



DEPARTMENT OF
ECOLOGY
State of Washington

Hangman Creek Watershed

Nutrients and Sediment Pollutant Source Assessment, 2018



April 2022

Publication 22-03-004

Publication Information

This report is available on the Department of Ecology's website at:
<https://apps.ecology.wa.gov/publications/SummaryPages/2203004.html>.

Data for this project are available in Ecology's [EIM Database](#). Study ID: tist0002.

The Activity Tracker Code for this study is 17-010.

Suggested Citation

Stuart, T. 2022. Hangman Creek Watershed Nutrients and Sediment Pollutant Source Assessment, 2018. Publication 22-03-004. Washington State Department of Ecology, Olympia.
<https://apps.ecology.wa.gov/publications/SummaryPages/2203004.html>.

Water Resource Inventory Area (WRIA) and 8-digit Hydrologic Unit Code (HUC) numbers for the study area:

- WRIA: 56
- HUC Number: 17010306

Contact Information

Publications Coordinator
Environmental Assessment Program
Washington State Department of Ecology
P.O. Box 47600
Olympia, WA 98504-7600
Phone: 360-407-6764

Washington State Department of Ecology – <https://ecology.wa.gov>

- Headquarters, Olympia 360-407-6000
- Northwest Regional Office, Bellevue 425-649-7000
- Southwest Regional Office, Olympia 360-407-6300
- Central Regional Office, Union Gap 509-575-2490
- Eastern Regional Office, Spokane 509-329-3400

COVER PHOTO: Hangman Creek looking downstream from Bradshaw Rd. bridge.
Photo credit: Tighe Stuart.

Any use of product or firm names in this publication is for descriptive purposes only and does not imply endorsement by the author or the Department of Ecology.

To request ADA accommodation for disabilities, or printed materials in a format for the visually impaired, call the Ecology ADA Coordinator at 360-407-6831 or visit ecology.wa.gov/accessibility. People with impaired hearing may call Washington Relay Service at 711. People with speech disability may call 877-833-6341.

Hangman Creek Watershed

Nutrients and Sediment Pollutant Source Assessment, 2018

by

Tighe Stuart

Environmental Assessment Program
Washington State Department of Ecology
Eastern Regional Office
Spokane, Washington

Table of Contents

	Page
List of Figures	3
List of Tables	3
Acknowledgments	4
Abstract	6
Introduction	7
Study area.....	7
Watershed description.....	9
Regulatory criteria and water quality standards.....	13
Field Methods and Data Sources	17
Ecology data collection.....	17
Non-Ecology data sources	26
Analytical Framework	28
Watershed mass balance	28
Long-term empirical model	29
QUAL2Kw.....	30
Stormwater.....	31
Results and Discussion	33
Observed sediment and nutrient patterns	33
Watershed sources of sediment and nutrients.....	36
Stormwater loads	43
Idaho loads	45
Long-term trends.....	47
Compliance with TMDLs and further reductions needed.....	50
Conclusions	62
Recommendations	63
References	64
Glossary, Acronyms, and Abbreviations	69
Appendices	73
Appendix A. Summary of data not available in EIM	74
Appendix B. Data quality	90
Appendix C. Watershed mass balance documentation.....	112
Appendix D. Long-term empirical model documentation.....	128
Appendix E. QUAL2Kw model documentation.....	136
Appendix F. Stormwater load estimation	205
Appendix G. Idaho high-flow season load estimation.....	217

List of Figures

	Page
Figure 1. Hangman Pollutant Source Assessment high-flow and low-flow study areas.	8
Figure 2. USGS stream-gage monthly flow statistics for Hangman Creek at the mouth, 1948-2016.	11
Figure 3. Land use patterns in the Hangman Creek watershed.....	12
Figure 4. Typical landscape in the Hangman Creek watershed, looking northeast toward Mica Peak near Rockford.	13
Figure 5. Map of high-flow study sampling locations.....	20
Figure 6. Map of low-flow study sampling locations.	21
Figure 7. Sample bottles and coolers in the field vehicle.	22
Figure 8. Gage station at Rock Creek at Hwy 27, with turbidity sensor mounted at the end of swing arm.....	24
Figure 9. Subbasins for watershed mass balance.....	28
Figure 10. Flowing stormwater outfalls to Lower Hangman Creek.	32
Figure 11. Observed flow, turbidity, total suspended solids (TSS), total phosphorus (TP), and dissolved inorganic nitrogen (DIN) in Hangman Creek at Meadowlane Rd.	33
Figure 12. Relationship between turbidity and total phosphorus (TP) throughout the Hangman Creek watershed.	34
Figure 13. Turbid water in upper Rock Creek, April 2018.....	35
Figure 14. Suspended sediment load contribution by subbasin, Mar-May 2018.....	38
Figure 15. Total phosphorus (TP) load contribution by subbasin, Mar-May 2018.	39
Figure 16. Example from Tekoa WWTP, showing algal nutrient uptake in upper Hangman Creek.	47
Figure 17. Declining trend in total suspended solids (TSS) at the mouth of Hangman Creek, 1978-2019, normalized for flow.....	48
Figure 18. Declining trend in total suspended solids (TSS) at the mouth of Hangman Creek, 1978-2019, as raw data.....	49
Figure 19. Turbid water from Hangman Creek meeting clear water from the Spokane River, at their confluence.....	50
Figure 20. Estimated total suspended solids (TSS) loads compared to TMDL load allocations.	53

List of Tables

Table 1. Applicable water quality criteria for Hangman Creek.....	14
Table 2. Spokane DO TMDL load allocations for Hangman Creek.....	14
Table 3. Spokane DO TMDL total phosphorus (TP) load reductions for Hangman Cr.	15
Table 4. Total suspended solids (TSS) load allocations for the Hangman Creek watershed.	15
Table 5. Total suspended solids (TSS) wasteload allocations for the Hangman Creek watershed.	16
Table 6. High-flow study sampling locations.....	18
Table 7. Low-flow study sampling locations including piezometers.	19
Table 8. Sample parameters and analytical methods.....	23
Table 9. High-flow study area-normalized subbasin load contribution estimates for suspended sediment (SSC), total phosphorus (TP), dissolved inorganic nitrogen (DIN), and flow.	37
Table 10. Total phosphorus (TP) loads for Lower Hangman Creek, June 2018.	41
Table 11. Total phosphorus (TP) loads for Lower Hangman Creek, July-October 2018..	41
Table 12. Dissolved inorganic nitrogen (DIN) loads for Lower Hangman Creek, June 2018.....	42
Table 13. Dissolved inorganic nitrogen (DIN) loads for Lower Hangman Creek, July-October 2018.....	42
Table 14. Estimated stormwater total phosphorus (TP) loads to Lower Hangman Creek, 2008-2018.....	44
Table 15. Estimated stormwater total suspended solids (TSS) loads to Lower Hangman Creek, water years 2009-2018.....	44
Table 16. Estimated phosphorus loads from Idaho, high-flow season 2009.	45
Table 17. Estimated sediment, phosphorus, and nitrogen loads from Idaho, high-flow season 2018.....	46
Table 18. Evaluation of total suspended solids (TSS) loads relative to Hangman TMDL load allocations.	52
Table 19. Evaluation of total phosphorus (TP) loads relative to Spokane TMDL load allocations for Hangman Creek.	55
Table 20. Total phosphorus (TP) reductions and degree of TMDL compliance, for four load reduction scenarios.....	57
Table 21. March-May TMDL season total phosphorus (TP) and suspended sediment (SSC) subbasin percent load reductions for “Meet Concentrations” scenario. .	58
Table 22. QUAL2Kw phosphorus reduction scenario sources summary, June-October 2018.	61
Table 23. QUAL2Kw phosphorus reduction scenario, effect at Hangman Creek mouth, June-October 2018.....	61

Acknowledgments

The author of this report thanks the following people for their contributions to this study:

- All of the landowners who granted permission for us to access their property to collect field data.
- Charlie Peterson, Spokane Conservation District, for providing stream gaging data.
- The many organizations, families, and individuals working to improve water quality in the Hangman Creek watershed.

Washington State Department of Ecology staff:

- Water Quality Program: Elaine Snouwaert, Mitch Redfern, and Chad Atkins for support and review.
- Environmental Assessment Program:
 - Eiko Urmos-Berry for organizing and leading the field sampling effort.
 - Tyler Buntain and Mike McKay for gage station installation.
 - Mitch Wallace and Mike Anderson for gage station operation and streamflow measurement support.
 - Melanie Redding and Brian Gallagher for leading the groundwater piezometer installation and sampling.
 - Andy Albrecht, Evan Newell, Austin Stewart, Steve Hummel, Mitch Redfern, Dan Dugger, Cathrene Glick, Eric Daiber, and Jonathan Ryskamp for assistance with the field study.
 - Janna Stevens for assistance with shade modeling and hemispherical photography analysis.
 - Manchester Environmental Laboratory staff including Nancy Rosenbower and Leon Weiks.
 - George Onwumere and Cathrene Glick for their support as managers.
 - Anise Ahmed and Jenny Wolfe for peer reviewing the report
 - Joan LeTourneau for formatting, editing, and publishing the report.

Abstract

Hangman Creek, a major tributary to the Spokane River, experiences water quality problems including high sediment and phosphorus conditions. This creek is an important contributor of sediment and phosphorus to the Spokane River. The Washington State Department of Ecology (Ecology) has developed Total Maximum Daily Load (TMDL) water cleanup plans that regulate the amount of sediment and phosphorus in Hangman Creek. The 2010 *Spokane River and Lake Spokane Dissolved Oxygen TMDL* plan set limits for phosphorus and other pollutants at the mouth of Hangman Creek. The 2009 *Hangman Creek Watershed Fecal Coliform, Temperature, and Turbidity TMDL* plan set limits for suspended sediment in Hangman Creek and its tributaries. In 2018, Ecology performed a pollutant source assessment to (1) evaluate current conditions in Hangman Creek with respect to these TMDL requirements, (2) assess long-term trends, and (3) quantify the actions needed throughout the watershed to meet TMDL goals.

During 2018, Ecology collected data for Hangman Creek and its tributaries. We sampled for suspended sediment, suspended solids, groundwater and surface water nutrients, and other parameters. We also collected continuous data for flow, turbidity, dissolved oxygen, pH, temperature, and conductivity. We used a mass-balance approach to quantify watershed contributions of sediment and nutrients during the springtime high-flow season. We used the QUAL2Kw water quality model to assess and quantify nutrient sources and processes in Lower Hangman Creek during the late spring, summer, and fall.

We found that the vast majority (~100%) of springtime sediment and phosphorus loading originates in the upper (southeastern) ~2/3 of the Hangman Creek watershed. However, per-square-mile loading varies greatly by subbasin within this area. The majority of summertime total phosphorus (~60%) and dissolved inorganic nitrogen (~95%) loading reaching the mouth of Hangman Creek originates in the lower watershed and is associated with groundwater.

Sediment conditions in Hangman Creek have improved substantially over the last four decades, but remain extremely high during the springtime high-flow season. Meeting the load allocation for total phosphorus established by the *Spokane River and Lake Spokane Dissolved Oxygen TMDL* will require eliminating the vast majority of springtime sediment (95%) and phosphorus (76%) loading to Hangman Creek. Although daunting, this is likely an achievable goal that would profoundly improve water quality in Hangman Creek and its tributaries.

Introduction

Hangman Creek, also known as Latah Creek, is a major tributary to the Spokane River. Hangman Creek and its tributaries have a long history of water quality problems, with 303(d) listings for temperature, bacteria, turbidity, dissolved oxygen (DO), and pH. Hangman Creek is a significant contributor of sediment and phosphorus to the Spokane River (Shultz, 2020; Moore and Ross, 2010).

Ecology developed a plan to address low oxygen and high nutrients (phosphorus) in the Spokane River and Lake Spokane (Long Lake). This plan, known as the *Spokane River and Lake Spokane Dissolved Oxygen Total Maximum Daily Load* (Moore and Ross, 2010; hereafter referred to as simply the *Spokane DO TMDL*), set limits for phosphorus and other pollutants from point and nonpoint sources. The Spokane DO TMDL set a load allocation for the mouth of Hangman Creek, requiring reductions in human-caused nonpoint phosphorus sources.

Another water quality improvement plan, the *Hangman Creek Watershed Fecal Coliform, Temperature, and Turbidity Total Maximum Daily Load* (Joy et al., 2009; hereafter referred to as the *Hangman Multiparameter TMDL*), addressed water quality concerns in Hangman Creek and its tributaries. To address turbidity, this plan set reductions for suspended sediment. Suspended sediment is strongly linked with phosphorus in the Hangman Creek watershed. Efforts to reduce sediment and phosphorus largely depend on the same set of best management practices.

The purpose of this 2018 pollutant source assessment is to quantify the sediment and nutrient reductions needed to meet the requirements of the *Spokane DO TMDL* and the *Hangman Multiparameter TMDL*. Our primary emphasis is on phosphorus, but we also evaluate sediment, nitrogen, DO, and pH, as appropriate. We evaluate the current status of Hangman Creek relative to each set of TMDL requirements, we examine long-term trends, and we detail the location and magnitude of reductions needed throughout the Hangman Creek watershed.

Study area

We divided this project into two distinct field study phases: a high-flow study, and a low-flow study:

- The **high-flow study** focused on conditions during the late winter-springtime runoff season. The area for the high-flow study included the entire portion of the Hangman Creek watershed in Washington.
- The **low-flow study** focused on conditions during the summertime low-flow period, although it also included the late spring and fall periods. Because a large portion of phosphorus loads reaching the mouth of Hangman Creek during the summer originate in the lower watershed, the low-flow study area focused on the lower ~15 miles of Hangman Creek.

Figure 1 presents a map of the Hangman Creek watershed showing the study areas for both study phases.

The Quality Assurance Project Plan (QAPP) for this project (Albrecht et al., 2017) included the activities described in this report. It also included an earlier study phase, the Tekoa receiving water study, which addressed nutrient contributions from the City of Tekoa Wastewater Treatment Plant. We published the *Tekoa Wastewater Treatment Plant Dissolved Oxygen, pH, and Nutrients Receiving Water Study* as a separate document (Stuart, 2020).

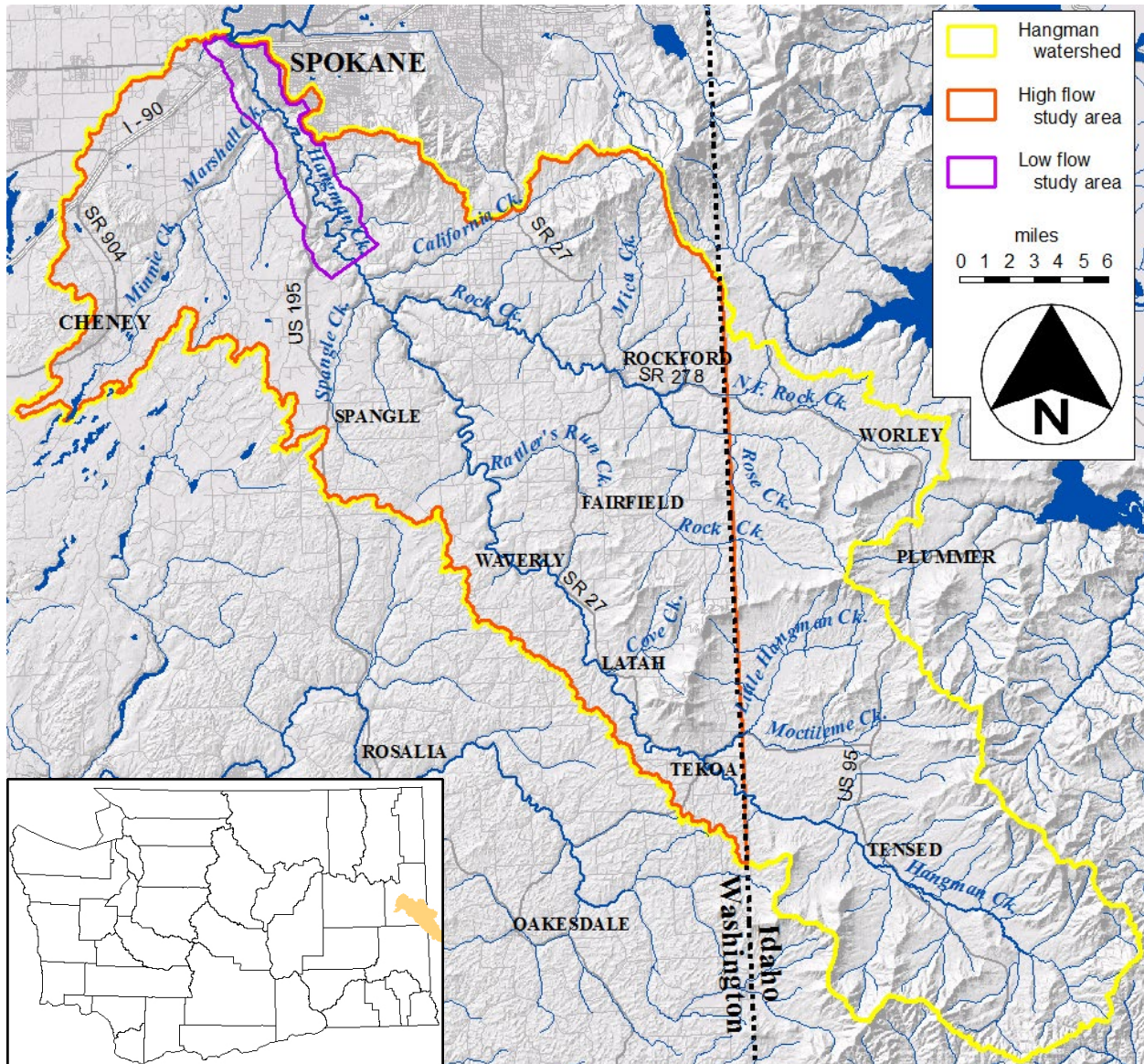


Figure 1. Hangman Pollutant Source Assessment high-flow and low-flow study areas.

Watershed description

The Hangman Creek (also known as Latah Creek) watershed drains about 431,000 acres and spans across four counties in two states. More than 60% of the watershed is in eastern Washington State (WRIA 56) while the remaining portion, including the headwaters, is located on the Coeur d'Alene Indian Reservation in Idaho. The major tributaries to Hangman Creek are the following creeks: Marshall, California, Spangle, Rock, Rattler Run, and the Little Hangman. Hangman Creek is a tributary to the Spokane River.

The watershed contains remnant populations of redband trout and other native and introduced fish species. According to watershed assessments of current and historical fish populations (SCD, 2005):

Fish habitat and distribution throughout the watershed has radically changed over the last one hundred years. Hangman Creek once had viable populations of native redband trout and healthy runs of salmon and steelhead. The removal of riparian vegetation, channel alterations, and heavy sedimentation has significantly reduced the spawning and rearing habitat on Hangman Creek. The primary species now found in the stream are adapted to warmer, slower waters and considered undesirable as gamefish. Resident trout populations are severely depressed.

California, Rock, and Marshall Creeks, as well as the Hangman Creek headwaters in Idaho, support remnant populations of redband trout (Western Native Trout Initiative, 2018; Lee, 2005). Improved water quality conditions (1) are needed to enhance and protect existing aquatic communities, and (2) would be a necessary first step for any possible future salmon or steelhead reintroduction.

Geology

Bedrock in the lower watershed is mainly Miocene basalt flows with pockets of Tertiary biotite granite and granodiorite (WDNR, 1998). During the Miocene epoch, basalt flows would periodically dam rivers and form lakes. Material deposited in these lakes formed the siltstones and sandstones of the Latah Formation. Pleistocene glacial deposits produced large amounts of wind-blown silt, known as loess. This wind-blown silt accumulated up to 200 feet over most of the basalt flows and formed dune-shaped hills. The Lake Missoula floods of the late Pleistocene (Waitt, 1980) left major channels in the region, removed the loess deposits covering the basalt, and deposited much of the sand, gravel, cobble, and boulders found in the lower reaches of Hangman Creek.

Easily erodible material is found throughout the Hangman Creek watershed. The unconsolidated material consists of three major deposits (Buchanan and Brown, 2003):

- Glacial Lake Missoula flood deposits of sand, gravel, and cobbles.
- Reworked Missoula flood deposits.
- Loess deposits found in the upper watershed.

The presence of these materials creates the potential for significant erosion and sediment transport, if land surfaces and streambanks are disturbed.

Hydrogeologic setting

There are two distinct aquifers in the area: the shallow, unconfined alluvial aquifer and the lower, confined water-bearing zones in the underlying basalt. The Hangman Valley is underlain primarily by glacio-alluvial deposits. These deposits are up to 200 feet thick and overlay the Columbia River Basalt Group. In the shallow alluvial aquifer, depth to water is about 10 to 20 feet below land surface.

There are significant groundwater inputs to Hangman Creek in the lower watershed, from about river mile (RM) 6 (near Qualchan golf course) to RM 1.5 (11th Ave.). (Figure 6, shown below in the *Field Methods and Data Sources* section, provides a map with some river mile locations indicated.) These include large subsurface groundwater inputs, as well as several surface springs. Together, lower-watershed groundwater inputs comprise the majority of flow at the mouth of Hangman Creek during the summer low-flow period.

Hydrology

Figure 2 illustrates streamflow patterns at the mouth of Hangman Creek. The spring runoff period typically occurs from January through May. Flows drop quickly from April through July, with the baseflows occurring during August and September. A wide seasonal variation in flows exists in Hangman Creek, with typical spring runoff flows about 40 times higher than typical flows during the summer low-flow period. Flows during the spring runoff period are very “flashy,” exhibiting a quick response to precipitation and snowmelt events. Peak flows in excess of 10,000 cfs occasionally occur.

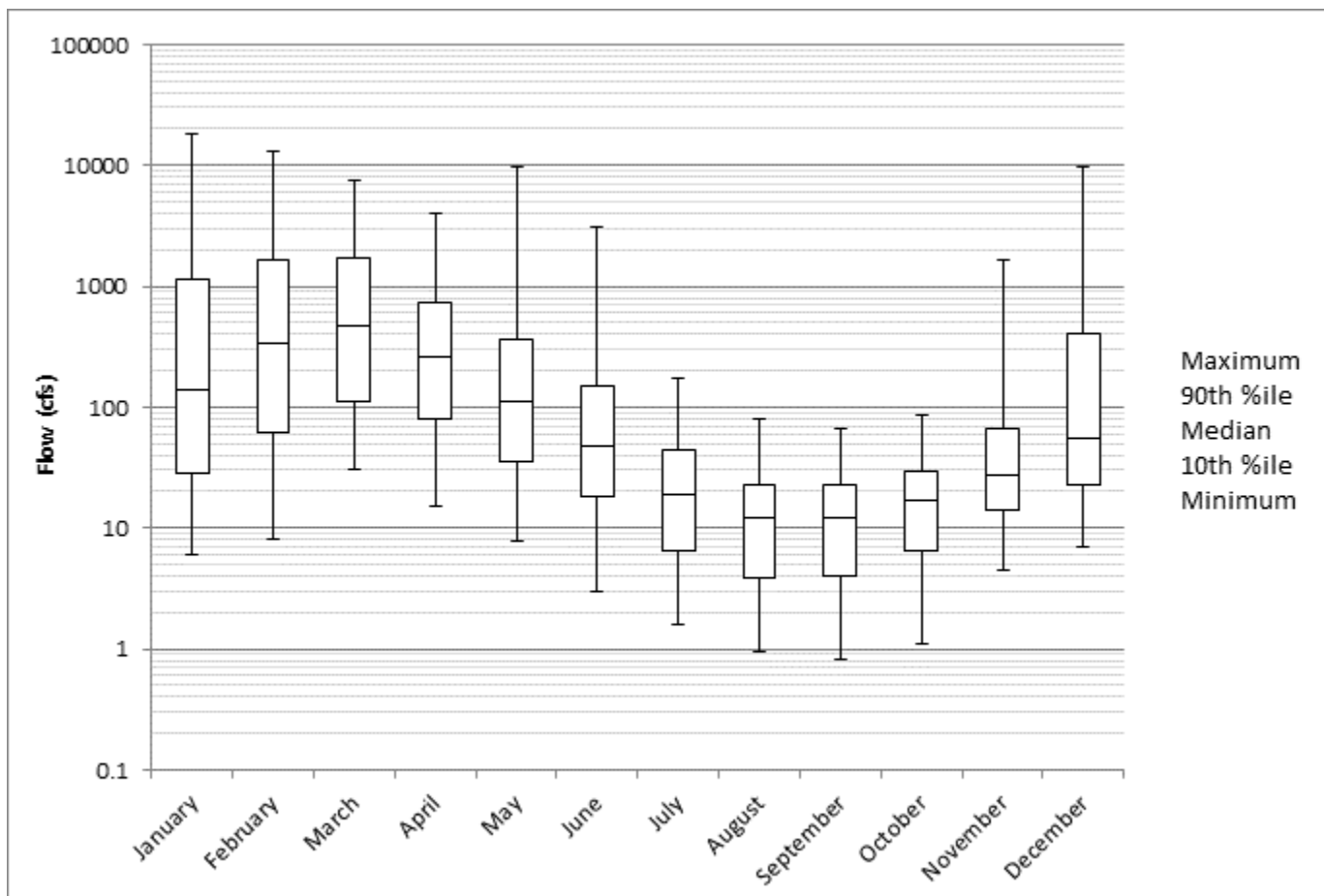


Figure 2. USGS stream-gage monthly flow statistics for Hangman Creek at the mouth, 1948-2016.

Land use

Figure 3 shows land use in the Hangman Creek watershed. The watershed is dominated by dryland agriculture, particularly in the south and eastern areas where loess soils occur. Forested areas occur on buttes and low mountains in the eastern part of the watershed, in canyons along Hangman and Rock Creeks, and in the channeled scablands that occur in the western part of the watershed. Urban development is concentrated in and around the city of Spokane, in the far northern part of the watershed. Figure 4 shows a photograph of a typical wintertime landscape in the Hangman Creek watershed.

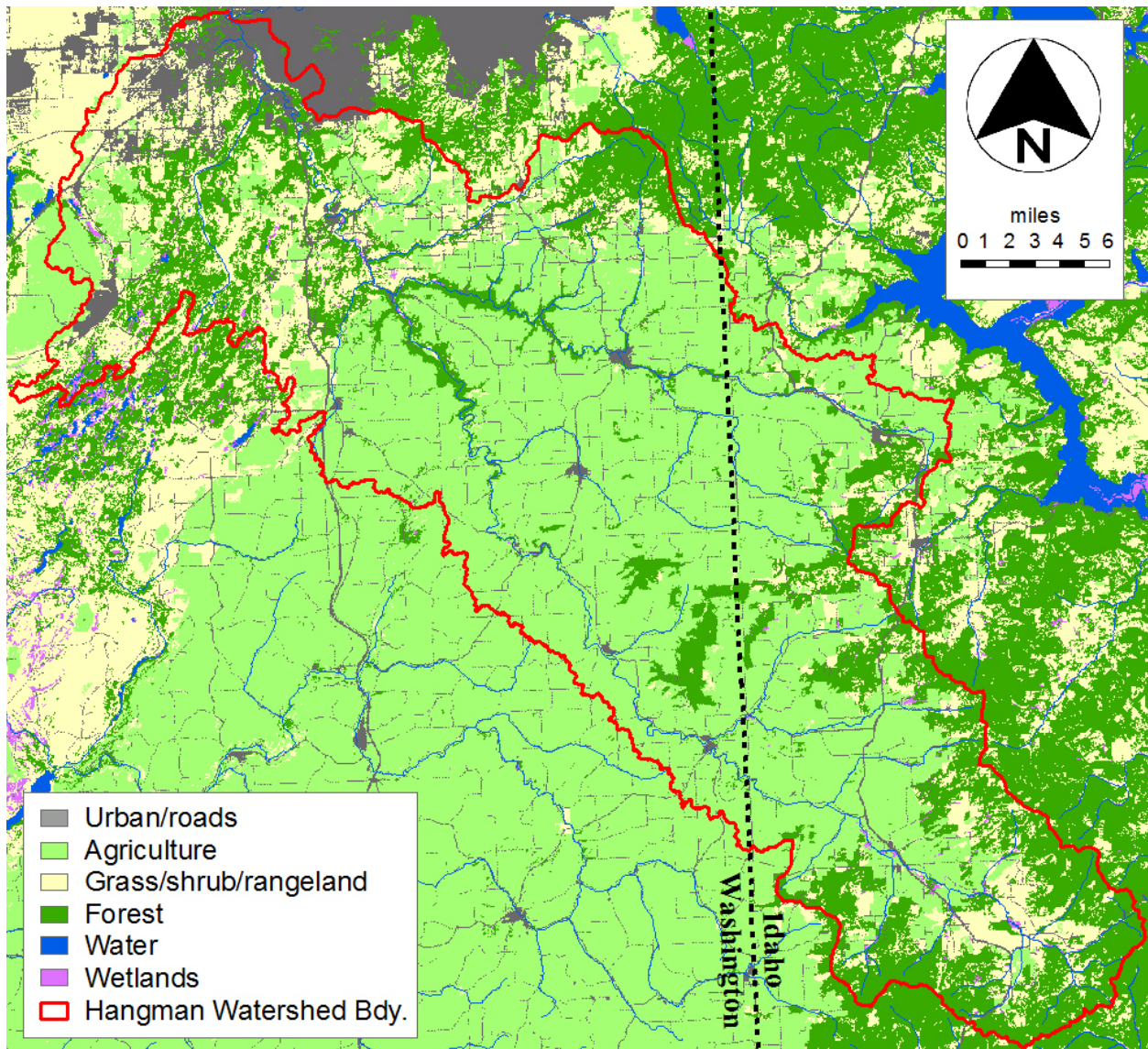


Figure 3. Land use patterns in the Hangman Creek watershed.

Source: National Land Cover Database (NLCD), 2006.



Figure 4. Typical landscape in the Hangman Creek watershed, looking northeast toward Mica Peak near Rockford.

Regulatory criteria and water quality standards

Dissolved oxygen (DO) and pH

In the Washington State water quality standards (WAC 173-201A), freshwater aquatic life use categories are described using key species (salmonid versus warm-water species) and life-stage conditions (spawning versus rearing). Hangman Creek has not been designated for protection of any special population of fish. Therefore, the statewide baseline designated aquatic life uses of “Salmonid Spawning, Rearing, and Migration” are to be protected.

The water quality criteria associated with the aquatic life use of “Salmonid Spawning, Rearing, and Migration” are biologically based. They are set to ensure the conditions necessary to fully support the aquatic life uses designated for the water body. As these criteria are based on biological requirements rather than the specific waterbody conditions, these criteria may not be achievable in all seasons. Hangman Creek is well known for its “flashy” and variable flow regime with extremely low and spatially stagnant flows in the summer. These conditions often

preclude the attainment of the numeric criteria. While Hangman Creek has been altered by human activities, extreme low summer flows are likely a natural feature in this watershed.

Table 1 summarizes the DO and pH water quality criteria associated with the “Salmonid Spawning, Rearing and Migration” use and therefore applicable to Hangman Creek. The *Programmatic QAPP for Water Quality Impairment Studies* (McCarthy and Mathieu, 2017) provides further information on these parameters.

Table 1. Applicable water quality criteria for Hangman Creek.

Parameter	Criteria
Dissolved Oxygen	DO concentration will not fall below 8.0 mg/L more than once every ten years on average.
pH	pH shall be within the range of 6.5 to 8.5 with a human-caused variation within above range of less than 0.5 units.

Phosphorus, ammonia, and CBOD

The *Spokane River and Lake Spokane Dissolved Oxygen TMDL* (*Spokane DO TMDL*; Moore and Ross, 2010) identified load allocations for the mouth of Hangman Creek. Table 2 summarizes the relevant allocations as reported in the TMDL, while Table 3 summarizes the load reductions for total phosphorus (TP). This pollutant source assessment study addresses TP, because Hangman Creek is a significant contributor of phosphorus. We are not addressing ammonia or CBOD in this study, because these pollutants are primarily associated with municipal and industrial point sources, not ambient tributary sources. For example, out of nine 5-day BOD (BOD5) samples taken from Hangman Creek and its tributaries during a 2009 storm event, all were non-detects (Ross, 2011). All ammonia samples taken at the mouth of Hangman Creek during this study were less than or equal to 0.011 mg/L.

Table 2. Spokane DO TMDL load allocations for Hangman Creek.

Season	2001 Flow (cfs)	Total Phosphorus		Ammonia (NH3-N)		CBOD	
		Allocation Concentration (mg/L)	2001 Load Allocation (lbs/day)	Allocation Concentration (mg/L)	2001 Load Allocation (lbs/day)	Allocation Concentration (mg/L)	2001 Load Allocation (lbs/day)
March – May Average	229	0.113	140.2	0.034	42.1	3.3	4102.1
June	31	0.044	7.5	0.012	2.1	2.8	479.0
July – October Average	9	0.030	1.4	0.009	0.4	2.3	107.9

Table 3. Spokane DO TMDL total phosphorus (TP) load reductions for Hangman Creek.

Month	Loads (lbs/day)			Load Reduction (lbs/day)	% Reduction	
	Natural (lbs/day)	2001 (lbs/day)	TMDL (lbs/day)		of 2001 Load (%)	of Human Load (%)
Mar-May	62.2	157.9	140.2	19.5	12	20
June	3.9	9.9	7.5	2.4	24	40
Jul - Oct	1.0	1.8	1.4	0.4	22	50

Total suspended solids (TSS)

The *Hangman Creek Watershed Fecal Coliform, Temperature, and Turbidity Total Maximum Daily Load (Hangman Multiparameter TMDL; Joy et al., 2009)* established load and wasteload allocations for TSS to address turbidity violations. Tables 4 and 5 show the load and wasteload allocations for TSS in the Hangman Creek watershed.

Table 4. Total suspended solids (TSS) load allocations for the Hangman Creek watershed.

For geographic subbasins and 303(d) listed stream segments.

	Sub-basin	303(d) listed segment	Estimated % reduction	
			Basin	303(d)
Hangman Creek	Upper Hangman Creek	Hangman Creek at Bradshaw Road (ID 40942)	26%	19%
	Hangman Creek from Tekoa to Bradshaw Rd		16%	
	Hangman Creek from Bradshaw Rd to Duncan	15%	n/a	
	Lower Hangman Creek	11%		
Tributaries	Little Hangman Creek	Little Hangman Creek (ID 40940)	16%	15%
	Rattler Run Creek	Rattler Run Creek (ID 40941)	15%	15%
	Rock Creek	Rock Creek at Jackson Road (40943)	18%	17%
	Marshall Creek		8%	n/a

n/a – There are no 303(d) listed segments in this geographic area.

Table 5. Total suspended solids (TSS) wasteload allocations for the Hangman Creek watershed.

Source	Permit Requirements		WLA
	Average Monthly Limit	Average Weekly Limit	
Tekoa WWTP	30 mg/L, 34.5 lbs/day	45 mg/L, 51.7 lbs/day	same
Fairfield WWTP	15 mg/L, 29.0 lbs/day	23 mg/L, 44.5 lbs/day	same
Spangle WWTP	15 mg/L, 8.5 lbs/day	23 mg/L, 12.8 lbs/day	same
Rockford WWTP	30 mg/L	45 mg/L	same
Freeman School District #358	20 mg/L, 7.2 lbs/day	30 mg/L, 10.8 lbs/day	same
Cheney WWTP	15 mg/L, 338 lbs/day	23 mg/L, 507 lbs/day	same
Industrial Facility Stormwater ¹	27 mg/L	88 mg/L ²	same
Spokane County Stormwater	All known and reasonable treatment		80% reduction ³
City of Spokane Stormwater	All known and reasonable treatment		80% reduction ³
Washington Dept. of Transportation Stormwater	All known and reasonable treatment		80% reduction ³
Construction Site Stormwater ⁴	All necessary best management practices Turbidity Benchmark: 25NTU Background and discharge sampling required Turbidity Limit: 5 NTU over background or when background is over 50 NTU less than a 10% increase over background		same

¹ No permitted industrial facilities currently exist in the watershed.

² Limit is a maximum daily (not average weekly).

³ Best management practices estimate 80% removal of TSS from stormwater sources (Ecology, 2004)

⁴ Construction stormwater NPDES permit regulates turbidity but does not regulate TSS.

Field Methods and Data Sources

Ecology data collection

Ecology collected field data in the Hangman Creek watershed during January-October of 2018. This data collection effort followed a project-specific Quality Assurance Project Plan (QAPP; Albrecht et al., 2017) as well as Ecology's *Programmatic QAPP for Water Quality Impairment Studies* (McCarthy and Mathieu, 2017). Our analysis also used some data from earlier field studies in the Hangman Creek watershed during 2008-2009 (Joy, 2008; Ross, 2011) and during 2016 (Stuart, 2016). The data collection occurred in two overlapping phases, corresponding to the high-flow and low-flow studies:

- **High-flow study:** January – May 2018; sites located throughout the portion of the Hangman Creek watershed located in Washington.
- **Low-flow study:** May – October 2018; sites located along Lower Hangman Creek, from Stevens Creek confluence to the mouth. Instream piezometers located from Qualchan Golf Course to the mouth. This study also included three synoptic flow (seepage) surveys during 2017, before the main data collection phase began.

Tables 6 and 7 list the sampling locations and the types of data that we collected at each location. Figures 5 and 6 show maps of the sampling sites for the high-flow study and the low-flow study, respectively.

Table 6. High-flow study sampling locations

Study Specific Location ID	Sampling Location	Latitude	Longitude	Laboratory samples		Turbidity field meas.		Continuous turbidity		Continuous streamflow		Discrete streamflow	
56HAN-58.5	Hangman Ck. at State Line	47.2028	-117.0406	2x	2x					U			
56HAN-55.1	Hangman Ck. above Little Hangman Ck.	47.2220	-117.0755	2x	2x	G	G						
56LIT-00.1	Little Hangman Ck. at Connell St.	47.2254	-117.0747	2x	2x	G	G						
56HAN-47.0	Hangman Ck. at Marsh Rd.	47.2761	-117.1532	2x	2x					P			
56COV-00.2	Cove Ck. at mouth	47.2788	-117.1531	2x	2x					P			
56HAN-32.8	Hangman Ck. at Bradshaw Rd.	47.3928	-117.2481	2x	2x	G	G						
56RAT-00.1	Rattler Run Ck. at mouth	47.3935	-117.2483	2x	2x					P			
56ROC-19.6	Rock Ck. at Bradshaw Rd.	47.3950	-117.0798	2x	2x					P			
56ROS-00.4	Rose Ck. at mouth	47.4169	-117.0667	2x	2x					P			
56ROC-17.1	Rock Ck. at Chatcholet Rd.	47.4201	-117.0883	2x	2x					P			
56MIC-00.2	Mica Ck. at mouth	47.4540	-117.1328	2x	2x					P			
56ROC-13.0	Rock Ck. at Hwy 27 in Rockford	47.4532	-117.1422	2x	2x	G	G						
56ROC-00.5	Rock Ck. at mouth	47.4955	-117.3228	2x	2x	G	G						
56HAN-20.2	Hangman Ck. blw Rock Ck.	47.4961	-117.3337	2x	2x	G	G						
56SPA-00.0	Spangle Ck. at mouth	47.5011	-117.3435	2x	2x					P			
56CAL-00.1	California Ck. at mouth	47.5127	-117.3469	2x	2x					P			
56HAN-06.2	Hangman Ck. at Meadowlane Rd.	47.6030	-117.4058	2x	2x	F	P						
56MIN-00.5	Minnie Ck. at mouth	47.5544	-117.4999	2x	2x					P			
56MAR-00.4	Marshall Ck. at Qualchan Dr.	47.6120	-117.4308							P			
56MAR-00.0	Marshall Ck. at mouth	47.6141	-117.4253	2x	2x								
56GAR-00.2	Garden Springs at Fish Lake trail	47.6443	-117.4509	S	S								S
56HAN-00.7	Hangman Ck. at mouth	47.6549	-117.4554	2x	2x					U			
56MS4-Chestnut	Stormwater outfall at Chestnut St., US RB	47.6402	-117.4430	(s)	(s)								(s)
56MS4-11thAve	Stormwater outfall at 11th Ave., DS RB	47.6458	-117.4473	(s)	(s)								(s)
56MS4-I90RB1	Stormwater outfall 100' US of I-90, RB	47.6485	-117.4461	S	S								S
56MS4-I90RB2	Stormwater outfall directly underneath I-90, RB	47.6488	-117.4463	S	S								S
56MS4-I90LB	Stormwater outfall 40' US of I-90, LB	47.6485	-117.4465	S	S								S
56CSO-19	CSO #19 outfall DS of I-90, RB	47.6493	-117.4464	(s)	(s)								(s)
56MS4-Sunset	Stormwater outfall DS Sunset Blvd. High Bridge Pk.	47.6503	-117.4487	S	S								S
56MS4-A-St	Stormwater outfall at A St. & Riverside Ave, US LB	47.6541	-117.4540	(s)	(s)								(s)

All data collected during 2018.

2x – Laboratory samples and turbidity measurements collected regularly twice per month.

S – Laboratory samples and discrete flow measurements collected during stormwater events only.

(s) – Outfall never observed to be flowing, or flow not sufficient to measure; no samples collected.

U – USGS streamflow gaging station.

G – Ecology streamflow gaging station with continuous turbidity.

P – Continuous streamflow and temperature measured using pressure transducers.

F – Continuous turbidity measured by probe and cellular telemetry datalogger

Table 7. Low-flow study sampling locations including piezometers.

Study Specific Location ID	Sampling Location	Latitude	Longitude	Laboratory samples	Periphyton biomass (2009)	Continuous streamflow	Discrete streamflow	Continuous turbidity	Continuous/diel sonde	Discrete sonde	Continuous temperature	Longitudinal depth (2016)	Time of travel (2009)
56HAN-14.5	Hangman Ck. abv. Hangman Vly. Golf Course	47.5403	-117.3718	2x		P	X	F	C		P	L	T
56HAN-13.2	Hangman Ck. above Latah WTP	47.5480	-117.3755	X			X		D			L	T
56HAN-12.6	Hangman Ck. below Latah WTP	47.5539	-117.3697	X			X		D			L	
56HAN-11.7	Hangman Ck. 1 mi. blw. Latah WTP	47.5583	-117.3829	X			X		D			L	
56HAN-08.9	Hangman Ck. at Yellowstone Pipeline	47.5812	-117.3959	X			X		D			L	
56HAN-08.6	Hangman Ck. abv Mullen Hill drainage	47.5830	-117.3995				E						
56Unk(MUL)-00.0	Unnamed drainage off Mullen Hill area	47.5820	-117.4014	X			X		D				
56HAN-08.2	Hangman Ck. just US Hatch Rd	47.5862	-117.4024				E						
56HAN-07.9	Hangman Ck. at Champion Park	47.5905	-117.4002	X			X		D			L	
56HAN-06.2	Hangman Ck. at Meadowlane Rd.	47.6030	-117.4058	2x		P	X	F	C		P	L	T
56HAN-05.8	Hangman Ck. at Qualchan GC up cart bridge	47.6058	-117.4135				E						T
56HAN-05.0	Hangman Ck. at Qualchan GC westward bend	47.6117	-117.4133				E						T
56HAN-04.6	Hangman Ck. blw. Qualchan Golf Course	47.6147	-117.4200	X			X		D			L	T
56MAR-00.4	Marshall Ck. at Qualchan Dr.	47.6120	-117.4308			P	X				P		
56MAR-00.0	Marshall Ck. at mouth	47.6141	-117.4253	2x			X		D				
56HAN-04.3	Hangman Ck. just DS Marshall Ck.	47.6156	-117.4254				E						T
56HAN-03.9	Hangman Ck. nr Cheney-Spokane Rd. intchg.	47.6199	-117.4308				E						T
56HAN-03.6	Hangman Ck. nr railroad overpass Hwy 195	47.6223	-117.4361				E						T
56HAN-03.3	Hangman Ck. at railroad bridge	47.6253	-117.4364	X		P	X		D		P	L	T
56Spr(VIN)-00.1	Vinegar flats US surface spring at Oak St.	47.6288	-117.4388	X			X		D				
56HAN-02.8	Hangman Ck. at end of 26th Ave	47.6327	-117.4367				E						T
56CRY-00.3	Crystal Springs at Inland Empire Way	47.6333	-117.4408	X			X		D				
56HAN-01.9	Hangman Ck. at Chestnut St.	47.6409	-117.4443	X			X		D			L	T
56GAR-00.0	Garden Springs at mouth	47.6456	-117.4477	X			X		D				
56HAN-01.4	Hangman Ck. just US I-90 bridge	47.6477	-117.4463				E						
56HAN-00.7	Hangman Ck. at mouth	47.6549	-117.4554	X	X	U	X		D			L	
56HAN-GW-1	Piezo in Hangman; DS of Meadowlane Rd.	47.6049	-117.4133	Z						Z			
56HAN-GW-2	Piezo in Hangman; blw Qualchan GC	47.6139	-117.4224	Z						Z			
56HAN-GW-3	Piezo in seeps; blw Qualchan GC	47.6138	-117.4232	Z						Z			
56HAN-GW-4	Piezo in Hangman; nr Cheney-Spokane Rd.	47.6189	-117.4303	Z						Z			
56HAN-GW-5	Piezo in Hangman; blw 11th ave.	47.6460	-117.4475	Z						Z			
56HAN-GW-6	Piezo in Hangman; abv. Riverside Ave.	47.6544	-117.4537	(z)						Z			

All data collected during 2018 unless otherwise noted.

2x – Laboratory samples collected twice per month.

Z – Groundwater laboratory samples and Sonde measurements collected from instream piezometer.

(z) – No groundwater nutrient samples collected; losing piezometer.

U – USGS streamflow gaging station.

P – Continuous streamflow and temperature measured using pressure transducers.

E – Discrete flow measured only during 2017 seepage surveys

F – Continuous turbidity measured by probe and cellular telemetry datalogger.

C – Water quality measurements (dissolved oxygen, pH, conductivity, temperature) collected continuously during study.

D – Water quality measurements collected continuously during 48-hour periods monthly (diel deployment).

L – Longitudinal depth recorded continuously along Hangman Creek (not just at sampling locations).

T – Time of travel measured along Hangman Creek for reaches including this location, at least once during 2009.

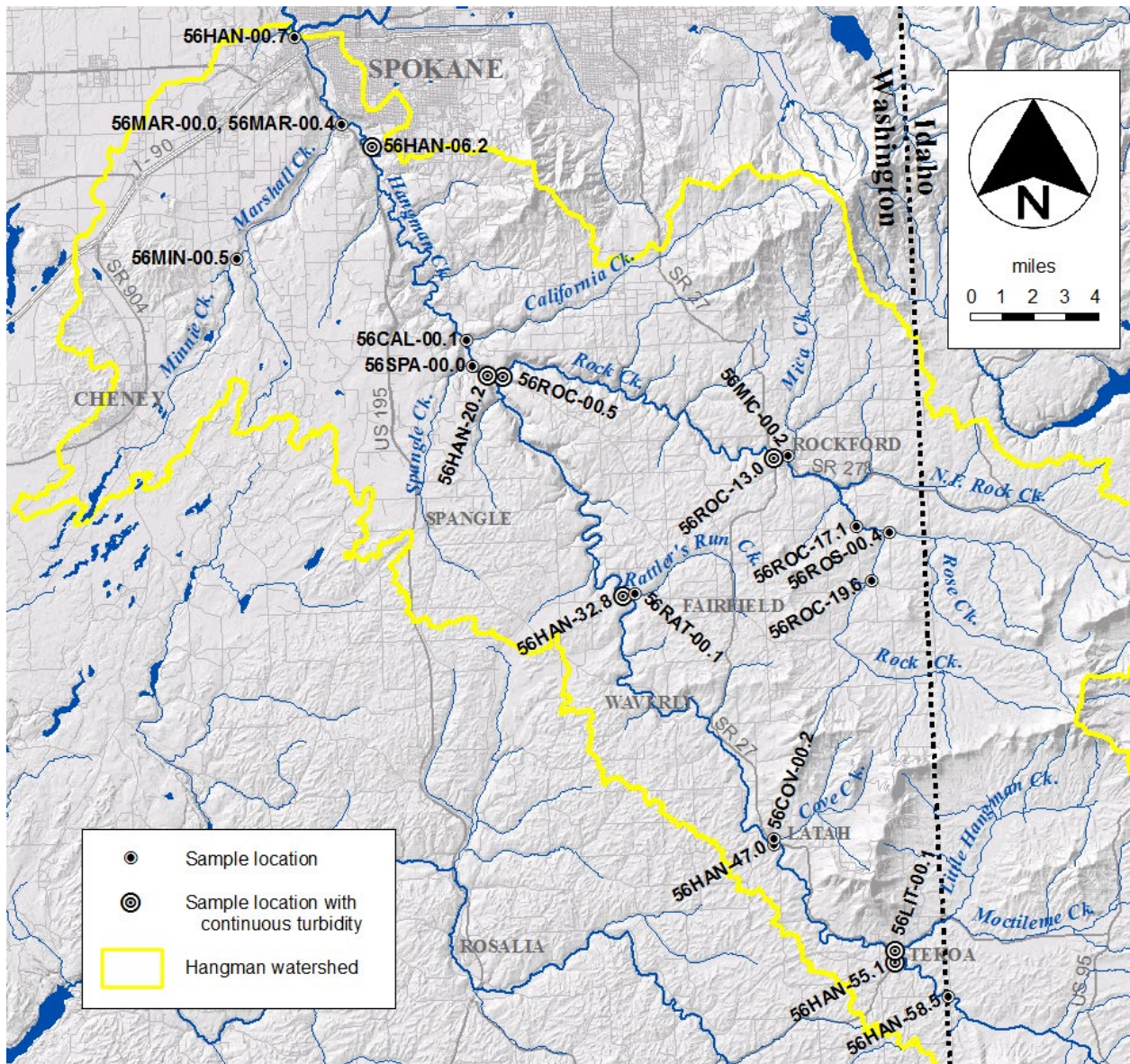


Figure 5. Map of high-flow study sampling locations.

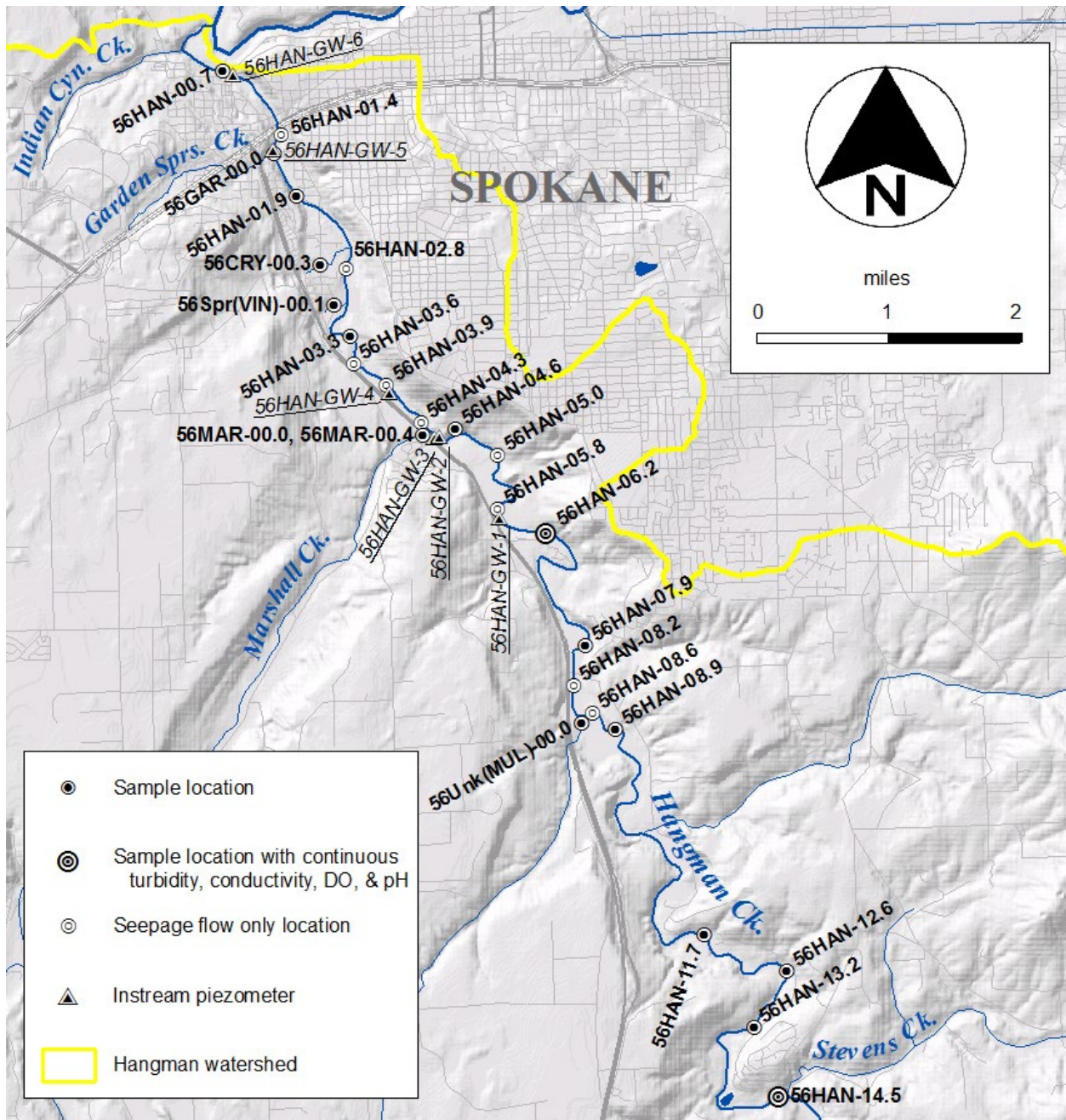


Figure 6. Map of low-flow study sampling locations.

Laboratory samples

During the January-May 2018 high-flow study, Ecology collected water samples (Figure 7) twice monthly at stream sampling locations, as well as during selected high-flow weather events. We also collected samples from urban stormwater outfalls during two stormwater-producing rain events. At stream sampling locations, we collected grab samples from the thalweg in a well-mixed part of the channel, using a bucket or pole sampler. We took two separate sets of field replicates at quality control (QC) sites during this study: (1) a set of grab samples, collected the same as the primary sample set, and (2) a set of depth-integrated samples, collected using an isokinetic sampler and processed using a churn splitter. For stormwater outfalls, we collected samples directly from the pipe end.

During the May-October 2018 low-flow study, we collected water samples monthly at stream sampling locations and at instream piezometers, as well as twice monthly at three selected locations. At stream sampling locations, we collected wading grab samples from the thalweg in a well-mixed part of the channel. For piezometers, we collected samples using a peristaltic pump after purging the well.

Ecology's Manchester Environmental Laboratory (MEL) analyzed all samples for this project. Table 8 lists the sample parameters and analytical methods.



Figure 7. Sample bottles and coolers in the field vehicle.

Table 8. Sample parameters and analytical methods.

Parameter	Method	High-flow study (surface water + stormwater)	Low-flow study (surface water)	Low-flow study (piezometers)
Total Persulfate Nitrogen	SM 4500-NB	X	X	X
Ammonia	SM 4500-NH ₃ -H	X	X	X
Nitrate/Nitrite	SM 4500-NO ₃ -I	X	X	X
Total Phosphorus	SM 4500-P H	X	X	X
Orthophosphate (Soluble Reactive Phosphorus)*	SM 4500-P G	X	X	X
Total Organic Carbon	SM 5310B		X	
Dissolved Organic Carbon	SM 5310B		X	X
Suspended Sediment Concentration	ASTM D3977B	X		
Total Suspended Solids	SM 2540D	X	X	
Total Non-Volatile Suspended Solids	EPA 160.4		X	
Turbidity	SM 2130	X		
Alkalinity	SM 2320B		X	X
Chloride	EPA 300.0		X	X
Bromide	EPA 300.0			X
Boron	EPA 200.8			X

SM = Standard Methods for the Examination of Water and Wastewater, 20th Edition (APHA, 2012).

ASTM = Formerly known as the American Society for Testing and Materials

EPA = EPA Method Code.

* Manchester Environmental Laboratory (MEL) refers to this parameter as orthophosphate. It is commonly referred to as soluble reactive phosphorus (SRP), and that is how we refer to it in this report.

Streamflow

For the high-flow study, Ecology’s Environmental Assessment Program (EAP) Freshwater Monitoring Unit (FMU) installed four stream gaging stations. In addition, we continued to use two gage stations that we installed in 2017 for the *Tekoa Receiving Water Study* (Stuart, 2020). We installed Hobo[®] stand-alone pressure transducers at 12 additional locations. These stations recorded stage height continuously through the study period. We measured flow and stage about twice monthly at all of these locations, and we used the measured relationship between stage and flow to convert the continuous stage record into a continuous flow record. At stormwater outfalls, we obtained discrete flow measurements by using either the partially full pipe or the timed bucket fill method.

For the low-flow study, we used Hobo[®] stand-alone pressure transducers to measure continuous flow at four locations, including two locations that were part of the high-flow study. At the remaining stream sampling locations, we measured flow monthly, concurrently with water sample collection. During the summer of 2017, prior to the main low-flow study period, we conducted three synoptic flow (seepage) surveys, consisting of discrete flow measurements to ascertain the locations of gaining and losing reaches in Lower Hangman Creek.

Turbidity

During the high-flow study, we collected continuous turbidity at the six FMU gaging stations using FTS® DTS-12 turbidity sensors (Figure 8). We also collected continuous turbidity at one additional site using a DTS-12 sensor linked to a stand-alone FTS® cellular telemetry datalogger. During the twice-monthly sampling events, field crews took triplicate spot measurements of turbidity at each sample location using a Hach® portable turbidity meter.

During the low-flow study, we measured continuous turbidity at two sites (including one site from the high-flow study) using DTS-12 sensors linked to stand-alone cellular telemetry dataloggers. We also collected routine spot turbidity measurements using a Hach® portable turbidity meter as a QC check on the continuous sensors.



Figure 8. Gage station at Rock Ck. at Hwy 27 (56ROC-13.0), with turbidity sensor mounted at the end of swing arm.

Continuous water quality

We did not measure field water quality parameters other than turbidity during the high-flow study.

During the low-flow study, we deployed Hydrolab[®] multiprobe sondes continuously throughout the study period to record dissolved oxygen (DO), pH, temperature, and conductivity at two locations. The sondes logged measurements of these parameters every 15 minutes. At the remaining 14 locations, we deployed Hydrolab[®] and/or YSI[®] EXO[®] sondes to record these same parameters for an approximate 48-hour period during each monthly sampling survey. We also collected routine spot measurements of these parameters as a QC check on the deployed instruments.

At instream piezometers, we measured the same four parameters using a Hydrolab[®] sonde attached to a flow cell and a peristaltic pump. These measurements served both to characterize groundwater quality and to monitor well purging before collecting lab samples.

Hydraulic geometry and time-of-travel

Stream channel width, depth, and velocity have an important influence on (1) the response of DO and pH to instream biological processes and (2) the downstream transport of nutrients and other substances.

To assess the widths of Hangman Creek, we digitized the wetted banks from 2017 12-inch resolution National Agriculture Imagery Program (NAIP) color orthophotos (aerial photographs geometrically corrected to have the same scale as a map). We calculated wetted widths every 10 meters using the TTools extension for ArcGIS (Ecology, 2015). TTools is a GIS-based tool used for spatial analysis of stream channels and riparian areas, including vegetation and shade.

During April 2016, we collected water depth data for the entirety of Hangman Creek within Washington and also for the portion of Rock Creek downstream of the North Fork (NF) Rock Creek confluence (Stuart, 2016). To measure water depths, we mounted a Hydrolab[®] Minisonde[®] equipped with a depth probe snugly inside a length of PVC pipe and dragged it along the bottom of the channel behind a canoe. A Surveyor[®] deck unit equipped with GPS recorded location coordinates and a corresponding depth measurement every 30 seconds.

To assess water velocities, we used data collected during two time-of-travel studies, on June 15-16 and July 14-17, 2009 (Joy, 2008; Ross, 2011) to represent two different flow conditions. The time-of-travel studies used rhodamine (a fluorescent, non-toxic tracer dye) to estimate travel times by measuring the time it takes for a slug of the dye to reach specific downstream locations.

Continuous water temperature

Ecology did not explicitly set out to monitor water temperature during the high-flow study. However, some of our monitoring instruments (such as gage stations, pressure transducers, and turbidity sensors) also monitored temperature. We performed a quality assurance (QA) assessment of these data and loaded them to EIM for public use.

For the low-flow study, Ecology obtained continuous water temperature data from deployed instruments including Hobo[®] pressure transducers and Hydrolab[®] multiprobe sondes. We used spot temperature measurements taken with Hydrolab[®] sondes as QC checks on the continuous temperature records from all instrument types.

Periphyton

Periphyton consists of a community of algae, fungi, microbes, and microscopic plants and animals that grow in shallow water habitats attached to submerged surfaces. Periphyton productivity is often one of the most important drivers of DO and pH changes in shallow streams and rivers.

On June 22 and July 27, 2009, Ecology collected periphyton biomass samples at Hangman Creek at the mouth (56HAN-00.7) using a modified version of USGS protocols (Porter et al., 1993; Mathieu, 2016). At this site, we collected three representative rocks from the streambed. We scraped periphyton from the rocks into the sample container along with deionized water. Ecology's Manchester Environmental Laboratory (MEL) analyzed the samples for Chlorophyll *a* and Ash-Free Dry Weight. We then calculated areal periphyton biomass as the total quantity of Chlorophyll *a* or Ash-Free Dry Weight collected divided by the rock surface area from which we had scraped the periphyton. Ash-Free Dry Weight represents total biomass, while Chlorophyll *a* represents photosynthetic biomass.

Non-Ecology data sources

USGS flow

The U.S. Geological Survey (USGS) operates a continuous streamflow gaging station on Hangman Creek at the mouth (Hangman Creek at Spokane, WA; Station ID 12424000). This is located very near our sampling site 56HAN-00.7 in this study. The USGS also operates a gaging station on upper Hangman Creek at the WA/ID state line (Hangman Creek at State Line Road near Tekoa, WA; Station ID 12422990). This is the same location as our sampling site 56HAN-58.5 in this study.

SCD flow

Spokane Conservation District (SCD) operated several streamflow gaging stations in the Hangman Creek watershed from about 2000-2010. We used 2009 SCD data from the Rock

Creek at Mouth site, in conjunction with 2009 Ecology data in one part of our loading analysis (see Appendix G).

Meteorology

We used meteorological data from the NOAA National Weather Service (NWS) weather stations at Spokane Airport (ID KGEG) and Felts Field (ID KSFF). We also used data from the interagency Remote Automatic Weather Station (RAWS) located at Turnbull National Wildlife Refuge (ID TWRW1), about 10 miles southwest of the study area. RAWS stations are operated jointly by agencies including the National Interagency Fire Center (NIFC), the National Oceanic and Atmospheric Administration (NOAA), and the Western Regional Climate Center (WRCC).

City of Spokane stormwater monitoring data

We used City of Spokane stormwater monitoring data from the Cochran Basin (City of Spokane, 2020) to estimate stormwater characteristics for a few parameters where we lacked data from Hangman-specific outfalls. The Cochran basin drains a large portion of the city of Spokane. Its outfall discharges stormwater to the Spokane River about 2 ½ miles downstream from the mouth of Hangman Creek.

We analyzed mass balances for total phosphorus (TP), suspended sediment concentration (SSC), and dissolved inorganic nitrogen (DIN). The analysis included the following steps:

1. We estimated the seasonal average load for each sampling location. We did this for two overlapping seasons: (1) January 18 – April 30, 2018, representing the period of peak flows, and (2) March 1 – May 31, 2018, representing the March-May season defined by the *Spokane DO TMDL* (Moore and Ross, 2010). For sampling sites with continuous turbidity, we used the relationship between turbidity and TP or SSC to estimate loads. (DIN does not correlate to turbidity.) For sampling sites without continuous turbidity (and for DIN at all sites), we used a multiple linear regression model approach (Cohn et al., 1989). Appendix C details these two methods, compares them, and discusses how we ensured comparability between them.
2. We calculated the contribution from each subbasin as the load flowing out of the subbasin minus all the loads flowing into the subbasin. This includes all sources in the subbasin (e.g., field, bank, groundwater). For example, for the “Hangman Tekoa-Latah-Waverly” subbasin:

$$U_{Hangman\ TekoaLatahWaverly} = U_{56HAN32.8} - U_{56HAN55.1} - U_{56LIT00.1} - U_{56COV00.2}$$

3. We divided each subbasin contribution by its corresponding drainage area. This results in an area-normalized subbasin contribution, expressed in units such as tons/day/mi² for sediment, or lbs/day/mi² for nutrients.¹
4. To test hypothetical implementation scenarios, we reversed the process to back-calculate the subbasin load contribution and sampling site loads that would occur, given particular areal contribution reductions.

We did not analyze watershed mass balances for total suspended solids (TSS), because the relationship between turbidity and SSC was much better than for TSS. SSC is generally considered a better method for quantifying suspended sediment (Galloway et al., 2005; Gray et al., 2000).

Long-term empirical model

To assess variability between years and to examine long-term trends, we used an empirical regression model, based on the long-term total suspended solids (TSS) dataset collected by Ecology’s ambient monitoring program at the mouth of Hangman Creek (Site ID 56A070; referred to as 56HAN-00.7 in this report). We used TSS data collected from 1978 through 2019. Our model is similar to a multiple linear regression approach, but uses the non-linear relationship between log[flow] and log[TSS], together with a long-term trend term.

¹ This area-normalized load contribution is sometimes referred to as “yield.” However, in this study we are not referring to it that way in order to avoid confusion with the agricultural usage of the same term.

We analyzed the correlation between TSS and TP using ambient monitoring data from late 2007 through 2019². We used this correlation to translate sediment reduction scenarios into forecasts for TP. We also analyzed the correlation between SSC and TSS (which, unlike TP vs TSS, appears to be constant throughout the watershed) using 2018 data from throughout the watershed collected during this study. We used this to translate between the watershed mass balances for SSC and the long-term loading model at the mouth for TSS.

During summer low-flow conditions, TP does not correlate as well with sediment. To estimate TP loads during low-flow, we used a regression model between flow and TP data collected during July-October, since late 2007. This model uses the linear relationship between flow and TP, together with a seasonal term.

Appendix D provides the details of these models.

QUAL2Kw

We used the QUAL2Kw water quality model (Pelletier and Chapra, 2008; Chapra 1997) to simulate nutrients, algal productivity, DO, and pH in Hangman Creek. The model domain includes Lower Hangman Creek from Stevens Creek (RM 14.5) to the mouth at the Spokane River, during May through October 2018. The model is based on data collected during the 2018 low-flow study.

QUAL2Kw is a one-dimensional numerical model capable of simulating a variety of conservative and non-conservative water quality parameters. The version used to model Hangman Creek (QUAL2Kw 6.0) is capable of simulating a river continuously throughout the course of a season. QUAL2Kw requires the following types of data:

- Channel geometry data
- Streamflow data
- Meteorology data and shade estimates
- Nutrient (nitrogen, phosphorus, and carbon) concentration data
- Diel or continuous DO, pH, and temperature data
- Algae biomass data
- Groundwater nutrient and flow data

² Ecology's ambient monitoring program has collected total phosphorus (TP) data at the mouth of Hangman Creek since 1972. However, the laboratory method employed to analyze the older samples did not produce reliable results under high-sediment conditions. A method change in October 2007 resulted in reliable TP data across the full range of conditions.

QUAL2Kw requires water quality input data to characterize water at all model boundaries, including the upstream end of the model reach, tributaries, point sources, and groundwater inputs. Water quality data at other locations in the model reach are used as a comparison to check model simulations.

There are several important concepts for modeling the effect of primary productivity in running waters. Among the most important are:

- Usually, only one nutrient can limit algal growth at a time. The limiting nutrient will be the least available relative to its demand. This principle is known as Liebig's law of the minimum (Chapra, 1997).
- For river modeling, it is important to limit the growth rate to control algal biomass yield. The growth rate is often limited by the concentration of the most limiting nutrient (i.e. the supply rate of the limiting nutrient),³ and by temperature. In some situations other factors limit growth instead of nutrients, such as space available for attachment, light availability, or the inherent rate that particular species can grow.
- It is appropriate to use the dissolved-fraction concentration of the limiting nutrient, such as soluble reactive phosphorus (SRP) and dissolved inorganic nitrogen (DIN), as the basis for modeling periphyton growth. This is because the nutrient must be in a readily-available form for biological uptake and growth to occur during solute transport (Welch and Jacoby, 2004).
- Total phosphorus (TP) and nitrogen are important to model since the particulate and organic fractions can be transformed into the dissolved fractions through various instream and hyporheic processes.

Appendix E provides detailed documentation of the model segmentation, inputs, calibration, and goodness-of-fit. We used the calibrated QUAL2Kw model to compare sources of nutrients in Lower Hangman Creek, accounting for the attenuation effects of algal uptake on nutrients reaching the Spokane River.

Stormwater

Several stormwater outfalls discharge to Hangman Creek in the Spokane area (Figure 10). Most of these outfalls discharge in the vicinity of the I-90 and Sunset Ave. bridges. The USGS Hangman Creek at Spokane gaging station (ID# 12424000) is located just downstream of these outfalls. Stormwater flows often show up in gaging station data as clear signals that are distinct from the natural watershed response to the precipitation. We used these signals, along with precipitation data, to estimate total stormwater flows to Hangman Creek. Appendix F presents the details of this analysis.

³ QUAL2Kw has the ability to limit algal growth based on any of three different principles: (1) Liebig's law of the minimum, as described above; (2) multiplicative; and (3) harmonic mean. The multiplicative and harmonic mean options allow for nutrient co-limitation, but each have particular drawbacks. The Liebig minimum option is most commonly used, and is used in this study.



Figure 10. Flowing stormwater outfalls to Lower Hangman Creek.

Results and Discussion

Observed sediment and nutrient patterns

Sediment and nutrient patterns in the Hangman Creek watershed are highly seasonal and flow-dependent. Consistent with previous studies in this watershed (Joy et al., 2009; Ross, 2011), we observed elevated sediment, turbidity, and nutrients during the winter-spring high-flow period, with lower levels during the summer low-flow period (Figure 11). Sediment, turbidity, and phosphorus (Figure 12) are all closely linked. During the high-flow period, these parameters are extremely variable, exhibiting “spikes” during precipitation/flow events. This extreme variability can be observed in Figure 11 as large turbidity spikes at the the corresponding flow spikes (which are themselves large). It is common for an order-of-magnitude change in turbidity to coincide with a half-order-of-magnitude change in flow.

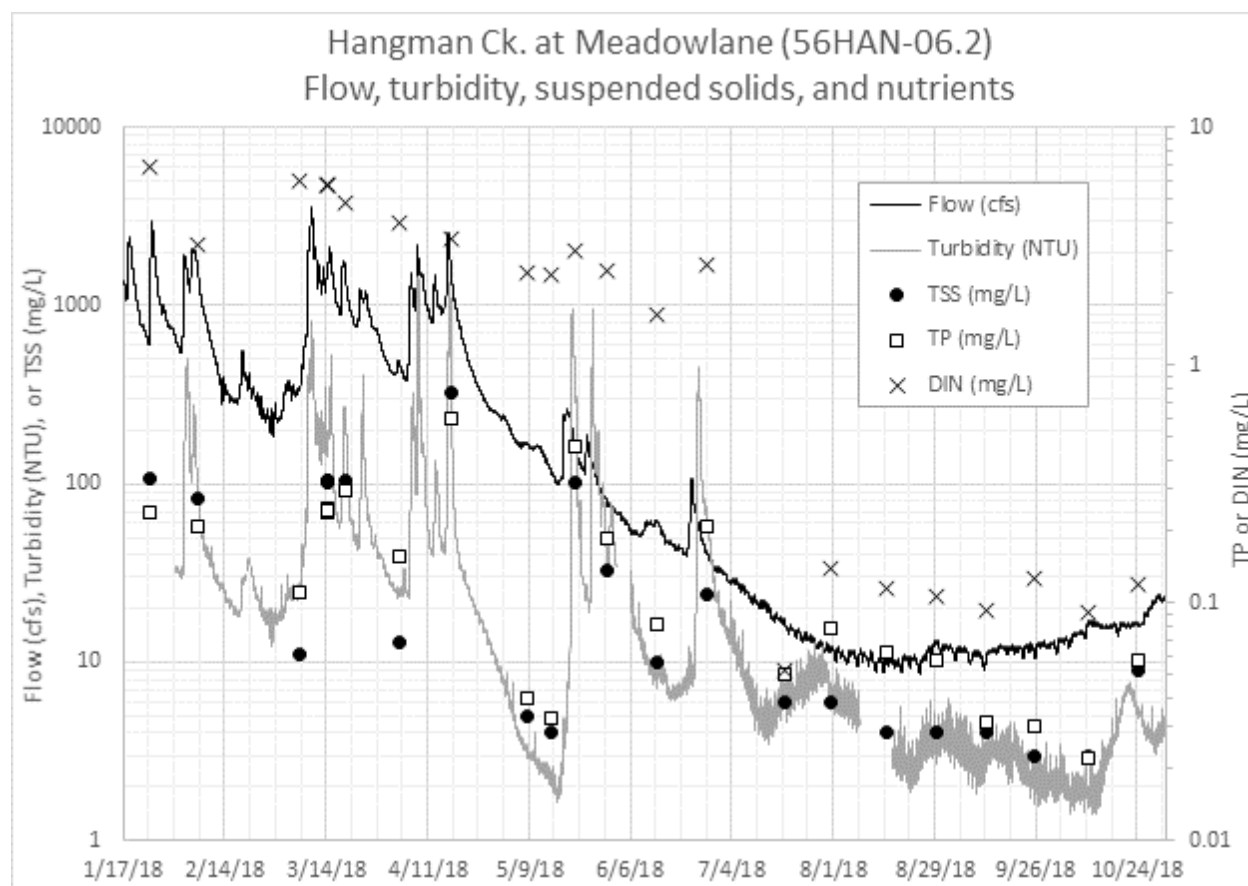


Figure 11. Observed flow, turbidity, total suspended solids (TSS), total phosphorus (TP), and dissolved inorganic nitrogen (DIN) in Hangman Ck. at Meadowlane Rd. (56HAN-06.2).

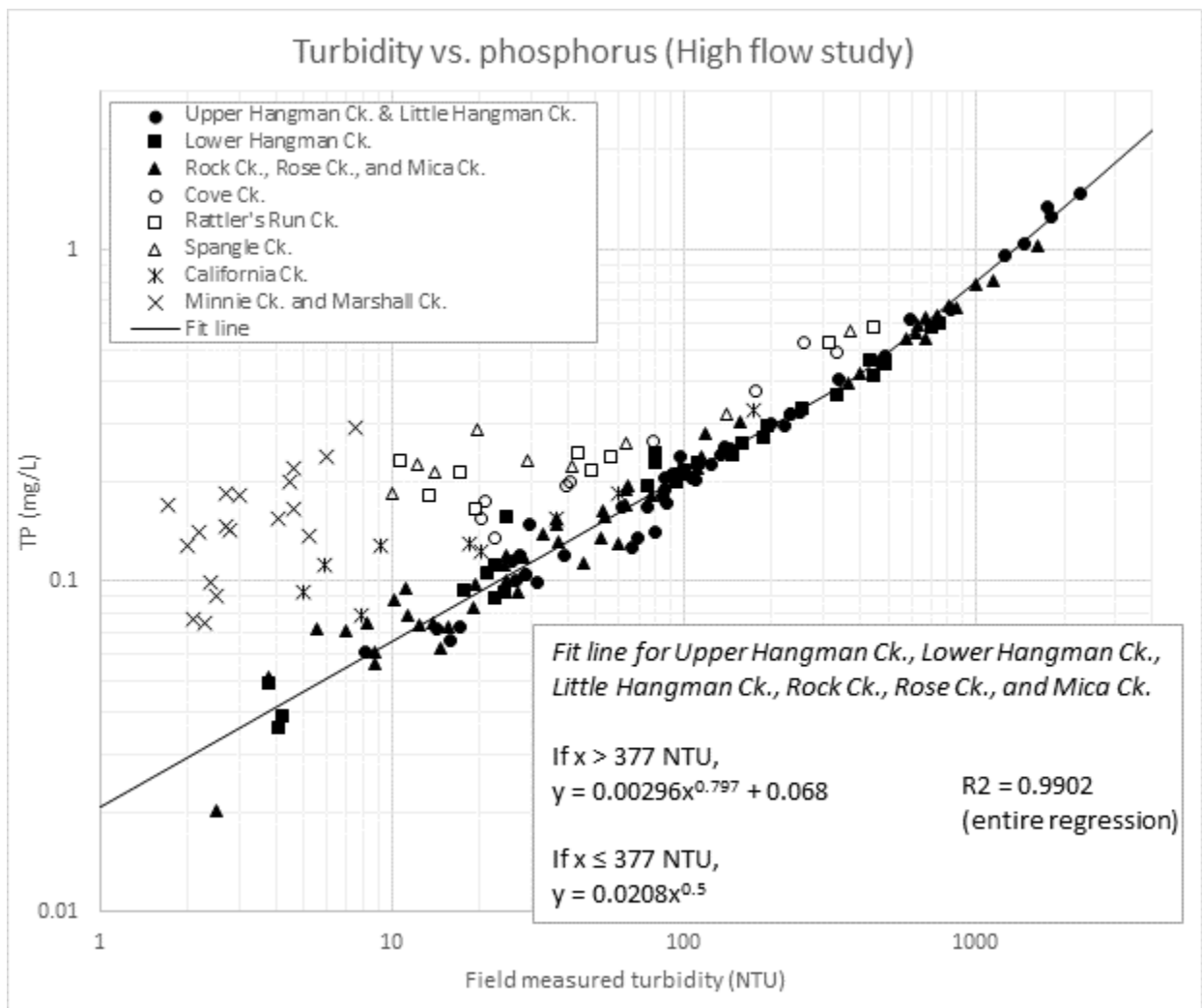


Figure 12. Relationship between turbidity and total phosphorus (TP) throughout the Hangman Ck. watershed.

The strong similarity between sediment, turbidity, and phosphorus trends reflects the fact that these three parameters are really three facets of the same phenomenon. The turbidity is caused by the suspended sediment in the water column. Also, during turbid conditions most of the phosphorus present is associated with the suspended soil particles (SCD, 2009). Turbid, high-sediment conditions are strongly related to high flows.

Figure 12 shows that a consistent relationship between turbidity and total phosphorus (TP) applies throughout most of the Hangman Creek watershed, including upper and Lower Hangman Creek, Little Hangman Creek, Rock Creek (Figure 13), Rose Creek, and Mica Creek. This relationship is different in some tributary streams, including Cove Creek, Rattler's Run Creek, Spangle Creek, California Creek, Minnie Creek, and Marshall Creek. These tributaries all have relatively higher proportions of soluble reactive phosphorus (average SRP/TP ratio > 50%), presumably from groundwater sources.

Dissolved inorganic nitrogen (DIN) displays strong seasonality, with higher concentrations during the high-flow period. However, unlike TP, DIN does not vary much *within* each season, and it does not correlate to turbidity (Figure 11). This is because DIN only includes the dissolved nitrate, nitrite, and ammonia fractions, and is not directly linked to sediment. DIN may enter waterways via groundwater, which is likely the main route, or via overland runoff. In fact there is probably a significant amount of organic and/or particulate nitrogen contained in suspended soil particles; however, this fraction is not included in DIN or entirely included in total persulfate nitrogen (TPN) lab results.



Figure 13. Turbid water in upper Rock Creek, April 2018.

Watershed sources of sediment and nutrients

Watershed mass balance (high-flow study)

Table 9 presents area-normalized subbasin load contribution estimates for sediment, nutrients, and flow. Figures 14 and 15 present suspended sediment (SSC) and total phosphorus (TP) data in map form for the March-May season defined in the *Spokane DO TMDL* (Moore and Ross, 2010).

Sediment and phosphorus

We observed that different subbasins contributed markedly different amounts of sediment and phosphorus during the high-flow period. In general, the vast majority (~100%) of sediment and phosphorus originated from the upper (i.e. southeastern) ~2/3 of the watershed, where loess soils occur and dryland agriculture is the predominant land use. However, within that area, differences between subbasins were stark. The highest area-normalized contributions came from Little Hangman Creek, followed by the Upper Rock and Rock Creek Canyon subbasins. In contrast, other subbasins with similar soil types and land use contributed far less.

To emphasize this, note that for the January-April peak flow season, median SSC contribution for “palouse-type” subbasins was 0.55 tons/day/mi². For Little Hangman Creek, it was 1.75 tons/day/mi², over three times higher than this. High-contributing subbasins tended to have extreme concentrations during precipitation/flow events. In Little Hangman Creek (56LIT-00.1) and upper Rock Creek (56ROC-19.6) we observed SSC concentrations in excess of 1000 mg/L, and in Little Hangman Creek we observed TP in excess of 1 mg/L.⁴

Nitrogen

Similar to phosphorus, we observed that the largest DIN contributions come from the upper ~2/3 of the watershed. However, there was less variability between subbasins. Elevated contribution from the Rattler’s Run and Rock Creek Canyon watersheds may be the result of point sources (Fairfield, Rockford, and Freeman School District WWTPs).

⁴ Note that SSC concentrations tend to be much higher than corresponding TP concentrations. SSC includes all material associated with sediment particles, only a small fraction of which consists of phosphorus. 1000 mg/L SSC and 1 mg/L TP are both extraordinarily high values for ambient streams.

Table 9. High-flow study area-normalized subbasin load contribution estimates for suspended sediment (SSC), total phosphorus (TP), dissolved inorganic nitrogen (DIN), and flow.

Subbasin name	SSC (tons/day/ mi ²)	SSC (tons/day/ mi ²)	TP (lbs/day/ mi ²)	TP (lbs/day/ mi ²)	DIN (lbs/day/ mi ²)	DIN (lbs/day/ mi ²)	Flow (cfs/mi ²)	Flow (cfs/mi ²)
	1/18/2018- 4/30/2018	3/1/2018- 5/31/2018	1/18/2018- 4/30/2018	3/1/2018- 5/31/2018	1/18/2018- 4/30/2018	3/1/2018- 5/31/2018	1/18/2018- 4/30/2018	3/1/2018- 5/31/2018
Upper Hangman	0.59	0.57	2.5	2.0	31	19	2.1	1.6
Little Hangman Creek	1.7	1.2	3.8	2.7	48	29	1.7	1.2
Cove Creek	0.26	0.23	1.6	1.2	28	20	1.1	0.88
Hangman Tekoa- Latah-Waverly	0.042	0.43	1.0	1.4	48	34	1.3	1.1
Rattler's Run Creek	0.32	0.27	1.8	1.4	65	50	1.1	0.92
Hangman Creek Canyon	-1.2 °	-0.97 °	-0.21 °	-0.12 °	26 °	33 °	0.89 °	0.82 °
Upper Rock	1.2	0.88	3.5	2.5	57	34	1.5	1.1
Rose Creek	0.56	0.49	2.5	2.1	62	39	1.4	1.0
Hoxie Valley - NF Rock Creek	0.55	0.48	1.4	1.0	42	24	1.5	1.1
Mica Creek	0.65	0.30	2.0	1.1	44	19	2.0	1.3
Rock Creek Canyon	1.6	0.88	3.7	2.1	72	51	1.9	1.4
Spangle Creek	0.093	0.062	1.3	0.85	36	27	0.82	0.64
California Creek	0.089	0.045	0.99	0.64	14	8.1	1.2	0.87
Hangman Valley	-0.53 °	-0.60 °	-1.4 °	-1.3 °	-33 °	-20 °	-0.34 °	-0.21 °
Minnie Creek	0.0066	0.0082	0.43	0.36	2.5	1.1	0.45	0.42
Marshall Creek	-0.0040	-0.0045	-0.23	-0.15	-1.2	-0.30	-0.13	-0.064
Lower Hangman	Estimates too uncertain to be usable °							
Indian Canyon Creek	No data ^d							

Colors in this table correspond to the colors in Figures 14 and 15. Redder colors indicate higher values, greener colors indicate lower values, and blue indicates negative values (sinks).

^a The season from 1/18/2018 – 4/30/2018 represents the season of peak flows, starting when we installed flow monitoring equipment throughout the watershed.

^b The season from 3/1/2018 – 5/31/2018 represents the March-May load allocation season established in the *Spokane River and Lake Spokane DO TMDL* (Moore and Ross, 2010).

^c We calculated subbasin load contributions by subtracting inflowing loads from outflowing loads. In some cases this creates large estimate uncertainty, where the inflowing and outflowing loads are both large, and the subbasin load is small. This is mainly an issue for mainstem Hangman Creek subbasins in the lower watershed. Subbasin load estimates for the Hangman Creek Canyon and Hangman Valley subbasins have large relative uncertainty and should be used with caution. Estimates for the Lower Hangman subbasin were unusable and are not listed here.

^d We did not sample Indian Canyon Creek during this project. Indian Canyon Creek flows into Hangman Creek downstream of the 56HAN-00.7 (Hangman Creek at mouth) sampling site and the USGS gage, and likely does not fully mix with Hangman Creek before reaching the Spokane River. Indian Canyon Creek has not historically been included in load and flow estimates for the mouth of Hangman Creek, but is technically part of the watershed.

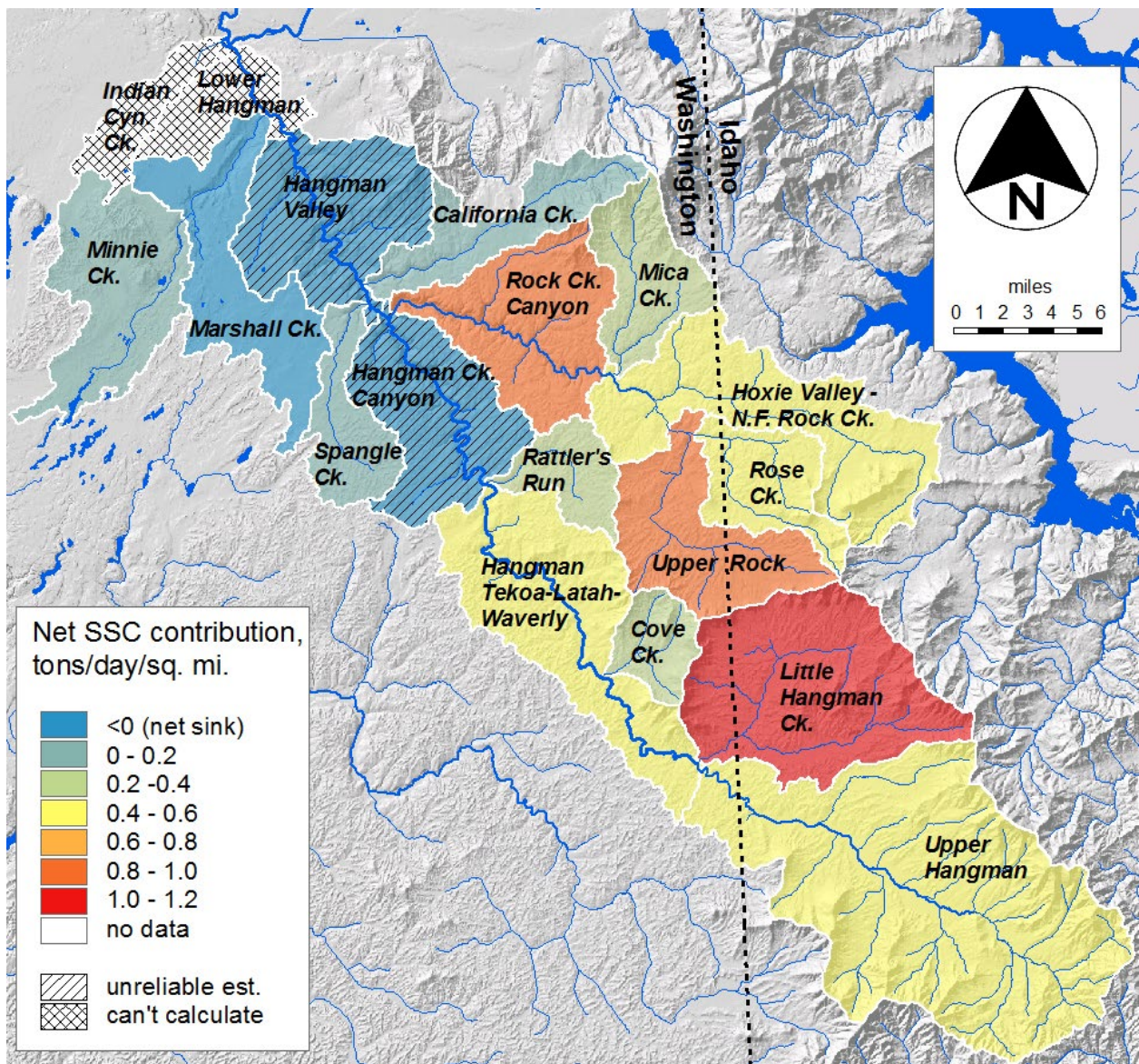


Figure 14. Suspended sediment load contribution by subbasin, Mar-May 2018.

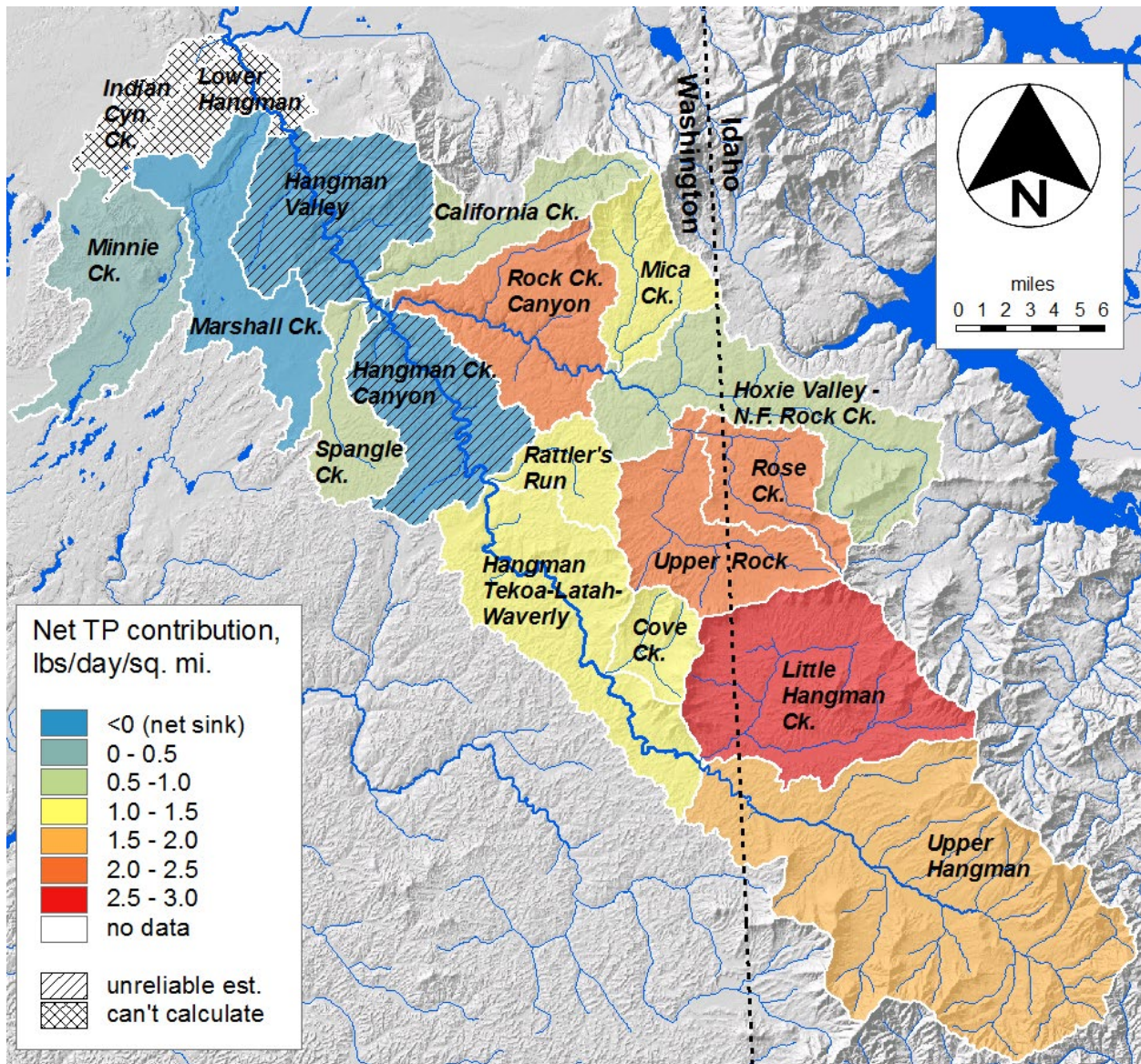


Figure 15. Total phosphorus (TP) load contribution by subbasin, Mar-May 2018.

QUAL2Kw model predictions (low-flow study)

Tables 10 through 13 present total phosphorus (TP) and dissolved inorganic nitrogen (DIN) load sources for Lower Hangman Creek. We present seasonal average loads for June and July-October 2018. We also present QUAL2Kw model-predicted estimates of nutrient attenuation.

Nutrient attenuation can occur through processes such as algal uptake, settling, and hyporheic exchange. The primary mechanism in Hangman Creek appears to be algal uptake of nutrients by bottom algae, or periphyton. Periphyton assimilate nutrients into their biomass throughout the warm-weather growing season. Significant downstream transport of these nutrients does not occur until late fall senescence and sloughing, or possibly even the next springtime high-flow period.

Attenuation occurs continuously along the length of a stream, so sources further upstream undergo more attenuation before reaching the mouth than do sources further downstream. Attenuation is also greater during the summer low-flow period, when slow travel times and ample algal activity result in high rates of nutrient cycling. This means that during higher-flow conditions, a greater proportion of the nutrient loads reaching the mouth of Hangman Creek originates higher in the watershed. During low-flow conditions, the majority of both TP and DIN reaching the mouth of Hangman Creek originates in the lower watershed.

Groundwater inputs to Lower Hangman Creek are the largest source of nutrients during the summer low-flow period. Diffuse groundwater contributed 43% of TP (Table 11) and 68% of DIN (Table 13) reaching the mouth of Hangman Creek during July-October 2018. These numbers are even higher if one includes surface springs – such as the upstream spring at Vinegar Flats, Crystal Springs, and Garden Springs – where groundwater surfaces and then flows a relatively short distance to Hangman Creek.

Marshall Creek, the largest tributary to Lower Hangman Creek, is a significant source of TP during June (Table 10) and July-October (Table 11). However, Marshall Creek is not a significant source of DIN (Tables 12 and 13), as DIN concentrations at the mouth of Marshall Creek are low.

Table 10. Total phosphorus (TP) loads for Lower Hangman Creek, June 2018.

Source	Location (km from mouth)	Source flow (cfs)	Load at source (lbs/day)	Load remaining at mouth (lbs/day)	% attenuation	% contribution to total load at mouth
Hangman Ck. at upstream model bdy ^a	24.2	48	40	32	20%	72%
Diffuse groundwater	(distributed)	22	7.2	7	3.7%	15%
Falling Springs ^b	17.2	0.40 ^b	0.15 ^b	0.13 ^b	12% ^b	0.3% ^b
Unnamed drainage off Mullen Hill area	14.1	0.80	0.3	0.27	9%	0.6%
Marshall Ck.	7.2	5.4	3.9	3.8	3.1%	8%
Upstream spring at Vinegar Flats	4.7	2.6	0.3	0.3	1.8%	0.7%
Crystal Springs	4.1	1.4	0.65	0.64	1.5%	1.4%
Garden Springs	2.5	0.66	0.43	0.43	0.8%	1.0%
Stormwater outfalls ^c	2.1	0.18	0.37	0.37	0.7%	0.8%

^a The QUAL2Kw upstream model boundary was located at the upstream end of the Hangman Valley Golf Course, downstream of the mouth of Stevens Creek.

^b We did not monitor Falling Springs. Load estimates assume the same concentrations as the Unnamed drainage off Mullen Hill area, and flows estimated from relative drainage area. The estimates should not be considered very reliable. Appendix E provides details.

^c This includes several stormwater outfalls, all of which discharge to Hangman Creek in the approximate vicinity of the I-90 bridge.

Table 11. Total phosphorus (TP) loads for Lower Hangman Creek, July-October 2018.

Source	Location (km from mouth)	Source flow (cfs)	Load at source (lbs/day)	Load remaining at mouth (lbs/day)	% attenuation	% contribution to total load at mouth
Hangman Ck. at upstream model bdy ^a	24.2	12	4.5	2.3	49%	28%
Diffuse groundwater	(distributed)	12	4.0	3.5	11%	43%
Falling Springs ^b	17.2	0.16 ^b	0.057 ^b	0.04 ^b	30% ^b	0.5% ^b
Unnamed drainage off Mullen Hill area	14.1	0.32	0.11	0.088	23%	1.1%
Marshall Ck.	7.2	1.8	1.4	1.3	8%	15%
Upstream spring at Vinegar Flats	4.7	2.1	0.3	0.29	3.9%	3.5%
Crystal Springs	4.1	0.87	0.39	0.38	3.3%	4.6%
Garden Springs	2.5	0.43	0.29	0.28	1.8%	3.5%
Stormwater outfalls ^c	2.1	0.032	0.068	0.067	1.3%	0.8%

^a The QUAL2Kw upstream model boundary was located at the upstream end of the Hangman Valley Golf Course, downstream of the mouth of Stevens Creek.

^b We did not monitor Falling Springs. Load estimates assume the same concentrations as the Unnamed drainage off Mullen Hill area, and flows estimated from relative drainage area. The estimates should not be considered very reliable. Appendix E provides details.

^c This includes several stormwater outfalls, all of which discharge to Hangman Creek in the approximate vicinity of the I-90 bridge.

Table 12. Dissolved inorganic nitrogen (DIN) loads for Lower Hangman Creek, June 2018.

Source	Location (km from mouth)	Source flow (cfs)	Load at source (lbs/day)	Load remaining at mouth (lbs/day)	% attenuation	% contribution to total load at mouth
Hangman Ck. at upstream model bdy ^a	24.2	48	640	430	33%	58%
Diffuse groundwater	(distributed)	22	250	230	8.0%	31%
Falling Springs ^b	17.2	0.40 ^b	5.1 ^b	3.9 ^b	23% ^b	0.5% ^b
Unnamed drainage off Mullen Hill area	14.1	0.80	10	8.3	19%	1.1%
Marshall Ck.	7.2	5.4	9.8	9.0	8.4%	1.2%
Upstream spring at Vinegar Flats	4.7	2.6	26	24	4.8%	3.3%
Crystal Springs	4.1	1.4	32	31	4.2%	4.2%
Garden Springs	2.5	0.66	3.6	3.5	2.2%	0.5%
Stormwater outfalls ^c	2.1	0.18	1.2	1.2	1.8%	0.2%

^a The QUAL2Kw upstream model boundary was located at the upstream end of the Hangman Valley Golf Course, downstream of the mouth of Stevens Creek.

^b We did not monitor Falling Springs. Load estimates assume the same concentrations as the Unnamed drainage off Mullen Hill area, and flows estimated from relative drainage area. The estimates should not be considered very reliable. Appendix E provides details.

^c This includes several stormwater outfalls, all of which discharge to Hangman Creek in the approximate vicinity of the I-90 bridge.

Table 13. Dissolved inorganic nitrogen (DIN) loads for Lower Hangman Creek, July-October 2018.

Source	Location (km from mouth)	Source flow (cfs)	Load at source (lbs/day)	Load remaining at mouth (lbs/day)	% attenuation	% contribution to total load at mouth
Hangman Ck. at upstream model bdy ^a	24.2	12	43	3.2	92%	2.5%
Diffuse groundwater	(distributed)	12	130	88	32%	68%
Falling Springs ^b	17.2	0.16 ^b	2.8 ^b	0.50 ^b	82% ^b	0.4% ^b
Unnamed drainage off Mullen Hill area	14.1	0.32	5.6	1.4	74%	1.1%
Marshall Ck.	7.2	1.8	1.6	1.1	33%	0.9%
Upstream spring at Vinegar Flats	4.7	2.1	20	17	16%	13%
Crystal Springs	4.1	0.87	18	16	14%	12%
Garden Springs	2.5	0.43	3.1	2.9	7.5%	2.2%
Stormwater outfalls ^c	2.1	0.032	0.21	0.20	6.0%	0.2%

^a The QUAL2Kw upstream model boundary was located at the upstream end of the Hangman Valley Golf Course, downstream of the mouth of Stevens Creek.

^b We did not monitor Falling Springs. Load estimates assume the same concentrations as the Unnamed drainage off Mullen Hill area, and flows estimated from relative drainage area. The estimates should not be considered very reliable. Appendix E provides details.

^c This includes several stormwater outfalls, all of which discharge to Hangman Creek in the approximate vicinity of the I-90 bridge.

Stormwater loads

Table 14 presents estimated stormwater total phosphorus (TP) loads for 2008-2018. Stormwater discharges to Lower Hangman Creek mostly in the vicinity of the I-90 and Sunset Ave. bridges. Stormwater loads vary greatly between seasons and years, depending heavily on the specific conditions of each precipitation event. Although stormwater TP load contributions are highest during the springtime, they make up a very small fraction of total load, because flows in Hangman Creek are so high during the spring.

During June through October, occasional intense rain events, coinciding with lower background flows in Hangman Creek, mean that stormwater loading can sometimes constitute a significant fraction (>10%) of the total seasonal TP load. During large precipitation events, stormwater can contribute the majority of flow in Hangman Creek, thus also contributing the majority of TP. For example, during October 30-31, 2016, a large precipitation event (1.3 inches of rain) contributed as much as 90 cfs of stormwater flow, as compared to about 70 cfs background flow. At the peak of this event, we estimate that stormwater contributed over 80% of the total TP load to Hangman Creek.

Table 15 presents estimated stormwater total suspended solids (TSS) loads. We present these loads on an annual basis, by water year, for ease of comparison to the *Hangman Multiparameter TMDL* (Joy et al., 2009). Stormwater contributes only a small fraction of total TSS loads in Hangman Creek most years, mainly because of the large nonpoint sediment loads during the springtime.

Table 14. Estimated stormwater total phosphorus (TP) loads to Lower Hangman Creek, 2008-2018.

Year	SW TP load (lbs/day) Mar-May	SW TP load (lbs/day) June	SW TP load (lbs/day) Jul-Oct	SW % of total TP load Mar-May ^a	SW % of total TP load June ^a	SW % of total TP load Jul-Oct ^a
2008	0.137	0.451	0.035	0.01%	1.25%	1.21%
2009	0.439	0.579	0.086	0.03%	4.08%	2.27%
2010	0.367	1.211	0.063	0.76%	1.30%	1.61%
2011	1.018	0.142	0.046	0.06%	0.16%	0.66%
2012	1.109	1.086	0.109	0.06%	1.69%	1.56%
2013	0.132	0.537	0.132	0.07%	6.47%	5.25%
2014	0.664	0.814	0.065	0.05%	13.02%	3.51%
2015	0.332	0.007	0.033	0.24%	0.22%	7.50%
2016	0.700	0.069	0.029	0.19%	1.73%	0.84%
2017	1.635	0.227	0.078	0.04%	1.00%	1.09%
2018	0.448	0.390	0.004	0.07%	1.73%	0.05%
Min	0.132	0.007	0.004	0.01%	0.16%	0.05%
10 %ile	0.133	0.019	0.009	0.01%	0.17%	0.17%
Median	0.448	0.451	0.063	0.06%	1.69%	1.56%
90 %ile	1.529	1.186	0.127	0.65%	11.71%	7.05%
Max	1.635	1.211	0.132	0.76%	13.02%	7.50%

^a Table 19 below presents the total TP loads to which we are comparing stormwater loads here.

Table 15. Estimated stormwater total suspended solids (TSS) loads to Lower Hangman Creek, water years 2009-2018.

Water Year	SW TSS load (tons/year)	SW % of total TSS load ^a
2009	15.4	0.02%
2010	26.7	1.53%
2011	30.3	0.04%
2012	29.2	0.03%
2013	18.4	0.40%
2014	19.2	0.03%
2015	15.5	0.30%
2016	21.8	0.24%
2017	61.3	0.01%
2018	24.2	0.04%
Min	15.4	0.01%
10 %ile	15.5	0.01%
Median	23.0	0.04%
90 %ile	58.2	1.42%
Max	61.3	1.53%

^a Table 18 below presents the total TSS loads to which we are comparing stormwater loads here.

Idaho loads

High-flow period

Tables 16 and 17 present estimated sediment and nutrient cross-boundary loads from Idaho. This includes estimates from data collected during 2009 (Joy, 2008; Ross, 2011), as well as 2018 data collected during this project. 36% of the total watershed area for Hangman Creek is located in Idaho. Five major waterways cross the WA/ID border: Hangman Creek, Little Hangman Creek, upper Rock Creek (sometimes referred to as South Fork, or SF, Rock Creek), Rose Creek, and North Fork (NF) Rock Creek. Moptileme Creek enters Little Hangman Creek just upstream of the WA/ID border; values for Little Hangman Creek include Moptileme Creek.

During the winter-springtime high-flow period, about half of the total streamflow in Hangman Creek originates in Idaho. We calculate that, typically, more than half of the total phosphorus (TP) load, as well as a large majority (over 2/3) of the suspended sediment load, originates in Idaho. The difference between TP and SSC Idaho contributions results from the fact that not all TP is linked to sediment. For example, soluble reactive phosphorus (SRP) may enter stream via nonpoint overland washoff or groundwater. In contrast to phosphorus, less than half of the dissolved inorganic nitrogen (DIN) load originates in Idaho.

Table 16. Estimated total phosphorus (TP) loads from Idaho, high-flow season 2009.

Waterbody	Idaho Drainage Area (mi ²) ^a	TP	TP	Flow	Flow
		(lbs/day) 1/1/09 - 4/30/09 ^b	(lbs/day) 3/1/09 - 5/31/09 ^b	(cfs) 1/1/09 - 4/30/09 ^b	(cfs) 3/1/09 - 5/31/09 ^b
NF Rock Ck.	29.7	97	65	44	44
Rose Ck.	19.9	48	40	23	23
Upper (SF) Rock Ck.	10.2	34	26	14	14
Little Hangman Ck.	61.3	160	150	94	94
Hangman Ck.	126.6	710	280	270	270
Total from Idaho ^c	--	1100	560	440	440
Estimated load or flow at Hangman Ck. mouth	--	1800	1700	820	860
Estimated % from Idaho	--	60%	33%	54%	52%

^a We estimated loads from Idaho for 2009 and 2018 using two slightly different approaches, due to the different sampling locations during each study. The drainage areas shown for 2009 are the areas draining to the state line sampling locations for each stream. These may in fact include areas in Washington, and may not include all areas in Idaho, depending on the vagaries of local topography.

^b The 1/1/2009 – 4/30/2009 period represents peak flow season, including an ice dam breakage event that occurred in early January. The season from 3/1/2009 – 5/31/2009 represents the March-May load allocation season established in the *Spokane DO TMDL* (Moore and Ross, 2010). We estimated 2009 seasonal average loads for each location using multiple-linear regression models based on twice-monthly sample data. See Appendix G for details of the analysis.

^c The total from Idaho is the sum of each of the waterbody loads. The values are rounded to two significant digits, and so may not add up exactly.

Table 17. Estimated sediment, total phosphorus (TP), and nitrogen loads from Idaho, high-flow season 2018.

Waterbody	Idaho Drainage Area (mi ²) ^a	SSC (tons/day)	SSC (tons/day)	TP (lbs/day)	TP (lbs/day)	DIN (lbs/day)	DIN (lbs/day)	Flow (cfs)	Flow (cfs)
		1/18/18 - 4/30/18 ^b	3/1/18 - 5/31/18 ^b	1/18/18 - 4/30/18 ^b	3/1/18 - 5/31/18 ^b	1/18/18 - 4/30/18 ^b	3/1/18 - 5/31/18 ^b	1/18/18 - 4/30/18 ^b	3/1/18 - 5/31/18 ^b
NF Rock Ck.	35.1	19	17	48	35	1500	830	54	37
Rose Ck.	17.4	9.7	8.4	43	36	1100	690	24	18
upper (SF) Rock Ck.	10.1	12	8.9	35	26	580	350	15	11
Little Hangman Ck.	52.9	92	63	200	140	2500	1500	91	66
Hangman Ck.	126.0	75	72	310	250	3900	2400	270	200
Total from Idaho ^c	--	210	170	640	490	9500	5700	450	330
Estimated load or flow at Hangman Ck. mouth	--	300	230	1100	860	22000	15000	940	730
Estimated % from Idaho	--	69%	72%	56%	57%	43%	39%	48%	45%

^a We estimated loads from Idaho for 2009 and 2018 using two slightly different approaches, due to the different sampling locations during each study. The drainage areas for 2018 are the exact areas within Idaho that contribute to each subbasin.

^b The period from 1/18/2018 – 4/30/2018 represents the season of peak flows, starting when we installed flow monitoring equipment throughout the watershed. The season from 3/1/2018 – 5/31/2018 represents the March-May load allocation season established in the *Spokane DO TMDL* (Moore and Ross, 2010). We estimated 2018 seasonal average loads from Idaho by multiplying the load from each cross-boundary subbasin (Upper Hangman, Little Hangman, Upper Rock, Rose, Hoxie Valley-NF Rock, and Mica) by the fraction of that subbasin contained in Idaho. See Figure 9.

^c The total from Idaho is the sum of each of the waterbody loads. The values are rounded to two significant digits, and so may not add up exactly.

Low-flow period

We did not explicitly quantify sediment or nutrient loads from Idaho for the summer low-flow period. Sediment concentrations in the summer are low (Figure 11), with clear water. Because of long travel times and nutrient attenuation, phosphorus and nitrogen loads crossing the state line during the summer do not reach the mouth of Hangman Creek during the low flow period. As discussed in the *Watershed sources of sediment and nutrients* section, nutrient attenuation in Hangman Creek appears to result from algal uptake of nutrients by periphyton. Significant downstream transport of these nutrients does not occur until late fall senescence and sloughing, or possibly even the next springtime high-flow period.

Figure 16 demonstrates this phenomenon using data from the 2017 *Tekoa Receiving Water Study* (Stuart, 2020). The phosphorus load from the Tekoa Wastewater Treatment Plant (WWTP) resulted in elevated concentrations downstream of the outfall. However, algal uptake resulted in TP concentrations returning to their upstream levels within about 4 miles. DIN loads return to their upstream levels even more quickly. Therefore, although nutrient loads originating from Idaho can contribute to water quality impairments locally in Hangman Creek and its tributaries, these loads do not reach the Spokane River during the summer low-flow period.

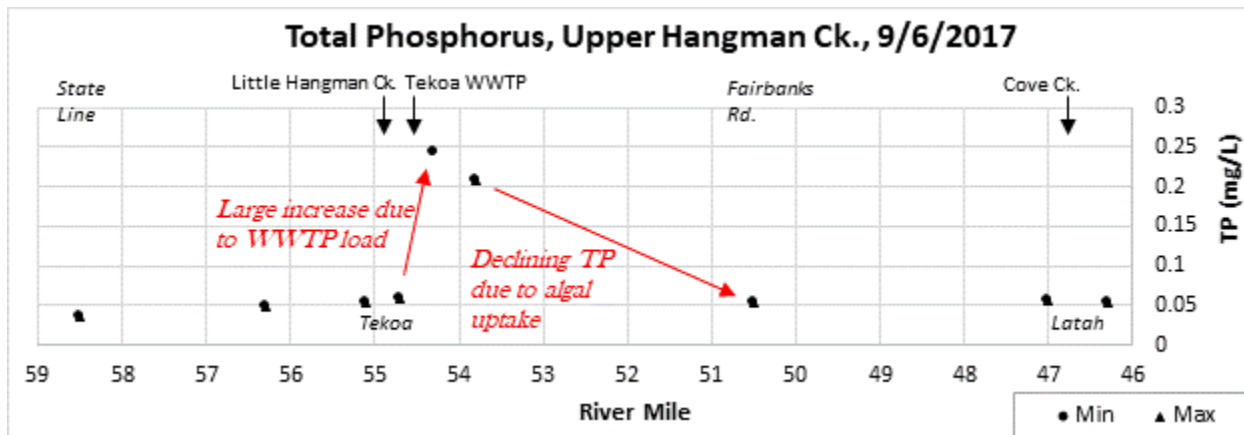


Figure 16. Example from Tekoa WWTP, showing algal nutrient uptake in upper Hangman Ck.

Long-term trends

Similar to Joy et al. (2009), we found a strong declining trend in sediment in Hangman Creek. Figures 17 and 18 present this trend for total suspended solids (TSS) data collected at the mouth of Hangman Creek from 1978 – 2019. To separate any long-term trend component from the strong seasonal effect of flow on sediment concentration, we first developed a nonlinear regression model relating TSS to flow, assuming no long-term trend. We then compared observed TSS values to the values predicted by the model. Appendix D provides the details of this analysis.

The reduction in sediment over the last four decades has been substantial. Flow-normalized sediment concentrations have declined by about 72%. This improvement has occurred during all seasons and flow conditions, with TSS conditions during low flow, medium flow, and high flow all showing similar reduction. This may be the result of improved land management and tillage practices throughout the Hangman Creek watershed.

Present-day (2018) sediment concentrations can still be very high, and human impacts to sediment delivery are substantial (Figure 19). Clearly there is still more work to do. However, these encouraging data results suggest that (1) efforts to improve water quality and reduce erosion in the Hangman watershed have already produced substantial, measurable improvements; and (2) best management practices are effective; their continued adoption can only result in further sediment reductions.

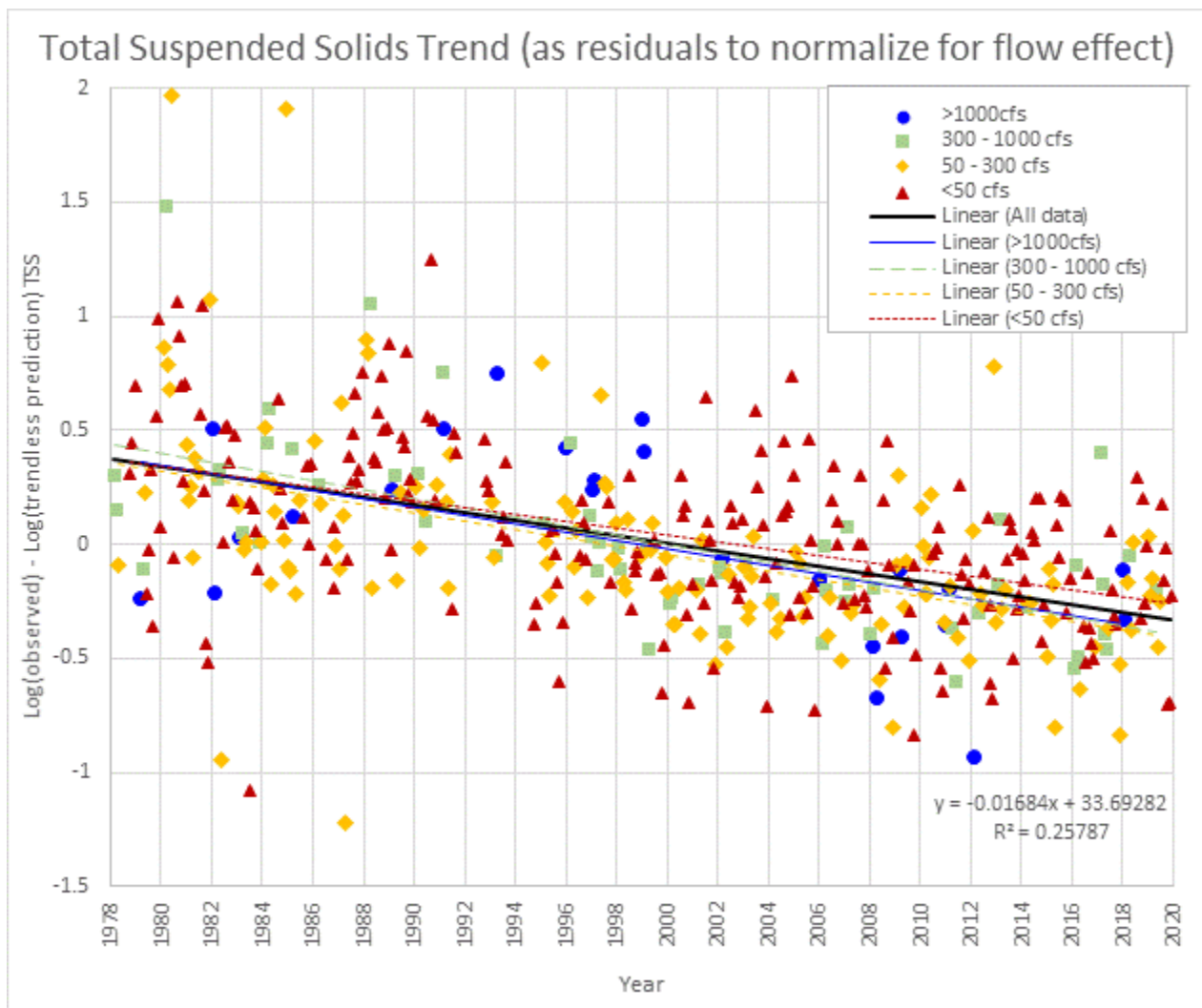


Figure 17. Declining trend in total suspended solids (TSS) at the mouth of Hangman Creek, 1978-2019, normalized for flow.

The units on this graph are the base-10 logarithm of observed TSS concentrations, minus the base-10 logarithm of the initial trendless model predicted concentration. Each unit represents an order of magnitude. For example, a value of 1 means that the observed concentrations were 10 times higher than would be expected based on that day's flow. A value of -1 means that the observed concentrations were 1/10th what would be expected based on flow. A value of 0 means the observed concentrations were exactly what would be expected based on flow.

Note that the initial trendless model prediction used here is **not** the final long-term model that we used for predicting TSS (Appendix D). Rather, this is a method of normalizing for flow conditions, to more clearly visualize the trend.

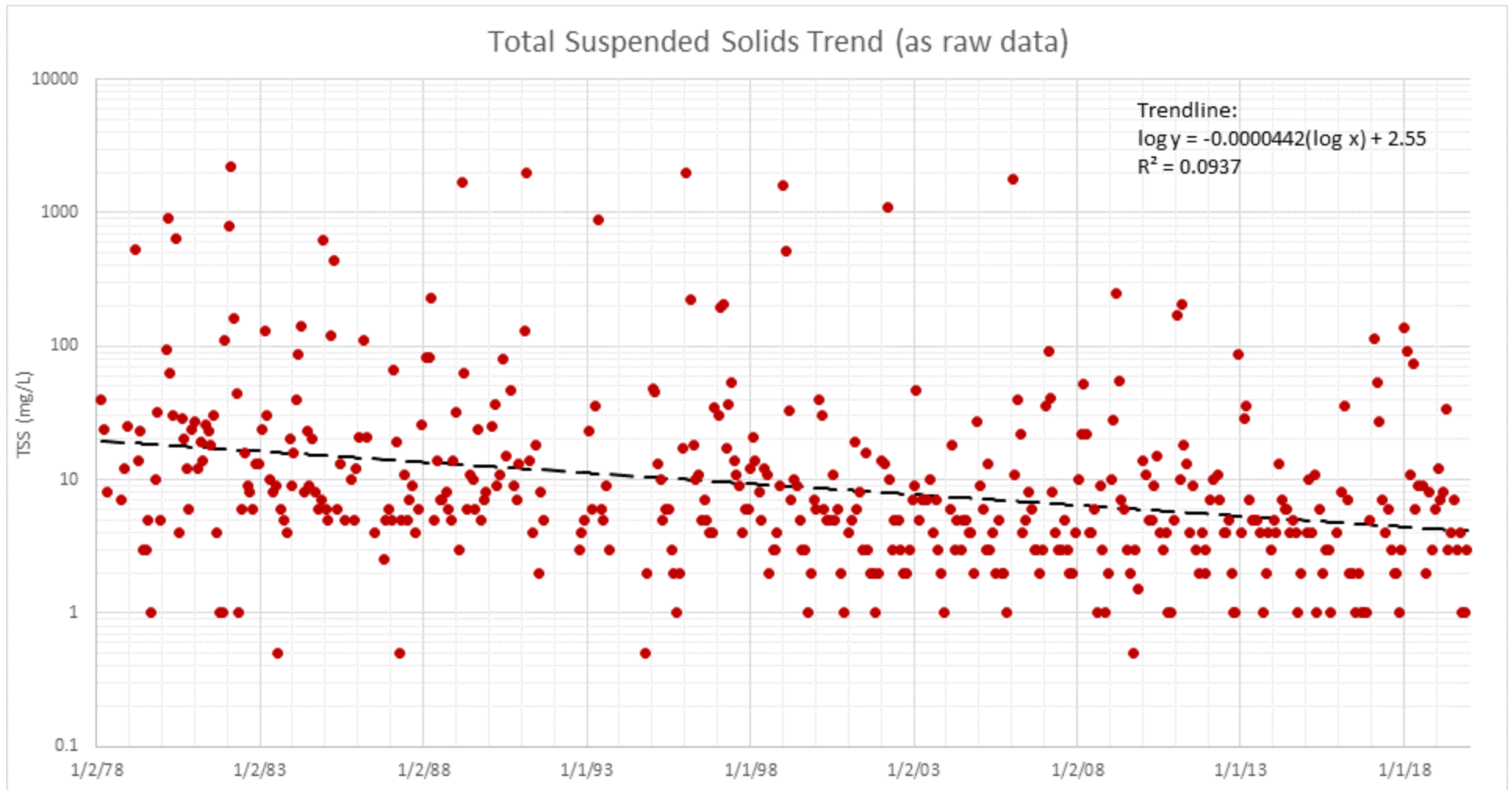


Figure 18. Declining trend in total suspended solids (TSS) at the mouth of Hangman Creek, 1978-2019, as raw data.

Higher values generally occur during late winter and springtime, while low values occur during the summer and fall.



Figure 19. Turbid water from Hangman Creek meeting clear water from the Spokane River, at their confluence.

Photo credit: Cutboard Studios/Spokane Riverkeeper

Compliance with TMDLs and further reductions needed

We evaluated compliance with TMDL limits for sediment and total phosphorus (TP) using the long-term empirical model, which accounts for the relationship between sediment and flow, as well as the observed long-term trend (see Appendix D).

Total Suspended Solids (Hangman Multiparameter TMDL)

The *Hangman Multiparameter TMDL* (Joy et al., 2009) prescribed 20-30% reductions in total suspended solids (TSS) relative to the 1999-2005 time period. The TMDL analysis also provided a set of equations that can be used to evaluate compliance with these load reductions.

Table 18 and Figure 20 compare estimated TSS loads to the load allocations set forth in the Hangman multiparameter TMDL. During the years prior to and during the TMDL evaluation data period (1999-2005), TSS loads in Hangman Creek generally exceeded the load allocations. However, beginning around 2006, TSS loads generally met the load allocations. Since 2006, TSS loads have exceeded the load allocations only once, in 2014.

This result is very much tied to the observed declining TSS trend described above. As noted previously, flow-normalized TSS concentrations since the late 1970s have decreased by almost 75%. Since the early 2000s when the Hangman TMDL dataset was collected, the observed decrease has been about 30-40%. Compared to the 20-30% reductions specified in the TMDL, this has meant that TSS loads in Hangman Creek have complied with the TMDL during recent years.

The *Hangman Multiparameter TMDL* sediment reductions were reasonable based on the available data at the time, and this TMDL contributed to a decade of water quality improvements in the Hangman Creek watershed. Although these modest reductions have now been achieved, it is clear that sediment problems persist. As noted, in 2018 we observed SSC in excess of 1000 mg/L and TP in excess of 1 mg/L at certain times and locations.

Further reductions are clearly needed. We observed TP concentrations greatly in excess of the limits set by the *Spokane DO TMDL*. Therefore, reductions will be driven by the load allocations for TP at the mouth of Hangman Creek established in the *Spokane DO TMDL*, not by the requirements of the *Hangman Multiparameter TMDL*. However, this does not mean that these improvements are only important to the Spokane River and Lake Spokane. The phosphorus reductions needed to comply with the Spokane TMDL will also have a profound positive effect on water quality in Hangman Creek and its tributaries.

Table 18. Evaluation of total suspended solids (TSS) loads relative to Hangman TMDL load allocations.

Water Year ^a	Mean annual flow (cfs)	Estimated TSS load (tons/year) ^b	2009 TMDL Full Protection Model / Load allocation (tons/year) ^c	% Reduction needed to meet TMDL load allocation	Meeting TMDL?
1979	232	719,548	56,278	92%	No
1980	116	10,082	6,835	32%	No
1981	179	107,925	25,624	76%	No
1982	296	681,212	118,551	83%	No
1983	283	101,062	103,865	0%	Yes
1984	361	383,559	216,892	43%	No
1985	195	53,379	33,535	37%	No
1986	220	202,145	48,164	76%	No
1987	97	11,559	3,950	66%	No
1988	58	1,388	848	39%	No
1989	217	314,029	46,488	85%	No
1990	181	85,250	26,475	69%	No
1991	155	56,611	16,453	71%	No
1992	61	5,787	974	83%	No
1993	208	46,679	40,634	13%	No
1994	32	285	136	52%	No
1995	247	71,669	68,707	4%	No
1996	362	2,360,979	220,035	91%	No
1997	629	6,299,276	1,183,738	81%	No
1998	166	7,189	20,538	0%	Yes
1999	315	188,252	143,165	24%	No
2000	273	90,677	92,714	0%	Yes
2001	84	1,604	2,533	0%	Yes
2002	229	73,770	54,357	26%	No
2003	139	16,503	11,838	28%	No
2004	124	30,605	8,413	73%	No
2005	74	2,832	1,708	40%	No
2006	272	54,934	91,960	0%	Yes
2007	192	14,036	32,029	0%	Yes
2008	274	25,139	93,686	0%	Yes
2009	305	71,591	130,078	0%	Yes
2010	108	1,745	5,497	0%	Yes
2011	425	84,924	359,411	0%	Yes
2012	273	84,918	93,096	0%	Yes
2013	172	4,660	22,584	0%	Yes
2014	187	69,020	29,317	58%	No
2015	135	5,119	10,802	0%	Yes
2016	188	9,234	29,767	0%	Yes
2017	526	604,593	687,799	0%	Yes
2018	377	57,740	248,763	0%	Yes
2019	257	46,392	77,462	0%	Yes

Key for Table 18

^a Water years are defined from October-September. For example, water year 2019 is October 1, 2018 through September 30, 2019.

^b We estimated TSS load using the long-term empirical TSS model (see Appendix D). This model has a very low bias over the entire 1978-2019 time period. However, it happens to be biased ~30% low for the 1999-2005 time period considered by the TMDL. For those years, we use the estimates from the TMDL Cohn multiple-regression model (Joy et al., 2009), which was calibrated to that more restricted time period.

^c This model is found in Figure 38 of Joy et al. (2009). It relates TSS load (tons/year) to mean annual flow (cfs) using the equation $y = 0.0035x^{3.0475}$.

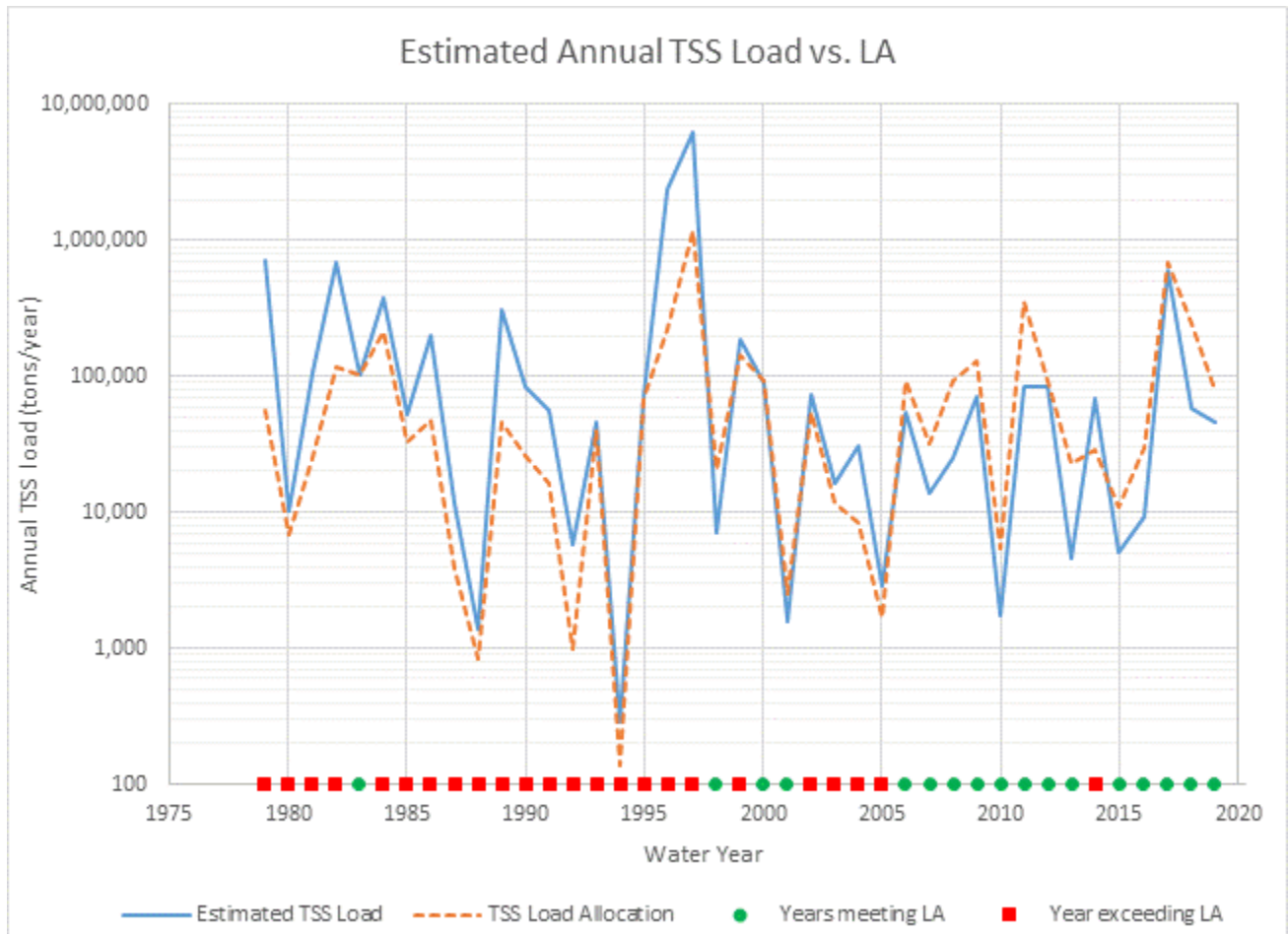


Figure 20. Estimated total suspended solids (TSS) loads compared to TMDL load allocations.

Total Phosphorus (Spokane DO TMDL)

The *Spokane DO TMDL* (Moore and Ross, 2010) set numeric load allocations for total phosphorus (TP) for the mouth of Hangman Creek. The TMDL set allocations in terms of both load and concentration for three seasonal periods: March-May, June, and July-October.

Evaluation of compliance, and reduction scenarios

Table 19 compares estimated TP loads and concentrations to the load allocations set forth in the *Spokane DO TMDL*. Despite the improving trend, TP loads and concentrations have generally not been in compliance with the load allocations. Significant further reductions will be needed to bring Hangman Creek into compliance with the *Spokane DO TMDL*.

We evaluated four scenarios for sediment and phosphorus reduction. These scenarios cover a spectrum of achievability and compliance with the *Spokane DO TMDL*:

- **Best of Today** – This scenario looks at the best-performing “Palouse-type” subbasins, characterized by loess soils and dryland agriculture land use, and reduces sediment and phosphorus contributions from all similar subbasins to that level.
- **California Creek** – This scenario reduces sediment and phosphorus contributions from all subbasins to match those of California Creek, a relatively high-performing subbasin draining a mixture of agricultural, residential, and forestland areas.
- **Meet Concentrations** – This scenario reduces sediment and phosphorus to the degree needed to meet load allocations, expressed as concentrations, during 90% of years.
- **Meet Loads** – This scenario reduces sediment and phosphorus to the degree needed to meet load allocations, expressed as loads, during 90% of years.

Table 20 summarizes the areal load contribution (yield) and percent reductions needed for each scenario and the degree of TMDL compliance each scenario would achieve. After comparing the implications of these scenarios, Ecology water quality managers have selected the “Meet Concentrations” option as the best goal to pursue. The “Best of Today” and “California Creek” scenarios do not fully comply with the *Spokane DO TMDL*, while the “Meet Loads” scenario is likely not achievable.

The *Spokane DO TMDL* set load allocations based on conditions during 2001, a low-flow year. Because load is the product of concentration and flow, and because phosphorus concentrations themselves increase with flow, loads tend to rise exponentially with increasing flow. This means that meeting low-flow loads during higher-flow years presents a mathematical near-impossibility. Meeting concentrations during higher-flow years, while still a challenge, is a more achievable goal.

Table 21 summarizes the phosphorus and sediment load reductions that would be needed from each subbasin for the preferred “Meet Concentrations” scenario.

Table 19. Evaluation of total phosphorus (TP) loads relative to Spokane TMDL load allocations for Hangman Ck.

Estimated loads and concentrations less than or equal to the assigned load allocation value are highlighted in green. Loads and concentrations exceeding the load allocation value are highlighted in red.

Year	Seasonal average flow (cfs) ^a	Seasonal average flow (cfs) ^a	Seasonal average flow (cfs) ^a	Estimated average TP load (lbs/day) ^b	Estimated average TP load (lbs/day) ^b	Estimated average TP load (lbs/day) ^b	Estimated average TP conc (mg/L) ^c	Estimated average TP conc (mg/L) ^c	Estimated average TP conc (mg/L) ^c
	Mar-May	Jun	Jul-Oct	Mar-May	Jun	Jul-Oct	Mar-May	Jun	Jul-Oct
Load Allocation	229 ^d	31 ^d	9 ^d	140.2 ^d	7.5 ^d	1.4 ^d	0.113 ^d	0.044 ^d	0.030 ^d
1978	320.2	44.0	22.5	407.5	27.7		0.236	0.117	
1979	448.8	26.6	9.2	1425.8	14.3		0.589	0.100	
1980	197.9	198.8	11.4	219.3	213.8		0.205	0.199	
1981	247.1	108.0	11.4	238.7	78.1		0.179	0.134	
1982	459.0	39.2	18.8	967.6	22.0		0.391	0.104	
1983	471.9	53.7	30.9	1003.1	31.8		0.394	0.110	
1984	693.9	165.0	34.7	2490.4	123.5		0.665	0.139	
1985	584.9	63.6	19.6	1499.8	37.8		0.475	0.110	
1986	276.4	44.9	17.7	301.3	23.6		0.202	0.098	
1987	164.7	17.9	6.1	172.9	6.3		0.195	0.065	
1988	116.0	29.8	4.5	87.1	13.0		0.139	0.081	
1989	690.7	38.1	11.9	4148.8	17.7		1.114	0.086	
1990	214.6	433.6	11.8	204.5	1380.6		0.177	0.590	
1991	263.6	53.2	8.3	432.6	25.8		0.304	0.090	
1992	53.0	6.2	2.0	27.3	1.3		0.096	0.039	
1993	671.8	32.0	16.8	1493.7	11.6		0.412	0.067	
1994	57.1	13.8	2.5	26.9	3.6		0.087	0.048	
1995	315.5	41.5	18.3	404.5	15.3		0.238	0.069	
1996	553.2	79.8	30.1	1178.3	38.1		0.395	0.089	
1997	884.1	143.5	54.0	2107.0	82.0		0.442	0.106	
1998	247.1	93.3	20.7	193.1	45.6		0.145	0.091	
1999	357.7	56.2	24.0	470.4	20.7		0.244	0.068	
2000	458.8	87.8	22.4	539.5	38.2		0.218	0.081	
2001	229.6	31.3	8.9	158.2	8.7		0.128	0.051	
2002	425.5	46.5	11.8	656.8	14.6		0.286	0.058	
2003	288.6	29.9	7.4	321.6	8.1		0.207	0.050	
2004	191.6	60.7	12.0	157.7	21.0		0.153	0.064	
2005	175.8	43.0	6.8	128.9	12.2		0.136	0.053	
2006	382.6	130.3	14.7	326.4	57.5		0.158	0.082	
2007	286.1	29.7	10.7	217.7	6.8		0.141	0.043	
2008	771.2	99.9	16.6	1116.0	36.0	2.9	0.268	0.067	0.032
2009	860.0	53.6	19.9	1702.7	14.2	3.8	0.367	0.049	0.035
2010	120.9	188.6	17.4	48.4	93.4	3.9	0.074	0.092	0.042
2011	1011.0	191.3	27.7	1821.7	88.6	7.0	0.334	0.086	0.047
2012	753.6	155.4	25.6	1799.3	64.3	7.0	0.443	0.077	0.051
2013	292.4	39.0	15.3	192.1	8.3	2.5	0.122	0.040	0.030
2014	472.3	32.2	12.1	1313.5	6.2	1.9	0.516	0.036	0.028
2015	210.7	18.3	4.7	139.3	3.1	0.4	0.123	0.031	0.018
2016	377.2	23.5	14.7	364.0	4.0	3.4	0.179	0.032	0.043
2017	1155.6	89.9	28.7	3862.8	22.7	7.1	0.620	0.047	0.046
2018	610.3	92.2	29.1	636.7	22.6	7.3	0.193	0.045	0.047
2019	696.2	59.1	25.3	1460.9	12.3	5.6	0.389	0.039	0.041

Key for Table 19

^a As measured by the USGS gage at the mouth of Hangman Creek

^b We estimated Mar-May and June TP loads using the long-term empirical TSS model, along with the translation from TSS to TP. For July-October, when TP and TSS are not as strongly linked, we used a dedicated TP model, which is only valid for data since 2008. See Appendix D.

^c We estimated seasonal average TP concentrations estimated by dividing the load (shown in the middle set of three columns) by the flow (first set of three columns) and applying the appropriate unit conversions.

^d Load allocations set in the *Spokane DO TMDL* (Moore and Ross, 2010), Table 6a.

Table 20. Total phosphorus (TP) reductions and degree of TMDL compliance for four load reduction scenarios.

Scenario	Areal TP load contribution Mar-May 2018 (lbs/day/mi ²)	Scenario TP % Reduction	Scenario TP % Reduction	Scenario TP % Reduction	% of years meeting LA load	% of years meeting LA load	% of years meeting LA load	% of years meeting LA conc.	% of years meeting LA conc.	% of years meeting LA conc.
		Mar-May	Jun	Jul-Oct	Mar-May	Jun	Jul-Oct	Mar-May	Jun	Jul-Oct
Best of Today	1.0	43%	-- ^a	-- ^a	40%	-- ^a	-- ^a	43%	-- ^a	-- ^a
California Creek	0.64	61%	-- ^a	-- ^a	50%	-- ^a	-- ^a	67%	-- ^a	-- ^a
Meet Concentrations (preferred option)	0.36	76%	39%	40%	64%	52%	43%	90%	90%	90%
Meet Loads	0.06	93%	88%	81%	93%	90%	90%	100%	100%	100%

^a The “best of today” and “California Creek” scenarios are based on areal TP load contributions observed during the high-flow study. We did not evaluate what the effect of these reductions would be during June and July-October.

LA = load allocation

Table 21. March-May TMDL season total phosphorus (TP) and suspended sediment (SSC) subbasin percent load reductions for “Meet Concentrations” scenario.

Subbasin Name	TP % reduction	SSC % reduction
Upper Hangman	82%	95%
Little Hangman Creek	86%	98%
Cove Creek	71%	88%
Hangman Tekoa-Latah-Waverly	72%	94%
Rattlers Run Creek	72%	90%
Hangman Creek Canyon	80%	96%
Upper Rock	86%	97%
Rose Creek	83%	94%
Hoxie Valley - NF Rock Creek	64%	94%
Mica Creek	68%	91%
Rock Creek Canyon	80%	97%
Spangle Creek	54%	57%
California Creek	44%	40%
Hangman Valley	79%	95%
Minnie Creek	1%	0%
Marshall Creek	1%	0%
Lower Hangman	* a	* a
Entire Hangman Watershed	76%	95%

^a We were not able to directly quantify nonpoint loads from the Lower Hangman subbasin (see Table 9 and footnotes). Anthropogenic loads to the Lower Hangman subbasin include urban stormwater (see *Stormwater Loads* section above, as well as Appendix F), and likely include urban nonpoint sources as well. Meeting the *Spokane DO TMDL* requirements will mean addressing these urban sources.

Achievability of preferred option, March-May

Ecology selected the “Meet Concentrations” scenario as a goal for phosphorus reductions. This scenario complies with the requirements of the *Spokane DO TMDL* by meeting the TP load allocations for the mouth of Hangman Creek, expressed as concentrations, during 90% of years.⁵ This will require wet-season (March-May) basin-wide phosphorus reductions of 76% relative to present-day (2018) levels. Eliminating 76% of phosphorus loading will mean eliminating 95%, or nearly all, suspended sediment. This is because not all phosphorus is associated with sediment; some phosphorus, such as that contained in groundwater, probably cannot be reduced.

This represents a significant, transformative effort that will qualitatively change Hangman Creek. It will require fundamentally eliminating the high-turbidity “brown plume” events (Figure 19) that the system is known for. Implementation of this goal will require a concerted effort over decades.

Although daunting, there are good reasons to think that this goal is achievable.

First, erosion control efforts thus far have already reduced sediment loads in Hangman Creek by almost 75% since the late 1970s. It appears this improvement has been realized through incremental operational conversion from conventional to conservation tillage practices, such as no-till, mulch till, and direct seeding, among other best management practices (BMPs). Despite the adoption of BMPs among some operators, less protective practices, such as conventional tillage, continue to be used by a significant portion of agricultural operators in the watershed. At present, high sediment concentrations and large loads still occur, and the vast majority of the sediment loading still appears to be anthropogenic. In short, there is still much room for improvement.

Second, recent research suggests that operators can substantially eliminate sediment runoff from fields while continuing the agricultural activities that are vital to the local and regional economy. For example, a paired watershed study in Kamiache and Thorn Creeks near St. John, WA has found a fourfold difference in sediment delivery between watersheds dominated by mulch tillage vs. conventional tillage (Boylan, 2021). Paired-subbasin studies near Pendleton, OR (Williams et al., 2009) and Pullman, WA (Singh et al., 2009) found that no-till farming practices eliminate nearly all field runoff, as compared to conventional tillage practices. The Spokane Conservation District is currently conducting a multi-year, paired-subbasin, no-till study in the Hangman Creek watershed near Spangle, WA (Flanders, 2018), which should verify the local applicability of these findings.

⁵ This analysis is based on hydrologic conditions that occurred from 1978-2019.

Thus, there is good reason to think that, if conservation tillage and complementary BMPs become widespread throughout the Hangman Creek watershed, field runoff could be mostly eliminated. This would leave bank erosion as the dominant erosion mechanism. Analyses of erosion in the Palouse ecoregion have attributed the vast majority of sediment loading to field, rather than bank, erosion (USDA, 1978).

The “Meet Concentrations” scenario requires a mean annual watershed-wide suspended sediment contribution of 0.026 tons/day/mi² (0.015 tons/acre/year). Based on 384 miles of streams in the Hangman Creek watershed with estimated mean annual flow of 1 cfs or greater, we calculated that this is equivalent to a channel erosion rate of 17 tons/mile/year. This compares to estimates of 120 tons/mile/year for moderate to severely eroding channels, 25 tons/mile/year for slightly eroding channels, and 0 tons/mile/year for non-eroding channels in the Palouse watershed during the 1970s (USDA, 1978). This value would need to be lower if some field erosion still persisted. However, this value seems achievable, provided reasonable controls on streambank erosion.

Although this numeric reduction goal is based on the TP load allocation from the *Spokane DO TMDL*, the effect of achieving this goal would not only be to protect the Spokane River and Lake Spokane. The effect would also be to significantly improve overall water quality throughout Hangman Creek and its tributaries. This would provide incalculable benefits to aquatic life, as well as aesthetic value and recreation.

Achievability of preferred option, June-October

We used the QUAL2Kw model to evaluate phosphorus source reductions that would meet the load allocation at the mouth of Hangman Creek for the June and July-October seasons. The phosphorus reduction model scenario meets the load allocation concentrations shown in Table 19, as well as the 39% (June) and 40% (July-October) overall TP reductions shown in Table 20. The model evaluates the effect of headwater, tributary, and groundwater reductions on loads at the mouth of Hangman Creek, while accounting for instream attenuation.

Tables 22 and 23 present this scenario. To achieve the needed phosphorus reductions at the mouth, we generally specified 60% reduction of surface water sources, 20% reduction of groundwater and surface spring sources, and elimination of urban stormwater. For the upstream model boundary, we specified a 60% reduction of soluble reactive phosphorus (SRP), and an 85% reduction of organic/particulate forms of phosphorus. The organic/particulate forms include phosphorus associated with sediment, which can be a large contributor during June.

This scenario demonstrates that significant phosphorus reductions are needed in the summer as well the springtime. However, the source reductions needed to achieve the ~40% overall summertime reduction at the mouth are reasonable and likely achievable.

Table 22. QUAL2Kw total phosphorus (TP) reduction scenario sources summary, June-October 2018.

Source	Location (km from mouth)	Avg TP, June (mg/L) original	Avg TP, July-Oct (mg/L) original	Avg TP, June (mg/L) reduced	Avg TP, July-Oct (mg/L) reduced	Scenario % reduction
Hangman Ck. at upstream model bdy ^a	24.2	0.150	0.0665	0.0583	0.0269	OrgP 85%; SRP 60% ^b
Diffuse groundwater	(distributed)	0.0613	0.0613	0.0491	0.0491	20%
Falling Springs ^c	17.2	0.0698	0.0666	0.0558	0.0533	20%
Unnamed drainage off Mullen Hill area	14.1	0.0698	0.0666	0.0558	0.0533	20%
Marshall Ck.	7.2	0.1314	0.1419	0.0526	0.0567	60%
Upstream spring at Vinegar Flats	4.7	0.0214	0.0274	0.0171	0.0219	20%
Crystal Springs	4.1	0.0848	0.0825	0.0678	0.0660	20%
Garden Springs	2.5	0.1219	0.1247	0.0488	0.0499	60% ^d
Stormwater outfalls ^e	2.1	0.3939	0.3939	0	0	100%

^a The QUAL2Kw upstream model boundary was located at the upstream end of the Hangman Valley Golf Course, downstream of the mouth of Stevens Creek.

^b OrgP, as defined by QUAL2Kw, includes organic and particulate forms of phosphorus. It does not include phosphorus associated with phytoplankton cells. We did not reduce boundary condition phytoplankton for this scenario.

^c We did not monitor Falling Springs. Load estimates assume the same concentrations as the Unnamed drainage off Mullen Hill area, and flows estimated from relative drainage area. The estimates should not be considered very reliable. Appendix E provides details.

^d Although Garden Springs is arguably a surface spring rather than a tributary, this scenario posits a 60% phosphorus reduction similar to other surface water sources. Garden Springs runs as a surface stream for a longer distance than the other springs. It has significantly higher phosphorus levels than the other springs, suggesting nonpoint pollution sources.

^e This includes several stormwater outfalls, all of which discharge to Hangman Creek in the approximate vicinity of the I-90 bridge.

Table 23. QUAL2Kw total phosphorus (TP) reduction scenario, effect at Hangman Creek mouth, June-October 2018.

	June	July-October
Average seasonal flow ^a	82.6 cfs	29.6 cfs
Current conditions TP average seasonal conc. ^a	0.102 mg/L	0.0514 mg/L
Reduction scenario TP average seasonal conc.	0.0431 mg/L	0.0296 mg/L
TMDL load allocation (LA) concentration	0.044 mg/L	0.030 mg/L
Overall % reduction at mouth	57.6%	42.5%

^a These values do not exactly match the values in Table 19. We calculated Table 19 using an empirical model (Appendix D). The values here are QUAL2Kw model predictions (Appendix E).

Conclusions

Results of this 2018 pollutant source assessment study support the following conclusions:

- Sediment and phosphorus are strongly linked in the Hangman Creek watershed. Large quantities of phosphorus are associated with the soil particles constituting the sediment load.
- The vast majority of Hangman Creek's sediment and phosphorus load during the springtime high-flow period originates in the upper (southeast) ~2/3 of the watershed. This is the area that is characterized by loess soils and dryland agriculture.
- Within the upper ~2/3 of the watershed, springtime sediment and phosphorus delivery vary greatly between subbasins. Average March-May sediment delivery in the upper watershed ranges from less than 0.1 tons/mi²/day to over 1 ton/mi²/day. Little Hangman Creek and certain parts of the Rock Creek drainage consistently showed the highest sediment and phosphorus delivery.
- Summertime phosphorus and nitrogen loads at the mouth of Hangman Creek mostly originate in the lower watershed. These loads are mostly associated with groundwater.
- Stormwater outfalls in the city of Spokane contribute less than 1% of overall total phosphorus (TP) load during March-May. However, stormwater typically contributes 1-2% of the overall load, and sometimes as much as 7-13%, during June-October. During individual stormwater flow events, the stormwater outfalls can contribute the majority of the overall TP load, as well as the majority of streamflow in Hangman Creek.
- Sediment concentrations, represented by total suspended solids (TSS), have declined by almost 75% since the late 1970s. This is likely the result of improved tillage and land management practices. However, unacceptably high sediment and phosphorus conditions persist, with suspended sediment concentration (SSC) over 1000 mg/L and TP over 1 mg/L observed at some times and places during 2018. Hangman Creek continues to deliver large quantities of sediment and phosphorus to the Spokane River.
- The wide variability of sediment and phosphorus delivery in different parts of the upper Hangman watershed, as well as the decline in sediment since the 1970s, taken together with other recent science, show the strong sensitivity of the Hangman Creek watershed to agricultural management practices. In a region with highly erodible soils, differences in tillage and other management practices can have a profound effect on erosion and runoff.
- Complying with the load allocation for TP at the mouth of Hangman Creek set by the Spokane DO TMDL will require large reductions in phosphorus and sediment beyond present-day conditions. A 76% TP reduction during March-May, 39% during June, and 40% during July-October will ensure compliance during 90% of years. This will require a transformational change in practices throughout the Hangman Creek watershed. Although daunting, this reduction is likely possible and achievable. In addition to protecting the Spokane River and Lake Spokane, this reduction would greatly improve water quality in Hangman Creek and its tributaries.

Recommendations

Results of this 2018 pollutant source assessment study support the following recommendations.

- Ecology, conservation districts, farm associations, and other stakeholders should continue to promote and encourage the widespread adoption of agricultural best management practices (BMPs) that have been evaluated for their protection of water quality, such as conservation tillage, residue management, and vegetated riparian buffers, among others.
- Ecology and other stakeholders should continue to implement BMPs that have been shown to be effective for mitigating human caused streambank erosion, such as bioengineered bank stabilization techniques, riparian plantings, and BMPs that reduce peak flow runoff, among others.
- Ecology and other stakeholders should also continue to work to reduce other nonpoint sources of nutrients, such as lawn fertilizer, septic tanks, and animal waste.
- Ecology should pursue and maintain close partnerships with the Idaho Department of Environmental Quality, the Coeur d'Alene Tribe, and other stakeholders to address sediment and phosphorus contributions originating in the Idaho portion of the Hangman Creek watershed.
- Agencies and local governments responsible for stormwater outfalls to Lower Hangman Creek in the downtown Spokane area should consider modifications to increase infiltration and reduce direct stormwater discharge to Hangman Creek.
- Ecology's Ambient Monitoring Program should continue long-term monthly sampling of TSS at the mouth of Hangman Creek. Any discussion about parameter changes (for example, adoption of SSC) should focus on the importance of maintaining comparability to the existing long-term record. The continuing long-term TSS record is invaluable for assessing sediment trends.

References

- Albrecht, A., T. Stuart, and M. Redding, 2017. Quality Assurance Project Plan: Hangman Creek Dissolved Oxygen, pH, and Nutrients Pollutant Source Assessment. Department of Ecology, Olympia, WA. Publication 17-03-111.
<https://apps.ecology.wa.gov/publications/SummaryPages/1703111.html>
- American Public Health Association (APHA). 2012. Standard Methods for the Analysis of Water and Wastewater, 23rd ed. Joint publication of the American Public Health Association, American Water Works Association, and Water Environment Federation.
www.standardmethods.org/
- Borchardt, M.A., 1996. Nutrients. Chapter 7 in Stevenson, R.J., Bothwell, M.L., and Lowe, R.L., eds., *Algal Ecology: Freshwater Benthic Ecosystems*. Academic Press, San Diego, CA.
- Bothwell, M., 1985. Phosphorus limitation of lotic periphyton growth rates: An intersite comparison using continuous-flow troughs (Thompson River system, British Columbia). *Limnology and Oceanography* 30:527-542.
- Bowie, G., W. Mills, D. Porcella, C. Campbell, J. Pagenkopf, G. Rupp, K. Johnson, P. Chan, S. Gherini, and C. Chamberlin, 1985. Rates, Constants, and Kinetics Formulations in Surface Water Quality Modeling (2nd Edition). U.S. Environmental Protection Agency, Athens, GA. Prepared by Tetra Tech and Humboldt State University.
- Boylan, R., 2021. Effectiveness Monitoring and the Whitman County VSP Program. Presentation of the Washington Conservation Commission. Palouse Conservation District, Pullman, WA.
- Buchanan, John P. and K. Brown, 2003. Hydrology of the Hangman Creek Watershed (WRIA 56), Washington and Idaho. Project completion report for WRIA 56 Planning Unit. Watershed Planning Grant # G0200292.
- City of Spokane, 2016. Quality Assurance Project Plan: Cochran Basin Dissolved Oxygen TMDL Stormwater Sampling. City of Spokane Wastewater Management. Spokane, WA.
- City of Spokane, 2020. Cochran Basin Dissolved Oxygen TMDL Stormwater Monitoring Report. Draft. City of Spokane Wastewater Management. Spokane, WA.
- Chapra, S.C., 1997. *Surface Water-Quality Modeling*. McGraw-Hill, New York, N.Y.
- Charbonneau, P. and B. Knapp, 1995. PIKAIA. A function optimization subroutine based on a genetic algorithm. Université de Montréal.
www.hao.ucar.edu/modeling/pikaia/pikaia.php
- Cohn, T., L. DeLong, E. Gilroy, R. Hirsch, and D. Wells, 1989. Estimating Constituent Loads. *Water Resources Research*, 25(5):937-942.
- Ecology, 2003. Shade.xls – A tool for estimating shade from riparian vegetation. Washington State Department of Ecology, Olympia, WA.
<https://www.ecology.wa.gov/models>

- Ecology, 2004. Stormwater Management Manual for Eastern Washington. Washington State Department of Ecology, Olympia, WA. Publication 04-10-076.
<https://apps.ecology.wa.gov/publications/SummaryPages/0410076.html>
- Ecology, 2015. TTools toolbar for ArcGIS. Updated and rewritten in Python from Oregon Department of Environmental Quality VBA version. Washington State Department of Ecology, Olympia, WA.
- Flanders, S, 2018. SCD Quality Assurance Project Plan: Edge of Field Monitoring. Spokane Conservation District, Spokane WA.
- Fondriest Environmental, Inc., 2014. Measuring Turbidity, TSS, and Water Clarity. Fundamentals of Environmental Measurements.
<https://www.fondriest.com/environmental-measurements/measurements/measuring-water-quality/turbidity-sensors-meters-and-methods/>
- Galloway, J., D. Evans, W. Green, 2005. Comparability of Suspended-Sediment Concentration and Total Suspended-Solids Data for Two Sites on the L'Anguille River, Arkansas, 2001 to 2003. United States Geological Survey. Scientific Investigations Report 2005-5139.
<https://pubs.usgs.gov/sir/2005/5193/>
- Gray, J., G. Glysson, L. Turcios, and G. Schwartz, 2000. Comparability of Suspended-Sediment Concentration and Total Suspended Solids Data. United States Geological Survey. Water Resources Investigations Report 00-4191.
<https://pubs.er.usgs.gov/publication/wri004191>
- Hill, W., 1996. Effects of Light. Chapter 5 in Stevenson, R.J., Bothwell, M.L., and Lowe, R.L., eds., Algal Ecology: Freshwater Benthic Ecosystems. Academic Press, San Diego, CA.
- Joy, J, 2008. Quality Assurance Project Plan: Hangman Creek Watershed Dissolved Oxygen and pH Total Maximum Daily Load Water Quality Study Design. Washington Department of Ecology, Olympia, WA. Publication 08-03-117.
<https://apps.ecology.wa.gov/publications/summarypages/0803117.html>
- Joy, J., R. Noll, and E. Snouwaert, 2009. Hangman (Latah) Creek Watershed Fecal Coliform, Temperature, and Turbidity Total Maximum Daily Load: Water Quality Improvement Report. Washington Department of Ecology, Olympia, WA. Publication 09-10-030.
<https://apps.ecology.wa.gov/publications/summarypages/0910030.html>
- Lee, C.D., 2005. Fish Distribution within the Latah (Hangman) Creek Drainage, Spokane and Whitman Counties, Washington, 2005. Eastern Washington University Biology Department Thesis Research.
- Mastin, M., 2017. Surface-Water Quality-Assurance Plan for the U.S. Geological Survey Washington Water Science Center. U.S. Geological Survey Open-File Report 2016-1020. Washington, D.C.
<https://pubs.er.usgs.gov/publication/ofr20161020>
- Mathieu, N., 2016. Standard Operating Procedures for the Collection of Periphyton Samples for TMDL Studies, Version 1.1. Washington Department of Ecology, Olympia, WA. SOP Number EAP085.

- McCarthy, S. and N. Mathieu, 2017. Programmatic Quality Assurance Project Plan: Water Quality Impairment Studies. Washington Department of Ecology, Olympia, WA. Publication 17-03-107.
<https://apps.ecology.wa.gov/publications/SummaryPages/1703107.html>
- Monod, J. 1950. La technique de culture continue, théorie et applications. *Annales de l'Institut Pasteur*, Paris, 79:390-410.
- Moore, D. and J. Ross, 2010. Spokane River and Lake Spokane Dissolved Oxygen Total Maximum Daily Load: Water Quality Improvement Report. Washington Department of Ecology, Olympia, WA. Publication 07-10-073.
<https://apps.ecology.wa.gov/publications/SummaryPages/0710073.html>
- Pelletier, G., 2012. rTemp. Response temperature: a simple model of water temperature. Washington State Department of Ecology, Olympia, WA.
<https://www.ecology.wa.gov/models>
- Pelletier, G. and S. Chapra, 2008. QUAL2Kw theory and documentation (version 5.1) A modeling framework for simulating river and stream water quality. Washington State Department of Ecology, Olympia, WA.
- Pelletier, G. S. Chapra, and H. Tao, 2006. QUAL2Kw – A framework for modeling water quality in streams and rivers using a genetic algorithm for calibration. *Environmental Modelling and Software* 21 (2006) 419-425. Publication 05-03-044
<https://apps.ecology.wa.gov/publications/SummaryPages/0503044.html>
- Porter, S.D., T.F. Cuffney, M.E. Gurtz, and M.R. Meador, 1993. Methods for Collecting Algal Samples as Part of the National Water-Quality Assessment Program; U.S. Geological Survey, Open-File Report 93-409, Denver, CO.
- Rantz, S. et al., 1982. Measurement and Computation of Streamflow. U.S. Geological Survey Water Supply Paper 2175. Washington, DC.
<https://pubs.er.usgs.gov/publication/wsp2175>
- Redding, M., 2020. Hangman (Latah) Creek Hydrogeologic Assessment, Focusing on the Latah Creek Wastewater Treatment Plant. Washington Department of Ecology, Olympia, WA. Publication 20-03-013.
<https://apps.ecology.wa.gov/publications/SummaryPages/2003013.html>
- Redfield, A.C., 1958. The biological control of chemical factors in the environment. *American Scientist* 46:205-222.
- Rier, S.T., and R.J. Stevenson, 2006. Response to periphytic algae to gradients in nitrogen and phosphorus mesocosms. *Hydrobiologia* 561:131-147.
- Ross, J., 2011. Hangman Creek Watershed Dissolved Oxygen, pH, and Nutrients Total Maximum Daily Load Study: Data Summary Report. Washington Department of Ecology, Olympia, WA. Publication 11-03-020.
<https://apps.ecology.wa.gov/publications/summaryPages/1103020.html>

- Rusydi, A., 2017. Correlation between conductivity and total dissolved solids in various types of water: a review. *Institute of Physics Conference Series: Earth and Environmental Science* 118:012019.
- Schultz, J., 2020. The effect of turbidity from Hangman Creek on the Spokane River. Spokane Riverkeeper, Spokane WA.
<https://www.spokaneriverkeeper.org/riverjournal/2020/12/8/2020-sediment-report-the-effect-of-turbidity-from-hangman-creek-on-the-spokane-river>
- Singh, P., J. Wu, D. McCool, S. Dun, C. Lin, and J. Morse. Winter hydrologic and erosion processes in the U.S. Palouse region: field experimentation and WEPP simulation. *Vadose Zone Journal* 8(2): 426-436.
- Snouwaert, E. and T. Stuart, 2015. North Fork Palouse River Dissolved Oxygen and pH Total Maximum Daily Load: Water Quality Improvement Report and Implementation Plan. Washington Department of Ecology, Olympia, WA. Publication 15-10-029.
<https://apps.ecology.wa.gov/publications/SummaryPages/1510029.html>
- Spokane Conservation District (SCD), 2005. The Hangman (Latah) Creek Water Resources Management Plan. Public Data File 05-02. Spokane, WA.
- Spokane Conservation District (SCD), 2009. The Hangman (Latah) Creek Soil Sampling Data Summary. Public Data File 09-01. Spokane, WA.
- Spokane Conservation District (SCD), 2010. Little Spokane River Stream Gage Report: Deadman Creek, Dragoon Creek, and the West Branch of the Little Spokane River. Spokane, WA.
- Stuart, T., 2016. Addendum to Quality Assurance Project Plan: Hangman Creek Watershed Dissolved Oxygen and pH Total Maximum Daily Load. Washington Department of Ecology, Olympia, WA. Publication 16-03-106.
<https://apps.ecology.wa.gov/publications/SummaryPages/1603106.html>
- Stuart, T., 2020. Tekoa Wastewater Treatment Plant Dissolved Oxygen, pH, and Nutrients Receiving Water Study. Department of Ecology, Olympia, WA. Publication 20-03-006.
<https://apps.ecology.wa.gov/publications/SummaryPages/2003006.html>
- USDA, 1978. Palouse Co-operative River Basin Study. US Department of Agriculture, Washington, DC. *Conservation*, 64(4), 253–264.
- USGS, 2006. Techniques of Water-Resources Investigations, Book 9, Handbooks for Water Resources Investigations. National Field Manual for the Collection of Water-Quality Data, Chapter A4. Collection Of Water Samples Revised 2006. U.S. Geological Survey, Washington, D.C.
<https://pubs.er.usgs.gov/publication/twri09A4>
- Valiantzas, J., 2006. Simplified versions for the Penman evaporation equation using routine weather data. *Journal of Hydrology*, 331:690-702.
- WAC 173-201A. Water Quality Standards for Surface Waters in the State of Washington. Washington State Department of Ecology, Olympia, WA.
<https://ecology.wa.gov/Water-Shorelines/Water-quality/Water-quality-standards>

- Waite, Richard B., Jr., 1980. About Forty Last-Glacial Lake Missoula Jökulhlaups Through Southern Washington. *Journal of Geology*, 88:653-679.
- Washington State Department of Natural Resources (WDNR), 1998. Geology and Earth Resources Map, Spokane County Water Quality Management Program.
- Washington State Department of Natural Resources (WDNR), 2020. Washington Lidar Portal. Division of Geology and Earth Sciences. Olympia, WA.
<https://lidarportal.dnr.wa.gov/>
- Western Native Trout Initiative, 2018. Western Native Trout Status Report: Redband Trout (*Oncorhynchus mykiss* sub-species).
<http://westernnativetrout.org/redband-trout/>
- Welch, E.B. and J.M. Jacoby, 2004. Pollutant Effects in Freshwater, *Applied Limnology*, Third Edition, Spon Press, New York, NY.
- Williams, J., H. Gollany, M. Siemens, S. Wuest, and D. Long. Comparison of runoff, soil erosion, and winter wheat yields from no-till and inversion tillage production systems in northeastern Oregon. *Journal of Soil and Water Conservation* 64(1): 43-52

Glossary, Acronyms, and Abbreviations

Glossary

Anthropogenic: Human-caused.

Clean Water Act: A federal act passed in 1972 that contains provisions to restore and maintain the quality of the nation's waters. Section 303(d) of the Clean Water Act establishes the TMDL program.

Conductivity: A measure of water's ability to conduct an electrical current. Conductivity is related to the concentration and charge of dissolved ions in water.

Diel: Of, or pertaining to, a 24-hour period.

Dissolved oxygen (DO): A measure of the amount of oxygen dissolved in water.

Effluent: An outflowing of water from a natural body of water or from a man-made structure. For example, the treated outflow from a wastewater treatment plant.

Hyporheic: The area beneath and adjacent to a stream where surface water and groundwater intermix.

National Pollutant Discharge Elimination System (NPDES): National program for issuing, modifying, revoking and reissuing, terminating, monitoring, and enforcing permits, and imposing and enforcing pretreatment requirements under the Clean Water Act. The NPDES program regulates discharges from wastewater treatment plants, large factories, and other facilities that use, process, and discharge water back into lakes, streams, rivers, bays, and oceans.

Nonpoint source: Pollution that enters any waters of the state from any dispersed land-based or water-based activities, including but not limited to atmospheric deposition, surface-water runoff from agricultural lands, urban areas, or forest lands, subsurface or underground sources, or discharges from boats or marine vessels not otherwise regulated under the NPDES program. Generally, any unconfined and diffuse source of contamination. Legally, any source of water pollution that does not meet the legal definition of "point source" in section 502(14) of the Clean Water Act.

Parameter: Water quality constituent being measured (analyte). A physical, chemical, or biological property whose values determine environmental characteristics or behavior.

pH: A measure of the acidity or alkalinity of water. A low pH value (0 to 7) indicates that an acidic condition is present, while a high pH (7 to 14) indicates a basic or alkaline condition. A pH of 7 is considered neutral. Since the pH scale is logarithmic, a water sample with a pH of 8 is ten times more basic than one with a pH of 7.

Point source: Sources of pollution that discharge at a specific location from pipes, outfalls, and conveyance channels to a surface water. Examples of point source discharges include municipal wastewater treatment plants, municipal stormwater systems, industrial waste treatment facilities, and construction sites where more than 5 acres of land have been cleared.

Pollution: Contamination or other alteration of the physical, chemical, or biological properties of any waters of the state. This includes change in temperature, taste, color, turbidity, or odor of the waters. It also includes discharge of any liquid, gaseous, solid, radioactive, or other substance into any waters of the state. This definition assumes that these changes will, or are likely to, create a nuisance or render such waters harmful, detrimental, or injurious to (1) public health, safety, or welfare; (2) domestic, commercial, industrial, agricultural, recreational, or other legitimate beneficial uses; or (3) livestock, wild animals, birds, fish, or other aquatic life.

Riparian: Relating to the banks along a natural course of water.

Salmonid: Fish that belong to the family *Salmonidae*. Species of salmon, trout, or char.

Stormwater: The portion of precipitation that does not naturally percolate into the ground or evaporate but instead runs off roads, pavement, and roofs during rainfall or snow melt. Stormwater can also come from hard or saturated grass surfaces such as lawns, pastures, playfields, and from gravel roads and parking lots.

Surface waters of the state: Lakes, rivers, ponds, streams, inland waters, salt waters, wetlands and all other surface waters and water courses within the jurisdiction of Washington State.

Total Maximum Daily Load (TMDL): Water cleanup plan. A distribution of a substance in a waterbody designed to protect it from not meeting water quality standards. A TMDL is equal to the sum of all of the following: (1) individual wasteload allocations for point sources, (2) the load allocations for nonpoint sources, (3) the contribution of natural sources, and (4) a Margin of Safety to allow for uncertainty in the wasteload determination. A reserve for future growth is also generally provided.

Watershed: A drainage area or basin in which all land and water areas drain or flow toward a central collector, such as a stream, river, or lake at a lower elevation.

303(d) list: Section 303(d) of the federal Clean Water Act requires Washington State to periodically prepare a list of all surface waters in the state for which beneficial uses of the water – such as for drinking, recreation, aquatic habitat, and industrial use – are impaired by pollutants. These are water quality limited estuaries, lakes, and streams that fall short of state surface water quality standards and are not expected to improve within the next two years.

90th percentile: A statistical number obtained from a distribution of a data set, above which 10% of the data exists and below which 90% of the data exists.

Acronyms and Abbreviations

ADCP	acoustic Doppler current profiler
BMP	best management practice
CBOD	carbonaceous biochemical oxygen demand
CV	coefficient of variation
DIN	dissolved inorganic nitrogen
DO	dissolved oxygen
DOC	dissolved organic carbon
Ecology	Washington State Department of Ecology
EIM	Environmental Information Management database

EPA	U.S. Environmental Protection Agency
FMU	Ecology's Environmental Assessment Program, Freshwater Monitoring Unit
GC	golf course
GIS	Geographic Information System software
GPS	global positioning system
HTS	hyporheic transient storage
ID	Idaho
ISS	inorganic suspended solids
LiDAR	Light Detection and Ranging
MAE	mean absolute error
MDL	method detection limit
MEL	Manchester Environmental Laboratory
MQO	measurement quality objective
MLR	multiple linear regression
NAIP	National Agriculture Imagery Program
NF	North Fork
NH4	ammonium nitrogen
NIFC	National Interagency Fire Center
NO2-3	nitrate-nitrite nitrogen
NOAA	National Oceanic and Atmospheric Administration
NPDES	National Pollutant Discharge Elimination System (see glossary)
NWS	National Weather Service
OSS	organic suspended solids
PVC	polyvinyl chloride
QA	quality assurance
QAPP	quality assurance project plan
QC	quality control
RAWS	Remote Automated Weather Station
RL	reporting limit
RM	river mile
RMSE	root mean squared error
RSD	relative standard deviation
SCD	Spokane Conservation District
SF	South Fork
SOP	standard operating procedures
SRP	soluble reactive phosphorus
SSC	suspended sediment concentration
SW	stormwater
TDS	total dissolved solids
TMDL	Total Maximum Daily Load (see glossary)
TN	total nitrogen
TNVSS	total non-volatile suspended solids
TOC	total organic carbon
TP	total phosphorus
TPN	total persulfate nitrogen
TSS	total suspended solids
USDA	U.S. Department of Agriculture

USGS	U.S. Geological Survey
VHG	vertical hydraulic gradient
WA	Washington
WAC	Washington Administrative Code
WDNR	Washington State Department of Natural Resources
WRCC	Western Regional Climate Center
WRIA	Water Resource Inventory Area
WWTP	Wastewater treatment plant (also WTP)
WY	Water Year

Units of Measurement

af	acre-feet
°C	degrees centigrade
cfs	cubic feet per second
cfs/mi ²	cubic feet per second per square mile, a unit of areal flow contribution (yield)
cms	cubic meters per second, a unit of flow
d	days
ft	feet
g	gram, a unit of mass
g/m ²	grams per square meter, a unit of areal biomass
hrs	hours
kg	kilograms, a unit of mass equal to 1,000 grams
km	kilometer, a unit of length equal to 1,000 meters
km ²	square kilometers
lbs/day	pounds per day, a unit of loading
lbs/day/mi ²	pounds per day per square mile, a unit of areal loading (yield)
m	meter
mg	milligram
mg/L	milligrams per liter (parts per million)
mg/m ²	milligrams per square meter, a unit of areal biomass
mi	miles
mi ²	square miles
mm	millimeters
mole	an International System of Units (IS) unit of matter
NTU	nephelometric turbidity units
ppb	parts per billion
s.u.	standard units
tons/day	tons per day, a unit of loading
tons/day/mi ²	tons per day per square mile, a unit of areal loading (yield)
µg/L	micrograms per liter (parts per billion)
µS/cm	microsiemens per centimeter, a unit of conductivity

Appendices

Appendix A. Summary of data not available in EIM

Four categories of data for this study are not available in Ecology’s Environmental Information Management (EIM) database. These data types either represent non-standard parameters, or are spatially oriented data types that are not compatible with the database format. This appendix presents these data.

- Periphyton biomass data collected during 2009 (Joy, 2008)
- Time-of-travel study data collected during 2009 (Joy, 2008)
- Longitudinal depth data collected during 2016 float (Stuart, 2016)
- Continuous gaged streamflow data collected during 2018 (Albrecht et al., 2017)

2009 Periphyton biomass data

Table A-1. Periphyton biomass data collected during 2009.

Location ID	Sampling Location	Chlorophyll a biomass (mg/m ²) June 22, 2009	Ash-free dry weight biomass (g/m ²) June 22, 2009	Chlorophyll a biomass (mg/m ²) July 27, 2009	Ash-free dry weight biomass (g/m ²) July 27, 2009
56HAN-57.7 ^a	Hangman Ck. at State Line	26.3	11.1	47.2	17.7
56HAN-54.3	Hangman Ck. below Tekoa	53.4	8.46	145	25.7
56HAN-41.2 ^b	Hangman Ck. at Roberts Rd.	77.4	14.0	106	21.6
56HAN-32.8	Hangman Ck. at Bradshaw Rd.	44.1	10.1	55.1	12.3
56ROC-15.4 ^b	Rock Ck. blw N fk. Confluence	68.6	12.5	125	13.2
56ROC-08.9 ^b	Rock Ck. at Jackson Rd.	195	38.0	100	11.2
56HAN-19.1 ^b	Hangman Ck. at Duncan	28.8	7.74	16.3	6.18
56HAN-00.7	Hangman Ck. at Mouth	53.2	6.76	91.6	11.0

^a This is located about 0.8 miles downstream of the 56HAN-58.5 state line site that we used during 2017.

^b Site not included in this field project. See Ross (2011) for location details.

2009 Time-of-travel data

Table A-2. Time-of-travel dye study data collected during 2009.

Upstream location	Downstream location	Reach length (mi)	Upstream date/time ^a	Downstream date/time ^b	Travel time (hrs)	Avg velocity (ft/s)
56HAN-31.1	56HAN-29.3	1.80	6/16/2009 11:35	6/16/2009 17:30	5.92	0.45
56HAN-20.2	56HAN-19.1	1.06	6/16/2009 15:15	6/17/2009 4:30	13.25	0.12
56HAN-14.5	56HAN-13.2	1.18	6/16/2009 14:40	6/16/2009 23:30	8.83	0.20
56HAN-06.2	56HAN-04.6	1.68	6/15/2009 17:22	6/16/2009 0:00	6.63	0.37
56HAN-04.6	56HAN-01.9	2.67	6/16/2009 0:00	6/16/2009 7:30	7.70	0.52
56HAN-47.0	56HAN-46.3	0.68	7/15/2009 10:22	7/15/2009 16:00	5.63	0.18
56HAN-14.5	56HAN-13.2	1.18	7/15/2009 9:00	7/16/2009 1:00	16.00	0.11
56HAN-06.2	56HAN-04.6	1.68	7/14/2009 9:14	7/14/2009 21:15	12.02	0.20
56HAN-03.6	56HAN-01.9	1.80	7/14/2009 9:49	7/14/2009 16:30	6.68	0.40

^a This is either the time of dye injection, or the time when we detected peak dye concentration at the upstream location.

^b This is the time when we detected peak dye concentration at the downstream location.

2016 Longitudinal depth float data

Note: Longitudinal depth float data are presented here in map and chart format. The continuous data records are too large to include in the report. Ecology will provide the dataset upon request.

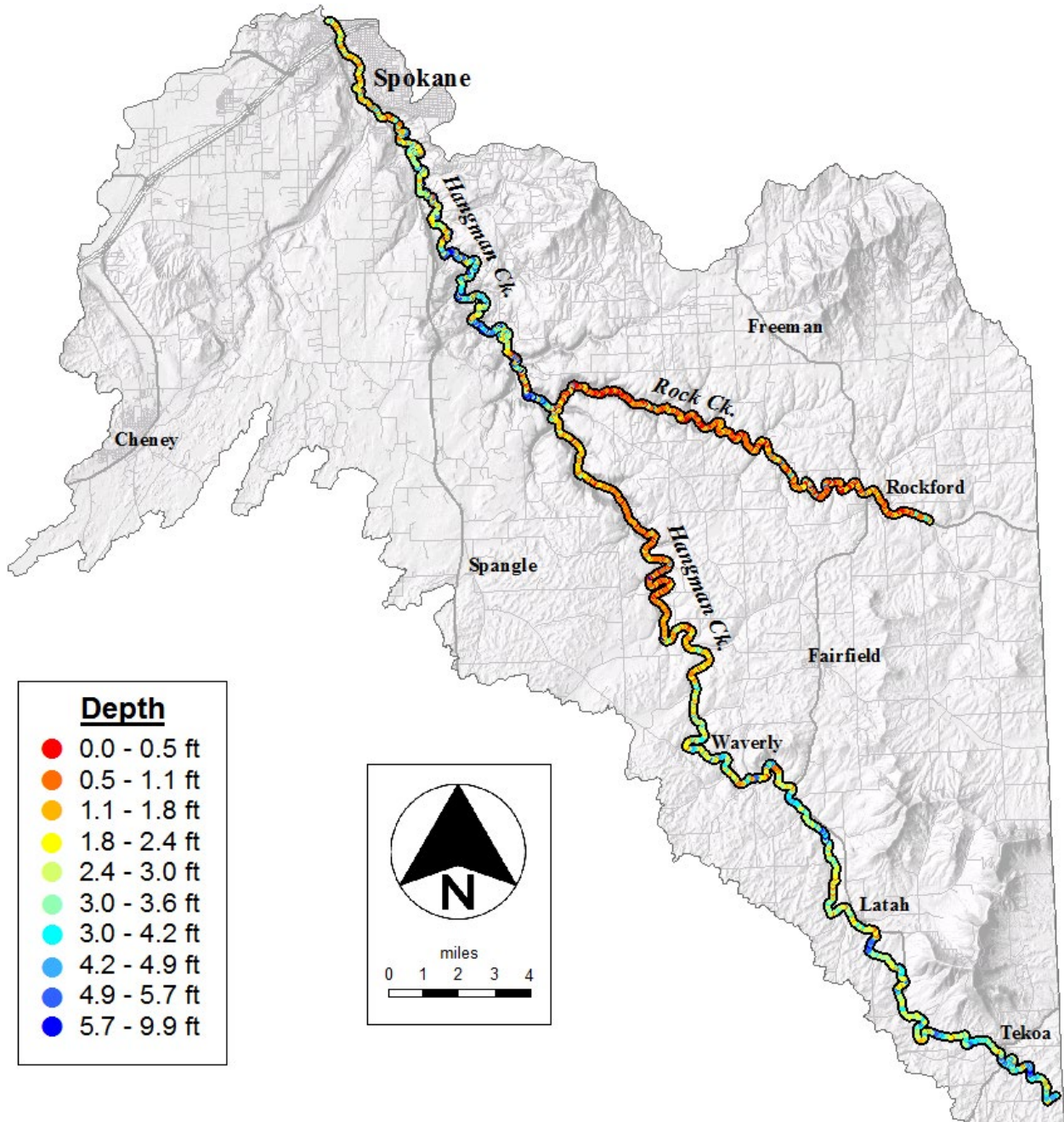


Figure A-1. Map of channel depths measured in Hangman and Rock Creeks, April 2016.

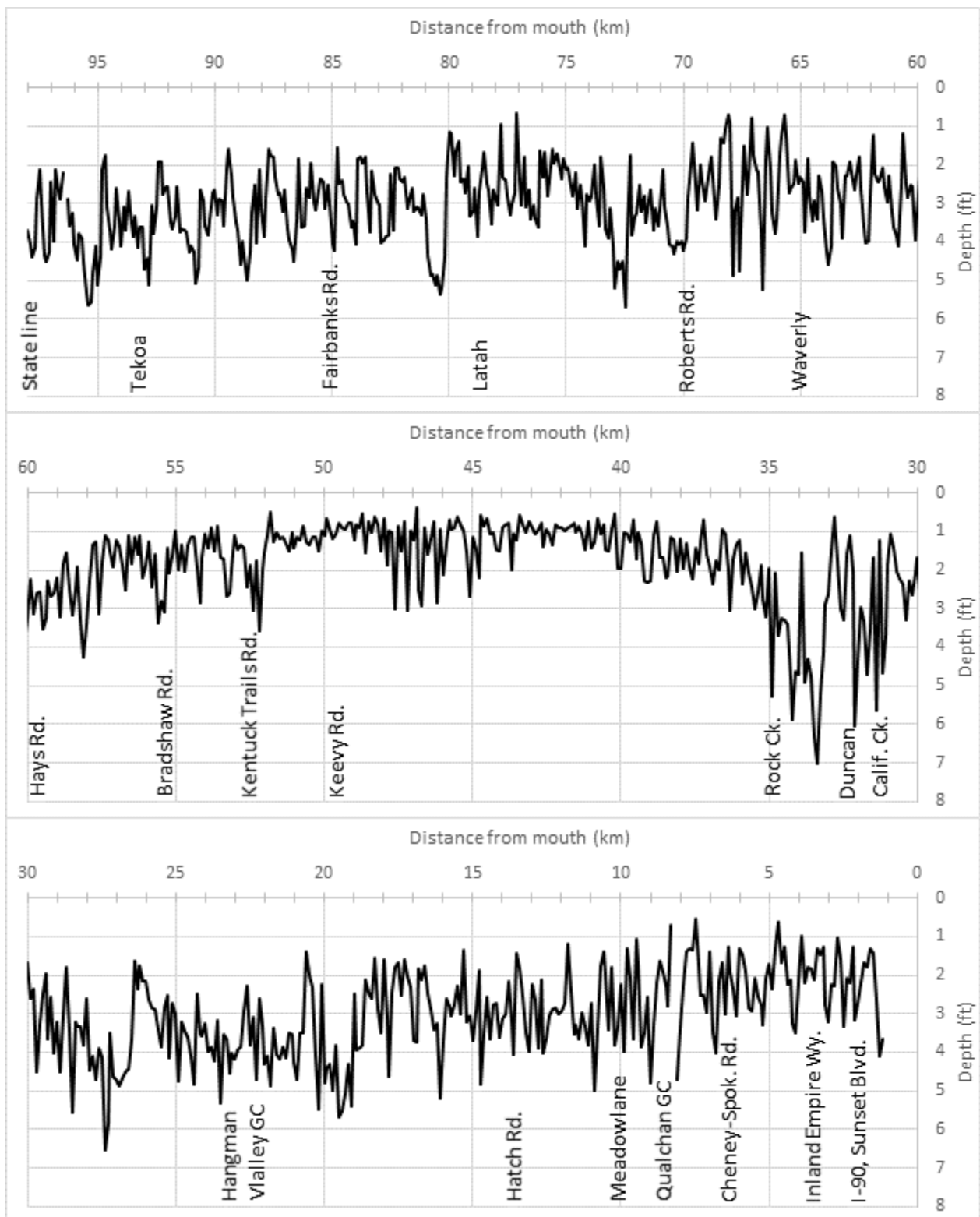


Figure A-2. Longitudinal depths measured in Hangman Creek, April 2016.

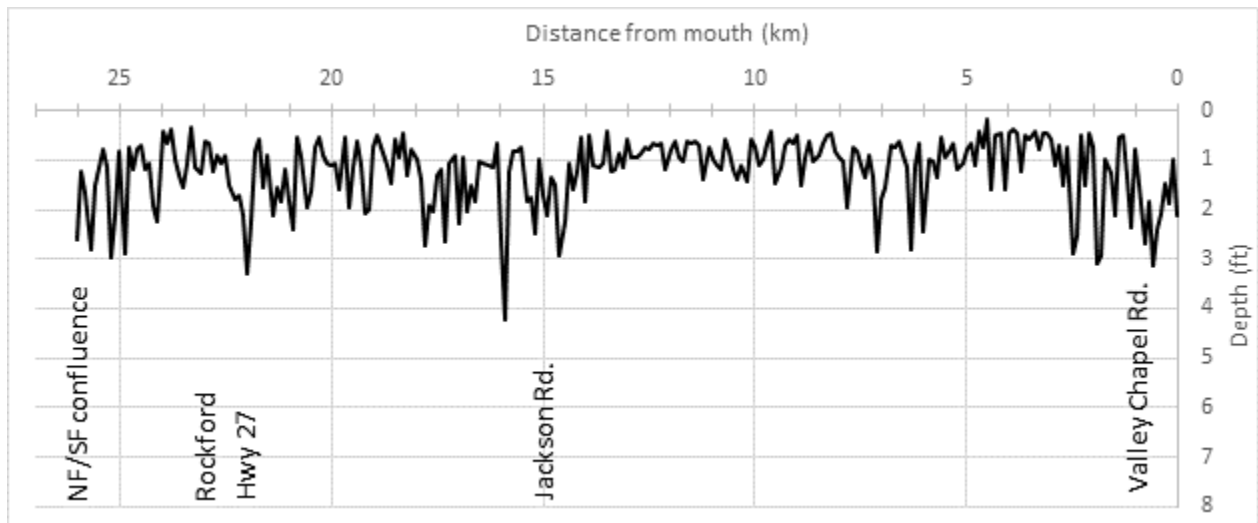
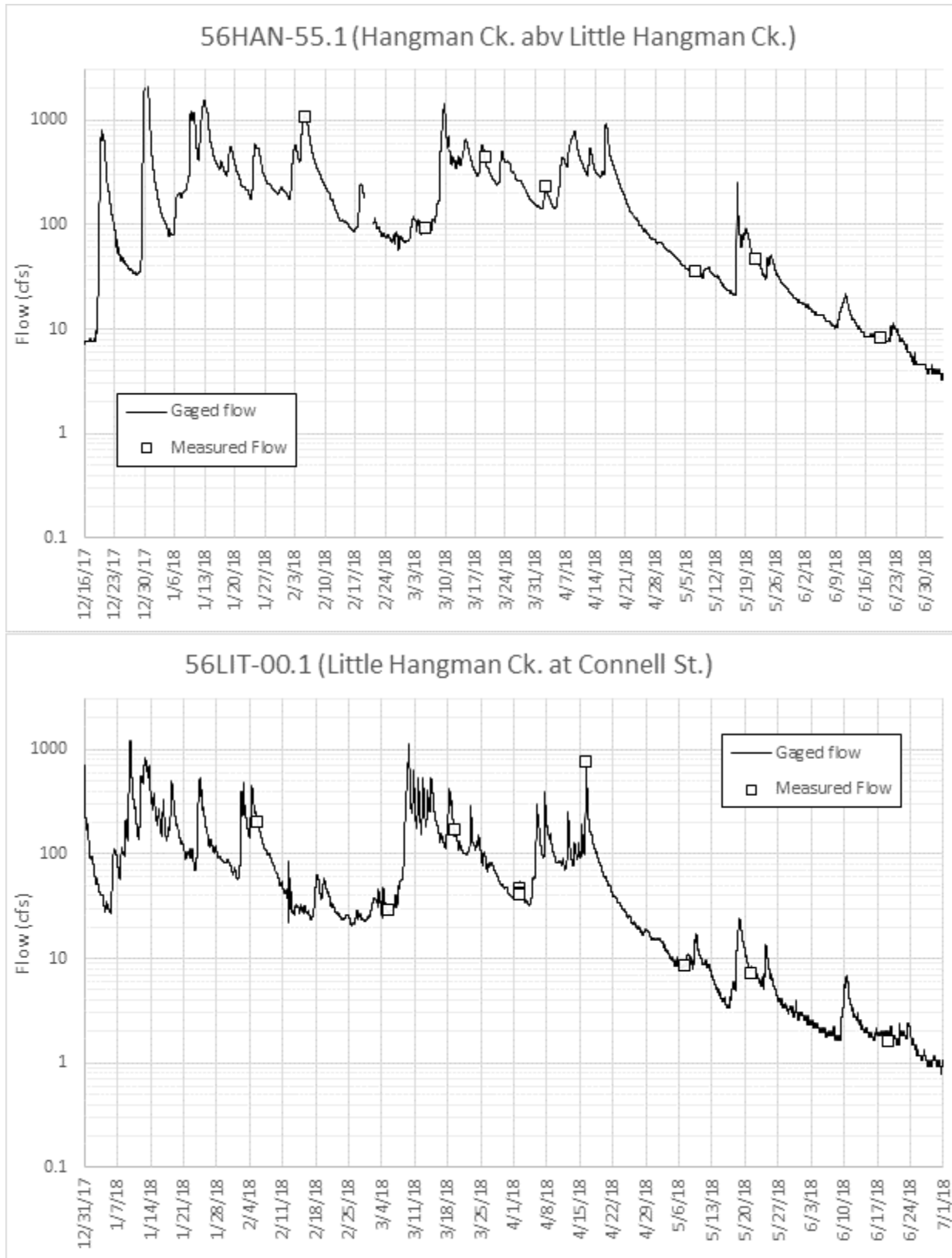


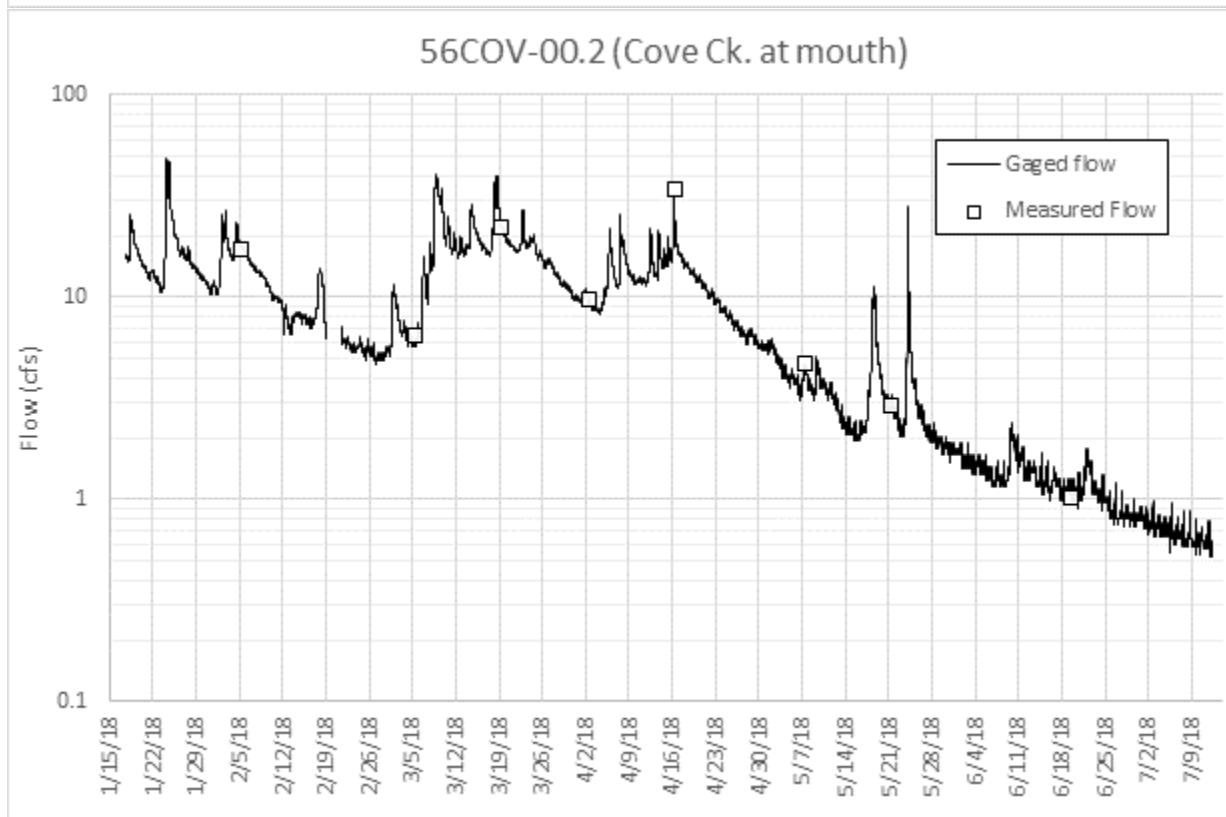
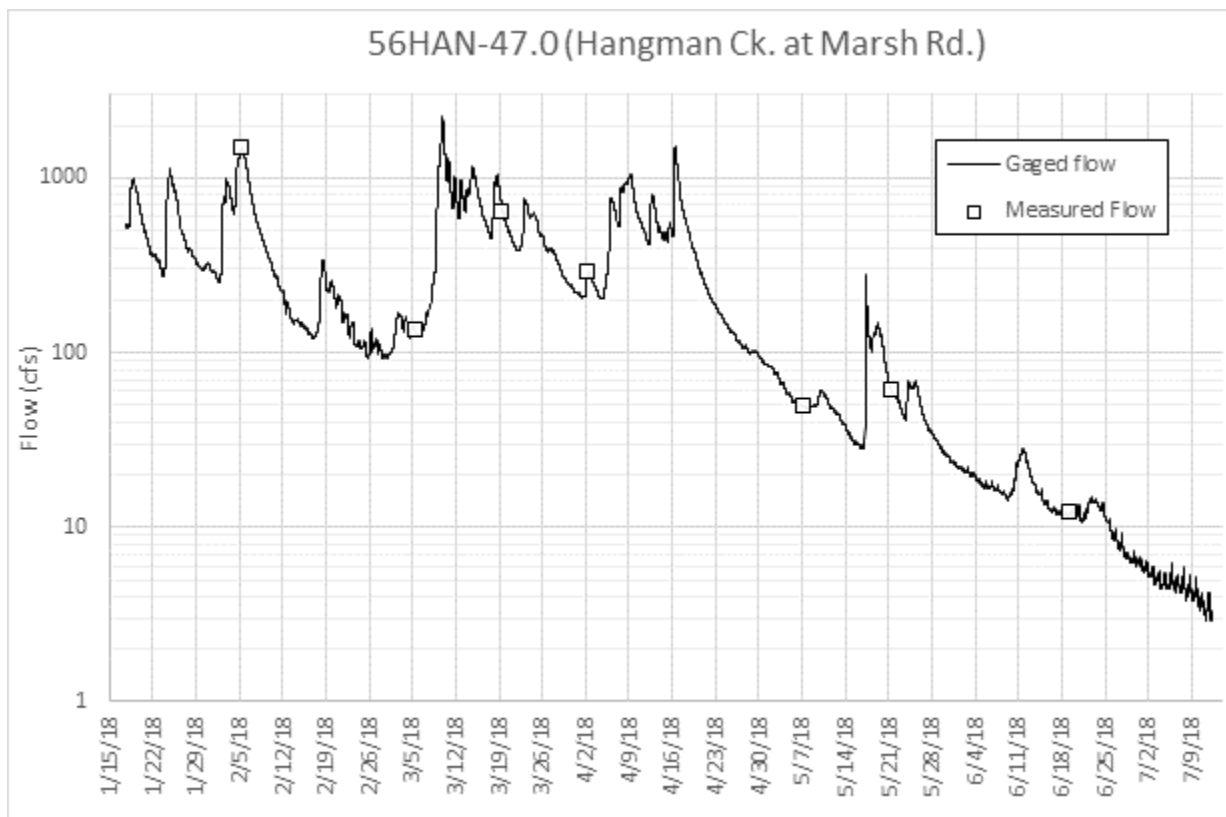
Figure A-3. Longitudinal depths measured in Rock Creek, April 2016.

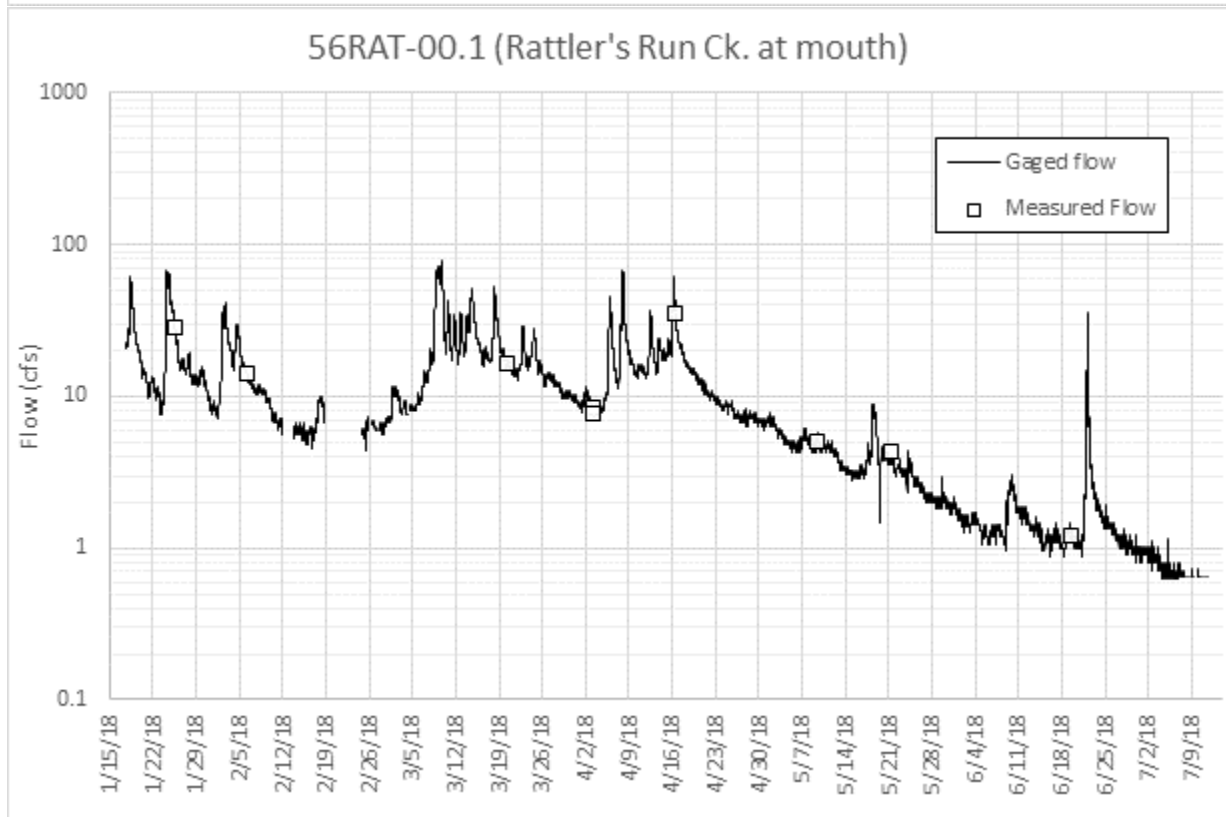
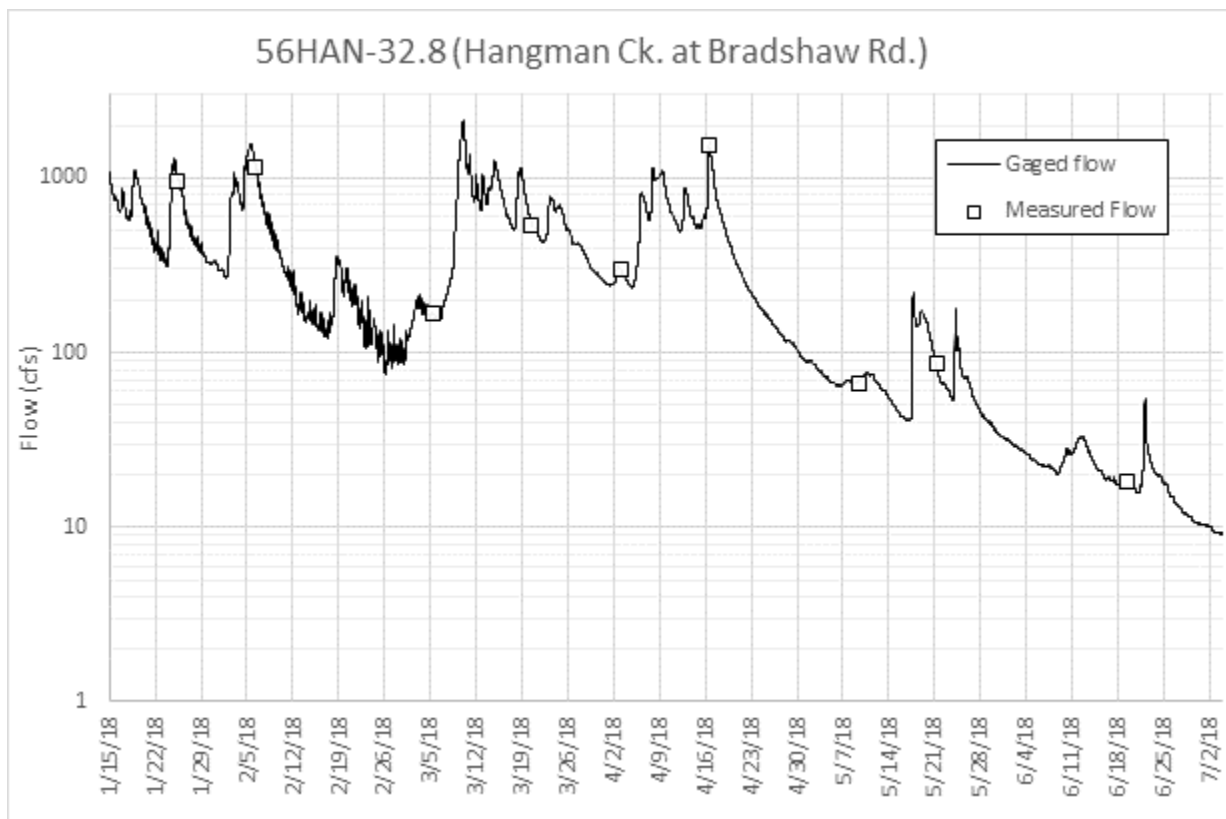
2018 Continuous gaged streamflow data

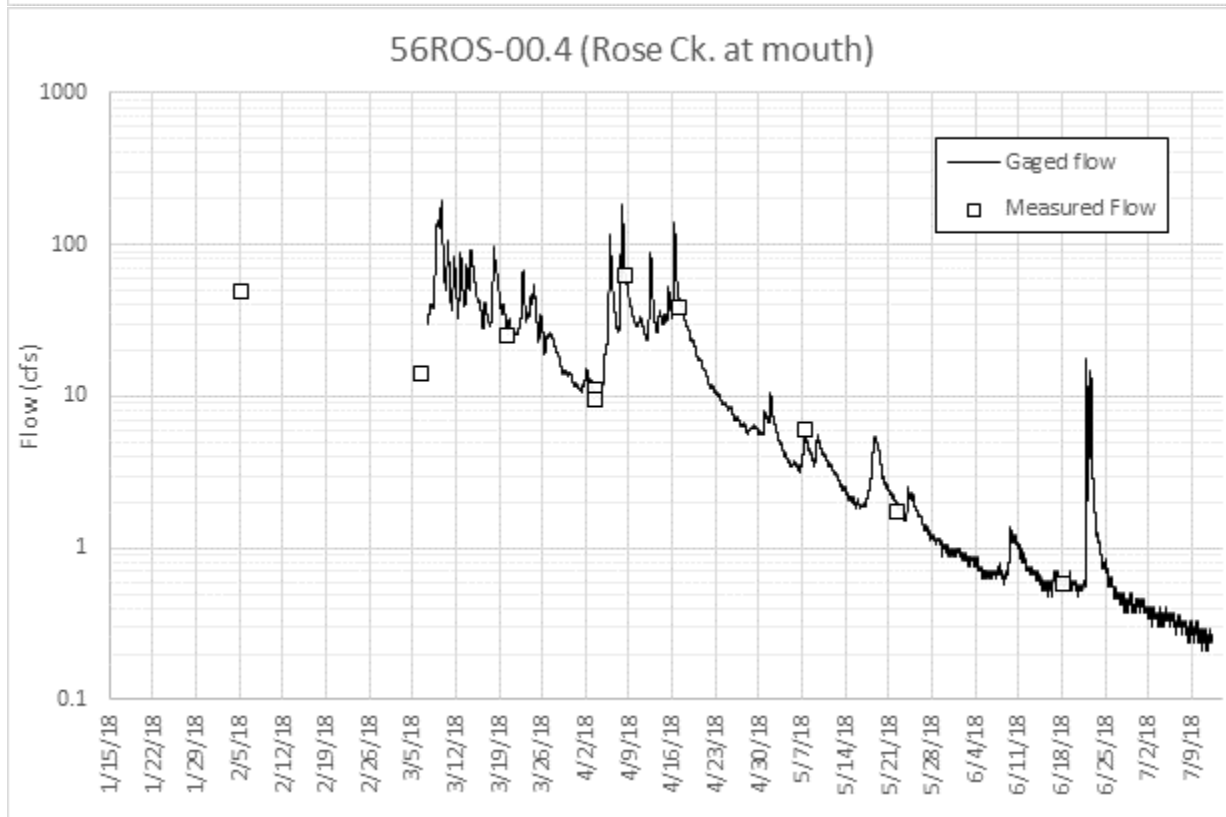
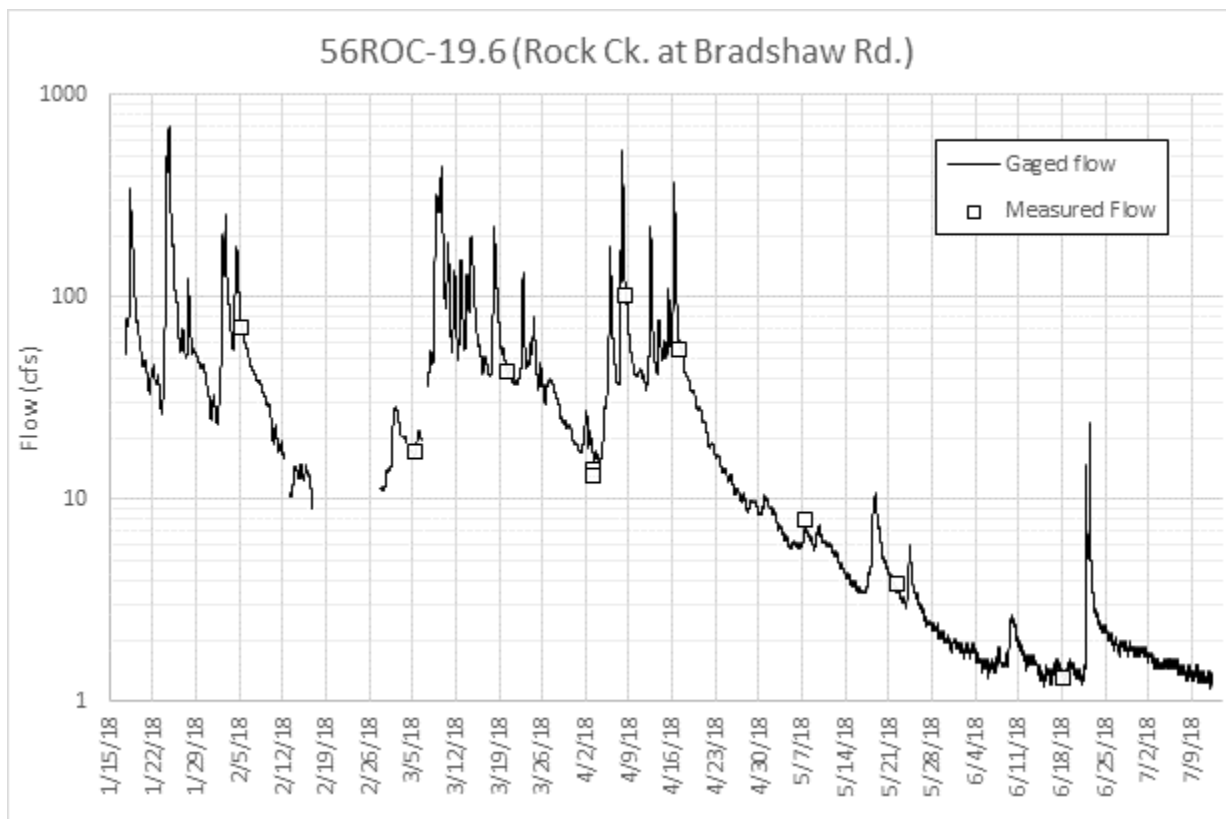
Continuous gaged streamflow data are presented here in chart format. The continuous data records are too large to include in the report. Ecology will provide the dataset upon request.

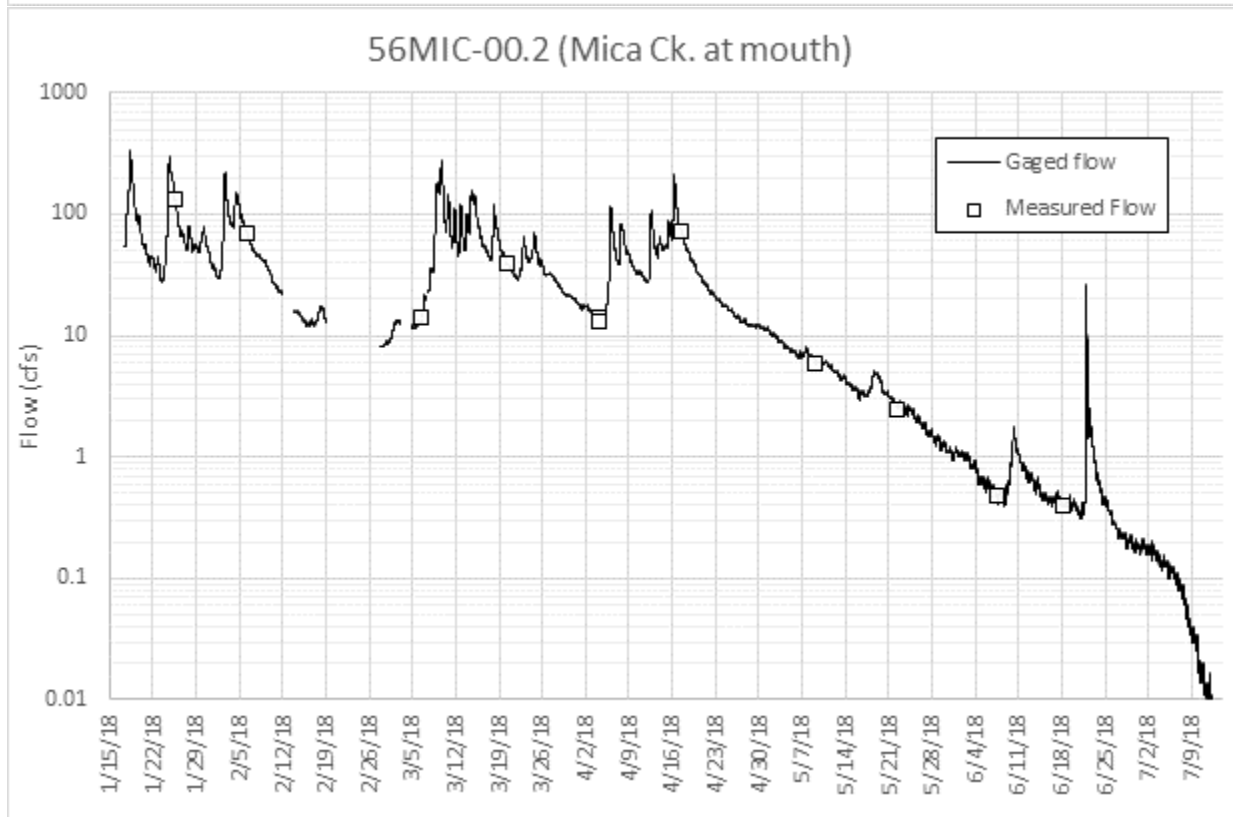
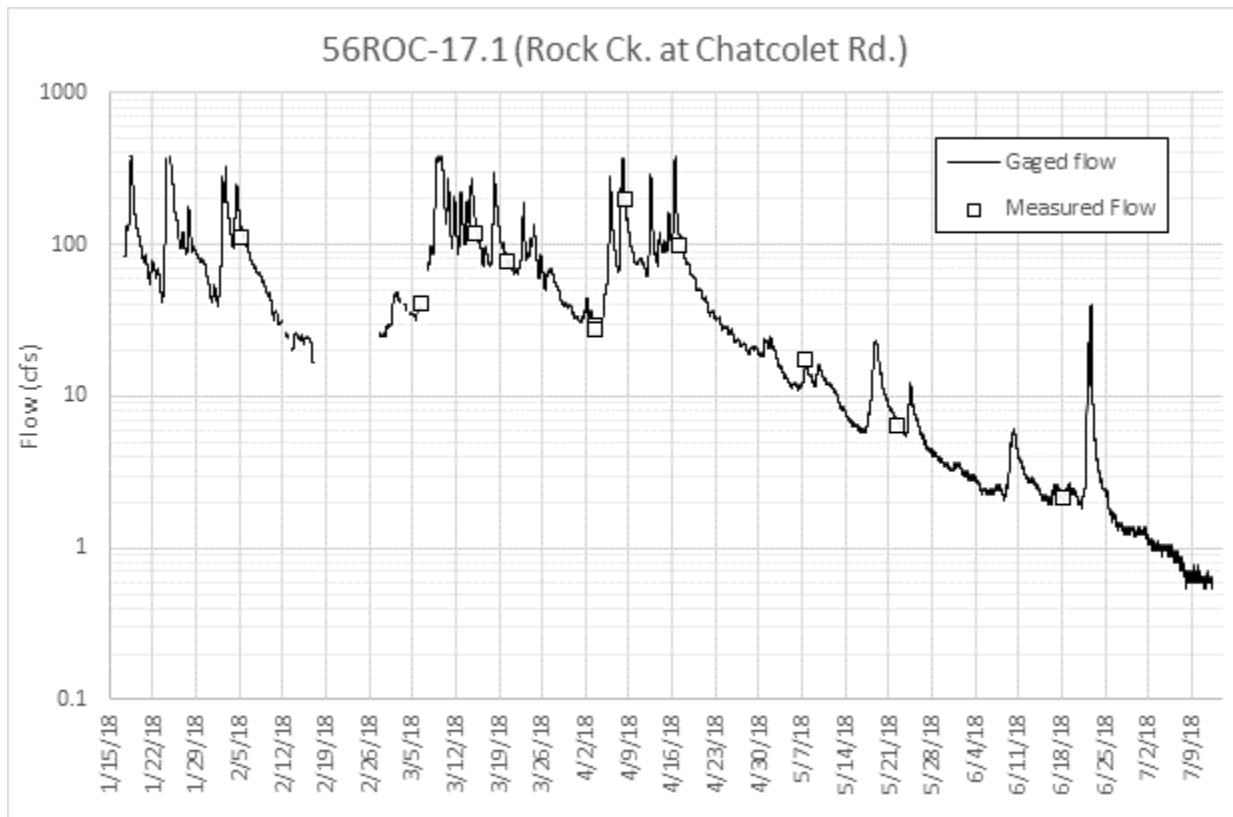
Figure A-4 (next 11 pages). Continuous gaged streamflow data collected during 2018.

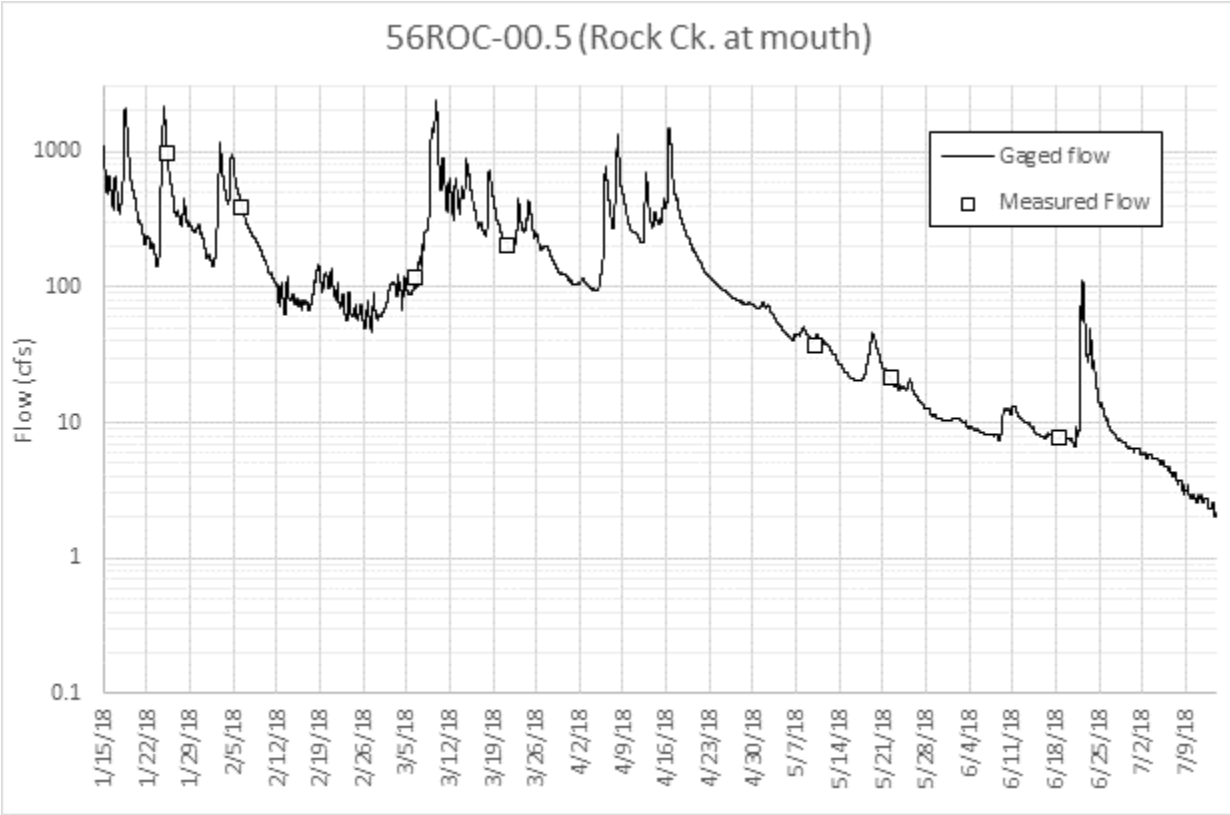
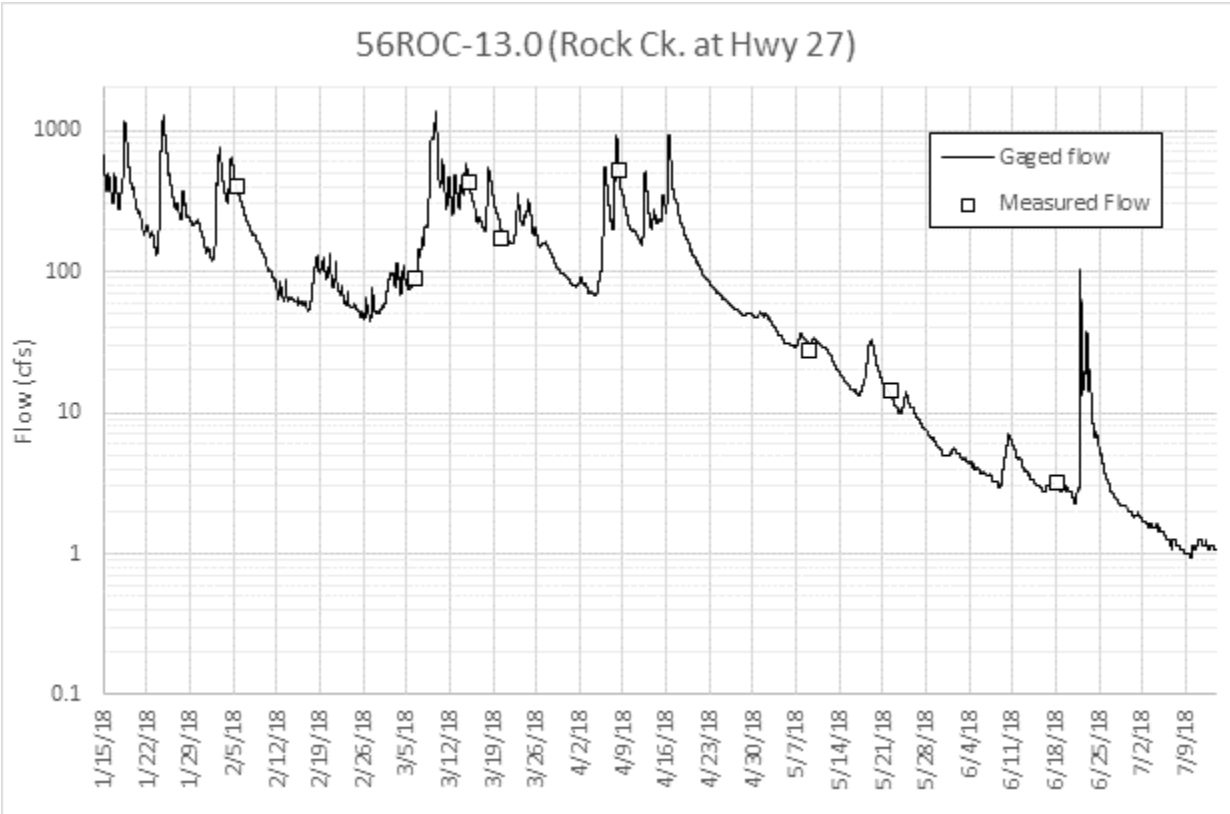


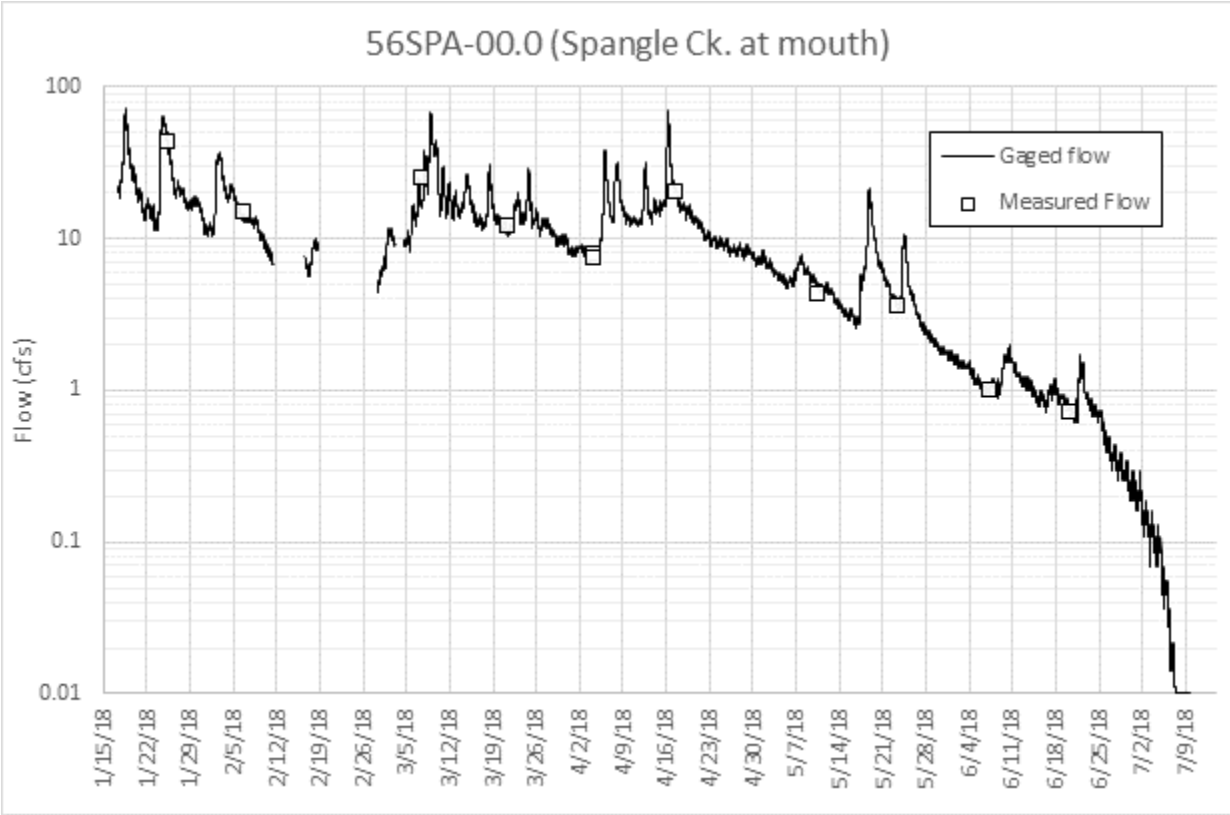
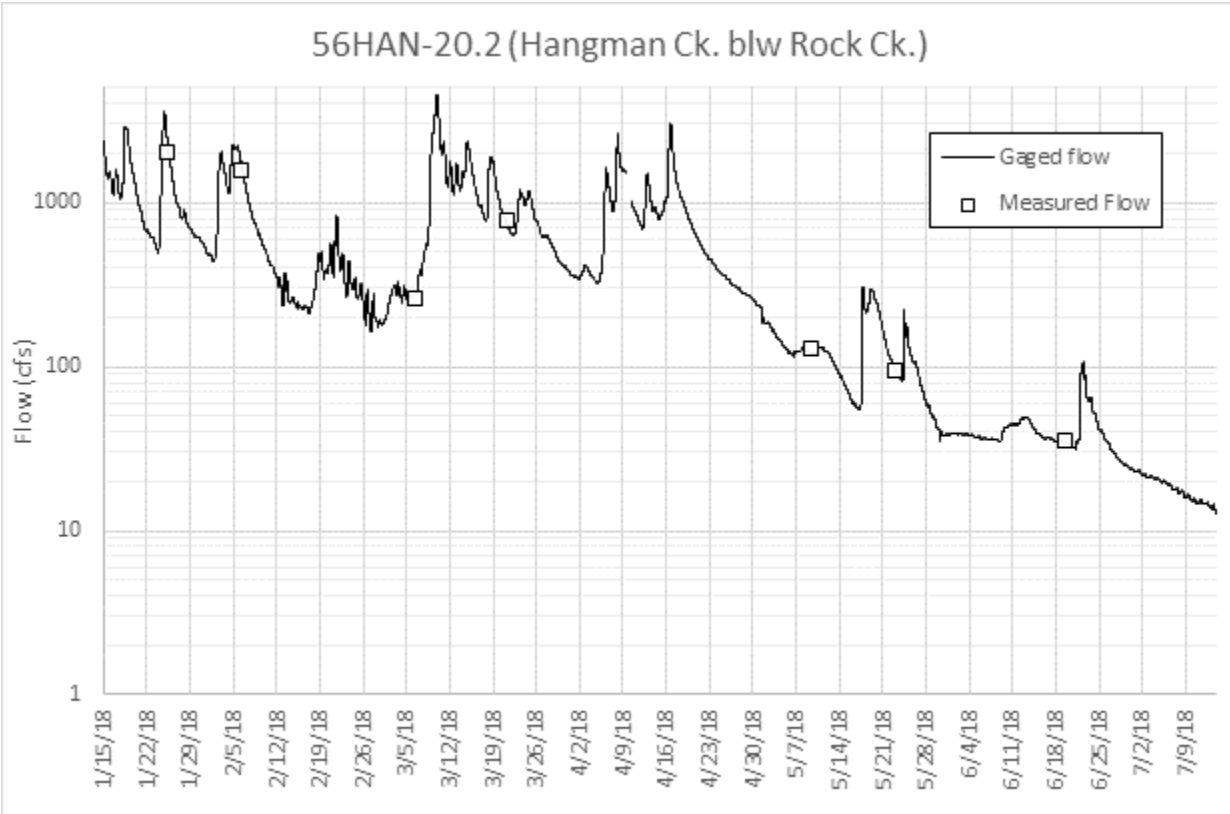


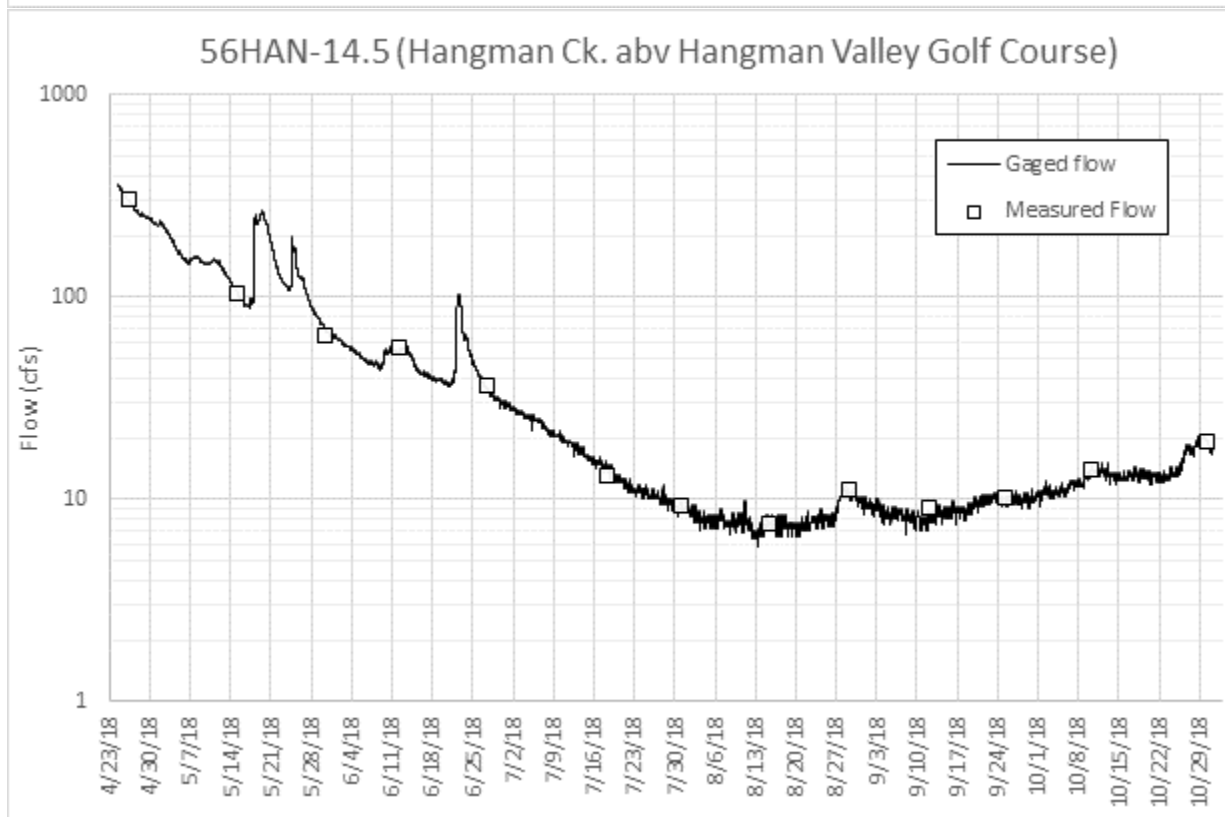
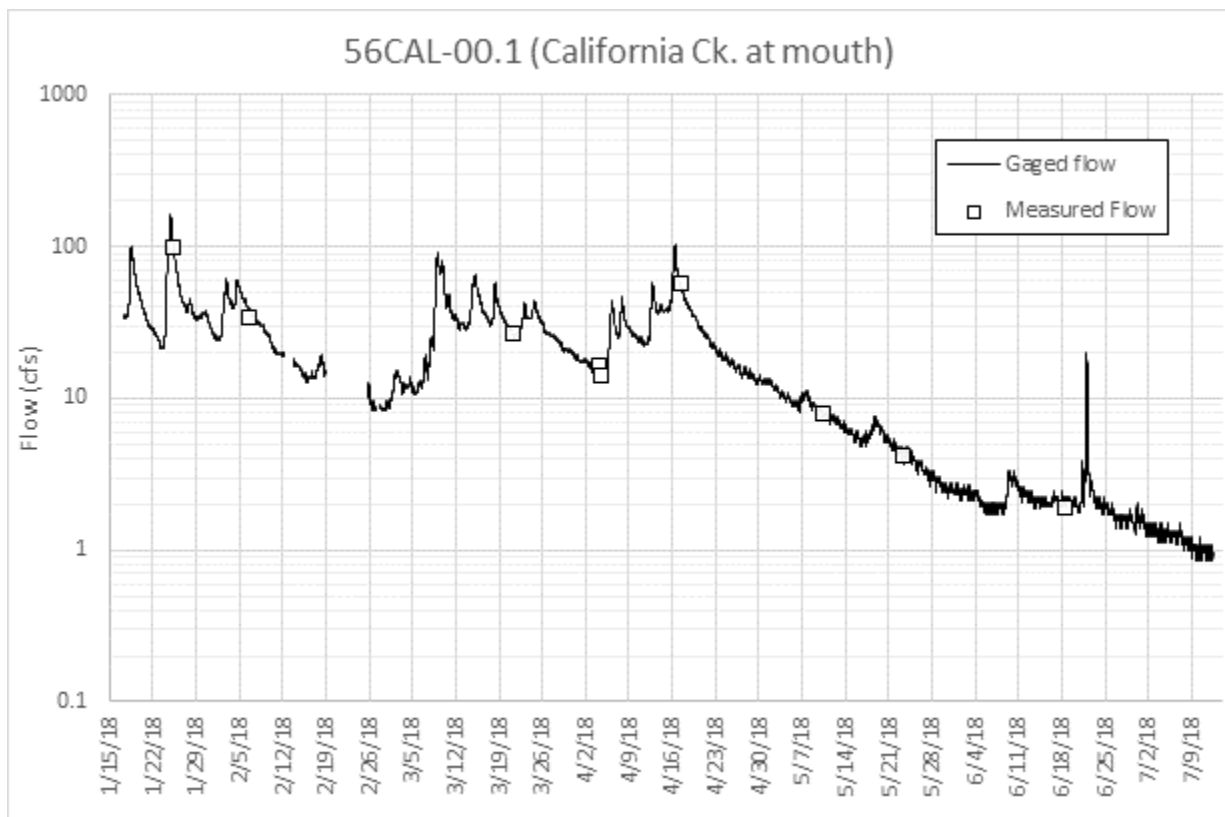


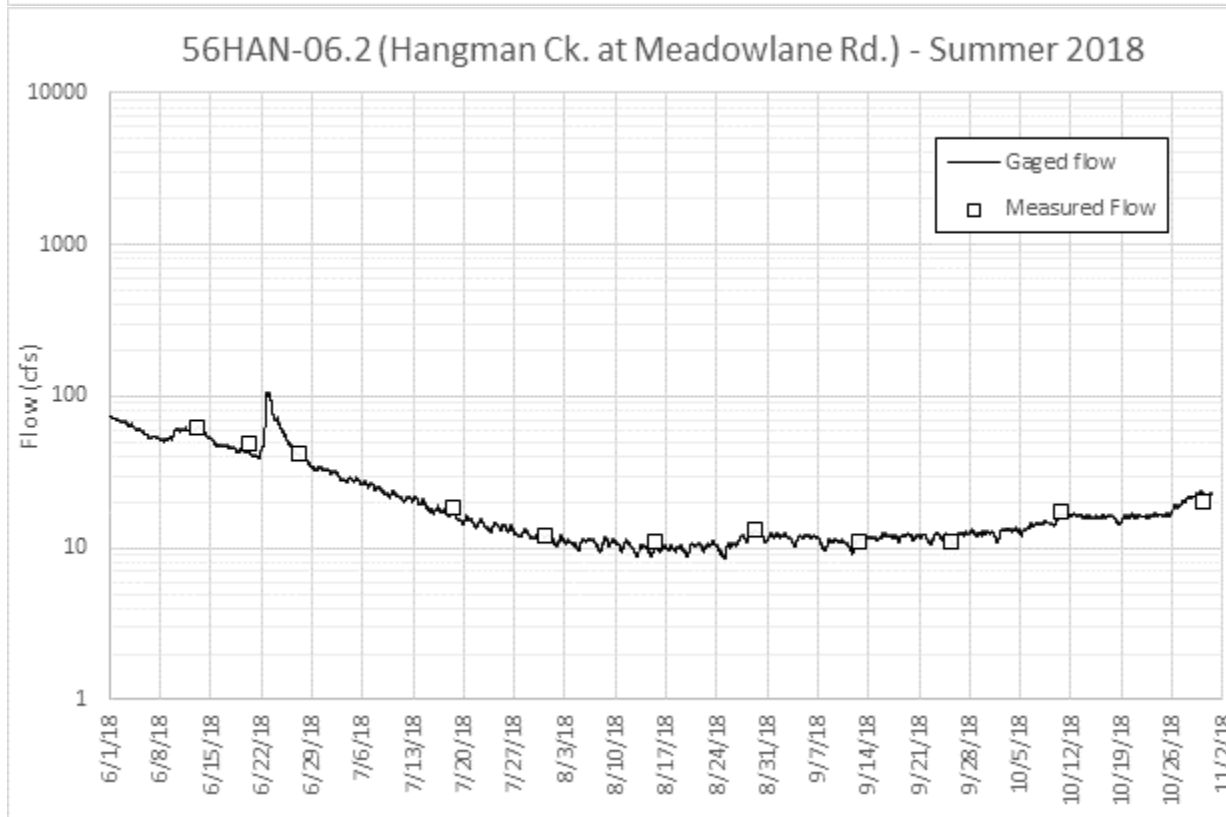
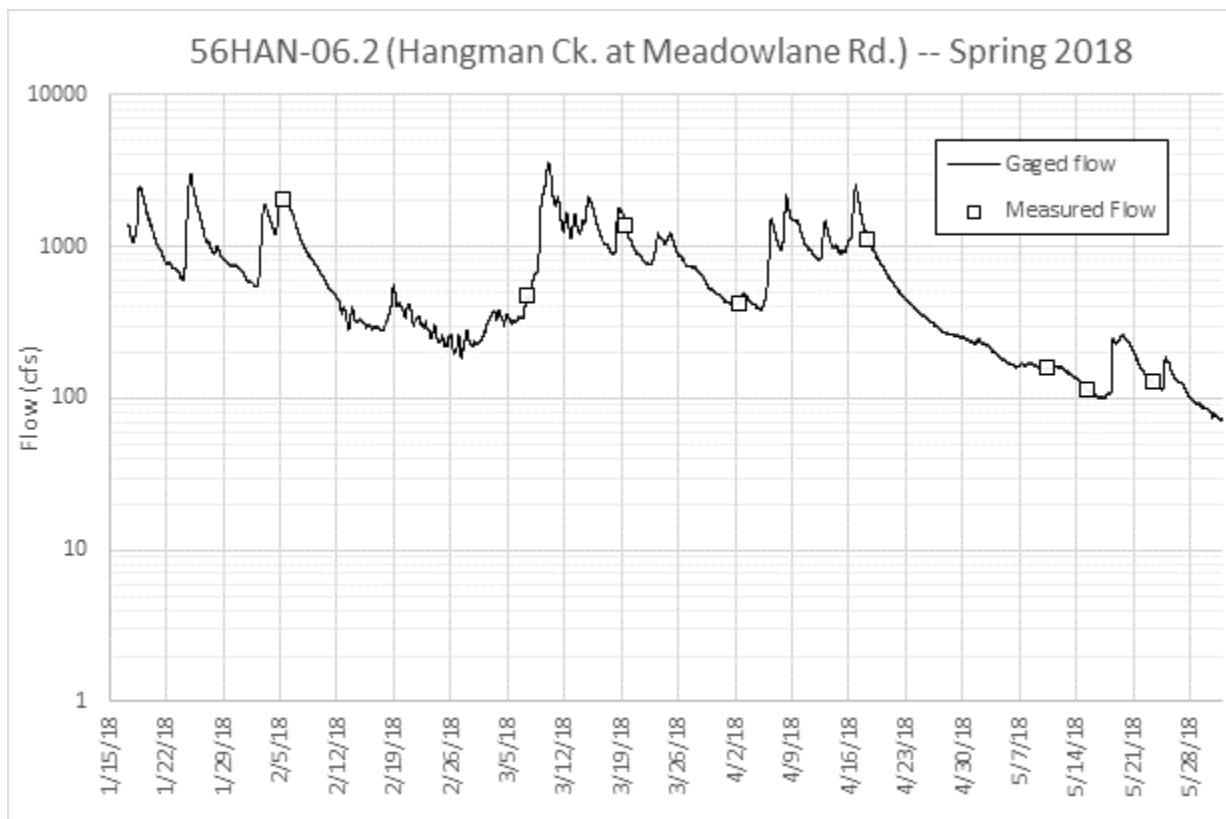


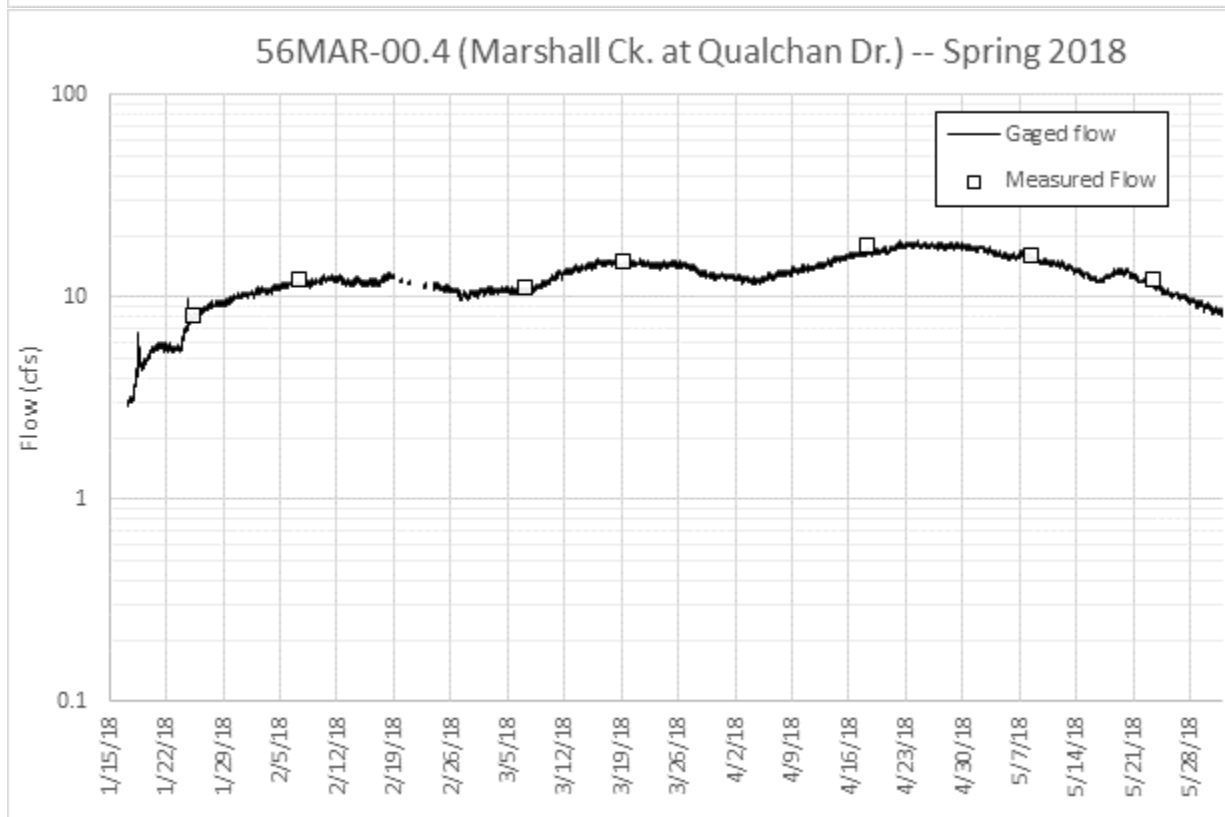
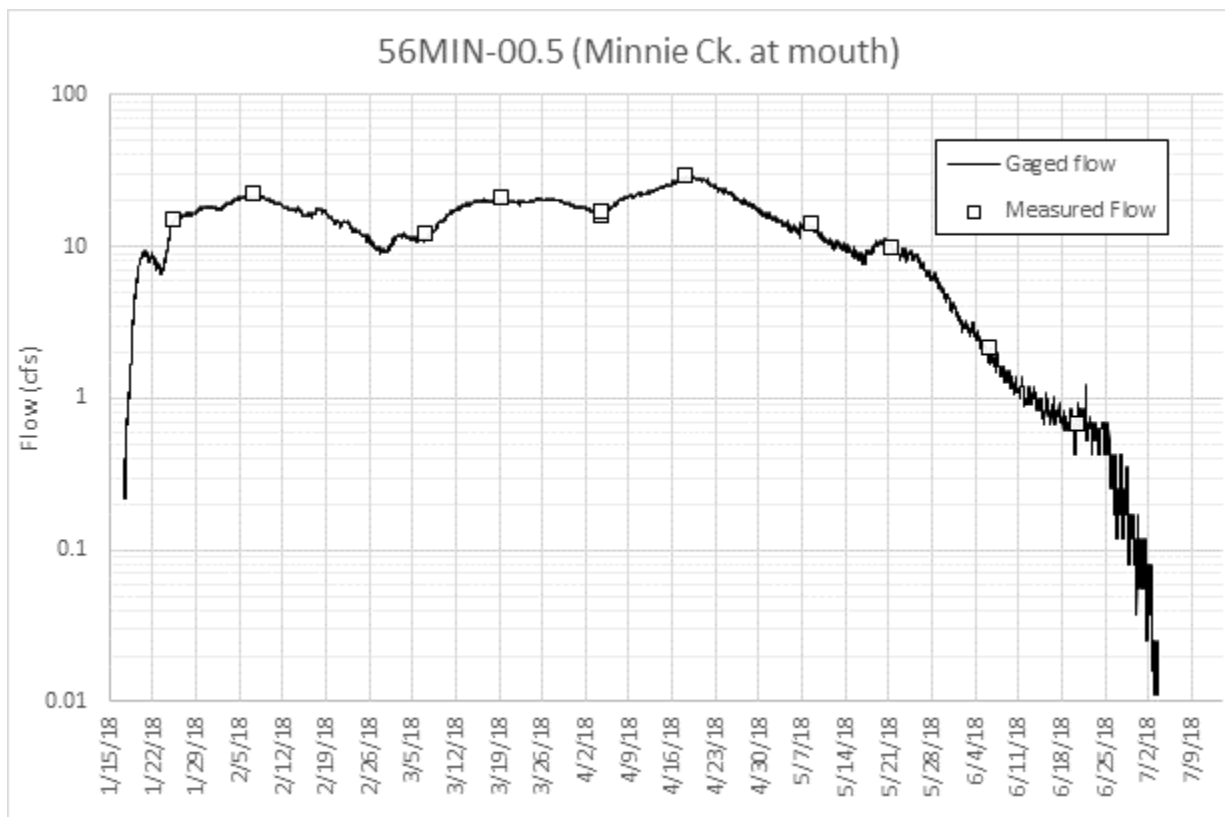


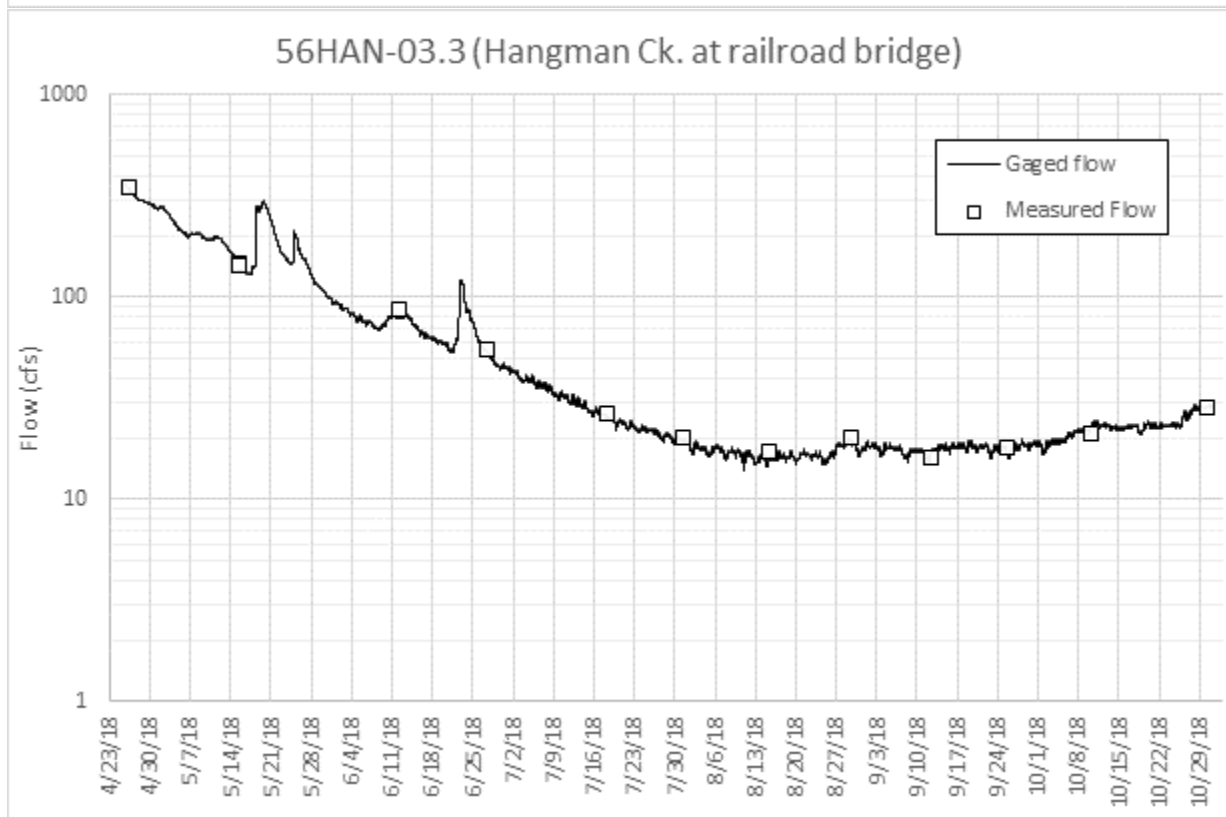
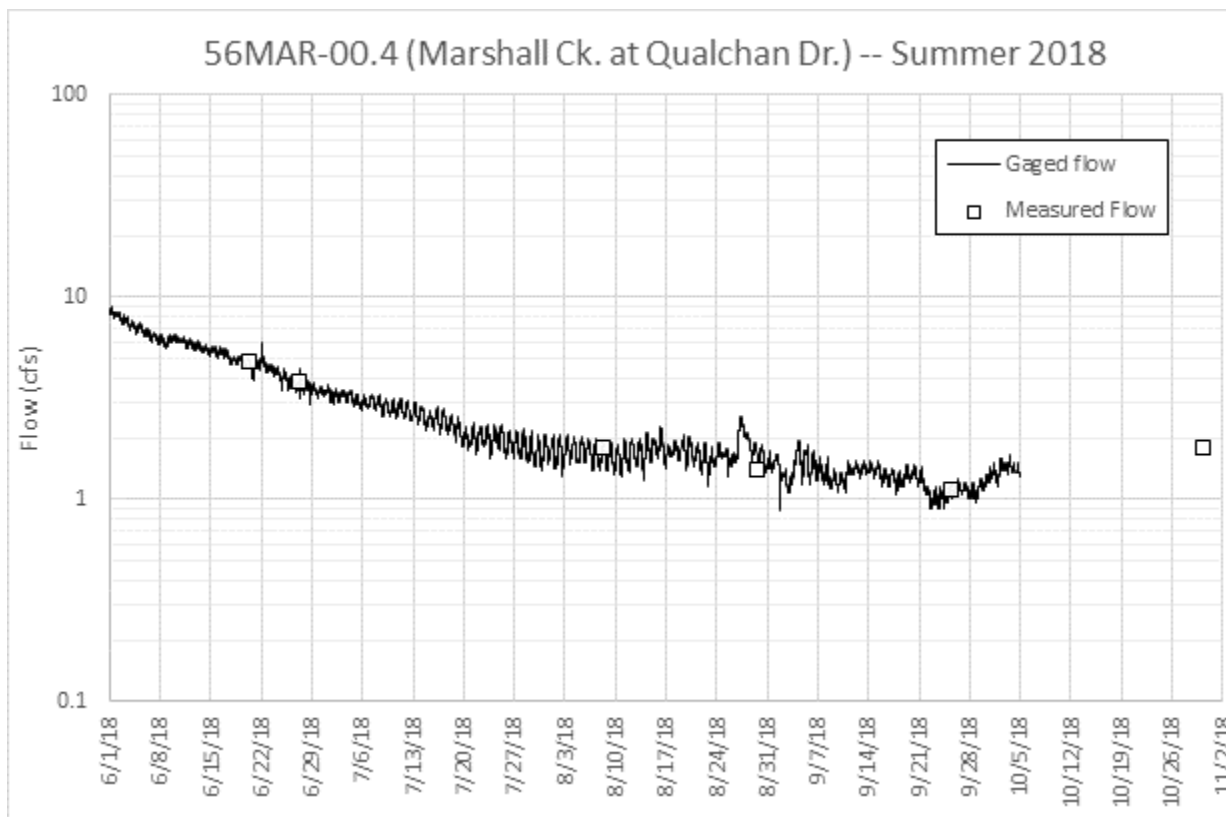












Appendix B. Data quality

This appendix describes the quality of data that Ecology collected during 2018 for the *Hangman Creek Pollutant Source Assessment* high-flow and low-flow studies. It also describes the quality of data obtained from other organizations and agencies that we used in our analysis. Our analysis also used Ecology data collected during 2009 and 2017 field studies. We assessed the quality of those data in previous reports (Ross, 2011; Stuart, 2020).

Typically, we assessed data by comparing quality metrics such as replicate precision statistics or instrument calibration end checks to a target Measurement Quality Objective (MQO). EAP's programmatic QAPP for water quality impairment studies (McCarthy and Mathieu, 2017) and the QAPP for the *Hangman Creek Pollutant Source Assessment* (Albrecht et al., 2017) define the MQOs for this study. We found all data to be acceptable for use in this study, unless otherwise noted.

Sample data quality

Replicates, duplicates, and matrix spikes

Ecology took replicate field samples for laboratory parameter analyses. Field replicates consisted of two samples collected from the same location and as close to the same time as possible.

Ecology collects field replicates to check the precision of the entire process of sampling and analysis. Tables B-1 and B-2 present the percentage of replicates taken per parameter and the assessed sample precision. Both the frequency of field replicates and the precision of the replicated samples generally fell within the target levels set in the QAPP. This indicates a high level of precision suitable for our analysis.

Laboratory duplicates consisted of two subsamples taken from the same sample container and analyzed separately. These serve as a check on the precision of the lab analysis. Ecology's Manchester Environmental Laboratory (MEL) standard operating procedure (SOP) calls for duplicating a minimum of 5% of all samples (1/20 samples or 1/analytical batch). However, MEL sometimes combines samples from different projects in lab batches, and the duplicates may come from other projects. Table B-1 only includes lab duplicates from this project. This is why the duplication rate is less than 5% for some parameters. MEL did not duplicate samples for suspended sediment concentration, the analytical procedure for which requires the entire sample volume, or for dissolved organic carbon, the laboratory analysis for which is identical to total organic carbon.

We analyzed field replicates and lab duplicates with result values of less than 5 times the reporting limit (RL) separately. These low-level sample results can have a higher relative variability than higher sample results.

Sample duplicate precision met targets for all parameters (Tables B-1 and B-2), except for total phosphorus (TP) and nitrate-nitrite for low-flow study groundwater samples. Those high values each reflect one “bad” duplicate pair out of a very small number of duplicates. In the case of nitrate-nitrite, the values of the “bad” duplicate pair were very near the RL.

MEL assesses bias for certain parameters through the use of matrix spikes. Matrix spike recoveries were within targets for all parameters (Table B-1).

Table B-1. Lab precision and bias results from 2018.

Parameter	Number Samples	Number Dups	% duplicated	Target Precision	Median %RSD < 5x RL	Median %RSD >= 5x RL	Matrix Spike % recovery Target range	Matrix Spike % recovery Actual range	Matrix Spike % recovery Avg %rec
High-flow study									
Suspended Sediment Conc.	190	0	0.0%	<15% RSD	--	--	--	--	--
Total Suspended Solids	190	26	13.7%	<15% RSD	0.0%	2.9%	--	--	--
Turbidity	190	21	11.1%	<15% RSD	--	2.6%	--	--	--
Total Phosphorus	190	11	5.8%	<10% RSD	--	1.2%	75% - 125%	85% - 110%	98.9%
Ortho-Phosphate	190	11	5.8%	<10% RSD	1.9%	0.4%	75% - 125%	88% - 118%	99.5%
Total Persulfate Nitrogen	190	5	2.6%	<10% RSD	--	0.8%	75% - 125%	89% - 105%	98.8%
Nitrate-Nitrite as N	190	5	2.6%	<10% RSD	--	0.9%	75% - 125%	89% - 97%	93.4%
Ammonia	190	10	5.3%	<10% RSD	3.6%	0.7%	75% - 125%	92% - 101%	96.0%
Low-flow study (surface water)									
Total Suspended Solids	113	18	15.9%	<15% RSD	10.1%	0.0%	--	--	--
Total Non-Volatile Susp. Solids	113	18	15.9%	<15% RSD	10.1%	2.7%	--	--	--
Total Phosphorus	113	4	3.5%	<10% RSD	--	0.8%	75% - 125%	99% - 106%	101.5%
Ortho-Phosphate	113	9	8.0%	<10% RSD	--	0.4%	75% - 125%	88% - 103%	96.8%
Total Persulfate Nitrogen	113	7	6.2%	<10% RSD	--	1.4%	75% - 125%	90% - 106%	95.5%
Nitrate-Nitrite as N	113	7	6.2%	<10% RSD	3.4%	0.3%	75% - 125%	87% - 104%	95.3%
Ammonia	113	3	2.7%	<10% RSD	7.5%	--	75% - 125%	84% - 102%	92.3%
Total Organic Carbon	113	2	1.8%	<10% RSD	--	1.8%	75% - 125%	99% - 104%	102.3%
Dissolved Organic Carbon	113	0	0.0%	<10% RSD	--	--	75% - 125%	--	--
Alkalinity, Total	113	8	7.1%	<10% RSD	--	0.4%	--	--	--
Chloride	113	8	7.1%	<5% RSD	--	0.3%	75% - 125%	91% - 104%	96.2%
Low-flow study (groundwater)									
Total Phosphorus	19	2	10.5%	<20% RSD	--	49.0%	75% - 125%	99% - 111%	105.0%
Ortho-Phosphate	21	2	9.5%	<20% RSD	0.0%	0.2%	75% - 125%	92% - 105%	98.5%
Total Persulfate Nitrogen	20	5	25.0%	<20% RSD	--	0.8%	75% - 125%	92% - 103%	97.2%
Nitrate-Nitrite as N	20	5	25.0%	<20% RSD	38.2%	0.4%	75% - 125%	91% - 102%	97.8%
Ammonia	20	0	0.0%	<20% RSD	--	--	75% - 125%	--	--
Dissolved Organic Carbon	19	2	10.5%	<20% RSD	1.9%	--	75% - 125%	98% - 99%	98.5%
Alkalinity, Total as CaCO3	19	2	10.5%	<20% RSD	--	--	75% - 125%	--	--
Chloride	20	3	15.0%	<20% RSD	--	0.0%	75% - 125%	91% - 102%	96.8%
Bromide	20	4	20.0%	<20% RSD	0.0%	--	75% - 125%	102% - 117%	107.3%
Boron	20	0	0.0%	<20% RSD	--	--	75% - 125%	100% - 108%	103.8%

Table B-2. Total precision (field + lab) results from 2018.

Parameter	Number Samples	Number Replicates	% replicated	Target Precision	Median %RSD < 5x RL	Median %RSD >= 5x RL
High-flow study						
Suspended Sediment Conc.	190	19	10.0%	<15% RSD	20.2%	2.0%
Total Suspended Solids	190	19	10.0%	<15% RSD	0.0%	4.1%
Turbidity	190	19	10.0%	<15% RSD	17.1%	4.0%
Total Phosphorus	190	19	10.0%	<10% RSD	--	1.7%
Ortho-Phosphate	190	19	10.0%	<10% RSD	--	0.8%
Total Persulfate Nitrogen	190	19	10.0%	<10% RSD	--	1.2%
Nitrate-Nitrite as N	190	19	10.0%	<10% RSD	1.7%	1.2%
Ammonia	190	19	10.0%	<10% RSD	2.7%	1.3%
Low-flow study (surface water)						
Total Suspended Solids	113	12	10.6%	<15% RSD	0.0%	0.0%
Total Non-Volatile Susp. Solids	113	12	10.6%	<15% RSD	20.2%	4.7%
Total Phosphorus	113	12	10.6%	<10% RSD	1.6%	1.7%
Ortho-Phosphate	113	12	10.6%	<10% RSD	--	0.6%
Total Persulfate Nitrogen	113	12	10.6%	<10% RSD	--	2.1%
Nitrate-Nitrite as N	113	12	10.6%	<10% RSD	4.6%	0.4%
Ammonia	113	12	10.6%	<10% RSD	0.0%	--
Total Organic Carbon	113	12	10.6%	<10% RSD	2.1%	2.6%
Dissolved Organic Carbon	113	12	10.6%	<10% RSD	0.7%	1.9%
Alkalinity, Total as CaCO ₃	113	12	10.6%	<10% RSD	--	0.6%
Chloride	113	12	10.6%	<5% RSD	--	0.2%
Low-flow study (groundwater)						
Total Phosphorus	19	5	26.3%	<20% RSD	--	1.1%
Ortho-Phosphate	21	5	23.8%	<20% RSD	--	0.3%
Total Persulfate Nitrogen	20	5	25.0%	<20% RSD	--	1.5%
Nitrate-Nitrite as N	20	5	25.0%	<20% RSD	--	0.4%
Ammonia	20	5	25.0%	<20% RSD	--	--
Dissolved Organic Carbon	19	5	26.3%	<20% RSD	2.8%	--
Alkalinity, Total as CaCO ₃	19	5	26.3%	<20% RSD	--	0.3%
Chloride	20	5	25.0%	<20% RSD	--	0.0%
Bromide	20	5	25.0%	<20% RSD	1.1%	--
Boron	20	5	25.0%	<20% RSD	--	2.9%

Blanks

Ecology submitted field blanks for analysis along with samples regularly throughout the project. In addition, MEL routinely ran lab blanks along with each analytical batch. All high-flow study and low-flow study surface water field and lab blanks resulted in values less than the reporting limit. For the nutrient and organic carbon parameters, some blanks did produce results that were higher than the method detection limit (MDL), but below the reporting limit (Table B-3). Because MEL reported all nutrient and organic carbon results down to the MDL for this project, this is of interest. We qualified all laboratory sample results less than the RL as estimates.

For the low-flow study groundwater samples, we had detections at or above the RL in some of our field blanks for total phosphorus, total persulfate nitrogen, nitrate-nitrite, dissolved organic carbon, and boron. This may have resulted from contamination in the sampling equipment and process. We qualified groundwater sample results for parameters and dates affected by this issue, as possible high biased estimates (qualifier “JL”).

Table B-3. Field and laboratory blank results from 2018.

Parameter	Number Samples	Number lab blanks	Number field blanks	Number results > RL	Number results > MDL*
High-flow study					
Suspended Sediment Conc.	190	56	5	0	--
Total Suspended Solids	190	52	5	0	--
Turbidity	190	35	5	0	--
Total Phosphorus	190	23	5	0	--
Ortho-Phosphate	190	26	5	0	--
Total Persulfate Nitrogen	190	28	5	0	--
Nitrate-Nitrite as N	190	28	5	0	--
Ammonia	190	22	5	0	--
Low-flow study (surface water)					
Total Suspended Solids	113	26	3	0	--
Total Non-Volatile Susp. Solids	113	26	3	0	--
Total Phosphorus	113	14	3	0	0
Ortho-Phosphate	113	15	3	0	0
Total Persulfate Nitrogen	113	17	3	0	0
Nitrate-Nitrite as N	113	17	3	0	9
Ammonia	113	14	3	0	1
Total Organic Carbon	113	17	3	0	1
Dissolved Organic Carbon	113	16	3	0	3
Alkalinity, Total as CaCO ₃	113	21	3	0	--
Chloride	113	14	3	0	--
Low-flow study (groundwater)					
Total Phosphorus	19	6	5	1	4
Ortho-Phosphate	21	6	5	0	0
Total Persulfate Nitrogen	20	5	5	3	3
Nitrate-Nitrite as N	20	5	5	1	5
Ammonia	20	7	5	0	0
Dissolved Organic Carbon	19	6	6	4	5
Alkalinity, Total as CaCO ₃	19	5	5	0	--
Chloride	20	5	5	0	--
Bromide	20	5	5	0	--
Boron	20	5	5	4	--

*Reported here only for parameters where MEL reported results down to the MDL. Dashes indicate that MEL reported results down to the RL.

Turbidity data quality

During this project, we collected turbidity data using three different methods:

- Discrete turbidity field measurements using Hach[®] 2100Q and 2100P portable meters, at all sampling locations during the high-flow study and at continuous turbidity stations during the low-flow study
- Continuous turbidity logging using FTS[®] DTS-12 sensors, at seven locations during the high-flow study and two locations during the low-flow study
- Water samples, analyzed for turbidity by Manchester Environmental Laboratory (MEL).

Discrete turbidity field measurement quality

We collected all discrete turbidity field measurements in triplicate throughout the high-flow and low-flow studies. Table B-4 presents replicate precision based on these triplicate measurements. Median %RSD were well within the MQO of 15% (McCarthy and Mathieu, 2017). To minimize error we averaged all three results for each measurement to get the final measurement values. The values in EIM are these averaged results.

We checked meter calibration regularly throughout the project using a 4-point check against StablCal[®] turbidity standards. All end checks were well within the $\pm 10\%$ MQO.

Table B-4. Replicate precision for Hach[®] meter discrete turbidity measurements

Result value range (NTU)	# of sample sets	# of duplicate pairs	Median %RSD	90 th percentile %RSD
High-flow study				
0 - 10	40	120	4.4%	13.7%
10 - 100	95	285	2.3%	6.5%
100 - 800	57	171	1.7%	4.9%
800 +	14	42	2.3%	8.6%
Low-flow study				
0 - 10	35	105	3.6%	11.1%
10 +	11	33	2.0%	11.9%

Comparison of turbidity methods

For many water quality parameters, there is a true value for any given sample. For example, in a liter of water, there is in reality a certain quantity of phosphorus; the goal of a total phosphorus laboratory assay is to measure this true quantity as accurately as possible. Turbidity, which is a measure of the optical properties of water, is different. Turbidity units such as NTU are arbitrary, and different probe and meter designs can interact differently with various suspended materials (e.g. algae, silt). Turbidity measurements taken by different instrument types are not directly comparable, even when calibrated to the same standard (Fondriest, 2014).

Figure B-1 shows the relationship between field turbidity measurements taken with the Hach® 2100Q/2100P meters and corresponding lab turbidity sample results. There is significant bias between the two methods, with field measurement results typically 1.5 times higher than corresponding lab sample results.

Figure B-2 shows the relationship between FTS® DTS-12 readings and the Hach® 2100Q/2100P meters. The FTS probes usually produced readings that were lower than the Hach meters, but higher than the lab samples. This relationship is evidently site-specific, with differing bias patterns at different sites. This could either reflect calibration differences between individual probes, or differing optical characteristics of sediment from different parts of the watershed, interacting differently with technologies used by each instrument type. There does appear to be some correspondence between parts of the watershed. For example, the two sites on Rock Creek (56ROC-13.0, 56ROC-00.5) have similar probe bias characteristics, while the sites on upper Hangman Creek (56HAN-55.1) and Little Hangman Creek (56LIT-00.1) also form a “like pair.” This could be a coincidence, but if not it suggests the “optical characteristics” explanation for the site-specific bias patterns may be more likely.

The natural question is, which of these three methods is best? Again, because of the inherent subjectivity of turbidity measurement, this is not a question of one method producing the “right” answer. Rather, it is a matter of which method is best suited to the purposes of this project. Because the primary goal of this project is to measure phosphorus loads, we chose the best turbidity method based on how well each method relates to phosphorus.

Figure B-3 shows plots of turbidity vs. total phosphorus (TP), at sites where all three types of turbidity data are available (i.e. continuous turbidity gage sites). Comparing the first three plots, it is evident that the Hach® 2100Q/2100P meter turbidity results have the cleanest correlation to TP, followed by the FTS® DTS-12 probe results, followed by the lab results. Therefore, we adopted the Hach® meter results as the standard for this project.

The continuous data logged by the FTS® probes are key to our analysis. Therefore we adjusted the FTS® probe results based on the site-specific relationships with the Hach® meter results (the lines in Figure B-2). The fourth plot in Figure B-3 shows that these final adjusted FTS® probe results correlate extremely well to TP, better even than the Hach® meter results. By using Hach® meter results to adjust the FTS® probe results, we combined the intra-site precision of the FTS® probes with the inter-site consistency and robustness of the Hach® meter.

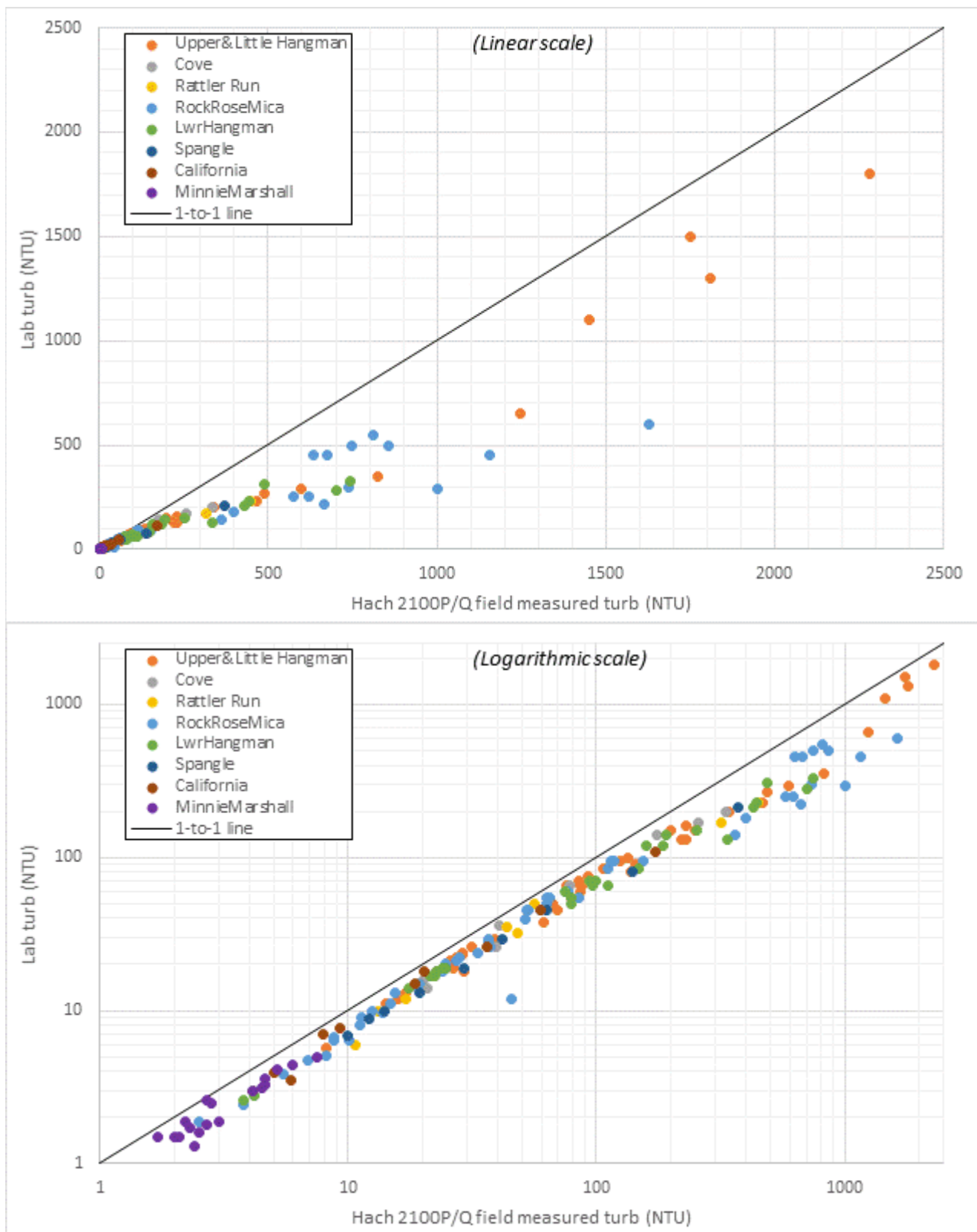


Figure B-1. Relationship between discrete field turbidity and lab turbidity

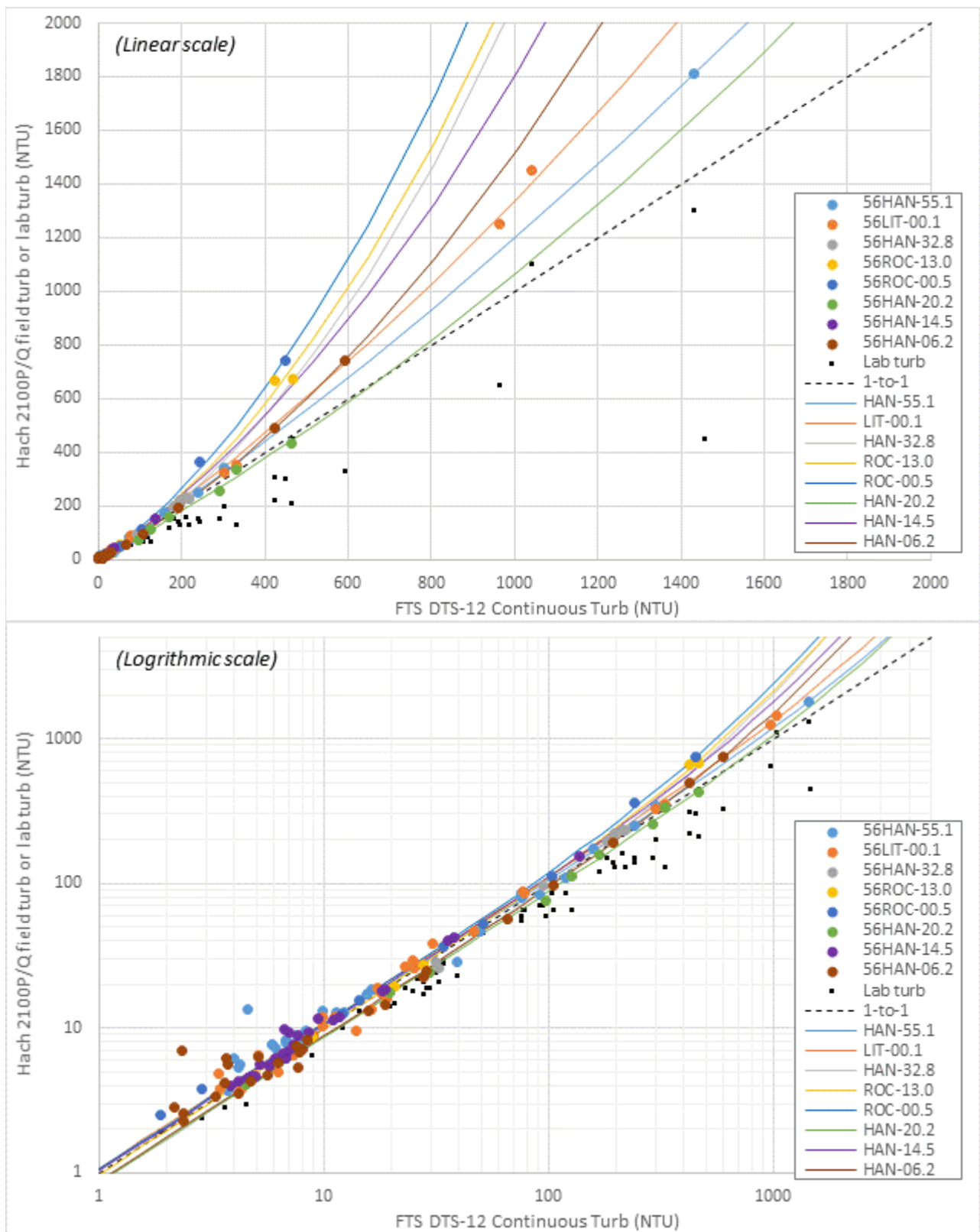


Figure B-2. Site-specific relationships between continuous and discrete field turbidity, also showing continuous vs. lab turbidity.

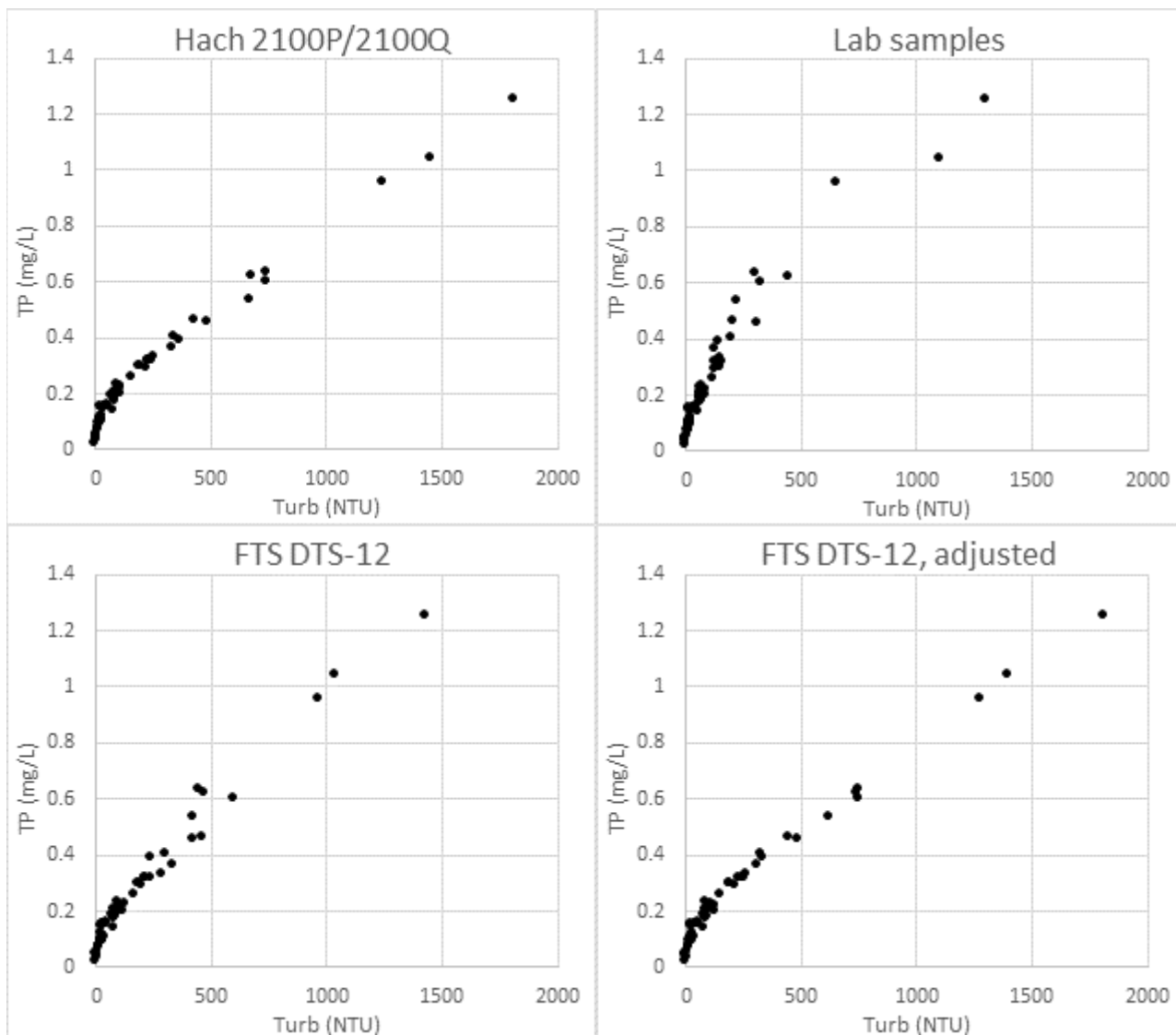


Figure B-3. Plots of turbidity vs TP, showing four turbidity data types: Hach meter, lab samples, FTS probe, and FTS probe adjusted using site-specific relationships based on Hach meter.

Adjusted continuous turbidity data quality

Table B-5 presents quality metrics for the continuous turbidity data, which was collected with FTS[®] DTS-12 probes and adjusted using the site-specific relationship with Hach[®] 2100Q/2100P meter results, as described previously. Median %RSDs were all well within the MQO of 15%. We qualified periods of data within the record as estimates (EIM data qualifier “EST”) for any of the following reasons:

- Data spikes, defined as any value greater than 1.5 times the 2-hour rolling average value.
- Probe range exceeded, any time the raw (uncorrected) probe value exceeded 1600 NTU, the top of the DTS-12 probe’s rated capability.
- Adjustment extrapolation, defined as any time the final (adjusted) result value was greater than 1.5 times the highest Hach[®] meter result used to define the adjustment.
- Data replacement, mostly when we removed obvious spikes and replaced with linear interpolation.

Table B-5. Continuous turbidity data quality summary

Location ID	FMU Gage ID	Gage location	# of check measurements	% RSD Median	%RSD 90 th percentile
56HAN-55.1	56A250	Hangman Ck. abv. Little Hangman Ck.	9 ^a	3.4%	13.0%
56LIT-00.1	56C070	Little Hangman Ck. at Connell St.	7 ^a	2.7%	5.7%
56HAN-32.8	56A200	Hangman Ck. at Bradshaw Rd.	7 ^a	2.2%	5.8%
56ROC-13.0	56B200	Rock Ck. at Hwy 27 in Rockford	7 ^a	4.2%	5.6%
56ROC-00.5	56B050	Rock Ck. at mouth	9 ^a	5.9%	15.2%
56HAN-20.2	56A100	Hangman Ck. blw. Rock Ck.	9 ^a	3.6%	6.8%
56HAN-14.5	--	Hangman Ck. abv. Hangman Valley GC	25 ^b	3.5%	12.0%
56HAN-06.2	--	Hangman Ck. at Meadowlane Rd.	28 ^c	6.7%	30.3%

^a We used these locations during the high-flow study only.

^b We used this location during the low-flow study only.

^c We used this location during both the high-flow and low-flow studies.

Grab vs. depth-integrated sample comparison

Throughout this project we collected grab samples from a well-mixed part of the stream, typically the thalweg, either using a bucket sampler operated from a bridge, an extension pole sampler from the bank, or by wading. We split grab samples by mixing the grab container and “pouring off” or syringe filtering into individual sample bottles.

One risk of using grab samples is that, particularly in high-sediment conditions, streams may not be well-mixed vertically. The tendency of sediment particles to settle can result in sediment stratification occurring, with lower concentrations near the surface and higher concentrations near the streambed. Since we take grab samples from near the surface, this could result in low biased sample results. This is a particular risk for parameters directly linked to sediment, such as suspended sediment concentration (SSC), total suspended solids (TSS), turbidity, and total phosphorus (TP).

During the high-flow study, to check for sample representativeness, we also collected a select number of depth-integrated samples (USGS, 2006). Depth-integrated sampling technique uses an isokinetic sampler such as the DH-48 or the DH-59, which collects a representative sample from the entire water column. We collected depth-integrated samples at three locations across the width of the stream, channel width permitting, to provide a degree of width integration as well. We split depth integrated samples into individual sample bottles using a churn splitter.

We collected depth-integrated samples whenever we collected field replicate QC samples during the high-flow study, or twice per sampling event. Thus, at each QC site, we collected three sets of samples: two sets of grab samples (primary and replicate) as well as a set of depth-integrated samples.

Figure B-4 shows plots comparing depth-integrated sample results to grab sample results, along a 1-to-1 line. The plots compare each depth-integrated result to both sets of grab results (primary and replicate). The only parameter that displayed any evidence of low-biased grab samples was the field turbidity measurements taken with the Hach® 2100P/2100Q meter, and only at extremely high values (>2000 NTU). It is remarkable that suspended sediment concentration (SSC), widely considered the best sediment metric, displayed near-perfect agreement between depth-integrated and grab samples. For total suspended solids (TSS), there was one sample set where one of the grab samples agreed well with the depth-integrated sample, and the other grab sample result was much higher. There was one “bad” result for ammonia, which appears to be an outlier.

Overall, the results of this method comparison show that, at least for the Hangman Creek watershed, depth-integrated and grab samples are broadly comparable, and that grab sample results are generally representative of the entire water column.

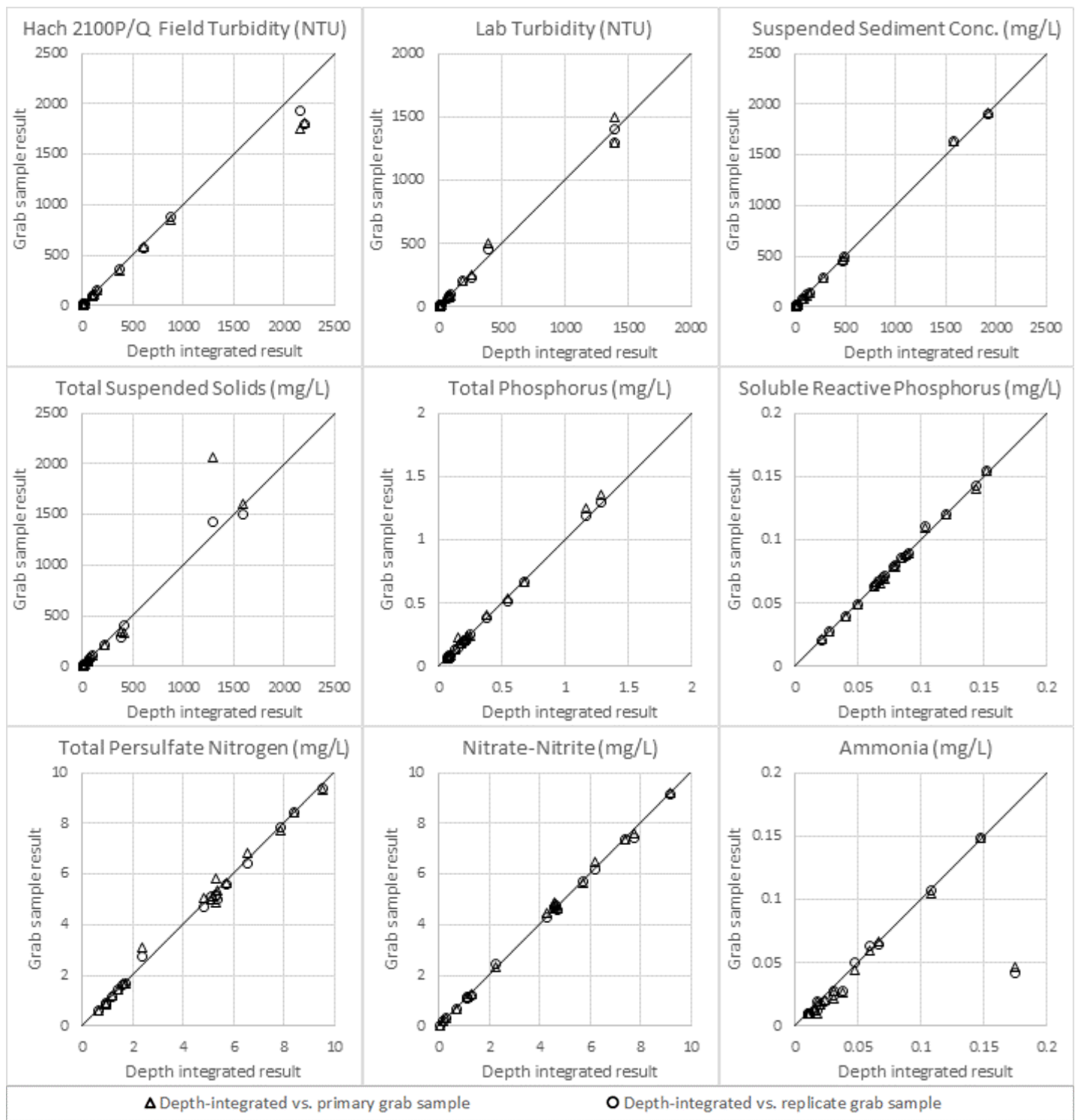


Figure B-4. Plots comparing depth-integrated vs. grab sample results.

Flow data quality

We assessed the quality of all flow measurement data. If a flow measurement contained issues likely to result in a measurement error $\geq \pm 10\%$, then we qualified the measurement as an estimate (EIM quality code “EST”). Table B-6 lists all instances of qualified flow data. We qualified 21 out of 367 flow measurements taken (5.7%).

Table B-6. Qualified (estimated) flow measurements

Location ID	Date	Measurement Method	Measured Flow (cfs)	Reason for qualification
56CAL-00.1	1/25/18	ADCP	97	Excessive variation between transects
56MS4-I90LB	2/15/18	Bucket	0.17	Bucket could not catch all flow from pipe. Estimated % captured and applied correction factor.
56MS4-I90RB1	3/14/18	Bucket	0.40	Very high velocity from pipe, very short bucket fills. Difficult to time exactly.
56MS4-I90LB	3/14/18	Culvert	0.44	High velocities and low depth in culvert.
56ROC-17.1	3/20/18	ADCP	77	Large estimated right edge flow.
56CAL-00.1	3/21/18	ADCP	26.4	Excessive variation between transects
56ROC-17.1	4/8/18	ADCP	194	Excessive variation between transects
56MS4-I90RB1	4/12/18	Culvert	1.8	Very fast, turbulent water. Meter struggled to get good measurement. Had to use shorter averaging interval.
56COV-00.2	4/16/18	ADCP	34.2	Large estimated left edge flow.
56HAN-55.1	5/7/18	ADCP	34.9	Excessive variation between transects
56HAN-11.7	5/15/18	ADCP	102	Large amount of macrophytes with water flowing through; Excessive variation between transects
56HAN-55.1	5/21/18	ADCP	46.8	Excessive variation between transects
56LIT-00.1	5/21/18	ADCP	7.2	Excessive variation between transects
56ROC-13.0	5/22/18	ADCP	14.0	Excessive variation between transects
56HAN-04.6	6/12/18	Wading	55	Poor cross-section, boulders and large depth variation.
56HAN-03.3	6/12/18	Wading	86	Too much flow concentrated in too few verticals
56GAR-00.0	6/12/18	Wading	0.60	Very narrow cross-section, small number of verticals.
56HAN-32.8	6/19/18	ADCP	17.9	Excessive variation between transects
56MAR-00.0	9/12/18	Wading	0.99	Excessive relative depth uncertainty
56MAR-00.0	10/10/18	Wading	1.2	Excessive relative depth uncertainty
56HAN-03.3	10/10/18	Wading	21.0	Possible misread depth could contribute up to 7% error

Multiprobe sonde data quality

Ecology calibrated Hydrolab® MiniSonde and HL4, and YSI® EXO multiprobe meters according to manufacturer’s specifications using certified standards. For meters that collected short-term diel continuous data or spot check data, we calibrated prior to each monitoring event, and we checked calibrations after each event to assess calibration drift. For meters that collected data continuously throughout the study period, we compared their in-situ readings weekly to a recently calibrated check instrument and/or to certified standards to check for biofouling and calibration drift. We cleaned biofouling from the continuous instrument probes and recalibrated to certified standards if drift occurred.

We used spot check measurements, calibration standard post-checks, and Winkler dissolved oxygen (DO) titration results to evaluate continuous instrument data. If indicated by the weight of evidence, we adjusted raw instrument data as follows:

- “Stable drift” bias adjustment to correct for moderate levels of miscalibration.
- “Sliding drift” bias adjustment to correct for slipping calibration or buildup of biofouling.
- “Linear” adjustment to correct for DO calibration issues that require a slope adjustment as well as a bias adjustment. We rarely used this option.

After applying any adjustments, we assessed the final data record according to the MQOs in Table B-7 (McCarthy and Mathieu, 2017). Table B-8 lists all instances where we qualified or rejected data, or where we lost data, for short-term diel continuous deployments. Table B-9 lists such instances for long-term continuous deployments. Table B-10 lists instances for groundwater quality measurements from piezometers. Adjusted data are flagged “IA” and qualified data are flagged “EST” in the EIM database.

Table B-7. Accuracy targets for water quality multiprobe sondes.

Parameter	Accept	Qualify	Reject
Temperature	≤ 0.2°C	> 0.2 and ≤ 0.8°C	> 0.8°C
Conductivity	≤ 10%	> 10% and ≤ 20%	> 20%
pH	≤ 0.2 S.U.	> 0.2 and ≤ 0.8 S.U.	> 0.8 S.U.
Dissolved oxygen	≤ 0.5 mg/L	> 0.5 and ≤ 0.1 mg/L	> 0.8 mg/L

Table B-8. Qualified, rejected, and lost data for short-term diel deployments.

Location	Temperature	Conductivity	pH	DO
56HAN-13.2 (Hangman Ck. abv. Latah WTP)				
56HAN-12.6 (Hangman Ck. blw Latah WTP)				
56HAN-11.7 (Hangman Ck. 1 mi. blw. Latah WTP)				
56HAN-08.9 (Hangman Ck. at Yellowstone Pipeline)				
56Unk(MUL)-00.0 (Unnamed drainage off Mullen Hill area)			May 14-16: Qualified due to poor agreement with spot checks	July 17-19: Qualified due to poor agreement with spot checks September 11-13: Qualified due to need for large sliding adjustment October 9-11: Qualified due to need for large sliding adjustment
56HAN-07.9 (Hangman Ck. at Campion Park)		August 14-16: Rejected due to probe malfunction		
56HAN-04.6 (Hangman Ck. blw. Qualchan GC)				July 17-19: Qualified due to poor agreement with spot checks August 14-16: Qualified due to poor agreement with spot checks
56MAR-00.0 (Marshall Ck. at mouth)			June 11-13: Qualified due to poor agreement with spot checks	May 14-16: Qualified due to questionable linearity of correction and lack of field checks at low end of diel cycle
56HAN-03.3 (Hangman Ck. at Railroad Bridge)				
56Spr(VIN)-00.1 (Vinegar Flats US surface spr. at Oak St.		October 9-11: Rejected due to spurious probe fluctuations	June 11-13: Qualified due to spurious probe fluctuations	May 14-16: Qualified due to questionable linearity of correction and lack of field checks at low end of diel cycle July 17-19: Qualified due to biofouling
56CRY-00.3 (Crystal Springs at Inland Empire Way)	August 14-16: Lost due to instrument failure	August 14-16: Lost due to instrument failure	August 14-16: Lost due to instrument failure	July 17-19: Qualified due to poor agreement with spot checks August 14-16: Lost due to instrument failure
56HAN-01.9 (Hangman Ck. at Chestnut St.)			October 9-11: Qualified due to poor agreement with spot checks	

Location	Temperature	Conductivity	pH	DO
56GAR-00.0 (Garden Springs at mouth)		May 14-16: Rejected due to spurious probe fluctuations October 9-11: Rejected due to spurious probe fluctuations		July 17-19: Qualified due to poor agreement with spot checks
56HAN-00.7 (Hangman Ck. at mouth)		July 17-19: Qualified some data points where removed spikes and replaced with linear interpolation	July 17-19: Qualified due to large calibration shifts and need for significant sliding drift adjustment	

WTP = Wastewater Treatment Plant (also WWTP)

Table B-9. Qualified, rejected, and lost data for long-term continuous deployments.

Location	Temperature	Conductivity	pH	DO
56HAN-14.5 (Hangman Ck. abv. Hangman Valley GC)	July 17-25: Lost due to instrument failure	July 17-25: Lost due to instrument failure August 29-Sept 5: Rejected due to probe malfunction September 11-15: Rejected due to probe malfunction September 16-25: Qualified due to messy data pattern October 3-31: Rejected due to probe malfunction	May 18-24: Qualified due to small spurious probe fluctuations July 15-17: Qualified due to poor agreement with spot checks July 17-25: Lost due to instrument failure September 19-Oct 24: Qualified due to poor agreement with spot checks	July 14-17: Qualified due to biofouling July 17-25: Lost due to instrument failure July 28-31: Qualified due to biofouling August 2-8: Qualified due to messy data pattern August 11-14: Qualified due to messy data pattern August 21-22: Qualified due to biofouling
56HAN-06.2 (Hangman Ck. at Meadowlane Rd.)		May 28-30: Rejected due to probe contamination by damselfly larva July 17-19: Qualified due to small spurious probe fluctuations	May 4-9: Qualified due to poor agreement with spot checks May 30-June 7: Qualified due to probe equilibration and calibration slippage issues August 8-14: Qualified due to probe equilibration and calibration slippage issues	May 15: Qualified due to biofouling May 16: Rejected due to biofouling July 9-11: Qualified due to biofouling July 23-25: Qualified due to biofouling July 29-31: Qualified due to biofouling August 3-8: Qualified due to biofouling October 30-31: Lost due to probe failure

Table B-10. Qualified, rejected, and lost data for piezometer groundwater quality measurements.

Location	Temperature	Conductivity	pH	DO
56HAN-GW-1 (Piezo in Hangman Ck.; DS of Meadowlane Rd.)	June 13: No measurements; couldn't find piezo July 18: Qualified. Could not do extended purge, readings may not have stabilized	June 13: No measurements; couldn't find piezo July 18: Qualified. Could not do extended purge, readings may not have stabilized	June 13: No measurements; couldn't find piezo July 18: Qualified. Could not do extended purge, readings may not have stabilized	June 13: No measurements; couldn't find piezo July 18: Qualified. Could not do extended purge, readings may not have stabilized
56HAN-GW-2 (Piezo in Hangman Ck.; blw Qualchan GC; AHL199)		July 18: Qualified due to failed calibration post-check		July 18: Qualified. Instrument also used for surface meas; required slope adjustment using Winklers. Could not extrapolate to adjust GW meas. September 12: Rejected due to probable sunlight interference
56HAN-GW-3 (Piezo in seeps; blw Qualchan GC; AHL198)		July 18: Qualified due to failed calibration post-check		July 18: Qualified. Instrument also used for surface meas; required slope adjustment using Winklers. Could not extrapolate to adjust GW meas. September 12: Rejected due to probable sunlight interference
56HAN-GW-4 (Piezo in Hangman Ck.; nr Cheney-Spokane Rd.; AHL197)		July 18: Qualified due to failed calibration post-check		July 18: Qualified. Instrument also used for surface meas; required slope adjustment using Winklers. Could not extrapolate to adjust GW meas. September 12: Rejected due to probable sunlight interference
56HAN-GW-5 (Piezo in Hangman Ck.; blw 11 th Ave.)	June 13: Qualified. Could not do extended purge, readings may not have stabilized All other dates: No measurements; losing vertical hydraulic gradient	June 13: Qualified. Could not do extended purge, readings may not have stabilized All other dates: No measurements; losing vertical hydraulic gradient	June 13: Qualified. Could not do extended purge, readings may not have stabilized All other dates: No measurements; losing vertical hydraulic gradient	June 13: Qualified. Could not do extended purge, readings may not have stabilized All other dates: No measurements; losing vertical hydraulic gradient
56HAN-GW-6 (Piezo in Hangman Ck.; abv. Riverside Ave.; AHL160)	All dates: No measurements; losing vertical hydraulic gradient			

Continuous temperature data quality

We evaluated low-flow study continuous water temperature data quality in two ways. First, we subjected Hobo® pressure transducers (which log temperature as well as pressure) to a two-point calibration checks after project completion using cold and warm water baths. Second, we compared spot measurements of temperature taken with either a Hydrolab® or with a Cole-Parmer® electronic thermistor to the continuous data. For continuous Hydrolab® sites, we did not post-check the temperature probes in calibration baths, but we took a larger number of field checks. Table B-11 presents calibration and field check results.

Post-deployment calibration bath results indicate that Hobo® pressure transducers were functioning within the MQO of +/- 0.2°C. Field checks indicate additional variability, likely related to the fact that temperatures in the field are nearly always changing, sometimes rapidly. Field checks indicate that the continuous water data are likely accurate to about +/- 0.4°C accounting for field variability.

During the high-flow study, some of our instruments, such as pressure transducers and turbidity probes, collected continuous temperature data as a secondary parameter. Temperature was not a part of our high-flow study analysis, and we did not use this data. However we did make it available in EIM for external use. We did not take spot temperature measurements to check these data. For temperature data collected by pressure transducers, the calibration bath gives us reasonable confidence in the data quality. For temperature data collected by turbidity probes, we qualified the data as estimates in EIM to reflect the lack of both calibration bath checks and field spot checks. High-flow study locations are not included in Table B-11.

Table B-11. Continuous water temperature logger calibration and field check results.

Location ID	Logger type	Calibration bath results	Number of field checks	Field check result (Mean absolute error °C)	Field check result (Bias °C)
56HAN-14.5 ^a	PT	OK	68	0.16	+0.09
56HAN-14.5 ^a	HL	--	56	0.11	+0.03
56HAN-06.2 ^b	HL	--	57	0.07	+0.05
56MAR-00.4 ^c	PT	OK	0	--	--
56HAN-03.3	PT	OK	20	0.16	-0.13

HL = Hydrolab® Minisonde5

PT = Hobo® pressure transducer

^a At 56HAN-14.5, both a Hydrolab® Minisonde and a Hobo® pressure transducer recorded continuous temperature. The quality of both data records is good, but the Hydrolab® is slightly better. However, the Hydrolab® record is missing an 8-day period during July 2018 due to instrument failure. Therefore we used both records to some degree, and we present both sets of statistics here.

^b At 56HAN-06.2, both a Hydrolab® Minisonde and a Hobo® pressure transducer recorded continuous temperature. The quality of both data records is good, but the Hydrolab® is slightly better. We used the Hydrolab® dataset and present only those statistics here.

^c At 56MAR-00.4, we monitored continuous temperature (and flow) upstream of the sampling location (56HAN-00.0) where we took the spot measurements. The two locations are not comparable for temperature, so we could not use the checks for this instrument.

Piezometer vertical hydraulic gradient data quality

We calculated piezometer vertical hydraulic gradient as

$$VHG = \frac{DH}{DL}$$

Where:

VHG = vertical hydraulic gradient (dimensionless)

DH = surface water - groundwater head difference (feet)

DL = depth below sediment surface to midpoint of open interval (feet)

Therefore the relative accuracy depends on the values of the individual measurements. We took the measurements used to derive DH and DL using either a steel measuring tape or an electronic water level tape (e-tape), both of which measure ± 0.01 ft. Therefore, VHG measurements are accurate to two significant digits.

Time-of-travel data quality

The protocol for conducting time-of-travel dye studies provides a robust method for determining the average amount of time it takes for water to travel through a given reach of a river. We released rhodamine dye into the river at an upstream location, and deployed Hydrolab® dataloggers equipped with a specialized probe to measure rhodamine concentrations at one or more locations downstream. We calculated the time of travel for a given reach as the time elapsed between dye injection at the upstream location and the time of peak dye concentration at the downstream location. Alternately, when placing multiple dataloggers downstream of a single dye injection, we calculated the time of travel for a given reach as the time as the time elapsed between the time of peak dye concentration at the upstream and locations.

This protocol was designed for measuring *average* time-of-travel, and therefore is based on the time of peak concentration, rather than leading edge. This differs significantly from protocols designed to estimate travel of toxic substances, where the emphasis is on human health considerations. Users of the data should take care not to misuse this data for purposes for which it was not intended.

Hydrolabs logged dye concentration every 15 minutes. Dye concentration curves were usually clear, and the peak concentration discernable. We assessed the accuracy of time of travel calculations as follows (Table B-12):

- We calculated the assessed accuracy, in hours, as the sum of upstream and downstream uncertainty.
- For reaches where we injected dye at the upstream end, the upstream uncertainty is zero, because the exact time of dye injection is known. For reaches that were a continuation of a further upstream dye cloud, the upstream uncertainty is the same as the downstream uncertainty of the previous reach.

- We estimated the downstream uncertainty based on the clarity and discernibility of the dye peak. We also accounted for dye curve skew; if the peak value appeared to be significantly different than the centroid, then we estimated a larger downstream uncertainty to account for this.

Table B-12. Time of travel data assessed accuracy.

Survey	Upstream Location	Downstream Location	Reach length (mi)	Time of Travel (hours)	Assessed uncertainty \pm time (hours)	Assessed uncertainty %
June 2009	56HAN-31.1 ^a	56HAN-29.3	1.80	5.92	1.00	17%
June 2009	56HAN-20.2 ^a	56HAN-19.1	1.06	13.25	0.50	4%
June 2009	56HAN-14.5 ^a	56HAN-13.2	1.18	8.83	0.50	6%
June 2009	56HAN-06.2 ^a	56HAN-04.6	1.68	6.63	0.50	8%
June 2009	56HAN-04.6 ^b	56HAN-01.9	2.67	7.50	0.75	10%
July 2009	56HAN-47.0 ^a	56HAN-46.3	0.68	5.63	1.00	18%
July 2009	56HAN-14.5 ^a	56HAN-13.2	1.18	16.00	1.50	9%
July 2009	56HAN-06.2 ^a	56HAN-04.6	1.68	12.02	0.50	4%
July 2009	56HAN-03.6 ^a	56HAN-01.9	1.80	6.68	0.50	7%

^a Dye drop location.

^b Continuation of upstream dye cloud.

Longitudinal depth data quality

The Hydrolab[®] depth probe uses an unvented pressure sensor to detect water depth. To guard against calibration drift due to changes in elevation and barometric pressure, we zeroed the depth probe at the put-in site at the beginning of each float day. 2-3 times during each float day, we checked the probe calibration by pulling the instrument to the water surface and checking the depth reading. If the calibration had begun to drift, we re-zeroed the probe. All zero check values taken throughout the 8 float days were within ± 0.04 m.

External data quality

USGS flow data

We obtained streamflow data from the U.S. Geological Survey (USGS) gaging stations Hangman Creek at Spokane (ID# 12424000) and Hangman Creek at State Line Road near Tekoa (ID# 12422990). The USGS Surface-Water Quality Assurance Plan (Mastin, 2017) describes the standard protocols used to insure data quality. Rantz et al. (1982) describes the field and data processing methods.

SCD flow data

We obtained streamflow data from the Spokane Conservation District (SCD) gaging station at the mouth of Rock Creek for 2009. SCD uses similar standard protocols to the USGS (SCD, 2010; Rantz et al., 1982).

NWS meteorological data

We obtained meteorological data from the National Oceanic and Atmospheric Administration (NOAA) National Weather Service (NWS) records for the Spokane Airport (KGEG), Felts Field (KSFF), and Turnbull National Wildlife Refuge (TWRW1) sites. NWS uses standard protocols to insure data quality. Information quality guidelines for NWS can be found here:

<https://www.noaa.gov/organization/information-technology/policy-oversight/information-quality>

City of Spokane stormwater monitoring data

We used City of Spokane stormwater monitoring data from the Cochran Basin (City of Spokane, 2020) to estimate stormwater characteristics for a few parameters where we lacked data from Hangman-specific outfalls. The *Cochran Basin Dissolved Oxygen TMDL Stormwater Sampling Quality Assurance Project Plan* (City of Spokane, 2016) describes the standard protocols used to insure data quality.

Appendix C. Watershed mass balance documentation

As described in the “Analytical Framework” heading above, the total phosphorus (TP), suspended sediment (SSC), and dissolved inorganic nitrogen (DIN) watershed mass balance analysis of the winter-spring 2018 High-flow Study data included the following steps:

1. Estimate seasonal average load for each sampling location
2. Calculate subbasin contributions as the load residual between sample locations
3. Normalize subbasin contributions by drainage area
4. Run scenarios: back-calculate subbasin load contributions and sampling location loads given particular areal contributions.

Sampling location seasonal average load estimates

We calculated seasonal average load estimates for two overlapping seasons: (1) January 18 – April 30, 2018, representing the period of peak flows, and (2) March 1 – May 31, 2018, representing the March-May season defined by the *Spokane River and Lake Spokane TMDL* (Moore and Ross, 2010). For sampling sites with continuous turbidity, we used the relationship between turbidity and TP or SSC to estimate loads. For sampling sites without continuous turbidity (and for DIN at all sites), we used a multiple-linear regression model approach.

Load estimates from continuous turbidity

To calculate the regression between turbidity and SSC (Figure C-1), we used data from all high-flow study locations except for stormwater outfalls. The relationship between turbidity and SSC is broadly consistent throughout the Hangman Creek watershed.

To calculate the regression between turbidity and TP (Figure C-2), we used data from upper and Lower Hangman Creek, Little Hangman Creek, Rock Creek, Rose Creek, and Mica Creek. These areas include all of the sites that had continuous turbidity gages, as well as some additional sites with the same fundamental turbidity-TP relationship. By including these additional sites, we were able to strengthen the regression and extend it upward to a higher range of values. We did not include sites on Cove Creek, Rattler’s Run Creek, Spangle Creek, California Creek, Minnie Creek, and Marshall Creek. These tributaries all have a different turbidity-TP relationship, presumably because of groundwater sources of soluble reactive phosphorus (average SRP/TP ratio > 50% at these sites).

DIN does not correlate to turbidity, so we could not use this method to estimate DIN loads.

We assessed the goodness-of-fit of the regression lines for SSC and TP (Table C-1). These statistics, along with a visual assessment of the “tightness” of the data cloud, give an indication of the amount of uncertainty associated with using these regressions.

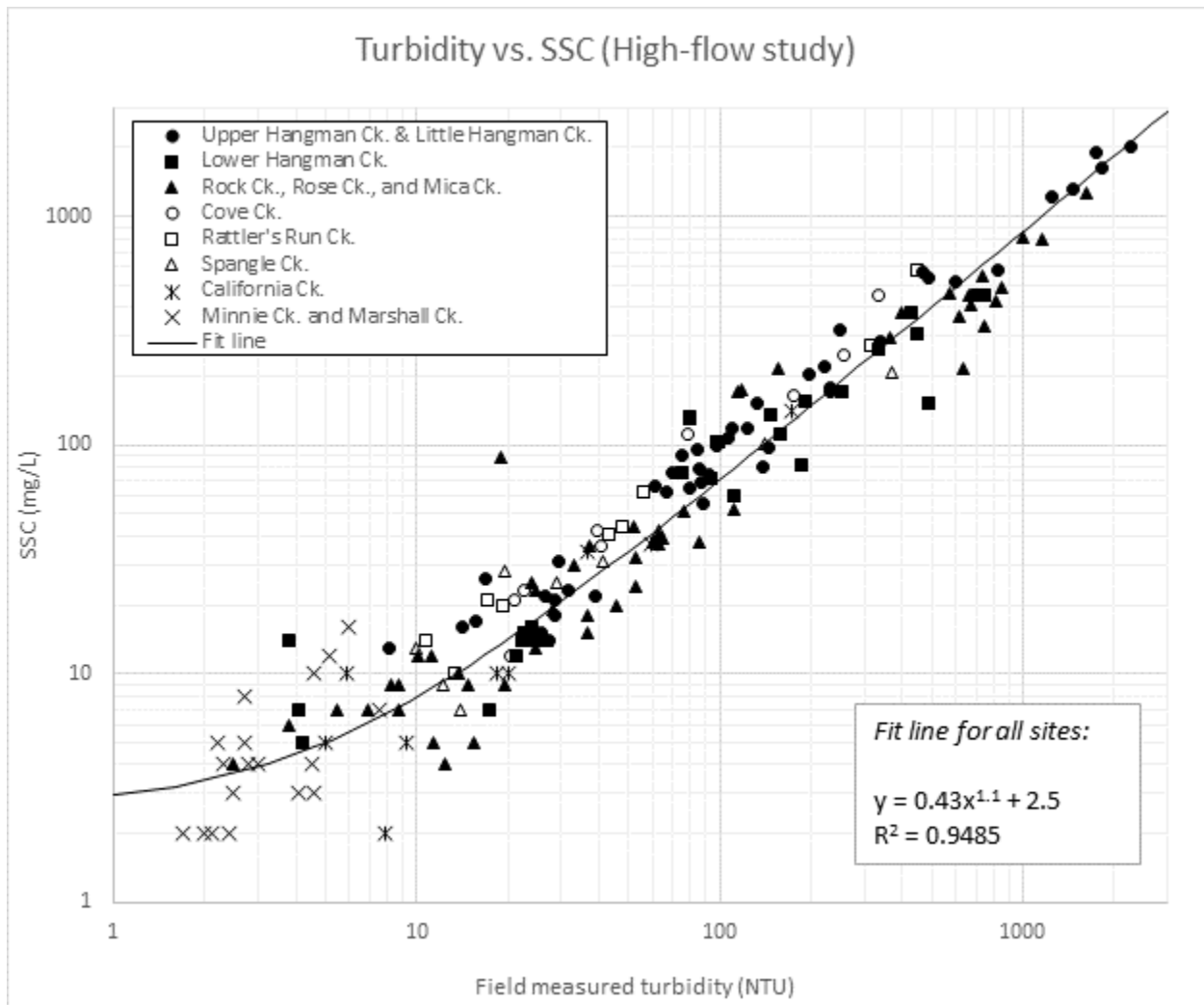


Figure C-1. Relationship between turbidity and suspended sediment concentration (SSC), showing regression line.

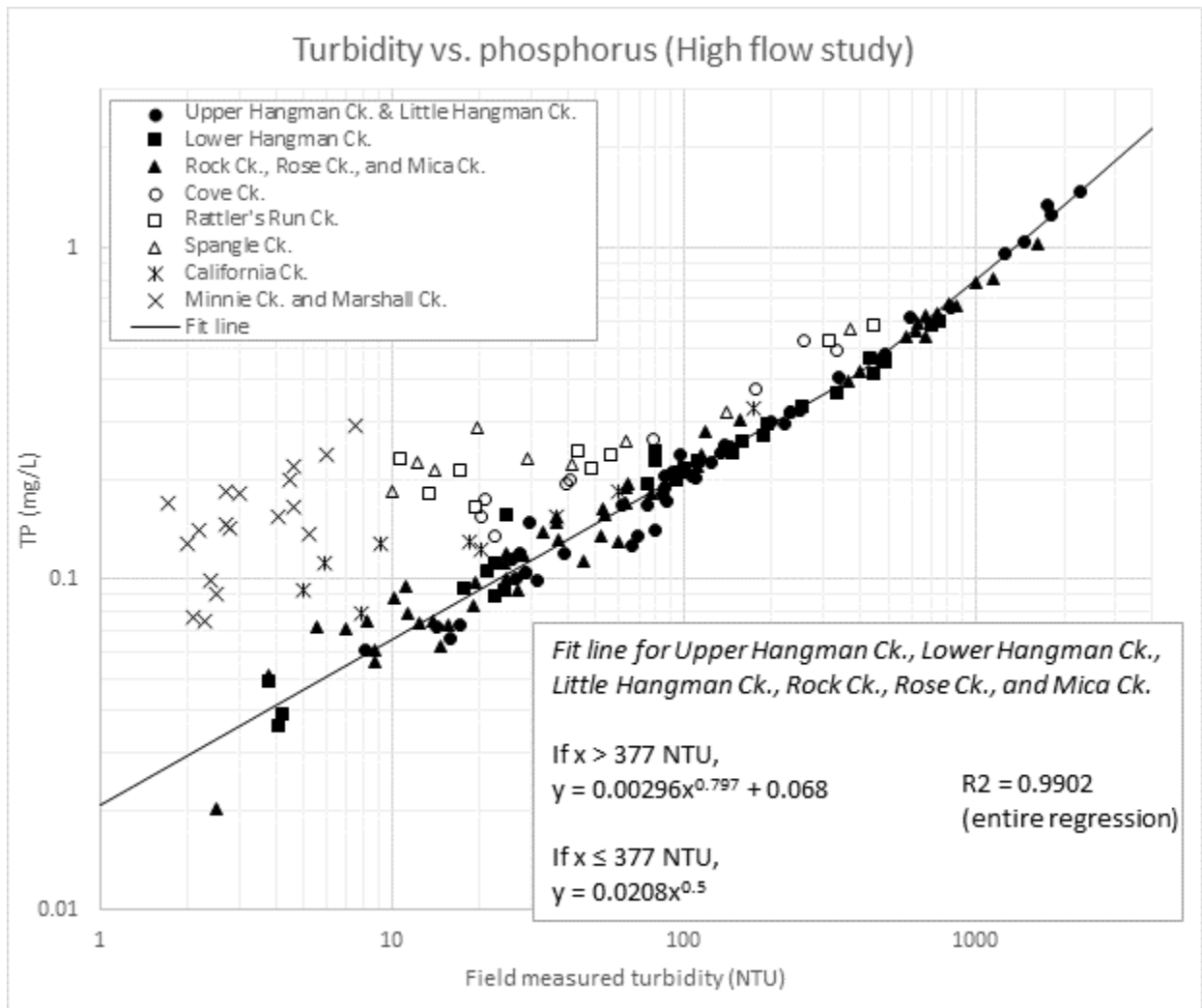


Figure C-2. Relationship between turbidity and total phosphorus (TP), showing regression line.

Table C-1. Goodness-of-fit statistics for turbidity vs. TP and turbidity vs. SSC regressions

Regression	Number of data points (n)	%RSD ^a	Weighted %RSD ^a	Average overall bias %
Turbidity vs. TP	124	13.6%	9.3%	+0.2%
Turbidity vs. SSC	179	44.0%	32.1%	+0.9%

^a %RSD and weighted %RSD reflect the distribution of relative residuals (predicted minus observed value, divided by the observed value). The standard %RSD considers all relative residuals equally. The weighted %RSD considers each relative residual in proportion to the associated observed value. This accounts for the fact that the regressions are a bit "tighter" (in proportional terms) at the upper end, and that the upper end of the curve contributes proportionally more to the overall seasonal load estimates. We calculated them as follows:

$$\%RSD = \sqrt{\frac{\sum \left(\frac{\text{Pred} - \text{Obs}}{\text{Obs}} \right)^2}{n}}$$

$$\text{Weighted \%RSD} = \sqrt{\frac{\sum \left[\left(\frac{\text{Pred} - \text{Obs}}{\text{Obs}} \right)^2 \times \text{Obs} \right]}{\sum \text{Obs}}}$$

At the seven locations with continuous turbidity data, we used the continuous turbidity record along with these regressions to estimate SSC and TP concentration at every 15 minute interval. We then used the estimated concentration along with the continuous flow record to estimate loads at each time interval (Figure C-3). From this, we calculated seasonal average loads (Table C-2).

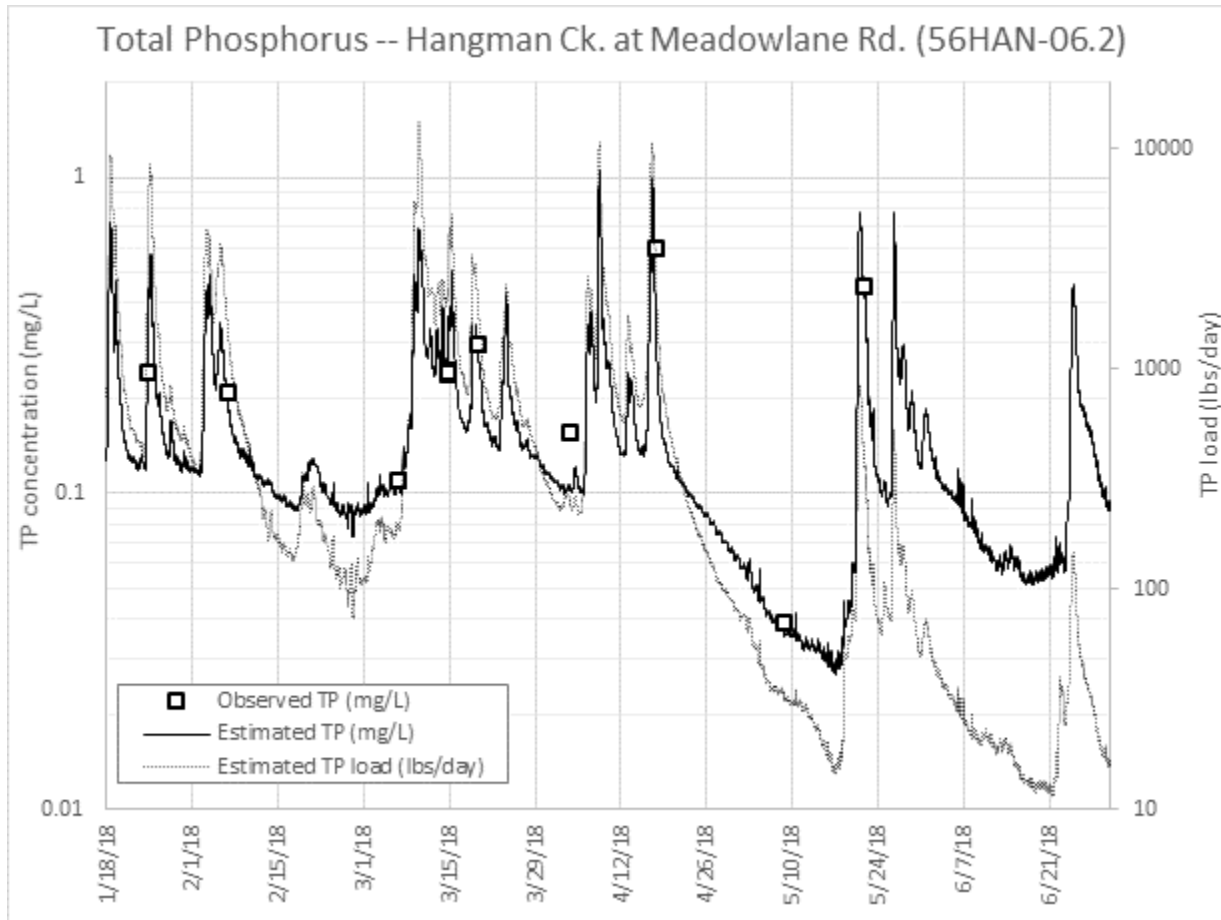


Figure C-3. Example time-series of TP concentration and load estimates for Hangman Ck. at Meadowlane Rd. (56HAN-06.2).

Table C-2. Seasonal average SSC and TP loads estimated from continuous turbidity data.

Location ID	Season	Seasonal Average SSC load (tons/day)	Seasonal Average TP load (lbs/day)	Seasonal Average Flow (cfs)
56HAN-55.1	1/18/18 - 4/30/18	78.5	331	280.1
56HAN-55.1	3/1/18 - 5/31/18	75.5	268	207.8
56LIT-00.1	1/18/18 - 4/30/18	112	241	110.4
56LIT-00.1	3/1/18 - 5/31/18	76.4	170	79.63
56HAN-32.8	1/18/18 - 4/30/18	196	648	477.9
56HAN-32.8	3/1/18 - 5/31/18	179	531	361.7
56ROC-13.0	1/18/18 - 4/30/18	102	303	215.5
56ROC-13.0	3/1/18 - 5/31/18	76	218	150.5
56ROC-00.5	1/18/18 - 4/30/18	170	454	292.5
56ROC-00.5	3/1/18 - 5/31/18	112	306	206.5
56HAN-20.2	1/18/18 - 4/30/18	322	1120	820.1
56HAN-20.2	3/1/18 - 5/31/18	258	852	612.3
56HAN-06.2	1/18/18 - 4/30/18	303	1100	849.6
56HAN-06.2	3/1/18 - 5/31/18	234	826	636.1

Load estimates from multiple linear regression modeling

Because we were not able to monitor continuous turbidity at all sampling locations, and because DIN cannot be calculated using that method, we also estimated seasonal loads using multiple-linear regression modeling (MLR; Cohn et al., 1989). We built and calibrated models for each parameter (SSC, TP, and DIN) at each sampling location. The models followed the form:

$$\log K = \beta_0 + \beta_1 \log(Q/A) + \beta_2 \log(Q/A)^2 + \beta_3 \sin(2\pi f_y) + \beta_4 \cos(2\pi f_y)$$

Where:

- K = constituent concentration (mg/L)
- Q = flow (cms)
- A = contributing watershed area (km²)
- f_y = year fraction (e.g. July 1, 2018 = 2018.50)
- β_0 = intercept parameter
- $\beta_{1,2}$ = parameters relating to flow dependence
- $\beta_{3,4}$ = parameters relating to seasonal variation

Tables C-3 through C-5 present the parameterization and selected goodness-of-fit statistics for the MLR models for SSC, TP, and DIN, respectively.

Table C-3. Parameterization and goodness-of-fit for multiple linear regression models for SSC.

Location ID	β_0 intercept	β_1 log(Q/A)	β_2 log(Q/A) ²	β_3 sin(2 π f _y)	β_4 cos(2 π f _y)	RMSE CV ^a	%Bias ^b	Slope ^c	R ² ^d
56HAN-58.5	4.500	1.962	0.316	-0.019	-0.165	140.2%	-43.3%	1.76	0.28
56HAN-55.1	5.091	1.702	0.146	-0.643	-0.648	103.7%	-29.3%	1.70	0.81
56LIT-00.1	5.788	2.173	0.241	-0.718	-0.609	62.6%	-11.5%	0.98	0.76
56HAN-47.0	6.478	2.589	0.324	-1.145	-0.751	82.1%	-26.4%	1.50	0.85
56COV-00.2	7.839	3.943	0.526	-0.409	-0.561	66.5%	-12.3%	1.18	0.68
56HAN-32.8	6.104	3.093	0.511	-0.554	-0.527	41.1%	-3.0%	0.93	0.68
56RAT-00.1	6.774	3.388	0.441	-0.270	-0.324	76.0%	-13.5%	1.21	0.79
56ROC-19.6	4.919	2.562	0.365	0.655	-0.397	74.5%	-7.6%	1.02	0.68
56ROS-00.4	5.016	1.940	0.178	-0.211	-0.529	82.0%	-11.7%	1.03	0.55
56ROC-17.1	5.074	2.374	0.261	0.277	-0.261	61.0%	-14.9%	1.18	0.83
56MIC-00.2	5.642	2.564	0.313	-0.711	-0.475	81.2%	-15.3%	1.14	0.65
56ROC-13.0	5.958	2.967	0.379	-0.220	-0.507	81.0%	-9.0%	0.89	0.62
56ROC-00.5	6.848	3.676	0.524	-0.657	-0.569	53.4%	-18.3%	1.26	0.96
56HAN-20.2	6.720	2.976	0.373	-0.969	-0.698	38.0%	-3.1%	1.00	0.86
56SPA-00.0	4.801	1.866	0.162	-0.164	-0.195	67.5%	-21.5%	1.27	0.74
56CAL-00.1	6.716	3.279	0.430	-1.037	-0.641	27.7%	-4.9%	1.08	0.97
56HAN-06.2	8.718	4.838	0.802	-0.865	-0.759	34.5%	-10.4%	1.08	0.89
56MIN-00.5	6.605	3.488	0.586	-1.049	-0.503	21.1%	-2.3%	1.00	0.89
56MAR-00.0	9.778	5.278	0.800	-0.947	-0.214	14.7%	-1.0%	1.01	0.90
56HAN-00.7	7.707	3.840	0.505	-0.379	-0.649	20.6%	-6.6%	1.08	0.97

Table C-4. Parameterization and goodness-of-fit for multiple linear regression models for TP.

Location ID	β_0 intercept	β_1 log(Q/A)	β_2 log(Q/A) ²	β_3 sin(2 π f _y)	β_4 cos(2 π f _y)	RMSE CV ^a	%Bias ^b	Slope ^c	R ² ^d
56HAN-58.5	1.207	1.376	0.227	-0.260	-0.187	92.1%	-22.3%	1.29	0.30
56HAN-55.1	1.412	1.497	0.243	-0.320	-0.309	74.2%	-15.9%	1.31	0.61
56LIT-00.1	1.605	1.597	0.260	-0.245	-0.189	30.1%	-6.4%	1.09	0.90
56HAN-47.0	1.964	1.665	0.253	-0.600	-0.393	61.6%	-15.3%	1.29	0.74
56COV-00.2	1.999	1.701	0.254	-0.321	-0.190	18.8%	-2.6%	1.05	0.87
56HAN-32.8	1.186	1.401	0.236	-0.231	-0.208	24.9%	-3.2%	1.01	0.66
56RAT-00.1	1.327	1.230	0.189	-0.311	-0.123	21.5%	-1.9%	1.02	0.82
56ROC-19.6	0.993	1.516	0.224	0.446	-0.107	22.9%	-1.6%	1.02	0.94
56ROS-00.4	1.516	1.693	0.260	0.080	-0.218	21.0%	-2.6%	1.04	0.93
56ROC-17.1	1.380	1.751	0.265	0.289	-0.108	21.4%	-2.5%	1.03	0.94
56MIC-00.2	0.991	1.405	0.230	-0.206	-0.090	34.3%	-5.4%	1.09	0.82
56ROC-13.0	1.515	1.812	0.282	0.061	-0.124	18.3%	-2.7%	1.03	0.96
56ROC-00.5	1.227	1.390	0.158	-0.146	-0.044	10.2%	-1.9%	1.02	0.99
56HAN-20.2	1.830	1.834	0.296	-0.320	-0.237	23.1%	-4.0%	1.02	0.84
56SPA-00.0	0.896	0.859	0.129	-0.332	-0.043	17.9%	-1.8%	1.02	0.83
56CAL-00.1	0.819	1.077	0.163	-0.271	-0.106	14.2%	-1.4%	1.03	0.91
56HAN-06.2	2.347	2.231	0.381	-0.256	-0.373	40.5%	-10.2%	1.11	0.61
56MIN-00.5	-0.973	-0.286	-0.022	-0.400	0.015	7.4%	-0.3%	1.00	0.92
56MAR-00.0	-0.071	0.449	0.120	-0.649	-0.061	12.4%	-0.5%	0.99	0.87
56HAN-00.7	2.527	2.388	0.381	-0.082	-0.292	29.0%	-6.8%	1.10	0.83

Table C-5. Parameterization and goodness-of-fit for multiple linear regression models for DIN.

Location ID	β_0 intercept	β_1 log(Q/A)	β_2 log(Q/A) ²	β_3 sin(2 π f _y)	β_4 cos(2 π f _y)	RMSE CV ^a	%Bias ^b	Slope ^c	R ² ^d
56HAN-58.5	-0.673	-0.839	-0.144	0.033	0.284	24.6%	-2.1%	1.01	0.61
56HAN-55.1	-0.632	-0.804	-0.137	0.055	0.273	25.4%	-2.3%	1.02	0.60
56LIT-00.1	0.003	-0.460	-0.079	0.084	0.292	19.2%	-1.5%	1.00	0.55
56HAN-47.0	-0.547	-0.790	-0.138	0.151	0.335	29.2%	-3.1%	1.01	0.50
56COV-00.2	0.194	-0.279	-0.053	0.096	0.175	11.8%	-0.8%	1.01	0.66
56HAN-32.8	-0.499	-0.766	-0.134	0.129	0.290	23.4%	-2.1%	1.00	0.45
56RAT-00.1	1.036	0.076	0.006	0.088	0.120	3.1%	-0.0%	1.00	0.96
56ROC-19.6	0.264	-0.301	-0.054	0.126	0.257	15.2%	-1.1%	1.00	0.67
56ROS-00.4	0.499	-0.102	-0.027	0.237	0.350	10.0%	-0.6%	1.00	0.93
56ROC-17.1	0.328	-0.244	-0.047	0.184	0.310	11.7%	-0.7%	1.00	0.85
56MIC-00.2	1.044	0.805	0.119	0.267	0.535	24.3%	-3.5%	1.03	0.89
56ROC-13.0	0.355	-0.062	-0.020	0.252	0.384	15.0%	-1.1%	1.01	0.87
56ROC-00.5	0.627	0.122	0.009	0.259	0.310	10.7%	-1.0%	1.01	0.93
56HAN-20.2	0.314	-0.214	-0.044	0.093	0.204	25.9%	-3.4%	1.04	0.40
56SPA-00.0	0.968	0.216	0.028	0.274	0.126	5.6%	-0.2%	1.00	0.91
56CAL-00.1	0.769	0.187	0.023	-0.274	0.105	27.6%	-3.9%	1.04	0.57
56HAN-06.2	0.217	-0.218	-0.046	0.167	0.225	22.8%	-2.5%	1.03	0.52
56MIN-00.5	-7.911	-4.417	-0.676	1.019	1.194	34.8%	+2.8%	0.89	0.85
56MAR-00.0	-7.826	-4.115	-0.536	0.287	0.547	22.6%	-0.8%	0.96	0.90
56HAN-00.7	-0.025	-0.417	-0.082	0.098	0.261	24.9%	-2.9%	1.03	0.59

^a RMSE CV is the Root Mean Squared Error coefficient of variation, or the RMSE divided by the average observed value:

$$RMSE\ CV = \frac{\sqrt{[\sum(K_{modeled} - K_{observed})^2]/n}}{K_{observed}}$$

^b % Bias is the overall bias divided by the average observed value:

$$\% Bias = \frac{[\sum(T_{modeled} - T_{observed})]/n}{K_{observed}}$$

^c The slope of the best fit line through the back-transformed predicted vs. observed scatter plot, with a specified zero intercept. The ideal value is 1.

^d The R² value of the best fit line through the back-transformed predicted vs. observed scatter plot, with a specified zero intercept.

At each location, we used the MLR model along with the continuous flow record to estimate constituent concentration at every 15 minute interval. We then estimated loads at each time interval. From this, we calculated seasonal average loads.

We assessed the comparability of seasonal average load estimates based on continuous turbidity vs. MLR by estimating SSC and TP loads using both methods at continuous turbidity sites. It is reasonable to assume that the load estimates based on turbidity are better, since SSC, TP, and turbidity are all inherently related. MLR estimates could have error, not only due to calibration uncertainty, but because they depend heavily on the flow record, and the timing, magnitude, and shape of flow event “spikes” can be different from sediment “spikes.” Therefore, for this comparison, where discrepancies occurred, we assumed that the turbidity-based estimate was correct, and that the MLR estimate was in error.

We found that discrepancies between MLR and turbidity load estimates for SSC and TP were related to the slope of the zero-intercept best fit line through the back-transformed MLR predicted vs. observed scatter plot (“slope” in Tables C-3 through C-5). Intuitively, this makes sense. The slope of the zero-intercept best-fit line through the scatter plot should ideally be 1; a divergence from this is likely to relate to model bias. This is also confirmation that discrepancies between MLR and turbidity-derived load estimates are mainly due to errors in the MLR estimate. Figure C-4 demonstrates this relationship.

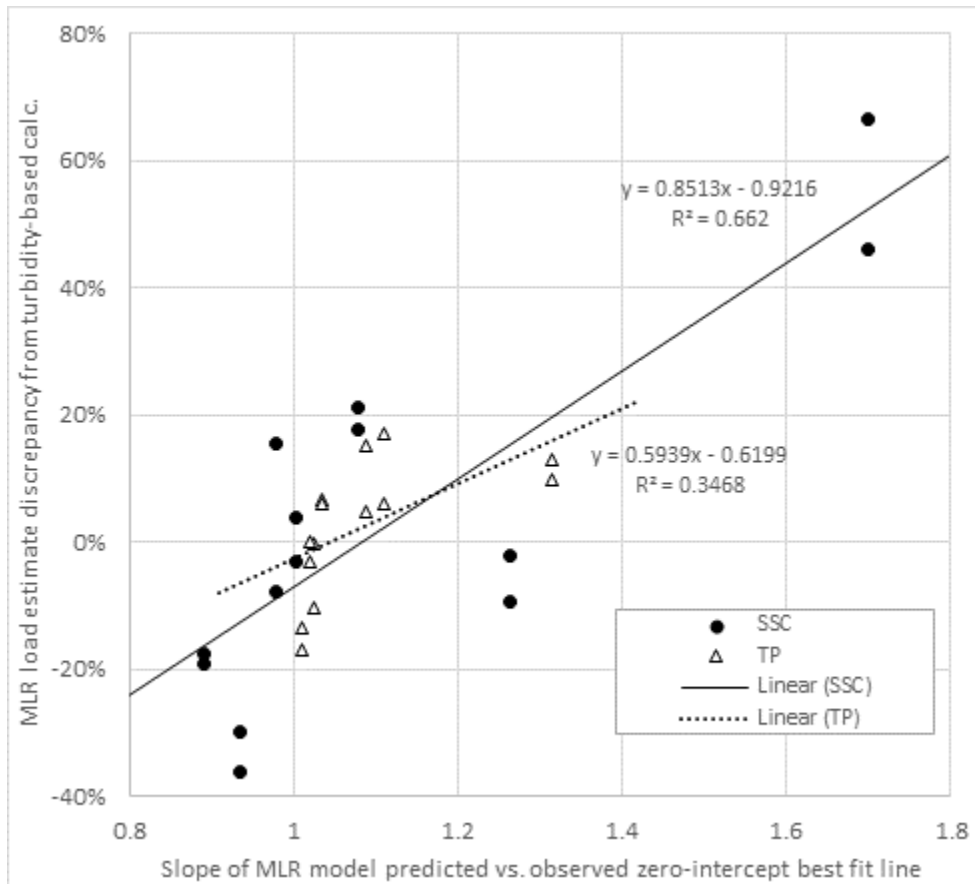


Figure C-4. The relationship between MLR model-derived load estimate error and the slope of the MLR model predicted vs. observed zero-intercept best fit line

We used the relationship shown in Figure C-4 to adjust the MLR load estimates for all sites. As shown in Figure C-5, this adjustment reduced bias and “tightened” the relationship between MLR and turbidity-derived load estimates for SSC and TP. It was not possible to independently compare MLR load estimates for DIN, since there were no turbidity-derived estimates to which they could be compared. However, as seen in Table C-5, the calibration bias were low and slopes very near 1 for MLR models for DIN. Therefore we expect MLR load estimates for DIN to be accurate without further adjustment. Table C-6 presents the final MLR load estimates for all sites.

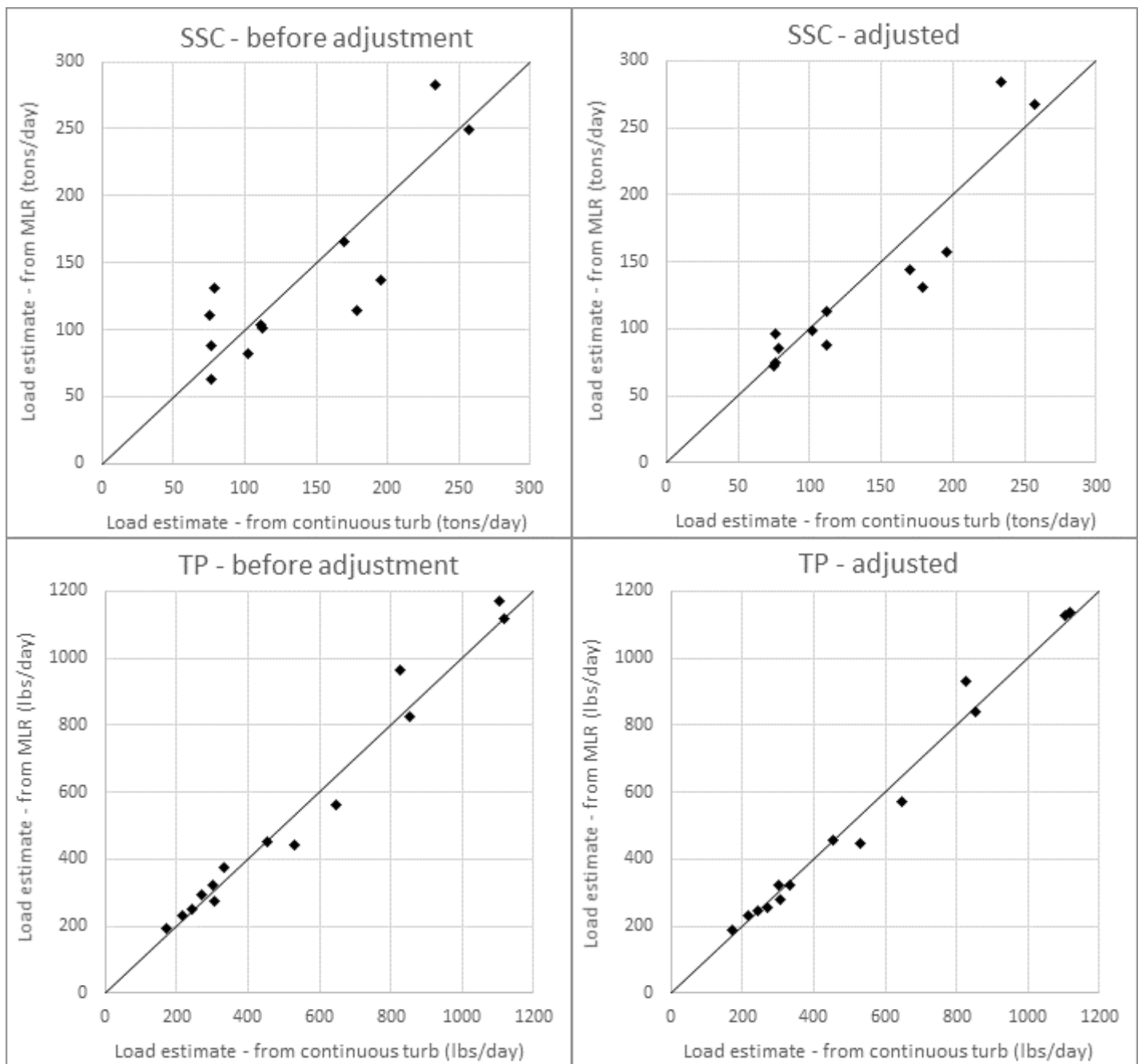


Figure C-5. Comparison of MLR and turbidity-derived load estimates, before and after MLR bias adjustment.

The diagonal black line shows the ideal 1-to-1 relationship.

Table C-6. Final adjusted seasonal average SSC, TP, and DIN loads estimated from multiple linear regression models.

Location ID	Season	Seasonal Average SSC load (tons/day)	Seasonal Average TP load (lbs/day)	Seasonal Average DIN load (lbs/day)	Seasonal Average Flow (cfs)
56HAN-58.5	1/18/18 - 4/30/18	115	416	4010	305.4
56HAN-58.5	3/1/18 - 5/31/18	89.0	310	2450	229.3
56HAN-55.1	1/18/18 - 4/30/18	85.8	322	4060	280.1
56HAN-55.1	3/1/18 - 5/31/18	72.4	254	2490	207.8
56LIT-00.1	1/18/18 - 4/30/18	113	246	3070	110.4
56LIT-00.1	3/1/18 - 5/31/18	96.6	190	1830	79.63
56HAN-47.0	1/18/18 - 4/30/18	173	600	9230	436.2
56HAN-47.0	3/1/18 - 5/31/18	134	457	5580	324.4
56COV-00.2	1/18/18 - 4/30/18	3.07	18.6	332	13.21
56COV-00.2	3/1/18 - 5/31/18	2.77	14.7	235	10.48
56HAN-32.8	1/18/18 - 4/30/18	157	573	10200	477.9
56HAN-32.8	3/1/18 - 5/31/18	131	450	6490	361.7
56RAT-00.1	1/18/18 - 4/30/18	4.41	24.4	889	15.31
56RAT-00.1	3/1/18 - 5/31/18	3.74	19.2	684	12.6
56ROC-19.6	1/18/18 - 4/30/18	77.3	140	1820	53.1
56ROC-19.6	3/1/18 - 5/31/18	66.8	108	1110	37.14
56ROS-00.4	1/18/18 - 4/30/18	12.0	53.0	1340	29.88
56ROS-00.4	3/1/18 - 5/31/18	10.4	44.3	847	22.26
56ROC-17.1	1/18/18 - 4/30/18	56.6	180	3410	85.33
56ROC-17.1	3/1/18 - 5/31/18	42.3	136	2090	61.56
56MIC-00.2	1/18/18 - 4/30/18	15.1	47.4	1010	45.62
56MIC-00.2	3/1/18 - 5/31/18	6.90	26.2	437	30.42
56ROC-13.0	1/18/18 - 4/30/18	98.5	325	6730	215.5
56ROC-13.0	3/1/18 - 5/31/18	74.7	232	3840	150.5
56ROC-00.5	1/18/18 - 4/30/18	144	459	9730	292.5
56ROC-00.5	3/1/18 - 5/31/18	88.2	278	5930	206.5
56HAN-20.2	1/18/18 - 4/30/18	359	1140	21800	820.1
56HAN-20.2	3/1/18 - 5/31/18	268	839	14400	612.3
56SPA-00.0	1/18/18 - 4/30/18	1.69	23.4	658	14.84
56SPA-00.0	3/1/18 - 5/31/18	1.14	15.4	492	11.57
56CAL-00.1	1/18/18 - 4/30/18	2.20	24.4	353	29.41
56CAL-00.1	3/1/18 - 5/31/18	1.11	15.8	200	21.35
56HAN-06.2	1/18/18 - 4/30/18	358	1130	21400	849.6
56HAN-06.2	3/1/18 - 5/31/18	284	930	14200	636.1
56MIN-00.5	1/18/18 - 4/30/18	0.261	16.9	101	17.75
56MIN-00.5	3/1/18 - 5/31/18	0.324	14.3	41.5	16.38
56MAR-00.0	1/18/18 - 4/30/18	0.104	7.69	53.0	12.58
56MAR-00.0	3/1/18 - 5/31/18	0.147	8.30	29.7	13.87
56HAN-00.7	1/18/18 - 4/30/18	468	1130	18300	787.2
56HAN-00.7	3/1/18 - 5/31/18	400	924	11700	611.8

Gray shading indicates values we did not ultimately use for the mass balance analysis. At continuous turbidity sites, we used turbidity-derived estimates for SSC and TP, but MLR estimates for DIN. At some sites, we did not use any of the estimates, because we did not use the sites to define subbasin boundaries.

Subbasin contribution estimates and area-normalization

To estimate subbasin contributions of sediment and nutrients, we began with the seasonal load estimates from sampling locations, as described in the previous section. For SSC and TP, we used turbidity-derived load estimates for locations where we collected continuous turbidity data. For the remainder of locations (generally tributaries), we used bias-adjusted multiple linear regression (MLR) estimates. For DIN, we used MLR estimates at all locations.

We calculated the contribution from each subbasin as the load flowing out of the subbasin minus all the loads flowing into the subbasin. So for example, for the “Hangman Tekoa-Latah-Waverly” subbasin (see Figure X):

$$U_{\text{Hangman TekoaLatahWaverly}} = U_{56\text{HAN}32.8} - U_{56\text{HAN}55.1} - U_{56\text{LIT}00.1} - U_{56\text{COV}00.2}$$

Then, we divided the estimated subbasin contribution by its corresponding drainage area. This results in an area-normalized subbasin contribution, expressed in units such as tons/day/mi² for sediment, or lbs/day/mi² for nutrients. (This area-normalized load contribution is sometimes referred to as “yield.”) Tables C-7 through C-9 present subbasin load contributions and area-normalized contributions for SSC, TP, and DIN, respectively. Table C-10 presents subbasin flow contributions, which we calculated in the same manner, using continuous flow data.

Table C-7. Estimated subbasin load contributions for suspended sediment (SSC).

Subbasin Name	Area (mi ²)	Calculate as ^a	1/18/18 – 4/30/18 Subbasin Load contribution (tons/day)	3/1/18 – 5/31/18 Subbasin Load contribution (tons/day)	1/18/18 – 4/30/18 Area-normalized contribution (tons/day/mi ²)	3/1/18 – 5/31/18 Area-normalized contribution (tons/day/mi ²)
Upper Hangman	132.5	HAN551	79	76	0.59	0.57
Little Hangman Creek	63.9	LIT001	110	76	1.7	1.2
Cove Creek	11.9	COV002	3.1	2.8	0.26	0.23
Hangman Tekoa-Latah-Waverly	57.3	HAN328 - HAN551 - LIT001 - COV002	2.4	24	0.042	0.43
Rattlers Run Creek	13.8	RAT001	4.4	3.7	0.32	0.27
Hangman Creek Canyon	38.6	HAN202 - HAN328 - RAT001 - ROC005	-48 ^b	-38 ^b	-1.2 ^b	-0.97 ^b
Upper Rock	36.1	ROC171 - ROS004	45	32	1.2	0.88
Rose Creek	21.5	ROS004	12	10	0.56	0.49
Hoxie Valley - NF Rock Ck	55.3	ROC130 - ROC171 - MIC002	30	27	0.55	0.48
Mica Creek	23.2	MIC002	15	6.9	0.65	0.30
Rock Creek Canyon	41.4	ROC005 - ROC130	68	36	1.6	0.88
Spangle Creek	18.2	SPA000	1.7	1.1	0.093	0.062
California Creek	24.7	CAL001	2.2	1.1	0.089	0.045
Hangman Valley	43.8	HAN062 - HAN202 - SPA000 - CAL001	-23 ^b	-26 ^b	-0.53 ^b	-0.60 ^b
Minnie Creek	39.4	MIN005	0.26	0.32	0.0066	0.0082
Marshall Creek	39.2	MAR000 - MIN005	-0.16	-0.18	-0.0040	-0.0045
Lower Hangman	16.3	HAN007 - HAN062 - MAR000	Could not calculate ^b	Could not calculate ^b	Could not calculate ^b	Could not calculate ^b
Indian Canyon Creek	12.0		No data ^c	No data ^c	No data ^c	No data ^c

^a To avoid confusion between dashes and minus signs, the Location ID's in this table are simplified; e.g. 56HAN-55.1 is shown as HAN551.

^b We calculated subbasin load contributions by subtracting inflowing loads from outflowing loads. In some cases this creates large estimate uncertainty, where the inflowing and outflowing loads are both large, and the subbasin load is small. This is mainly an issue for mainstem Hangman Creek subbasins in the lower watershed. Subbasin load estimates for the Hangman Creek Canyon and Hangman Valley subbasins have large relative uncertainty and should be used with caution. Estimates for the Lower Hangman subbasin were unusable and are not listed here.

^c We did not sample Indian Canyon Creek during this project. Indian Canyon Creek flows into Hangman Creek downstream of the 56HAN-00.7 (Hangman Creek at mouth) sampling site and the USGS gage, and likely does not fully mix with Hangman Creek before reaching the Spokane River. Indian Canyon Creek has not historically been included in load and flow estimates for the mouth of Hangman Creek, but is technically part of the watershed.

Table C-8. Estimated subbasin load contributions for total phosphorus (TP).

Subbasin Name	Area (mi ²)	Calculate as ^a	1/18/18 – 4/30/18 Subbasin Load contribution (lbs/day)	3/1/18 – 5/31/18 Subbasin Load contribution (lbs/day)	1/18/18 – 4/30/18 Area-normalized contribution (lbs/day/mi ²)	3/1/18 – 5/31/18 Area-normalized contribution (lbs/day/mi ²)
Upper Hangman	132.5	HAN551	330	270	2.5	2.0
Little Hangman Creek	63.9	LIT001	240	170	3.8	2.7
Cove Creek	11.9	COV002	19	15	1.6	1.2
Hangman Tekoa-Latah-Waverly	57.3	HAN328 - HAN551 - LIT001 - COV002	57	78	1.0	1.4
Rattlers Run Creek	13.8	RAT001	24	19	1.8	1.4
Hangman Creek Canyon	38.6	HAN202 - HAN328 - RAT001 - ROC005	-8.3 ^b	-4.6 ^b	-0.21 ^b	-0.12 ^b
Upper Rock	36.1	ROC171 - ROS004	130	92	3.5	2.5
Rose Creek	21.5	ROS004	53	44	2.5	2.1
Hoxie Valley - NF Rock Ck	55.3	ROC130 - ROC171 - MIC002	76	55	1.4	1.0
Mica Creek	23.2	MIC002	47	26	2.0	1.1
Rock Creek Canyon	41.4	ROC005 - ROC130	150	89	3.7	2.1
Spangle Creek	18.2	SPA000	23	15	1.3	0.85
California Creek	24.7	CAL001	24	16	0.99	0.64
Hangman Valley	43.8	HAN062 - HAN202 - SPA000 - CAL001	-62 ^b	-58 ^b	-1.4 ^b	-1.3 ^b
Minnie Creek	39.4	MIN005	17	14	0.43	0.36
Marshall Creek	39.2	MAR000 - MIN005	-9.2	-6	-0.23	-0.15
Lower Hangman	16.3	HAN007 - HAN062 - MAR000	Could not calculate ^b	Could not calculate ^b	Could not calculate ^b	Could not calculate ^b
Indian Canyon Creek	12.0		No data ^c	No data ^c	No data ^c	No data ^c

^a To avoid confusion between dashes and minus signs, the Location ID's in this table are simplified; e.g. 56HAN-55.1 is shown as HAN551.

^b We calculated subbasin load contributions by subtracting inflowing loads from outflowing loads. In some cases this creates large estimate uncertainty, where the inflowing and outflowing loads are both large, and the subbasin load is small. This is mainly an issue for mainstem Hangman Creek subbasins in the lower watershed. Subbasin load estimates for the Hangman Creek Canyon and Hangman Valley subbasins have large relative uncertainty and should be used with caution. Estimates for the Lower Hangman subbasin were unusable and are not listed here.

^c We did not sample Indian Canyon Creek during this project. Indian Canyon Creek flows into Hangman Creek downstream of the 56HAN-00.7 (Hangman Creek at mouth) sampling site and the USGS gage, and likely does not fully mix with Hangman Creek before reaching the Spokane River. Indian Canyon Creek has not historically been included in load and flow estimates for the mouth of Hangman Creek, but is technically part of the watershed.

Table C-9. Estimated subbasin load contributions for dissolved inorganic nitrogen (DIN).

Subbasin Name	Area (mi ²)	Calculate as ^a	1/18/18 – 4/30/18 Subbasin Load contribution (lbs/day)	3/1/18 – 5/31/18 Subbasin Load contribution (lbs/day)	1/18/18 – 4/30/18 Area-normalized contribution (lbs/day/mi ²)	3/1/18 – 5/31/18 Area-normalized contribution (lbs/day/mi ²)
Upper Hangman	132.5	HAN551	4100	2500	31	19
Little Hangman Creek	63.9	LIT001	3100	1800	48	29
Cove Creek	11.9	COV002	330	230	28	20
Hangman Tekoa-Latah-Waverly	57.3	HAN328 - HAN551 - LIT001 - COV002	2800	1900	48	34
Rattlers Run Creek	13.8	RAT001	890	680	65	50
Hangman Creek Canyon	38.6	HAN202 - HAN328 - RAT001 - ROC005	990 ^b	1300 ^b	26 ^b	33 ^b
Upper Rock	36.1	ROC171 - ROS004	2100	1200	57	34
Rose Creek	21.5	ROS004	1300	850	62	39
Hoxie Valley - NF Rock Ck	55.3	ROC130 - ROC171 - MIC002	2300	1300	42	24
Mica Creek	23.2	MIC002	1000	440	44	19
Rock Creek Canyon	41.4	ROC005 - ROC130	3000	2100	72	51
Spangle Creek	18.2	SPA000	660	490	36	27
California Creek	24.7	CAL001	350	200	14	8.1
Hangman Valley	43.8	HAN062 - HAN202 - SPA000 - CAL001	-1400 ^b	-870 ^b	-33 ^b	-20 ^b
Minnie Creek	39.4	MIN005	100	42	2.5	1.1
Marshall Creek	39.2	MAR000 - MIN005	-48	-12	-1.2	-0.30
Lower Hangman	16.3	HAN007 - HAN062 - MAR000	Could not calculate ^b	Could not calculate ^b	Could not calculate ^b	Could not calculate ^b
Indian Canyon Creek	12.0		No data ^c	No data ^c	No data ^c	No data ^c

^a To avoid confusion between dashes and minus signs, the Location ID's in this table are simplified; e.g. 56HAN-55.1 is shown as HAN551.

^b We calculated subbasin load contributions by subtracting inflowing loads from outflowing loads. In some cases this creates large estimate uncertainty, where the inflowing and outflowing loads are both large, and the subbasin load is small. This is mainly an issue for mainstem Hangman Creek subbasins in the lower watershed. Subbasin load estimates for the Hangman Creek Canyon and Hangman Valley subbasins have large relative uncertainty and should be used with caution. Estimates for the Lower Hangman subbasin were unusable and are not listed here.

^c We did not sample Indian Canyon Creek during this project. Indian Canyon Creek flows into Hangman Creek downstream of the 56HAN-00.7 (Hangman Creek at mouth) sampling site and the USGS gage, and likely does not fully mix with Hangman Creek before reaching the Spokane River. Indian Canyon Creek has not historically been included in load and flow estimates for the mouth of Hangman Creek, but is technically part of the watershed.

Table C-10. Estimated subbasin flow contributions.

Subbasin Name	Area (mi ²)	Calculate as ^a	1/18/18 – 4/30/18 Subbasin Flow contribution (cfs)	3/1/18 – 5/31/18 Subbasin Flow contribution (cfs)	1/18/18 – 4/30/18 Area-normalized contribution (cfs/mi ²)	3/1/18 – 5/31/18 Area-normalized contribution (cfs/mi ²)
Upper Hangman	132.5	HAN551	280	210	2.1	1.6
Little Hangman Creek	63.9	LIT001	110	80	1.7	1.2
Cove Creek	11.9	COV002	13	11	1.1	0.88
Hangman Tekoa-Latah-Waverly	57.3	HAN328 - HAN551 - LIT001 - COV002	74	64	1.3	1.1
Rattlers Run Creek	13.8	RAT001	15	13	1.1	0.92
Hangman Creek Canyon	38.6	HAN202 - HAN328 - RAT001 - ROC005	34 ^b	32 ^b	0.89 ^b	0.82 ^b
Upper Rock	36.1	ROC171 - ROS004	56	39	1.5	1.1
Rose Creek	21.5	ROS004	30	22	1.4	1.0
Hoxie Valley - NF Rock Ck	55.3	ROC130 - ROC171 - MIC002	85	59	1.5	1.1
Mica Creek	23.2	MIC002	46	30	2.0	1.3
Rock Creek Canyon	41.4	ROC005 - ROC130	77	56	1.9	1.4
Spangle Creek	18.2	SPA000	15	12	0.82	0.64
California Creek	24.7	CAL001	29	21	1.2	0.87
Hangman Valley	43.8	HAN062 - HAN202 - SPA000 - CAL001	-15 ^b	-9.1 ^b	-0.34 ^b	-0.21 ^b
Minnie Creek	39.4	MIN005	18	16	0.45	0.42
Marshall Creek	39.2	MAR000 - MIN005	-5.2	-2.5	-0.13	-0.064
Lower Hangman	16.3	HAN007 - HAN062 - MAR000	Could not calculate ^b	Could not calculate ^b	Could not calculate ^b	Could not calculate ^b
Indian Canyon Creek	12.0		No data ^c	No data ^c	No data ^c	No data ^c

^a To avoid confusion between dashes and minus signs, the Location ID's in this table are simplified; e.g. 56HAN-55.1 is shown as HAN551.

^b We calculated subbasin flow contributions by subtracting inflowing flows from outflowing flows. In some cases this creates large estimate uncertainty, where the inflowing and outflowing flows are both large, and the subbasin flows is small. This is mainly an issue for mainstem Hangman Creek subbasins in the lower watershed. Subbasin flow estimates for the Hangman Creek Canyon and Hangman Valley subbasins have large relative uncertainty and should be used with caution. Estimates for the Lower Hangman subbasin were unusable and are not listed here.

^c We did not sample Indian Canyon Creek during this project. Indian Canyon Creek flows into Hangman Creek downstream of the 56HAN-00.7 (Hangman Creek at mouth) sampling site and the USGS gage, and likely does not fully mix with Hangman Creek before reaching the Spokane River. Indian Canyon Creek has not historically been included in load and flow estimates for the mouth of Hangman Creek, but is technically part of the watershed.

Scenario back-calculations

We calculated hypothetical scenarios for TP and SSC essentially by running the subbasin contribution estimates and area-normalization steps in reverse. This process included the following steps:

1. We used the long-term empirical model (see Appendix D) to scale back sediment loading, and therefore phosphorus loading, to meet a particular condition. For example, for the “Meet Concentrations” scenario, we scaled back sediment loading proportionately until TP met the March-May Spokane TMDL load allocation concentrations during 90% of years.
2. Because the watershed mass balance analysis is specific to 2018, we used the scaled-back long-term empirical model to find the scenario concentration (for concentration-based scenarios) or the load (for load-based scenarios) for March-May 2018.
3. We ran the subbasin contribution and area-normalization steps in reverse, finding the area-normalized subbasin contribution (yield) that would result in the correct March-May 2018 load or concentration at the mouth of Hangman Creek. For subbasins that had previously been estimated to have a negative load contribution, we scaled the negative load proportionately to loads upstream of that subbasin. This reflects the possibility that negative loads may have been an artifact of load estimate uncertainties, and avoids unrealistic scenario back-calculations with small positive contributions and large sinks.
4. We accounted explicitly for Wastewater Treatment Plant (WWTP) sources of TP during the back-calculation, to avoid unrealistic assumptions about nonpoint TP in subbasins with WWTPs.

Table C-11 summarizes the assumptions and values used for each scenario.

Table C-11. Assumptions and values used for TP scenario back-calculations.

Scenario	Basis assumption	Areal TP load contribution (lbs/day/mi ²)	TP % reduction at mouth of Hangman Ck.
Best of Today	Specify areal load contribution = 1.0 lbs/day/mi ² , reflecting approximate observed value for Spangle Ck., Hoxie Valley – NF Rock Ck., Mica Ck., and Cove Ck. subbasins	1.0	43%
California Creek	Specify areal load contribution = 0.64 lbs/day/mi ² , reflecting observed value for California Ck., subbasin	0.64	61%
Meet Concentrations (<i>preferred option</i>)	Average TP concentration at mouth of Hangman Ck. for March-May 2018 = 0.053 mg/L. Value derived by using long-term empirical model to scale back sediment loads to meet Spokane TMDL TP load allocation concentration during 90% of years.	0.36	76%
Meet Loads	Average TP load at mouth of Hangman Ck. for March-May 2018 = 61.3 lbs/day. Value derived by using long-term empirical model to scale back sediment loads to meet Spokane TMDL TP load allocation, as load, during 90% of years.	0.06	93%

Appendix D. Long-term empirical model documentation

To assess variability between years and to examine long-term trends, we used an empirical regression model, based on the long-term total suspended solids (TSS) dataset collected by Ecology's ambient monitoring program at the mouth of Hangman Creek (Site ID 56A070; referred to as 56HAN-00.7 in this report). We used TSS data collected from 1978 through 2019. Our model is similar to a multiple-regression approach (Cohn et al., 1989), but uses the non-linear relationship between $\log[\text{flow}]$ and $\log[\text{TSS}]$, together with a long-term trend term.

Step 1: Comparison of flow and TSS

For the first step toward developing the long-term empirical model, we adopted the preliminary (but, as it turns out, untrue) assumption that there has been no long-term trend in TSS, and that TSS concentration is solely a function of flow. Figure D-1 presents the comparison between mean daily flow reported by the USGS and observed TSS. The relationship is not linear. Rather, it is a curved relationship that is different for high vs. low-flow conditions. The relationship at high-flow is best described by a quadratic equation in logarithmic space, while for low-flow a proportional relationship (linear in logarithmic space) provides a better approximation.

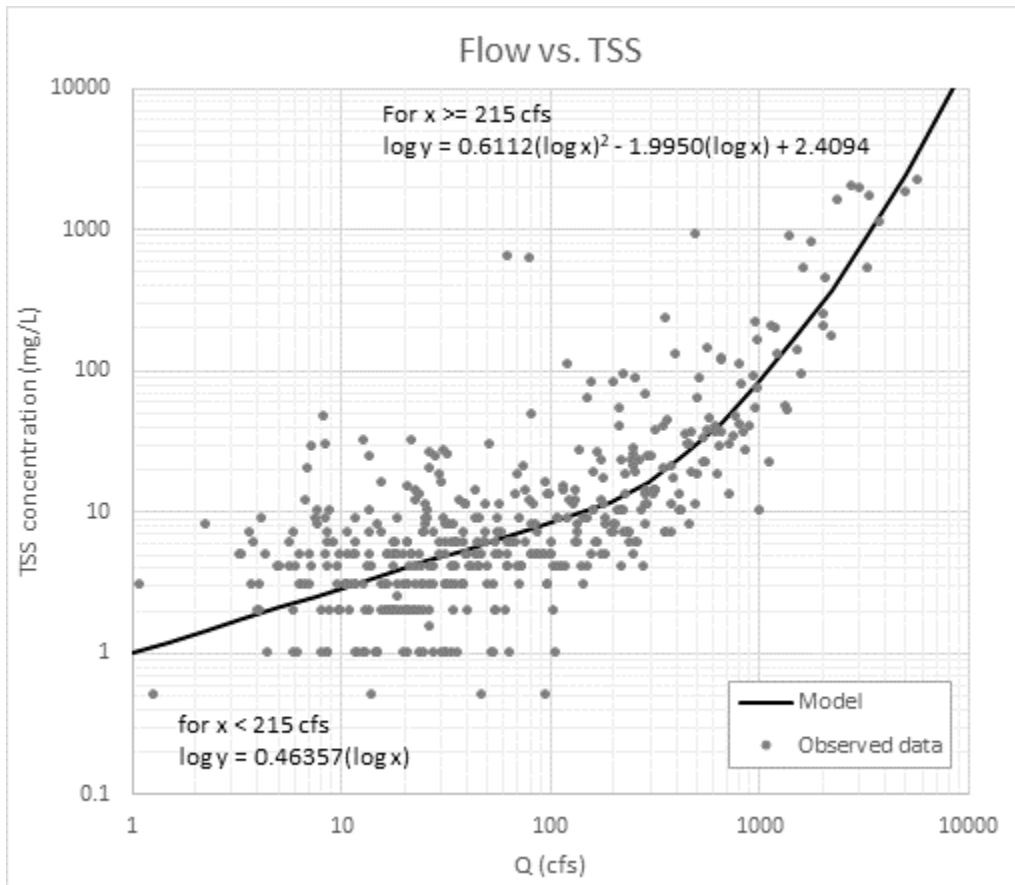


Figure D-1. Relationship between flow and total suspended solids (TSS) at the mouth of Hangman Creek, assuming no long-term trend.

Step 2: Trends analysis

For our second step, we compared observed TSS data to the predictions of the initial trendless regression shown in Figure D-1. Because TSS values span multiple orders of magnitude, we made this comparison in logarithmic space, as the base-10 logarithm of observed TSS concentrations minus the base-10 logarithm of the predicted concentration. We plotted these residuals against time to look for long-term trends. As shown in Figure D-2 (also presented as Figure 17 in the main report body), there is a strong declining trend across results from all flow ranges. We discuss the water quality management implications of this in the **results and discussion** section of the main report body.

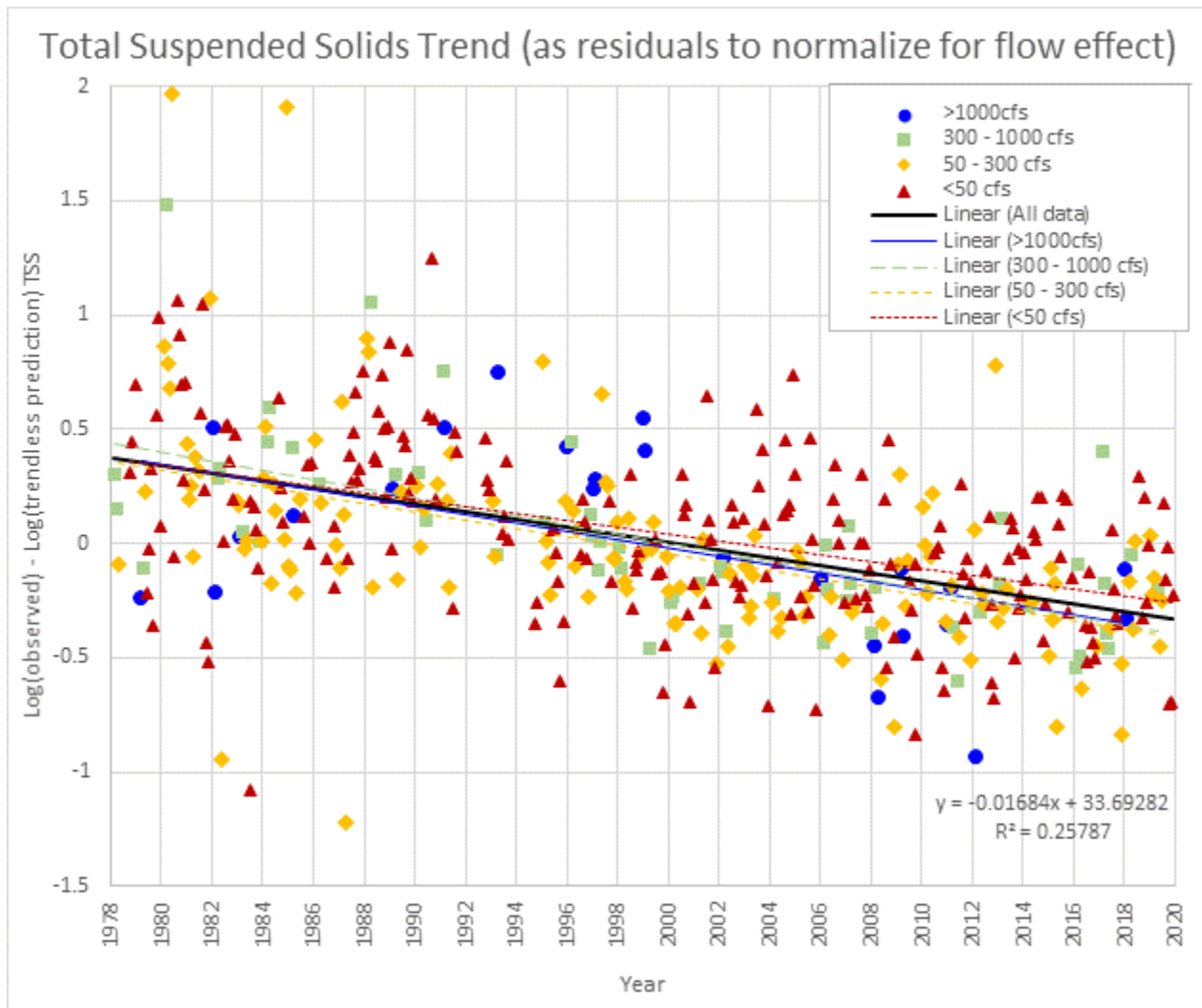


Figure D-2. Declining trend in total suspended solids (TSS) at the mouth of Hangman Creek, 1978-2019, normalized for flow.

The presence of this trend accounts for some of the variability in the relationship between TSS and flow shown in Figure D-1. Therefore, for our final model prediction, we added a bias correction term based on the “all data” (thick black line) trend in Figure D-2. The final model is expressed as:

If $Q \geq 215$ cfs,

$$\log K = [0.6112(\log Q)^2 - 1.995(\log Q) + 2.4094] - [0.01684f_y - 33.69282]$$

If $Q < 215$ cfs

$$\log K = [0.46357(\log Q)] - [0.01684f_y - 33.69282]$$

Where:

K = TSS concentration (mg/L)

Q = mean daily flow, as reported by USGS (cfs)

f_y = year fraction (e.g. July 1, 2016 = 2016.5)

For both versions of the equation, the first set of square brackets describes the flow-dependency, while the second set of square brackets describes the long-term trend.

Translation from TSS to TP

To predict TP during the November-June period when phosphorus is most strongly linked to sediment, we compared TSS and TP data to build a “translation” between parameters. To do this, we used the following data:

- Ambient data collected at the mouth of Hangman Creek from October 2007 through December 2019. TP data collected prior to 2007 used a different lab method, which could underestimate results during high-sediment conditions.
- TP and TSS data collected during the 2018 high-flow study from upper and Lower Hangman Creek, Little Hangman Creek, Rock Creek, Rose Creek, and Mica Creek. These areas all display a fundamentally consistent relationship between TP and TSS (see Figure 12 in the main report body).

This “TSS to TP” approach has several advantages over using a dedicated “TP only” model relating flow directly to TP:

- This approach allowed us to use sites other than the mouth of Hangman Creek for building the TSS to TP translation, from a dataset that targeted high flow, high sediment conditions. This meant we could use many data points at higher concentrations than were present in the ambient dataset from the mouth, resulting in a much stronger “high end” of the curve.
- The period of reliable TP data from the mouth of Hangman Creek begins in WY 2008. This means a “TP only” model would only be valid since that time.
- This approach allows us to easily predict the impact of hypothetical sediment reductions on TP in Hangman Creek.

Figure D-3 presents the comparison between TSS and TP data. The relationship between these parameters was best described using quadratic equations in logarithmic space. There is a clear inflection (bend) in the relationship at around 10 mg/L TSS or 0.1 mg/L TP.

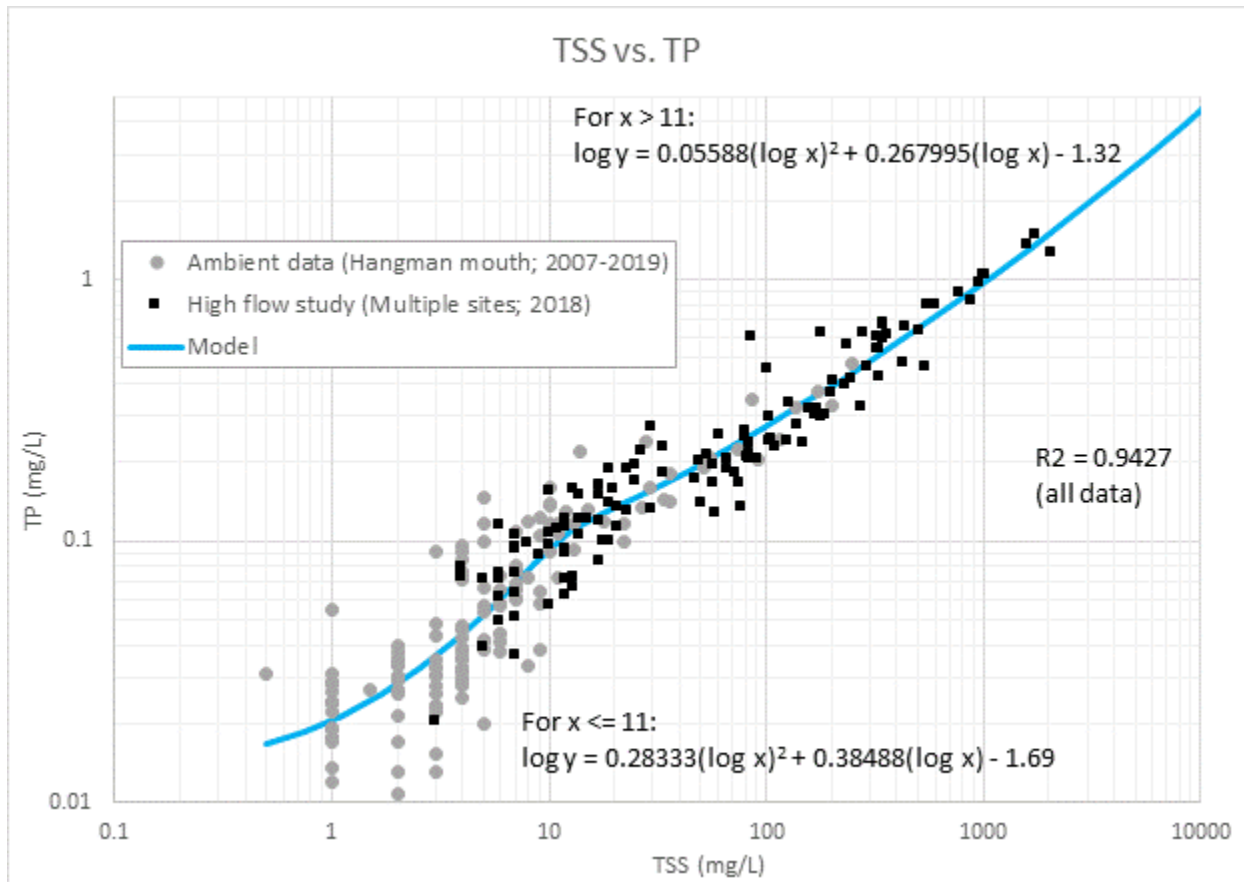


Figure D-3. Relationship between total suspended solids (TSS) and total phosphorus (TP) at mouth of Hangman Creek and comparable locations.

Dedicated “TP only” model

Despite the advantages of the TSS-to-TP approach, the TSS-to-TP translation has one downside. It does not accurately predict TP during low-flow summertime conditions. During this period, phosphorus often originates from groundwater sources and does not strongly correlate to sediment. Therefore, we used a dedicated “TP-only” model to predict TP during the July-October low-flow period. Its predictions are valid starting October 2007, the period of reliable TP data. This model is a simple correlation between flow and observed TP with a correction for seasonality:

$$K = [0.001085Q + 0.01248] - [0.0001439d_j - 0.034535]$$

Where:

K = TP concentration (mg/L)

Q = mean daily flow, as reported by USGS (cfs)

D_j = Julian date (e.g. Jan 1 = 1; July 1 = 182)

Model evaluation

Table D-1 presents goodness-of-fit statistics for the long-term empirical model. We provide statistics for TSS, for the translation to TP, and for the TP-only model. For TSS, we compare to ambient data collected at the mouth of Hangman Creek since 1978. For TP, we compare to ambient data collected since October 2007, the period of reliable TP data. Figure D-4 presents logarithmic-scale scatter plots of observed vs. predicted data for TSS and TP, and Figures D-5 and D-6 present time-series plots showing observed vs. predicted data.

Table D-1. Goodness-of-fit statistics for the long-term empirical model.

Metric	TSS	TP (TSS-to-TP translation of long-term TSS model)	TP (dedicated “TP only” model)
RMSE	284 mg/L	0.044 mg/L	0.0092 mg/L
RMSE CV	504%	55.5%	28.3 %
Bias	-0.3 mg/L	-0.005 mg/L	+0.0000 mg/L
% Bias	-0.5%	-6.3%	+0.03%

$$RMSE = \sqrt{\frac{\sum (K_{modeled} - K_{observed})^2}{n}}$$

$$Bias = \frac{\sum (K_{modeled} - K_{observed})}{n}$$

$$RMSE\ CV = \frac{RMSE}{K_{observed}}$$

$$\% Bias = \frac{Bias}{K_{observed}}$$

The results of this model reflect the inherent variability in the relationship between flow, TSS, and TP. For any single daily model prediction, there is some uncertainty. However, the strength of this model lies in the large number of data points, which allows the model to find the central

tendency of the data, while accurately accounting for flow-dependency and long-term trends. We expect model estimates of seasonal and yearly average loads to be robust.

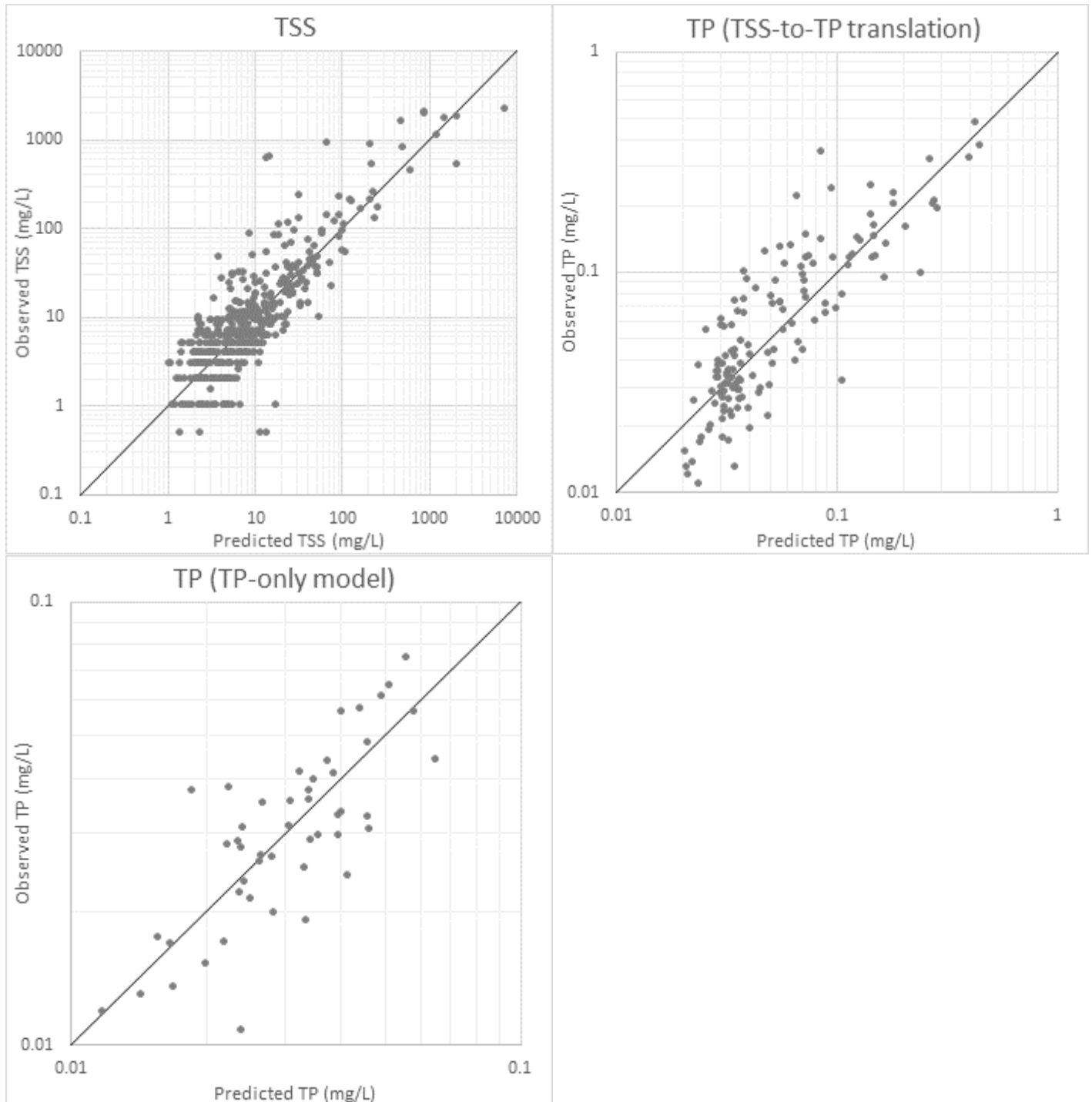


Figure D-4. Scatter plots comparing predicted vs. observed results for the long-term empirical model.

The black line shown on each plot is the ideal 1-to-1 line.

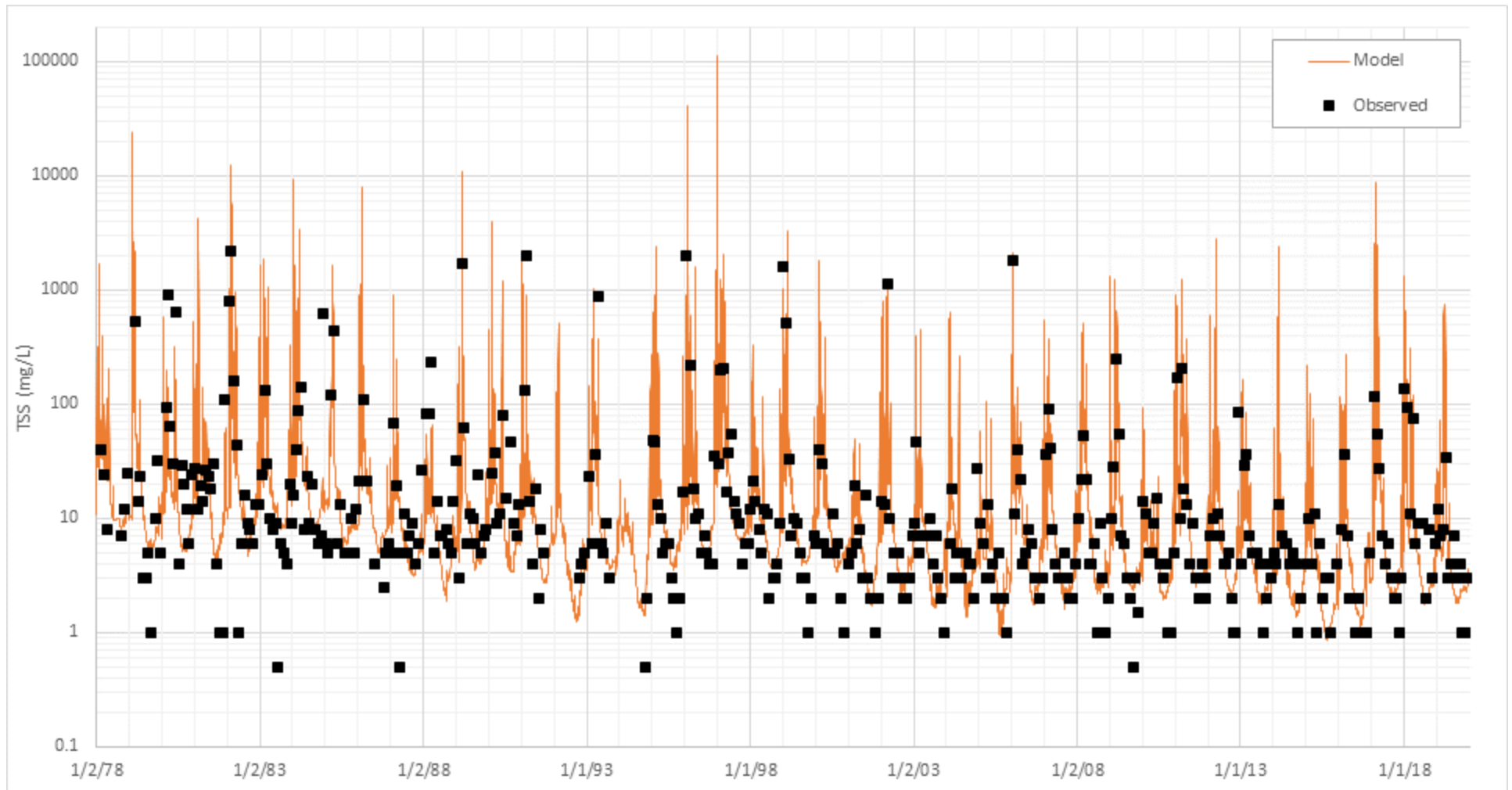


Figure D-5. Time-series plot showing observed vs. predicted total suspended solids (TSS).

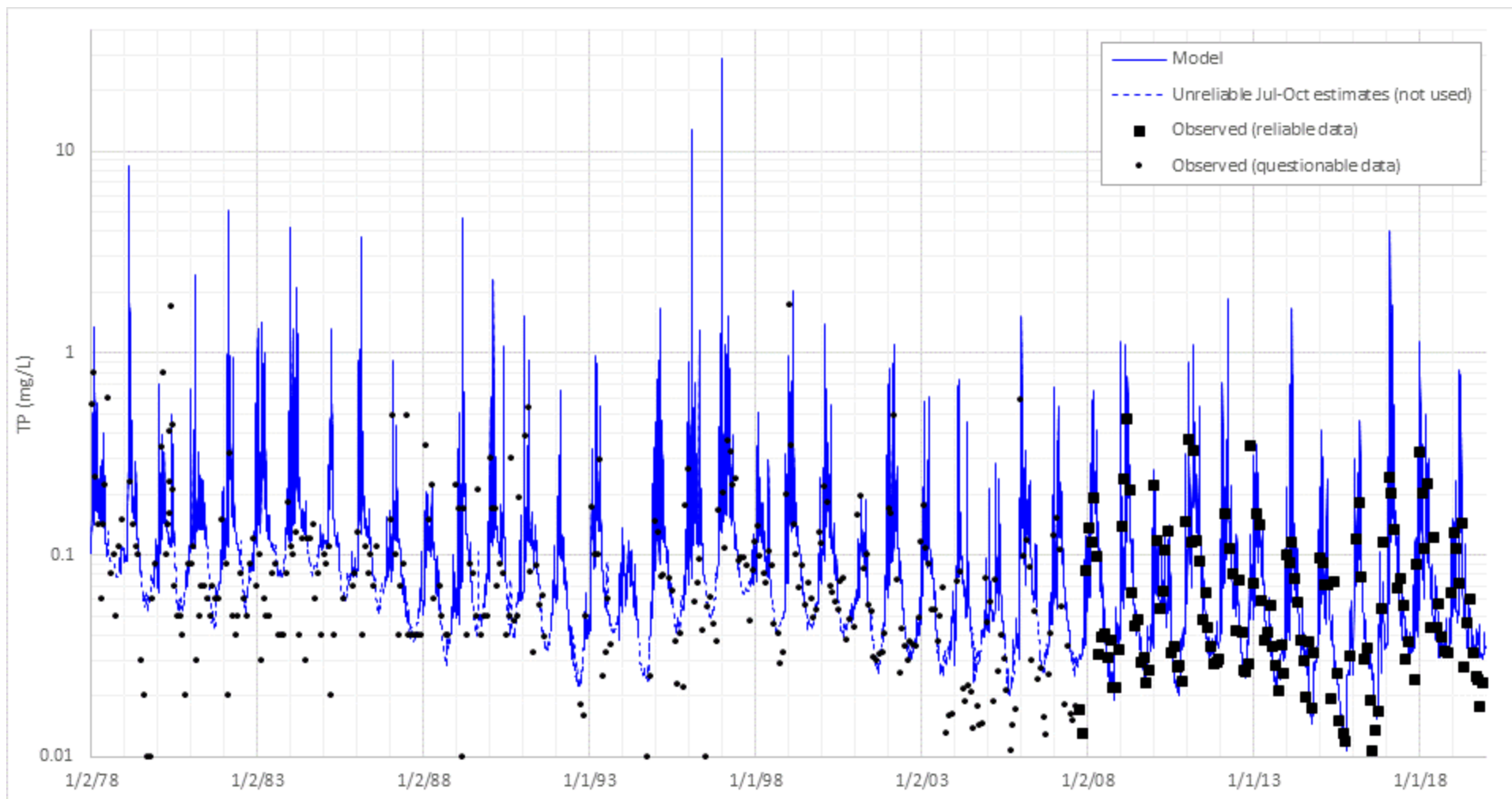


Figure D-6. Time-series plot showing observed vs. predicted total phosphorus (TP)

November-June predictions come from the TSS-to-TP translation of the long-term TSS model.

July-October predictions come from the dedicated TP model, which is only valid after October 2007.

Appendix E. QUAL2Kw model documentation

QUAL2Kw Modeling Framework

We used the QUAL2Kw 6.0 modeling framework (Pelletier and Chapra, 2008) to develop the loading capacity for nutrients and to make predictions about water quality under various scenarios. The QUAL2Kw model framework and complete documentation are available at <http://www.ecy.wa.gov/programs/eap/models.html>.

The QUAL2Kw 6.0 modeling framework has the following characteristics:

- One dimensional. The channel is well-mixed vertically and laterally. Also includes up to two optional transient storage zones connected to each main channel reach (surface and hyporheic transient storage zones).
- The option to use steady-state flow routing or non-steady, non-uniform flow using kinematic wave flow routing. Repeating diel or fully continuous simulation with time-varying boundary conditions for periods of up to one year.
- Dynamic heat budget. The heat budget and temperature are simulated as a function of meteorology on a continuously varying or repeating diel time scale.
- Dynamic water-quality kinetics. All water quality state variables are simulated on a continuously varying or repeating diel time scale for biogeochemical processes.
- Heat and mass inputs. Point and non-point loads and abstractions are simulated.
- Three groups of algae can be simulated. This includes bottom algae (periphyton), as well as two general algal groups that can be used to represent phytoplankton or macrophytes.
- Sediment diagenesis and heterotrophic metabolism in the hyporheic zone can both be optionally included.
- Variable stoichiometry. Luxury uptake of nutrients by the bottom algae (periphyton) is simulated with variable stoichiometry of N and P.

For this study, we used the fully continuous dynamic simulation option. This is the preferred option for modeling streams like Hangman Creek that have slow movement of water and long travel times during the summer. This option allows for changes in upstream boundary conditions to impact simulated downstream water quality after the appropriate travel time, which can be multiple days.

Model Segmentation

We used QUAL2Kw to model about 15 miles of Lower Hangman Creek. The modeled reach extends from the upstream edge of the Hangman Valley Golf Course, just below the confluence of Stevens Creek, to the mouth of Hangman Creek at the Spokane River. We divided this reach into 118 model segments, each 200m in length (Figure E-1).

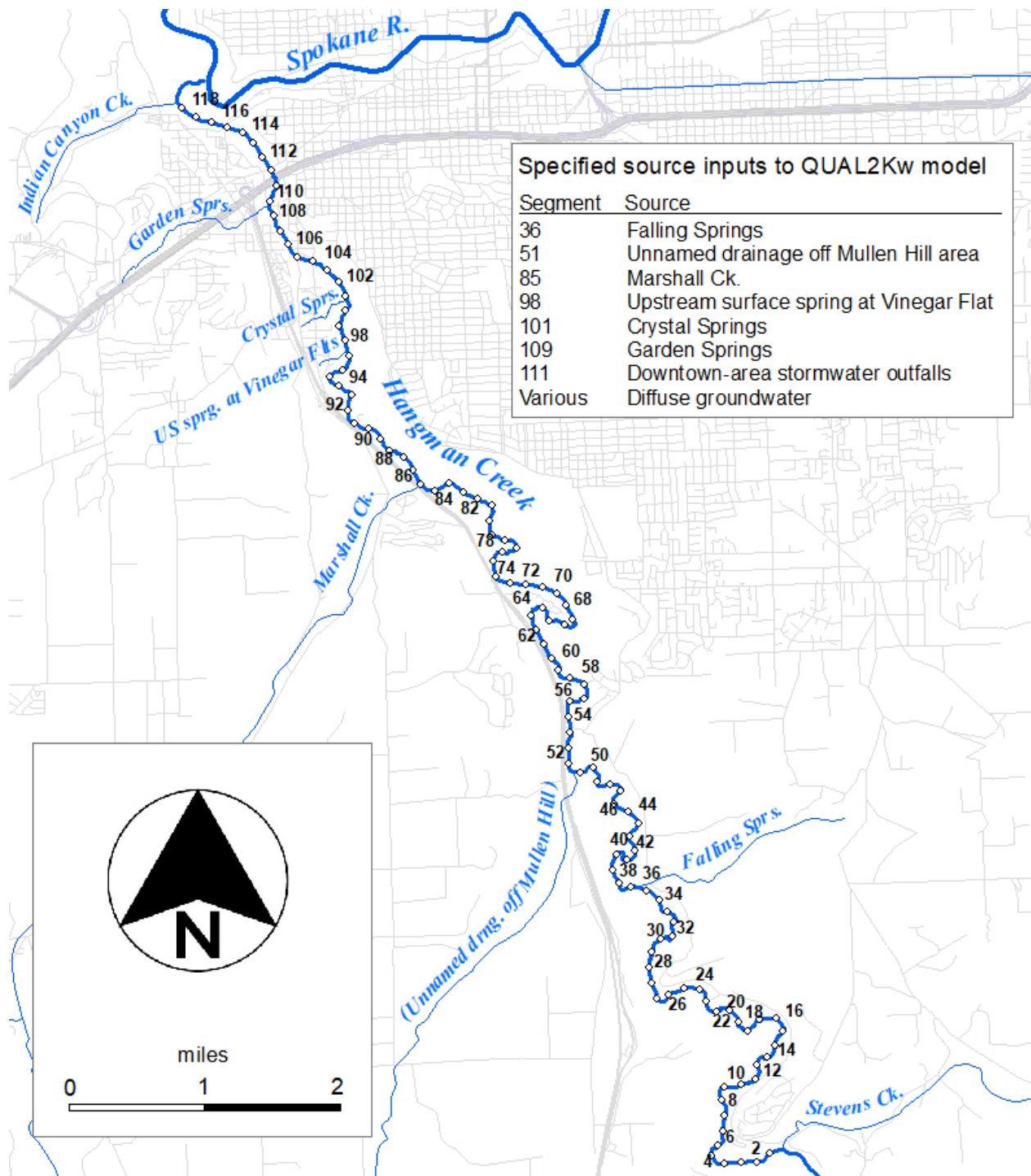


Figure E-1. Model segmentation and specified source inputs for Lower Hangman QUAL2Kw model.

Channel Geometry

We calculated channel geometry for each model segment as power functions relating width, depth, and velocity to flow:

$$W=aQ^b \quad D=cQ^f \quad V=kQ^m$$

Where:

W = width (m)	a = width coefficient	b = width exponent
D = depth (m)	c = depth coefficient	f = depth exponent
V = velocity (m/s)	k = velocity coefficient	m = velocity exponent
Q = flow (cms)		

These power functions are related by the continuity equation:

$$Q = WDV = (aQ^b)(cQ^f)(kQ^m)$$

Therefore:

$$b + f + m = 1 \quad \text{and} \quad ack = 1$$

Table E-1 summarizes the data sources we used to determine the power function for each model segment. The kinematic wave dynamic flow routing means that channel geometry and flow balance both affect one another. Therefore, we developed geometry and flow balances together, in an iterative adjustment process until the model provided good simulations of width, depth, and velocity, as well as flow.

Channel geometry in Hangman Creek varies greatly from one location to the next, with wide, deep, slow pools punctuated by narrow, shallow, fast riffles. Capturing this variability is key to an accurate simulation of temperature and water quality. Figures E-2 through E-4 present modeled and observed width, depth, and time-of-travel.

The model provides good representations of width, depth, and velocity. One limitation of the model geometry is that it overestimates longitudinal dispersion. This can be seen in Figure E-4 as the predicted dye curve being too “wide”, with the leading edge arriving too soon, and the tailing edge lingering too long, even though the timing of the peak is reasonable. This is the result of “numerical dispersion” relating to model segment size. The only fix for this would be to use a smaller model segment size, such as 100m rather than 200m. However, that would result in a model size that would exceed the memory limitations, and a model run time that would be prohibitive. For the intended purpose of simulating water quality and continuous nutrient transport, the extra dispersion is acceptable.

Table E-1. Data sources and approach for calculating QUAL2Kw channel geometry

Geometric dimension	Low-flow end of power curve (~20-50 cfs at Hangman mouth)	Medium-flow end of power curve (~100-300 cfs at Hangman mouth)
Width	2017 National Agriculture Imagery Program (NAIP) orthophotos. Digitized at 1:1000 scale using ArcGIS, sampled using TTools (Ecology, 2015).	Google Earth historical imagery for 4/7/2016. Sampled manually using Google Earth measure tool.
Depth	Match summertime diel temperature ranges (shallower channel results in wider temperature range, deeper results in narrower range)	High-resolution longitudinal depth data collected by Ecology April 27-28, 2016 during float survey.
Velocity	Time-of-travel dye studies conducted by Ecology June 16, 2009 and July 15, 2009. Simulated dye injection explicitly using the model, and match observed timing of dye curves at downstream site.	Match timing of sediment/turbidity spikes recorded above Hangman Valley Golf Course (56HAN-14.5, represented as headwater boundary condition in the model) and at Meadowlane Road (56HAN-06.2, represented by segment 70 in the model).

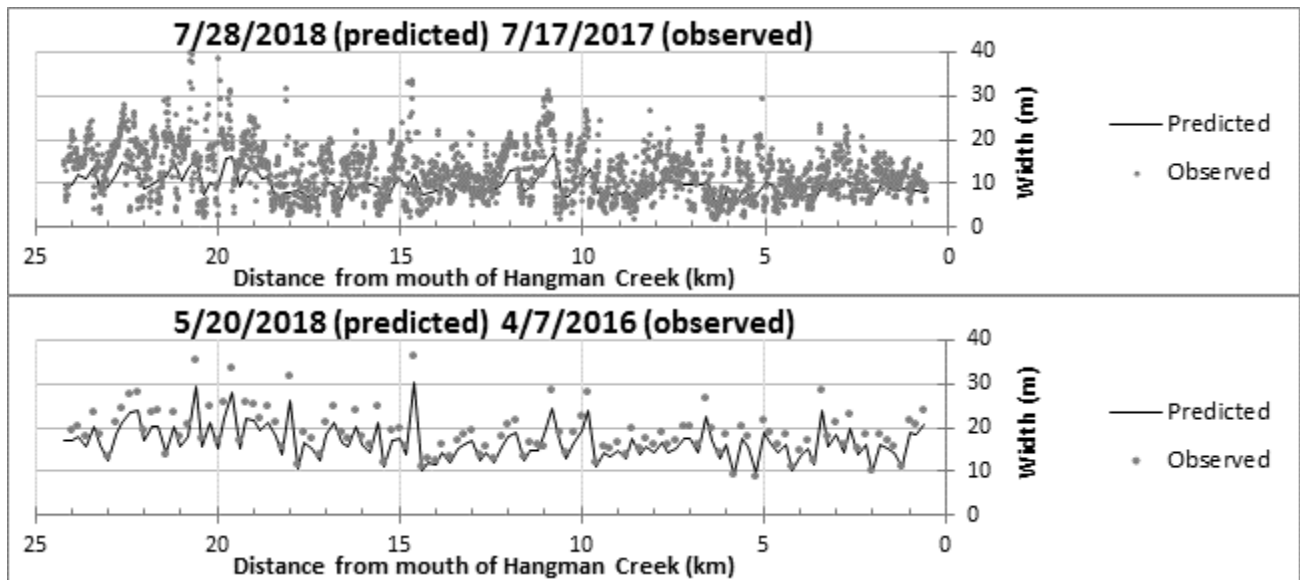


Figure E-2. Modeled and observed channel width

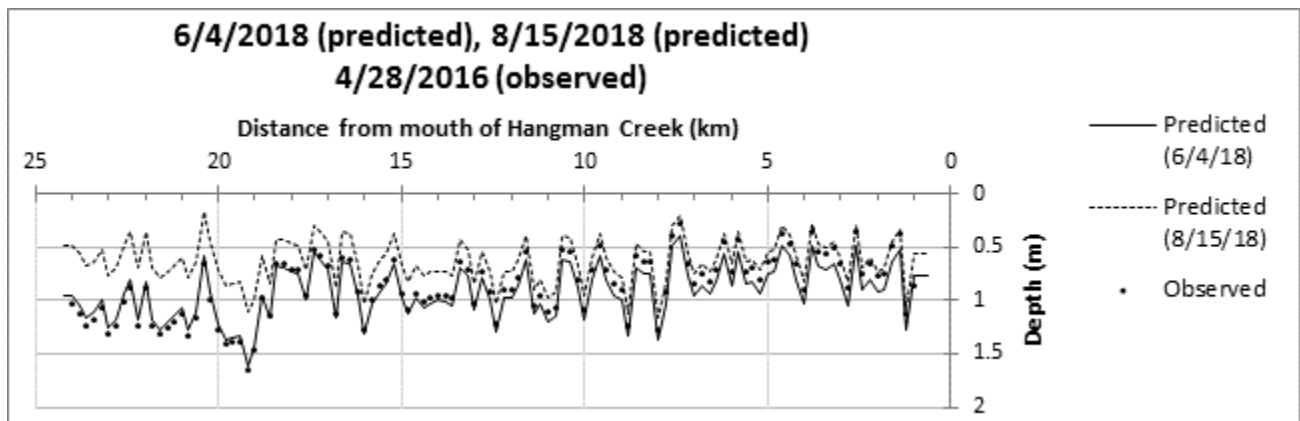


Figure E-3. Modeled and observed channel depth.

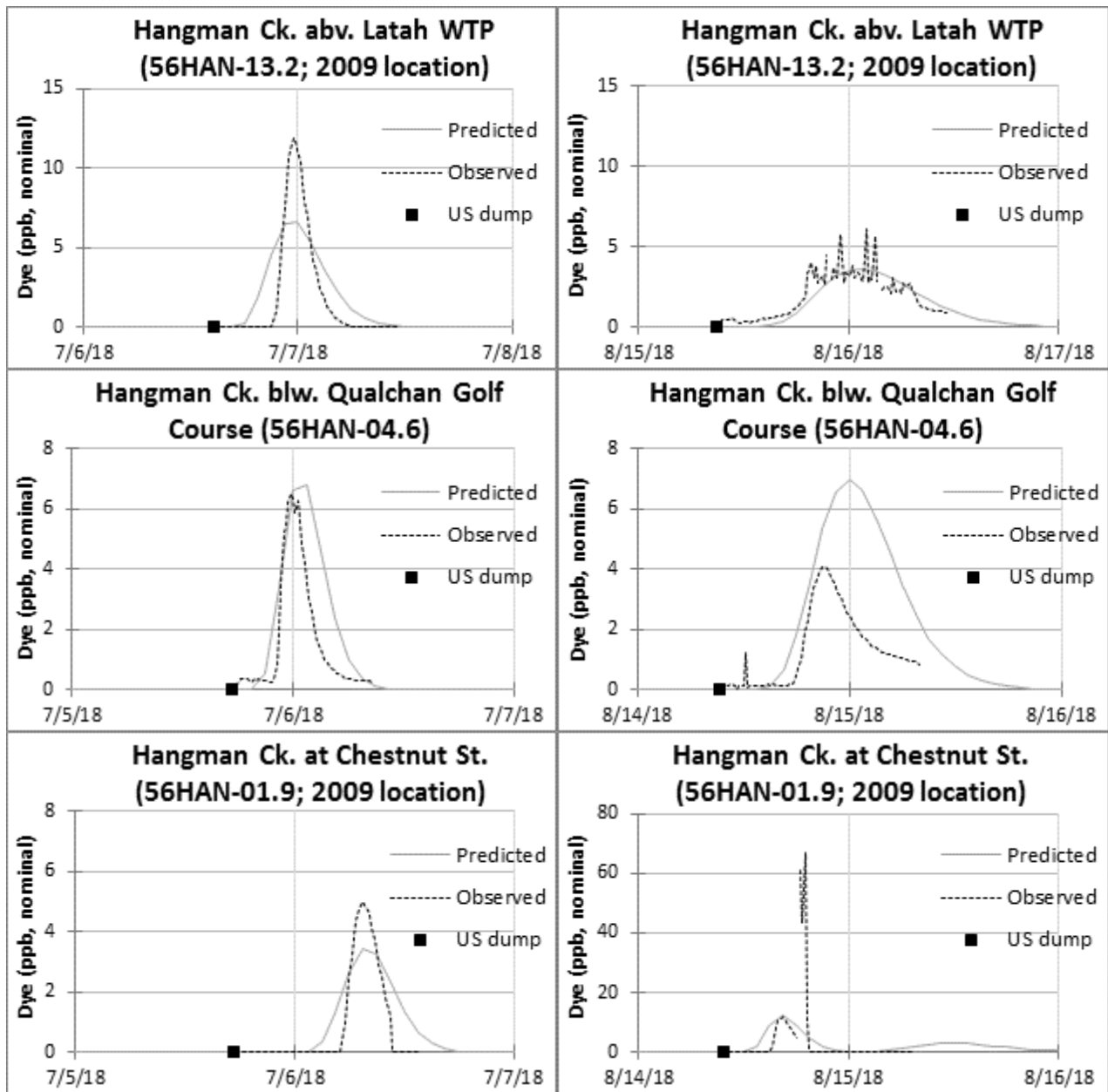


Figure E-4. Modeled and observed time-of-travel, as indicated by rhodamine WT dye concentration.

Time of travel dye studies actually occurred June 15-17, 2009, and July 14-16, 2009. We chose the July 5-7, 2018 and August 14-16, 2018 time periods for comparison in the model, because these periods had equivalent streamflow conditions. We did not calibrate the rhodamine WT sensors during the study, as exact concentrations are unimportant. Dye curve timing is the important consideration.

Simulation Time Period

We used the QUAL2Kw model to simulate a period from May 5 through October 30, 2018.

Flow Balances

The flow balance describes the volume of water entering and exiting the model domain, and the “balance” of water remaining in the model domain, representing mainstem river flow. The primary ways in which water enters the model domain are:

- The upstream model boundary (Hangman Creek above Hangman Valley Golf Course; 56HAN-14.5)
- Six natural tributaries, including streams and surface springs
- Stormwater discharge through outfalls
- Diffuse inputs over multiple model segments, representing gains from groundwater

We did not specify any abstractions, or any reaches that lost flow to groundwater. All reaches in the model domain appeared to be either gaining or neutral. Table E-2 summarizes upstream boundary, tributary and stormwater inflows. Table E-3 summarizes diffuse groundwater inflows.

The diffuse groundwater inflows shown in Table E-3 reflect a large groundwater input to Lower Hangman Creek. This input occurs mainly between Meadowlane Rd. (RM 6.2) and Chestnut St. (RM 1.8). Along with the surface springs that occur in this area, this groundwater contributes a large fraction of the flow at the mouth of Hangman Creek during the summer months.

Table E-2. Summary of upstream boundary, tributary, and stormwater inflows included in the QUAL2Kw model.

Source	Monitoring station ID	Flow basis	Range of Values (cfs) ^a min-max (mean)	10%ile flow (cfs) ^{a b}
Upstream model boundary	56HAN-14.5	Continuous gaged flow data	5.84-268 (36.5)	7.81
Falling Springs	(N/A)	Assume flow is half of flow observed at 56Unk(MUL)-00.0. (Watershed area 5.9 mi ² vs 9.1 mi ² for UnkMUL)	0.104-1.23 (0.313)	0.13
Unnamed drainage off Mullen Hill area	56Unk(MUL)-00.0	Excellent correlation between measured flows here and at Marshall Ck. ($R^2 = 0.99967$). Used measured flows here along with continuous gaged Marshall Ck. record to estimate continuous flows.	0.208-2.46 (0.626)	0.26
Marshall Ck.	56MAR-00.0	Continuously gaged flow data at 56MAR-00.4, just upstream of the old oxbow swamp at Qualchan Dr., confirmed by measurements taken at 56MAR-00.0.	0.901-16.5 (4)	1.31
Upstream surface spring at Vinegar Flats	56Spr(VinUS)-00.1	Linear interpolation between measured flows	1.8-2.7 (2.2)	1.85
Crystal Springs	56CRY-00.3	Linear interpolation between measured flows	0.69-2.2 (1.14)	0.69
Garden Springs	56GAR-00.0	Use correlation with Marshall Creek record to approximate, because of high-flow measurement uncertainty at this site.	0.336-1.01 (0.54)	0.39
Stormwater outfalls	Various monitored and unmonitored outfalls	Based on stormwater patterns evident in Hangman USGS flow record (See Appendix F).	0-24.6 (0.073)	0

^a QUAL2Kw uses metric units, so flow is simulated in cms. We present model input and output flow values in this report in cfs for the sake of reader familiarity.

^b The 10th percentile of flow model input values represents typical (non-extreme) conditions during summer low-flow months.

Table E-3. Per-reach groundwater inflows, in cfs, through the QUAL2Kw simulation period.
Groundwater input volumes in the QUAL2Kw model smoothly interpolate between the dates shown in this table.

Reach	# of model segments	5/15/18	6/12/18	7/18/18	8/15/18	9/12/18	10/10/18
Model Boundary – Yellowstone Pipeline	48	2.18	1.36	0.93	0.93	1.02	1.55
Yellowstone – Campion Park	8	2.82	1.76	1.20	1.20	1.32	2.00
Campion – Meadowlane Rd.	14	0.64	0.40	0.27	0.27	0.30	0.45
Meadowlane – Blw Qualchan GC	14	2.29	1.70	1.50	1.50	1.50	2.30
Blw Qualchan – RR bridge	10	16.17	12.58	3.76	2.55	2.77	2.90
RR bridge – Chestnut St.	11	4.00	5.00	6.34	3.75	2.75	3.25
Chestnut – Mouth	13	0	0	0	0	0	0
Total groundwater inflow		28.1	22.8	14.0	10.2	9.7	12.5

Boundary Condition Water Quality Inputs

The boundary conditions in a water quality model are a description of water quality wherever water enters the model domain. The boundary conditions in the Lower Hangman Creek QUAL2Kw model include the upstream model boundary, tributaries, stormwater, and diffuse groundwater. The continuous version of QUAL2Kw requires an hourly time-series of data for each model variable⁶, for each of these boundary points. Table E-4 summarizes the range of values for each boundary condition input variable, along with the data or calculation method used to generate the input time-series.

⁶ When talking about water quality models, the convention is to use the term “variable” to refer to a modeled quantity of something (e.g. dissolved oxygen, ammonia nitrogen). This is analogous to the term “parameter” when talking about sampling and data collection. Confusingly, when talking about models, we use the term “parameter” to refer to a calibration constant or a rate parameter that governs model processes (e.g. algal growth rate, phosphorus remineralization rate).

Table E-4. Summary of continuous boundary condition water quality inputs for the Lower Hangman Creek QUAL2Kw model.

We present values in the format: Min-Max (Mean)

Model variable	Temp (C)	Cond (uS/cm @25 C)	ISS (mg/L)	DO (mg/L)	CBODf (mg/L) ^a	Org N (ug/L)	NH4 (ug/L)	NO2-3 (ug/L)	Org P (ug/L)	Inorg P (ug/L)	Phyto (ug/L)	Detritus (mg/L)	Chloride (mg/L)	Alk (mg/L)	pH (S.U.)
Sample parameter equivalent	Temp (C)	Cond (uS/cm @25 C)	TNVSS (mg/L)	DO (mg/L)	DOC * 2.69 ^b	TPN -NH4 - NO23 ^c	NH4	NO2-3	TP-SRP- (Phyto* 1:1) ^d	SRP	9.97*(TSS - TNVSS) - 17.8 ^e	(TOC-DOC) *2.5 ^f	Chloride (mg/L) ^g	Alk (mg/L)	pH (S.U.)
Upstream model bdy	6.09-25.5 (17.2) ^h	217-366 (328) ^h	2.68-498 (12.6) ⁱ	5.24-15.7 (9.19) ^h	6.13-14 (9.84) ^j	223-2740 (380) ^k	3-100 (14.8) ⁱ	11.2-3480 (1150) ⁱ	10-259 (36.3) ⁱ	1.28-229 (46.7) ⁱ	2.15-42 (10.1) ^m	1.5 ⁿ	4.52-6.62 (5.77) ^j	96.7-179 (149) ^k	7.34-9.09 (8.07) ^h
Falling Springs	3.76-18 (11.2) ^o	372-400 (385) ^o	0.5-14 (3.7) ^o	7.41-10.6 (8.98) ^o	5.23-22.5 (9.9) ^o	0.0763-618 (268) ^o	3-12 (5.67) ^o	1440-3740 (2930) ^o	0-23.8 (3.87) ^o	57.4-76 (66.3) ^o	0 ^{or}	0-1.63 (0.729) ^o	8.04-8.89 (8.73) ^o	173-175 (174) ^o	7.59-8.17 (7.9) ^o
56Unk(MUL)-00.0	3.76-18 (11.2) ^p	372-400 (385) ^j	0.5-14 (3.7) ^j	7.41-10.6 (8.98) ^q	5.23-22.5 (9.9) ^j	0.0763-618 (268) ^j	3-12 (5.67) ^j	1440-3740 (2930) ^j	0-23.8 (3.87) ^j	57.4-76 (66.3) ^j	0 ^r	0-1.63 (0.729) ^j	8.04-8.89 (8.73) ^j	173-175 (174) ^j	7.59-8.17 (7.9) ^s
56MAR-00.0	2.22-22.3 (14.1) ^t	268-427 (300) ^k	2-31 (17) ^j	2.3-10.1 (5.38) ^q	11.7-25.6 (15.2) ^j	296-579 (384) ^j	19-57 (32.2) ^j	38-351 (157) ^j	20-116 (71.7) ^j	22.9-130 (70.7) ^j	0 ^r	0.5-2.3 (1.31) ^j	13.2-23.9 (15.4) ^j	116-156 (128) ^j	7.12-7.56 (7.37) ^s
56Spr(VinUS)-00.1	8.92-18.6 (13.6) ^p	429-447 (441) ^j	0.5 ^u	5.73-24.4 (11.1) ^q	3.2-5.27 (3.97) ^j	102-233 (143) ^j	3-17 (10.7) ^j	1520-2020 (1810) ^j	0-1.3 (0.581) ^j	16.7-35.2 (25.1) ^j	0 ^r	0-1.69 (1.07) ^j	16.7-17.3 (17) ^j	193-201 (197) ^j	7.44-8.81 (7.92) ^s
56CRY-00.3	8.53-11.3 (9.66) ^p	395-424 (407) ^j	0.5-3 (0.844) ^j	8.65-10 (9.29) ^q	5.3-10.3 (6.54) ^j	0-747 (242) ^j	3 ^u	3670-5600 (4150) ^j	0 ^j	78.8-87.5 (83.6) ^j	0 ^r	0-0.675 (0.377) ^j	30.8-33.3 (31.8) ^j	130-134 (133) ^j	7.61-7.67 (7.64) ^s
56GAR-00.0	5.68-19.4 (12.7) ^p	687-720 (708) ^j	13-20 (15.5) ^j	8.14-11.7 (9.47) ^q	5.94-8.61 (6.79) ^j	137-217 (165) ^j	3-8 (4.23) ^j	914-1410 (1270) ^j	11-24 (17) ^j	99.3-139 (112) ^j	0 ^r	0.325-1.15 (0.79) ^j	107-117 (111) ^j	168-171 (170) ^j	8.17-8.4 (8.28) ^s
Stormwater	16.53 ^v	89 ^w	133 ^x	9.15 ^y	8 ^v	333 ^z	254 ^z	991 ^z	309 ^z	84.9 ^z	0 ^r	0 ^{aa}	4 ^{bb}	38 ^{cc}	6.87 ^v
Groundwater (segs 1-61)	11.4 ^{dd}	547 ^{dd}	0 ^{ee}	2.53 ^{dd}	8.88 ^{dd}	0 ^{dd}	5 ^{dd}	1110 ^{dd}	4.3 ^{ff}	56.8 ^{ff}	0 ^{ee}	0 ^{ee}	11.3 ^{dd}	312 ^{dd}	7.15 ^{dd}
Groundwater (segs 62-118)	9.94-13.7 (12.59) ^{gg}	528 ^{hh}	0 ^{ee}	1.5 ^{hh}	2.39 ^{hh}	104 ⁱⁱ	3 ⁱⁱ	2250 ⁱⁱ	0 ^{hh}	61.6 ^{hh}	0 ^{ee}	0 ^{ee}	16.9 ^{hh}	240 ^{hh}	7.41 ^{hh}

^a QUAL2Kw also has a model variable for slow CBOD (CBODs). We did not use this variable, but rather assigned all DOC to the fast CBOD (CBODf) variable because of the way the model handles carbon exchange with the hyporheic zone. In fact all DOC was apparently recalcitrant. See the **Model calibration and rate parameters** section below for more information.

^b 2.69 represents the stoichiometric ratio of oxygen:carbon for purposes of carbonaceous oxygen demand.

^c Ideally, the calculation for organic N would also involve subtracting out the phytoplankton N stoichiometric equivalent (see Org P calculation). However this did not work for N, because the TPN lab method involves a decanting step whereby particulate material, likely including phytoplankton, is removed. Therefore, the TPN lab result does not include N associated with phytoplankton (or other particulate material) anyway.

^d The TP lab method digests all material in the sample, there is no decanting step. Therefore, to calculate organic P it is necessary not only to subtract the inorganic fraction, but also the phytoplankton P fraction. We used a stoichiometric ratio of 1 g Chlorophyll a : 1 g P. See the **Model calibration and rate parameters** section below for the complete stoichiometric ratios used in the model.

^e Based on regression between observed Chlorophyll a samples and associated organic suspended solids (OSS; equivalent to TSS – TNVSS) results. See **phytoplankton** heading below for more details. We used the General Algae 1 model variable to simulate phytoplankton. We did not use the General Algae 2 variable.

^f QUAL2Kw represents detritus in terms of algal dry weight. We used a stoichiometric ratio of 100 g dry weight : 40 g carbon; or 100/40 = 2.5.

^g Chloride is a conservative tracer and does not interact with other model variables. We used the pathogen model variable, with all decay rates set to zero, to simulate chloride.

- ^h Input time-series taken directly from continuous monitoring data
- ⁱ Input time-series based on continuous turbidity data, using regression between lab results and field turbidity.
- ^j Input time-series based on linear interpolation between lab result or field measurement values taken every 2 to 4 weeks.
- ^k Input time-series based on continuous flow data, using regression between lab results or field measurements, and gaged flow.
- ^l Input time-series based on continuous flow data during higher flow conditions, and interpolation between lab results during lower flow conditions.
- ^m For the first 1/3 of the period between lab results, use value of previous lab result. For second 1/3 of the period, use linear interpolation. For the last 1/3 of the period, use next lab result. The reason for this approach is to avoid peaky “spikes” at high values when phytoplankton blooms clearly lasted for multiple days.
- ⁿ Used single mid-range value for the entire model period. Because of subtraction of DOC from TOC, the lab data is too noisy to attach much meaning to any one result value.
- ^o We did not monitor Falling Springs at segment 36. Assume values are the same as for 56Unk(MUL)-00.0.
- ^p Input time-series based on rTemp (Pelletier, 2012) model calibrated to 48-hour continuous data collected once per month.
- ^q DO estimated based on diel %saturation pattern observed during 48-hour continuous deployments, and continuous water temperature estimate.
- ^r We did not observe phytoplankton blooms in tributaries, nor is there any reason to think this would be the case, as these are all small, narrow, more quickly-flowing streams. Phytoplankton can also reasonably be assumed to be absent from stormwater.
- ^s pH estimated based on diel pattern observed during 48-hour continuous deployments, with pattern smoothly varying from one month to the next.
- ^t Input time-series based on continuous temperature data collected upstream at 56MAR-00.4 (Qualchan Drive), adjusted based on 48-hour continuous deployments at 56MAR-00.0.
- ^u All sample results were non-detects.
- ^v Average of sample/measurement results taken by City of Spokane during May-Oct, 2016-2019 at the Cochran Basin outfall (City of Spokane, 2020). No data available from Hangman outfalls.
- ^w Value based on median total dissolved solids (TDS) value recorded by Ecology’s Spokane River Urban Waters samplers in City of Spokane stormwater conveyances and outfalls. Assumed TDS/conductivity ratio of 0.75, per information from Rusydi (2017). No data available from Hangman outfalls.
- ^x Used flow-weighted average of four stormwater outfalls to Hangman Creek, monitored by Ecology during Mar-Apr 2018. Assumed all TSS was ISS.
- ^y Starting with temperature estimate of 16.53 C (see footnote v), we assumed 100% DO saturation, based on the fact that stormwater starts as rainwater, and plunges into Hangman Ck. via high-turbulence culvert pipes. No data available from Hangman outfalls.
- ^z Used flow-weighted average of four stormwater outfalls to Hangman Creek, monitored by Ecology during Mar-Apr 2018.
- ^{aa} Assumed zero detritus, because we assumed that all stormwater TSS was ISS, and detritus is based on TSS minus ISS.
- ^{bb} Starting with conductivity value of 89 uS/cm (see footnote w), we used the relationship on Hangman Creek between conductivity and chloride to estimate a chloride value of 4 mg/L. No data available from Hangman outfalls.
- ^{cc} Estimated value based on median hardness value recorded by Ecology’s Spokane River Urban Waters samplers in City of Spokane stormwater conveyances and outfalls. Although hardness and alkalinity are not the same thing, they often vary together and have results of similar magnitude. No data available from Hangman outfalls.
- ^{dd} Average of push-point sample/measurement values from locations 2GW and 4GW in Redding (2020). Temperature and conductivity data at these locations suggest these represent *bona fide* groundwater, whereas other push-point locations may not.
- ^{ee} We assume there is no appreciable ISS, phytoplankton, or detritus in groundwater.
- ^{ff} Upper watershed groundwater phosphorus values are taken only from the 8/18/201 measurement at 4GW in Redding (2020). Averaging all 2GW and 4GW values results in a higher value that clearly is inconsistent with instream loading evidence.
- ^{gg} Piezometer data from this study indicated a seasonal trend in groundwater temperatures, with summertime values a bit warmer than spring and fall values. Input time-series based on interpolation between monthly measurements.
- ^{hh} Average of measurement/sample values from piezometer sampling during this study, at locations 56HAN-GW-2, 56HAN-GW-3, and 56HAN-GW-4. These three locations represent the three strongly gaining piezometers.
- ⁱⁱ Lower watershed groundwater nitrogen values are taken only from 56HAN-GW-4 (piezometer nr. Cheney-Spokane Rd. interchange). Averaging all 56HAN-GW-2, 56HAN-GW-3, and 56HAN-GW-4 values results in a lower value that clearly is inconsistent with instream loading evidence.

Phytoplankton

We did not collect routine Chlorophyll *a* samples during 2018. However, in the absence of high-sediment conditions, it is possible to approximate suspended phytoplankton chlorophyll concentration using organic suspended solids (OSS), which is calculated as total suspended solids (TSS) minus total non-volatile suspended solids (TNVSS). We used a small number of Chlorophyll *a* sample results from upper Hangman Creek collected during 2017 (Stuart, 2020), along with concurrent solids results, to estimate the relationship between OSS and Chlorophyll *a* (Figure E-5).

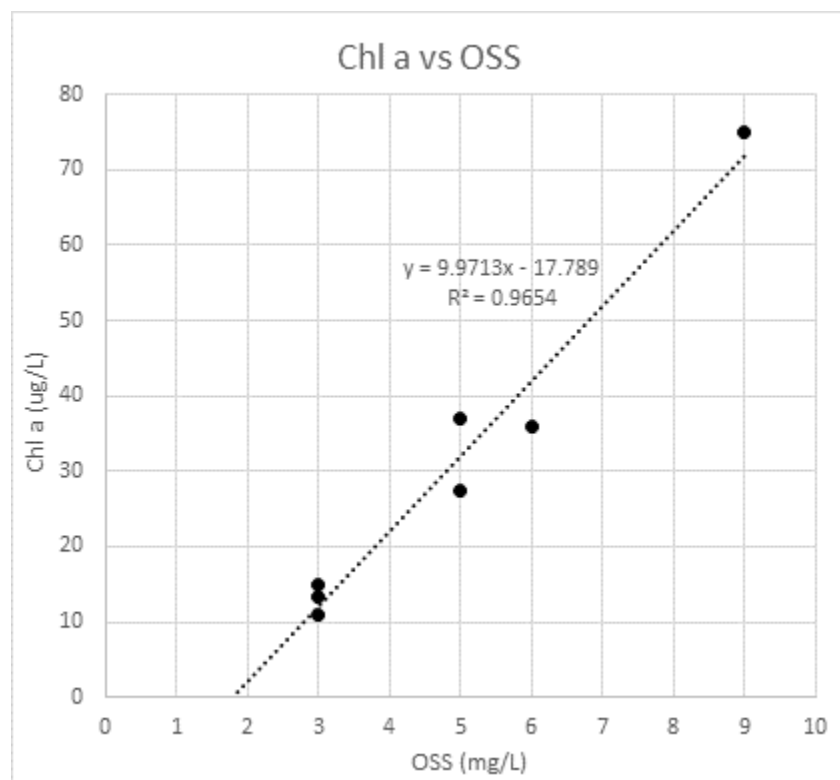


Figure E-5. Observed relationship between organic suspended solids (OSS), and Chlorophyll *a*.

We then used this relationship along with OSS data collected during 2018 to estimate a continuous time-series for suspended phytoplankton, as represented by chlorophyll *a*. Figure E-6 presents this estimate for the upstream boundary condition (56HAN-14.5). We also present daily average pH for comparison. Overall high pH appears to be associated with phytoplankton blooms.

This method provides a reasonable approximation of suspended chlorophyll *a* that captures some of the general patterns in phytoplankton growth. In particular, it does a good job capturing blooms that occurred during mid-June and late July. It may miss other blooms, such as a possible bloom in mid-October that occurred between sampling runs.

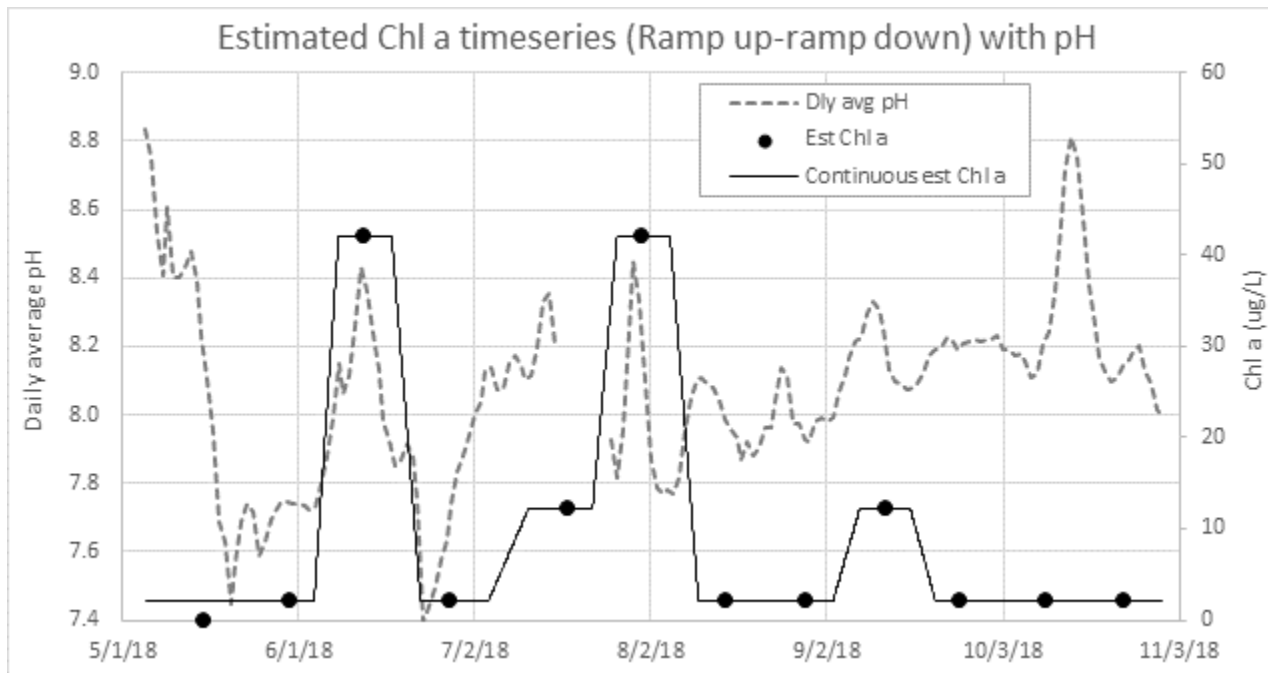


Figure E-6. Estimated Chlorophyll a time-series shown along with daily average pH, at upstream model boundary.

Initial Conditions

We did not specify initial conditions. Absent specified initial conditions, QUAL2Kw sets constituent values throughout the model domain to the upstream boundary condition at the first time step. At the beginning of the simulation period, relatively uniform water quality conditions associated with early May flows of about 200 cfs make this an acceptable simplification. Furthermore, the time of travel for the entire model domain is about a day under those flow conditions, so the initial conditions are quickly flushed out of the model domain.

Climate Inputs

Table E-5. Data sources for climate model inputs

Parameter	Data Source
Air temperature	National Weather Service/Spokane International Airport (KGEG)
Dew point	National Weather Service/Felts Field (KSFF)
Windspeed	National Weather Service/Spokane International Airport (KGEG), modified by a wind sheltering factor of 0.25
Cloud cover	National Weather Service/Spokane International Airport (KGEG)
Solar radiation	Remote automated weather station (RAWS) Turnbull National Wildlife Refuge (TWRW1), modified by site adjustment factor of 1.08

Shade Inputs

We estimated effective shade using Ecology's shade model (Ecology, 2003). We used the TTools toolbar for ArcGIS (Ecology 2015) to sample a 2015 LiDAR coverage of the Spokane area (WDNR, 2020). Because of the high-resolution nature of LiDAR coverage, we used a vegetation density of 100%. We used a standard stream-edge overhang value of 10% of the height of the vegetation at the edge of the stream. Figures E-7 and E-8 show model predicted shade values along with observed effective shade values calculated from hemispherical photographs taken at the center of the stream channel.

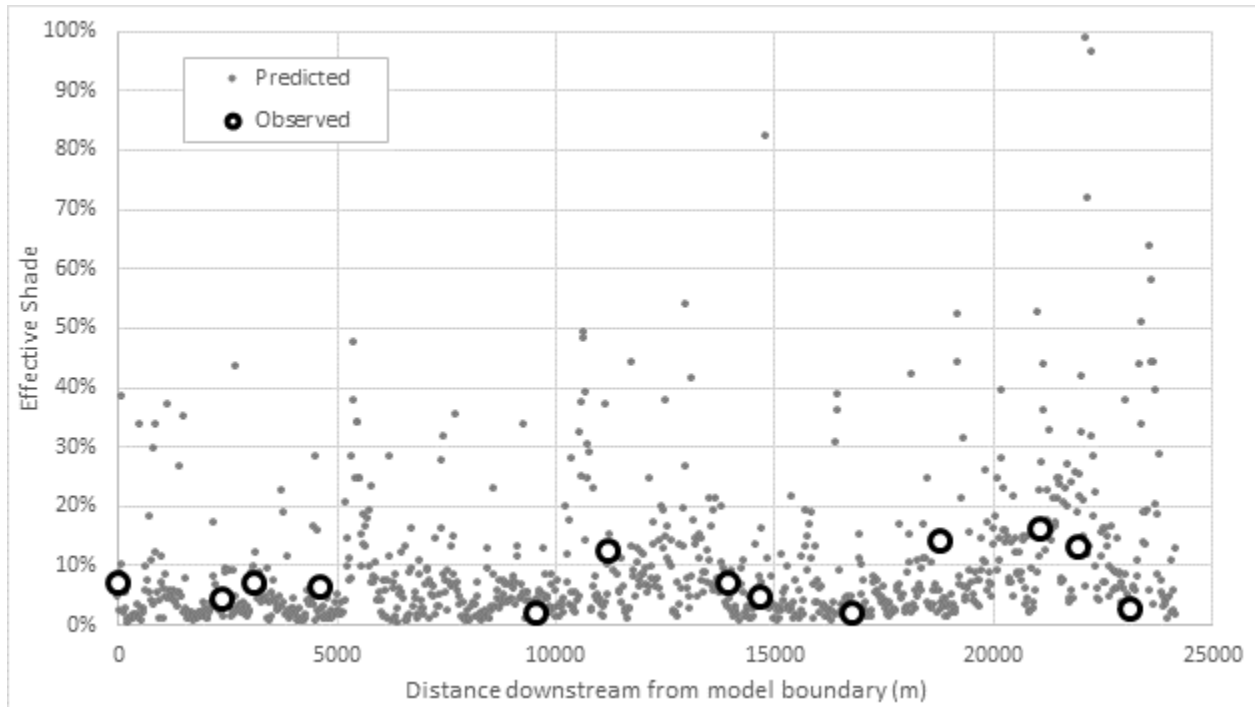


Figure E-7. Longitudinal graph of model predicted shade, along with observed values from hemispherical photos.

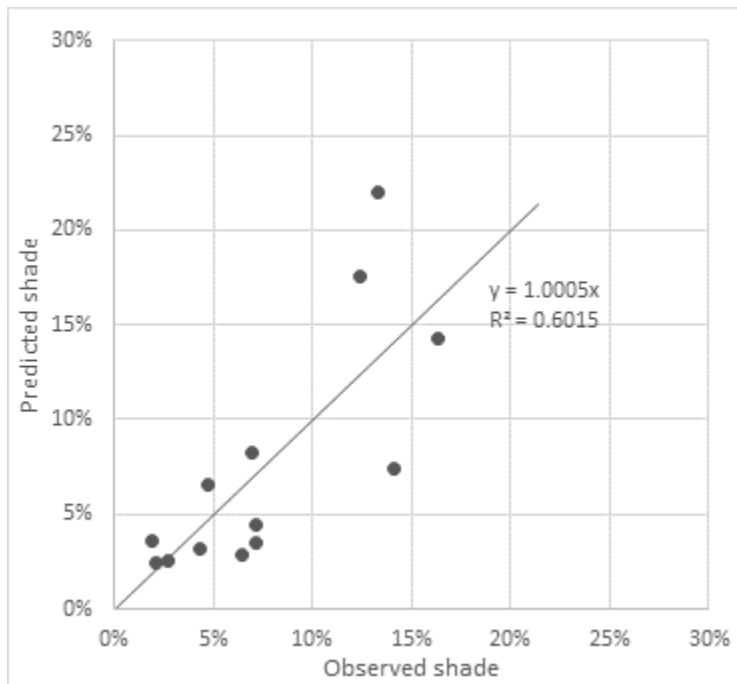


Figure E-8. Model predicted effective shade, plotted against observed values from hemispherical photos.

QUAL2Kw model settings

Table E-6 lists the QUAL2Kw model settings. The substrate of Hangman Creek typically consists of irregular-shaped basalt cobbles cemented by fine sediment. Sand occurs in some lower watershed locations. Sediment-water interactions tend to be much less significant than in streams with a greater substrate porosity. We found that including the hyporheic transient storage (HTS) zone, with a small amount of flow exchange and a low biofilm growth rate, helped provide the heterotrophic respiration needed to correctly simulate DO and pH.

We did not use the sediment diagenesis module. This module simulates sediment oxygen demand (SOD) resulting from the downward flux of organic matter from the water column. Observed DO data in Hangman Creek do not suggest significant SOD. Furthermore, Hangman Creek clearly does not have a significant downward flux of organic matter – we had to treat DOC (simulated as CBODfast) as recalcitrant (zero oxidation rate) to correctly predict observed concentrations.

Table E-6. QUAL2Kw model settings.

Simulation option	Setting
Calculation step	1.40625 minutes
Number of days for the simulation period	179 days
Simulation mode	Continuous
Solution method (integration)	Euler
Solution method (pH)	Brent
Simulate hyporheic transient storage zone (HTS)	Level 2 (mass transfer between the water column and the hyporheic pore water, with water quality kinetics with attached heterotrophic bacteria as a state variable in the hyporheic sediment zone with growth limitation from fast-reacting DOC, nitrate, ammonia, soluble reactive P, and dissolved oxygen)
Simulate surface transient storage zone (STS)	No
Option for conduction to deep sediments in heat budget	Lumped
State variables for simulation	All
Simulate sediment diagenesis	No
Simulate alkalinity change due to nutrient change	Yes

Model Calibration and Rate Parameters

We performed calibration of the QUAL2Kw model using the genetic auto-calibration algorithm (Pelletier et al., 2006). We based the fitness function used to evaluate the quality of various calibrations on two factors:

- Goodness of model fit to the observed data
- The sensitivity of algal productivity to instream nutrient concentrations. A part of the fitness function tested how well the simulated growth limitation factors for N and P adhered to ranges shown in research literature (Bothwell, 1985; Rier and Stevenson, 2006). The *Model Sensitivity to Nutrients* section later in this appendix provides more details.

Calibration was an iterative process. We performed a total of 9 batches of auto-calibrations. Each batch consisted of between 4 and 12 individual auto-calibrations, identical except for random number seed. This provided an approximate Bayesian distribution of values for each parameter. We then used this distribution to adjust the lower and upper bounds for each parameter during subsequent batches. We made various other changes between batches as well as need became apparent. These included adding growth limitation factors to the fitness function, turning on the hyporheic transient storage zone (HTS) simulation, adding phytoplankton to the simulation, and adjusting the parameter weighting in the fitness function.

Table E-7 lists the final rate parameters.

Table E-7. QUAL2Kw rate parameters.

We do not show temperature corrections; these are equal to 1.07 unless indicated otherwise.

Parameter	Value	Units	Value source or calibration basis ^a
Stoichiometry:			
Carbon	40	gC	Default values based on Redfield cellular ratio (Redfield, 1958).
Nitrogen	7.2	gN	
Phosphorus	1	gP	
Dry weight	100	gD	
Chlorophyll	1	gA	Default ratio for phytoplankton
Inorganic suspended solids:			
Settling velocity	0.125	m/d	Hand-calibrated to observed ISS data
Oxygen:			
Reaeration model	User model		Calibrated reaeration model to match phase timing of diel DO fluctuations
Reaeration user model parameter A	9		
Reaeration user model parameter B	0.547		
Reaeration user model parameter C	-1.939		
Temp correction	1.024		Default values
Reaeration wind effect	None		
O2 for carbon oxidation	2.69	gO2/gC	Standard stoichiometric ratios
O2 for NH4 nitrification	4.57	gO2/gN	
Oxygen inhib model CBOD oxidation	Exponential		Default values
Oxygen inhib parameter CBOD oxidation	0.60	L/mgO2	
Oxygen inhib model nitrification	Exponential		
Oxygen inhib parameter nitrification	0.60	L/mgO2	
Oxygen enhance model denitrification	Exponential		
Oxygen enhance parameter denitrification	0.60	L/mgO2	
Oxygen inhib model phyto resp	Exponential		
Oxygen inhib parameter phyto resp	0.60	L/mgO2	
Oxygen enhance model bot alg resp	Exponential		
Oxygen enhance parameter bot alg resp	0.60	L/mgO2	
Slow CBOD:			
Hydrolysis rate	100	/d	Arbitrary very high rate to pass through all material to "Fast CBOD" compartment.
Oxidation rate	0	/d	
Fast CBOD:			
Oxidation rate	0	/d	We used this category to represent all DOC. However the DOC is not actually fast-reacting; it's very recalcitrant, hence the zero oxidation rate.
Organic N:			
Hydrolysis	0.0435	/d	Autocal min = 0; max = 0.06
Settling velocity	0.5	m/d	Hand-calibrated
Ammonium:			
Nitrification	0.288	/d	Autocal min = 0.1; max = 3
Nitrate:			
Denitrification	1.48	/d	Autocal min = 1; max = 2
Sed denitrification transfer coeff	0.1	m/d	Assumed value; midrange of default settings
Organic P:			
Hydrolysis	0.6	/d	Hand-calibrated
Settling velocity	0.25	m/d	Hand-calibrated
Inorganic P:			
Settling velocity	0	m/d	Inorg P is dissolved, settling very unlikely

Parameter	Value	Units	Value source or calibration basis ^a
Sed P oxygen attenuation half sat constant	1	mgO ₂ /L	Assumed value; midrange of default settings
General Algae 1 (Phytoplankton):			
Max Growth rate	3	/d	Hand-calibrated
Respiration rate	0.1	/d	Default value
Death rate	0	/d	Default value
Temp correction	1		Phyto death likely doesn't increase with temp
Nitrogen half sat constant	15	ugN/L	Default value
Phosphorus half sat constant	2	ugP/L	Default value
Inorganic carbon half sat constant	1.3E-05	moles/L	Assumed value; midrange of default settings
General algae 1 use HCO ₃ ⁻ as substrate	Yes		Standard assumption
Light model	Half-saturation		Standard model
Light constant	50	langleys/d	Upper end of literature range (Hill, 1996; Bowie et al., 1985)
Ammonia preference	25	ugN/L	Default value
Settling velocity	0.5	m/d	Hand-calibrated. Higher than normal value reasonable due to slow pools with little to no turbulence
Include transport of general algae 1	Yes		Setting for suspended phytoplankton
Nitrogen uptake water column fraction	1		Setting for suspended phytoplankton
Phosphorus uptake water column fraction	1		Setting for suspended phytoplankton
General Algae 2: not used			
Bottom Algae:			
Growth model	Zero-order		Standard model for periphyton
Max Growth rate	22.2	gD/m ² /d	Autocal min = 13; max = 30
Basal respiration rate	0.267	/d	Autocal min = 0.25; max = 0.39
Photo-respiration rate parameter	0.389	unitless	Default value; autocal favored similar values
Excretion rate	0.00311	/d	Autocal min = 0; max = 0.06
Death rate	0.0632	/d	Autocal min = 0; max = 0.1
Scour function	Not used		
External nitrogen half sat constant	425	ugN/L	Autocal min = 150; max = 500
External phosphorus half sat constant	63.1	ugP/L	Autocal min = 50; max = 200
Inorganic carbon half sat constant	1.3E-05	moles/L	Assumed value; midrange of default settings
Bottom algae use HCO ₃ ⁻ as substrate	Yes		Standard assumption
Light model	Half saturation		Standard model
Light constant	50	langleys/d	Upper end of literature range (Hill, 1996; Bowie et al., 1985)
Ammonia preference	24.1	ugN/L	Autocal min = 15; max = 30
Nutrient limitation model for N and P	Minimum		Standard model
Subsistence quota for nitrogen	35.9	mgN/gD	Autocal min = 25; max = 36
Subsistence quota for phosphorus	0.401	mgP/gD	Autocal min = 0.05; max = 2
Maximum uptake rate for nitrogen	252	mgN/gD/d	Autocal min = 200; max = 1000
Maximum uptake rate for phosphorus	20	mgP/gD/d	Hand-calibrated
Internal nitrogen half sat ratio	1.26		Autocal min = 1.05; max = 2
Internal phosphorus half sat ratio	2.43		Autocal min = 1.05; max = 2.5
Nitrogen uptake water column fraction	1		Standard assumption for periphyton
Phosphorus uptake water column fraction	1		Standard assumption for periphyton
Detritus (POM):			
Dissolution rate	0.47	/d	Autocal min = 0.25; max = 0.5
Settling velocity	0	m/d	Assume value would be very low; 0 value means all detritus can be passed to CBOD.
Pathogens: (used this constituent to represent chloride, all loss rates set to zero)			
pH:			

Parameter	Value	Units	Value source or calibration basis ^a
Partial pressure of carbon dioxide	410	ppm	Atmospheric CO ₂ value for 2018
Hyporheic metabolism:			
Model for biofilm oxidation of fast CBOD	Zero-order		Standard model
Max biofilm growth rate	2	gO ₂ /m ² /d	Hand-calibrated to result in sustained biofilm mass. Higher values result in rapid growth followed by die-off due to carbon limitation.
Fast CBOD half-saturation	0.5	mgO ₂ /L	Default value
Oxygen inhib model	Exponential		Standard model
Oxygen inhib parameter	0.60	L/mgO ₂	Default value
Respiration rate	0.2	/d	Default value
Death rate	0.05	/d	Default value
External nitrogen half sat constant	0	ugN/L	Turned off nutrient limitation of hyporheic biofilm, to reflect hyporheic access to groundwater nutrients, which the model framework does not include.
External phosphorus half sat constant	0	ugP/L	
Ammonia preference	25	ugN/L	Default value
Generic constituent: (used this constituent to represent rhodamine tracer dye, all loss rates set to zero)			
Photosynthetic quotient and respiratory quotient for bottom algae			
Photosynthetic quotient for NO ₃ vs NH ₄ use	1.71		Autocal min = 1.3; max = 1.8
Respiratory quotient	1.00		Default value

^a Auto-calibration min and max bounds are for the batch in which the final value for that parameter was determined. Bounds for other autocalibration batches varied.

Model Goodness-of-Fit

Table E-8 summarizes the Lower Hangman Creek QUAL2Kw model goodness of fit to observed data. The Root Mean Squared Error (RMSE) and Mean Absolute Error (MAE) statistics express the magnitude of typical model error for a variable in the same units as that variable. RMSE is more sensitive to a few large error values, whereas MAE is more forgiving of large outliers. The Root Mean Squared Error Coefficient of Variation (RMSE CV) and Mean Absolute Error Coefficient of Variation (MAE CV) express the proportion of typical model error to the typical value of the variable. The overall bias statistic expresses the tendency of the model to over- or under-predict the value of a given variable. % Bias expresses this tendency as a proportion of the typical value of the variable. We also provide the average observed values from this study for reference. We did not include statistics for bottom algae (periphyton) because there are only two data points, from a different year than the model predictions. The comparison for bottom algae is a general check, not a precise calibration.

For all variables, we calculated RMSE, MAE, and bias by comparing modeled daily average values to observed daily average or grab sample values. For variables that display a marked diel swing, such as temperature, dissolved oxygen (DO), and pH, we calculated the RMSE, MAE, and bias for daily maximums and minimums as well. We also calculated RMSE CV, MAE CV and %Bias, which express error as a proportion of typical variable values, for those variables that express a quantity or concentration of something. These “relative” statistics are not appropriate for temperature or pH, which use arbitrary (and in the case of pH, exponential) unit scales where zero does not represent the total absence of the thing being measured.

The QUAL2Kw model provides a reasonable and acceptable simulation of DO, pH, and nutrients in Lower Hangman Creek. Daily minimum DO had a minimal amount of error (RMSE = 0.64 mg/L; overall bias = +0.38). Daily maximum pH also had a minimal amount of error (RMSE = 0.26 S.U.; overall bias = -0.07 S.U.). The same is true for total phosphorus (RMSE = 0.016 mg/L; overall bias = -0.005 mg/L). These variables are particularly relevant for comparison to water quality standards for DO and pH, and load allocations from the Spokane TMDL for TP. These model fit statistics compare well to results from models used for TMDLs by Ecology in the past (Sanderson and Pickett, 2014).

Figure E-9 presents calibration plots for all key model variables. Calibration plots are able to give a better context for understanding model performance than error statistics alone can provide.

Table E-8. Summary statistics for goodness-of-fit of the QUAL2Kw model to observed data.

Variable	RMSE [MAE] Daily Min	RMSE [MAE] Daily Max	RMSE [MAE] Daily Avg	RMSE CV [MAE CV] Daily Min	RMSE CV [MAE CV] Daily Max	RMSE CV [MAE CV] Daily Avg	Ovl. Bias Daily Min	Ovl. Bias Daily Max	Ovl. Bias Daily Avg	%Bias Daily Min	%Bias Daily Max	%Bias Daily Avg	Abg Obs Value Daily Min	Abg Obs Value Daily Max	Abg Obs Value Daily Avg
Temperature (degC)	0.52 [0.42]	0.44 [0.36]	0.40 [0.32]				-0.28	-0.12	-0.19				15.8	18.2	16.9
Dissolved oxygen (mgO ₂ /L)	0.64 [0.54]	1.25 [1.04]	0.67 [0.53]	8.0% [6.7%]	11.9% [9.9%]	7.3% [5.8%]	+0.38	-0.16	+0.18	+4.7%	-1.5%	+2.0%	8.0	10.5	9.2
pH	0.16 [0.13]	0.26 [0.19]	0.19 [0.15]				+0.04	-0.07	-0.02				7.8	8.3	8.1
Conductivity (uS/cm 25C)			17.5 [14.3]			4.9% [4.0%]			-6.8			-1.9%			355
Chloride (mg/L)			2.49 [1.95]			27.1% [21.2%]			-1.95			-21.1%			9.21
Total suspended solids (mgD/L)			14.6 [3.6]			162.1% [40.3%]			+2.1			+23.0%			9.0
Inorganic suspended solids (mgD/L)			2.07 [1.30]			42.4% [26.6%]			+0.14			+2.9%			4.88
Total N (mgN/L)			0.29 [0.22]			22.0% [16.3%]			+0.06			+4.9%			1.33
Organic N (mgN/L)			0.20 [0.12]			64.9% [40.2%]			+0.06			+18.8%			0.30
Ammonium N (mgN/L)			0.012 [0.004]			97.4% [31.6%]			-0.002			-15.2%			0.012
Nitrate + nitrite N (mgN/L)			0.19 [0.12]			18.4% [11.9%]			-0.064			-6.3%			1.01
Total P (mgP/L)			0.016 [0.011]			23.0% [16.1%]			-0.005			-7.7%			0.068
Organic P (mgP/L)			0.030 [0.012]			82.3% [33.6%]			-0.008			-21.5%			0.036
Inorganic P (mgP/L)			0.023 [0.012]			73.2% [37.8%]			+0.003			+8.1%			0.032
Total organic C (mgC/L)			0.83 [0.54]			21.5% [14.1%]			+0.27			+7.0%			3.84
Dissolved organic C (mgC/L)			0.66 [0.51]			19.4% [15.2%]			-0.36			-10.5%			3.39
Detritus (mgD/L)			0.90 [0.67]			69.0% [51.5%]			+0.39			+29.6%			1.31
Alkalinity (mgCaCO ₃ /L)			9.6 [7.2]			5.8% [4.3%]			+5.9			+3.5%			166
Phytoplankton (ugA/L)			9.0 [5.3]			72.8% [42.8%]			-1.3			-10.6%			12.3

$$RMSE = \sqrt{\frac{\sum(T_{modeled} - T_{observed})^2}{n}}$$

$$RMSE CV = \frac{RMSE}{Avg\ observed\ value}$$

$$MAE = \frac{\sum Abs(T_{modeled} - T_{observed})}{n}$$

$$MAE CV = \frac{MAE}{Avg\ observed\ value}$$

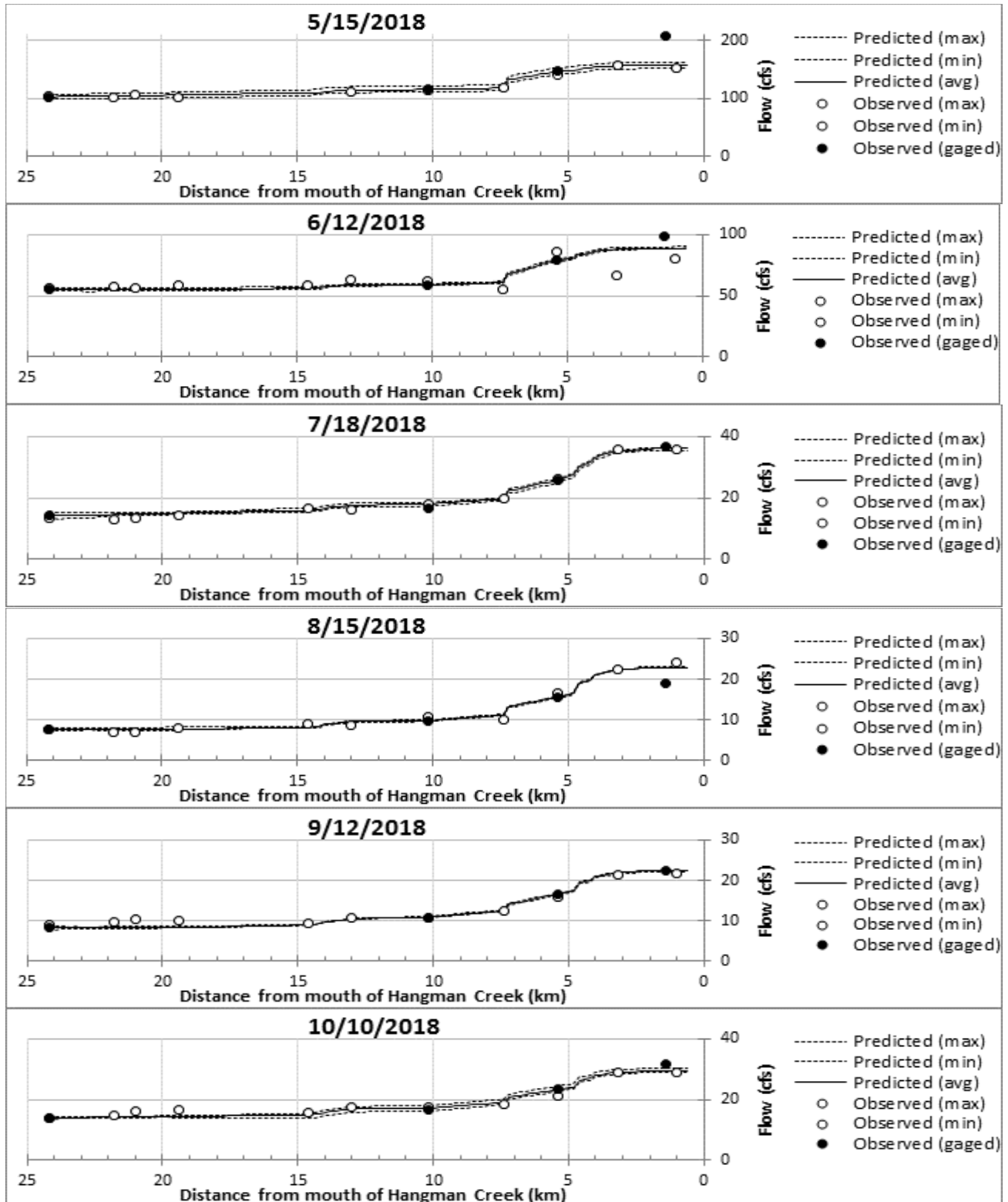
$$Bias = \frac{\sum(T_{modeled} - T_{observed})}{n}$$

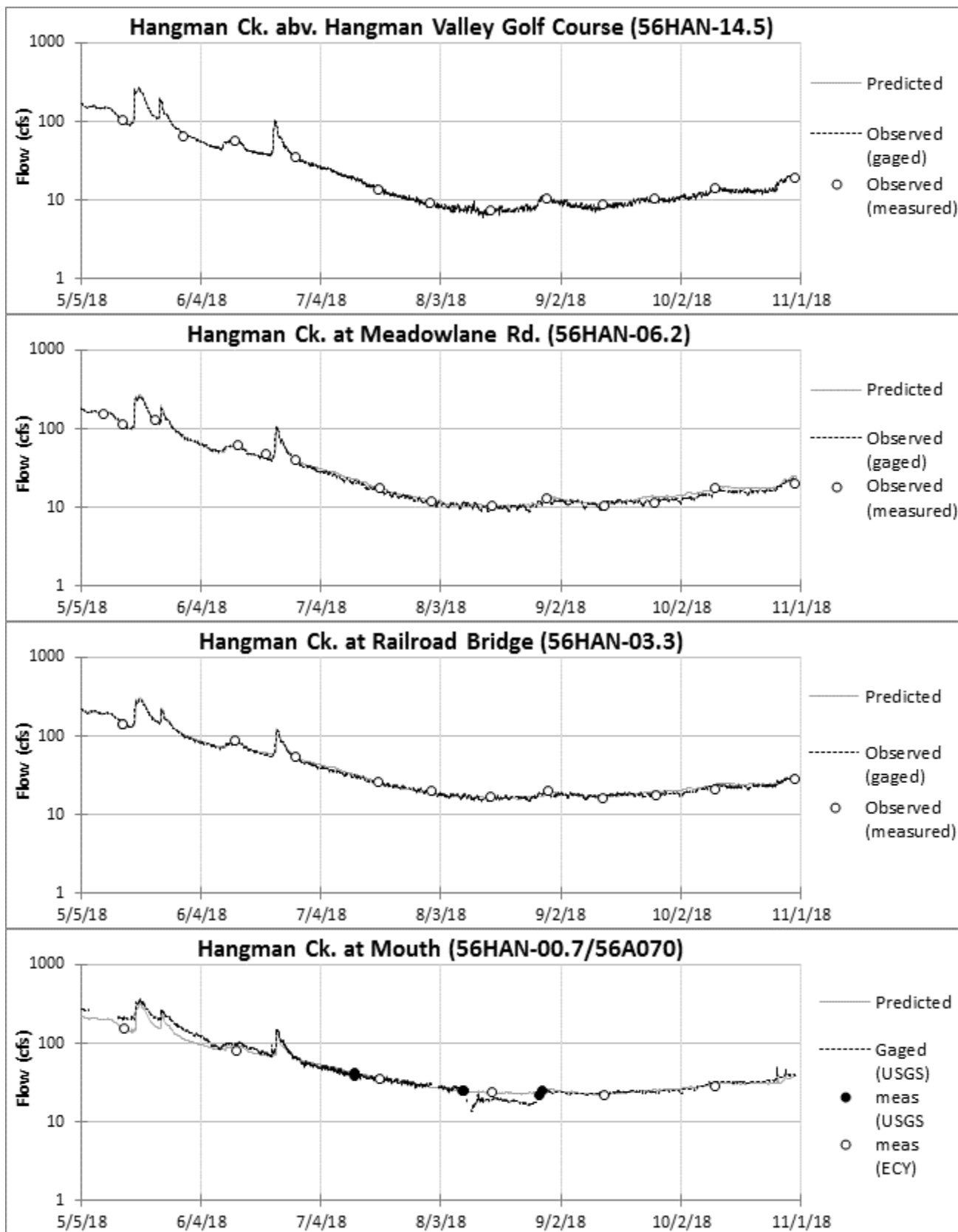
$$\%Bias = \frac{Bias}{Avg\ observed\ value}$$

Figure E-9. Longitudinal and time-series plots of modeled vs. observed values for all key model variables.

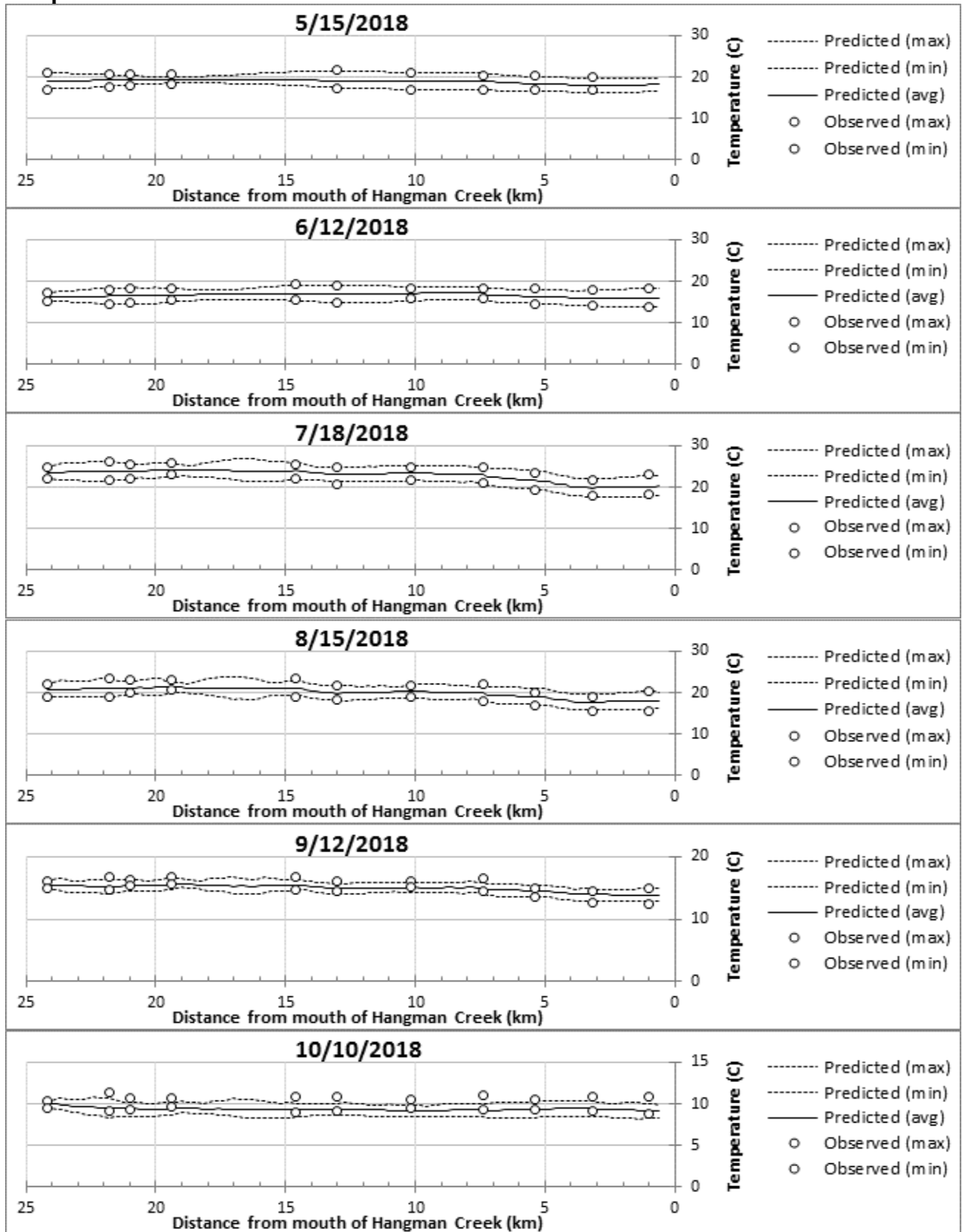
This figure includes all plots in the next 43 pages.

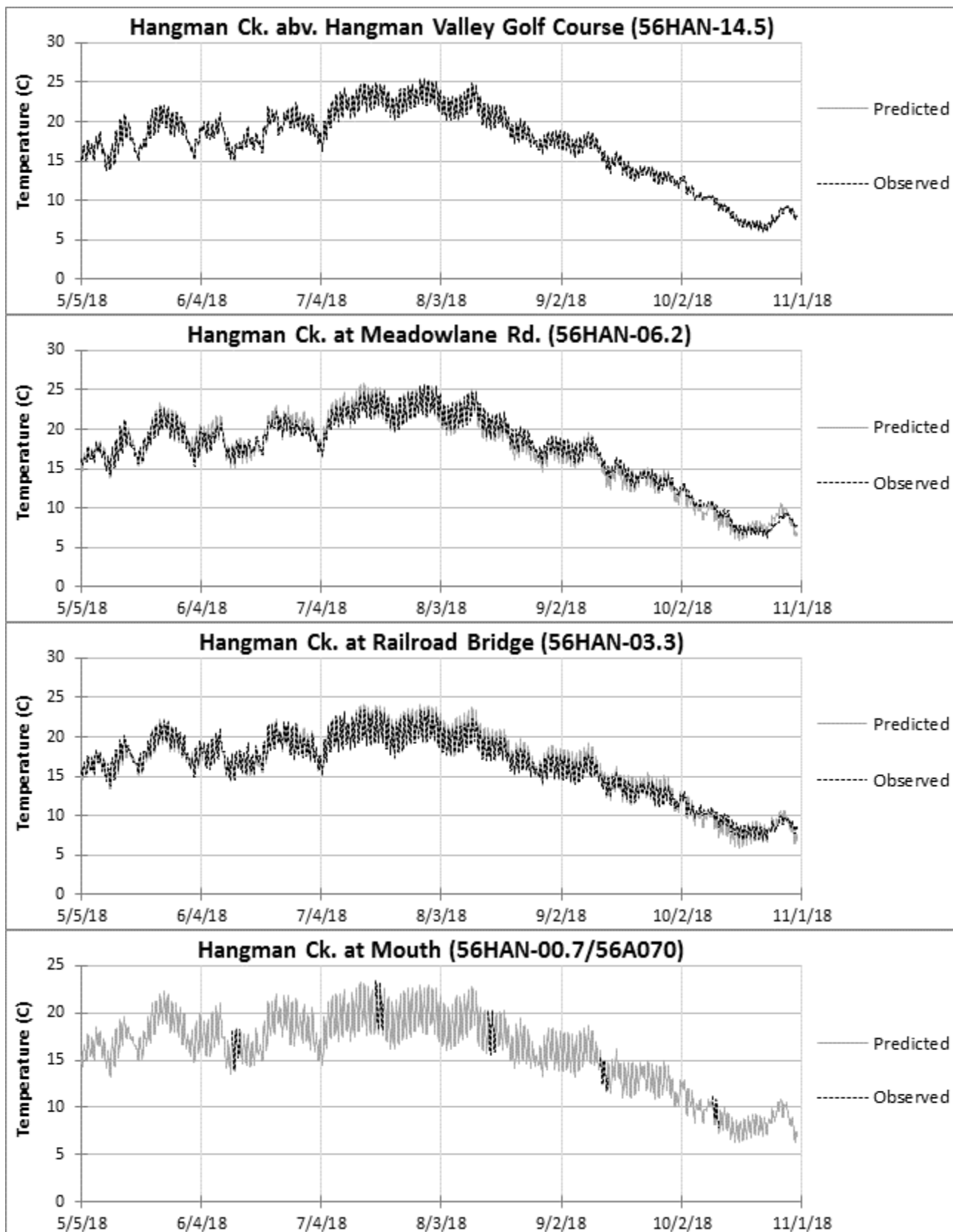
Streamflow



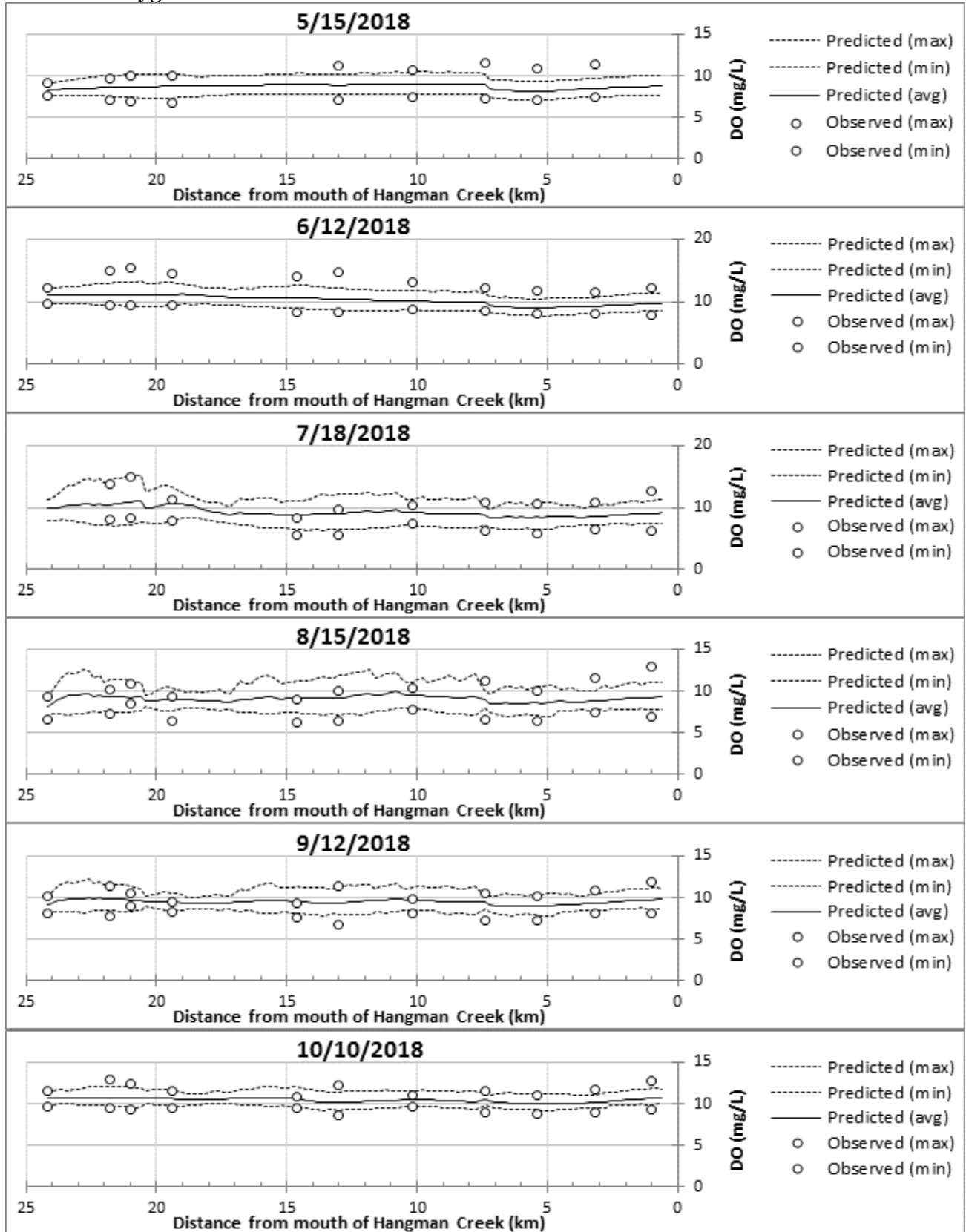


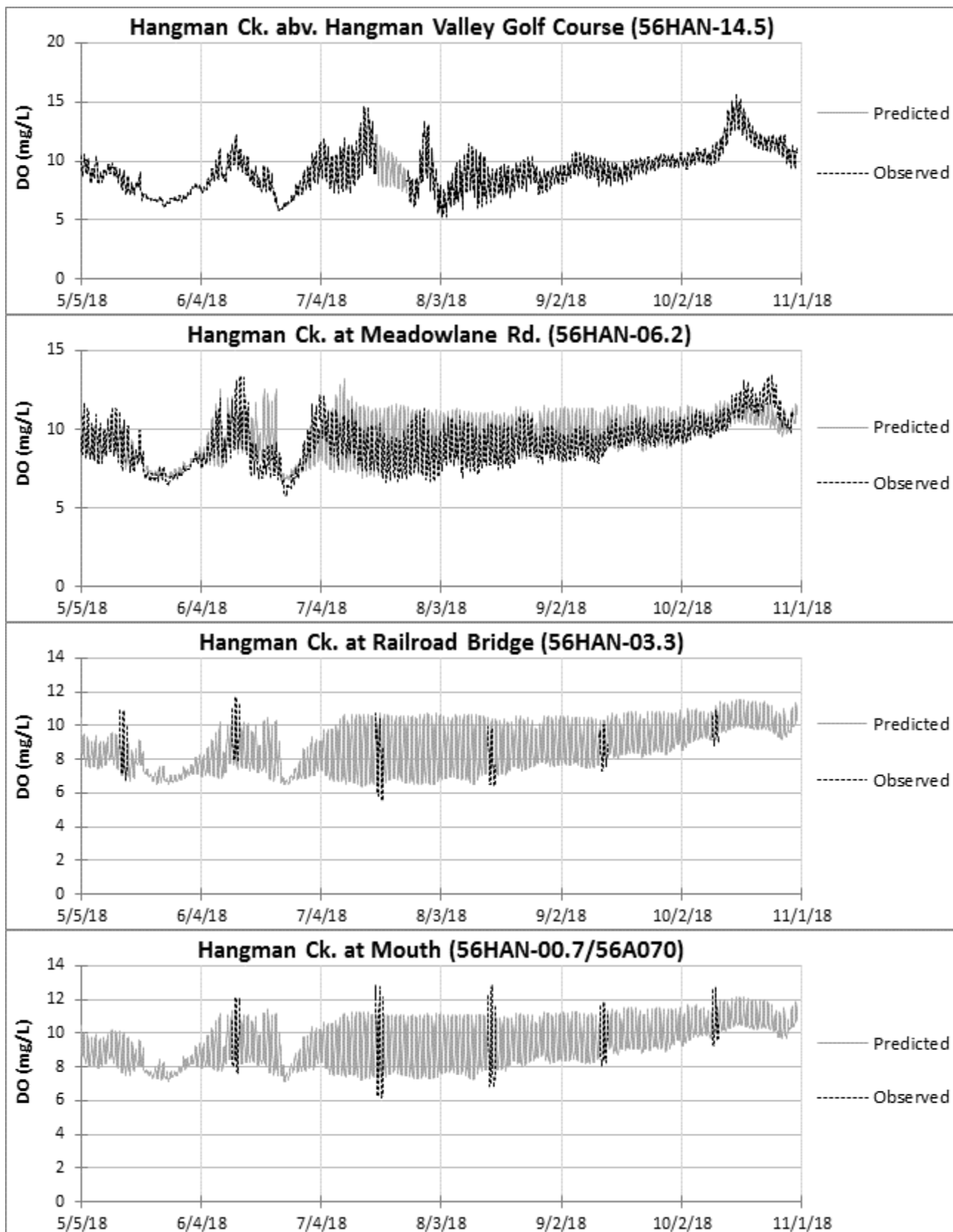
Temperature



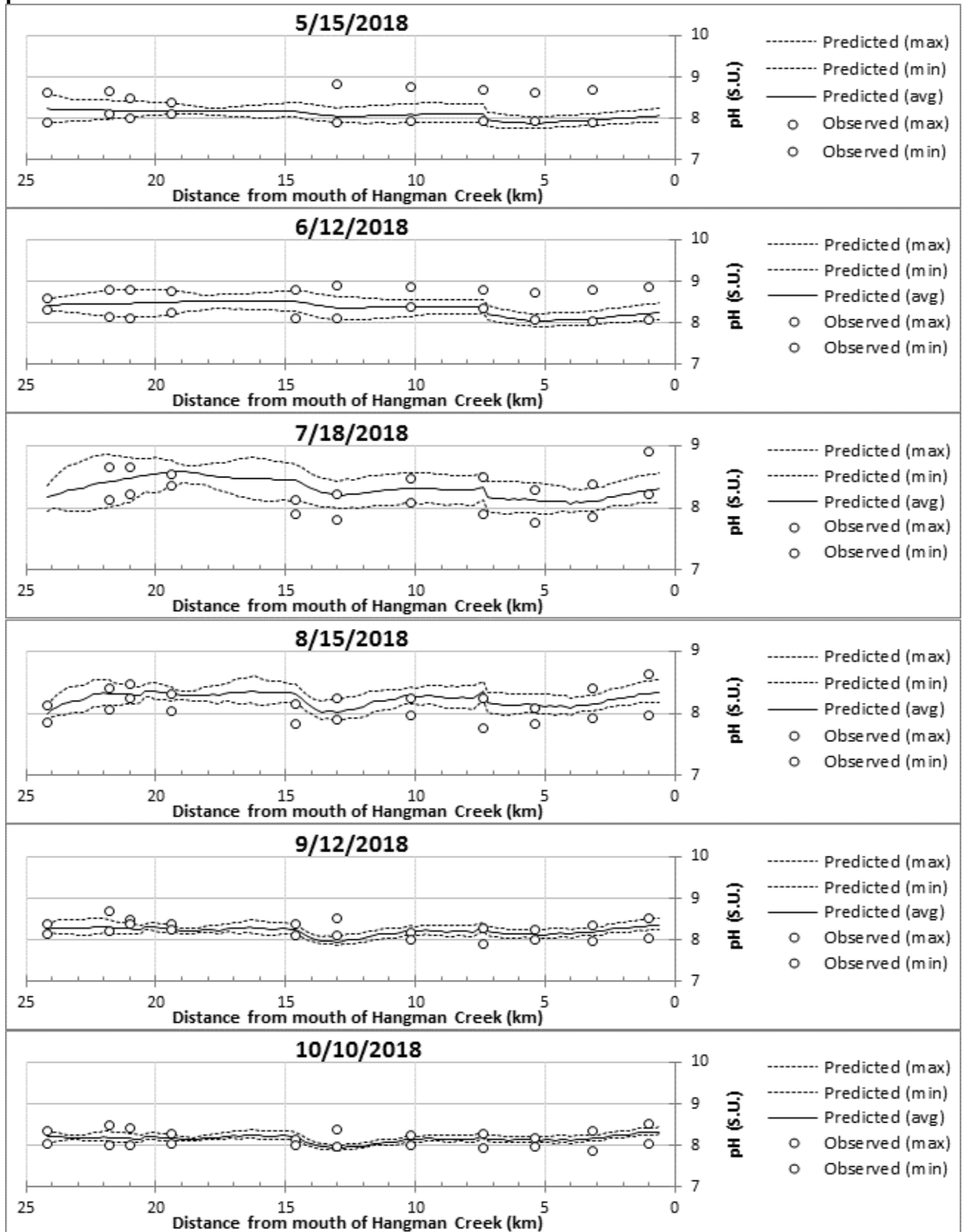


Dissolved Oxygen

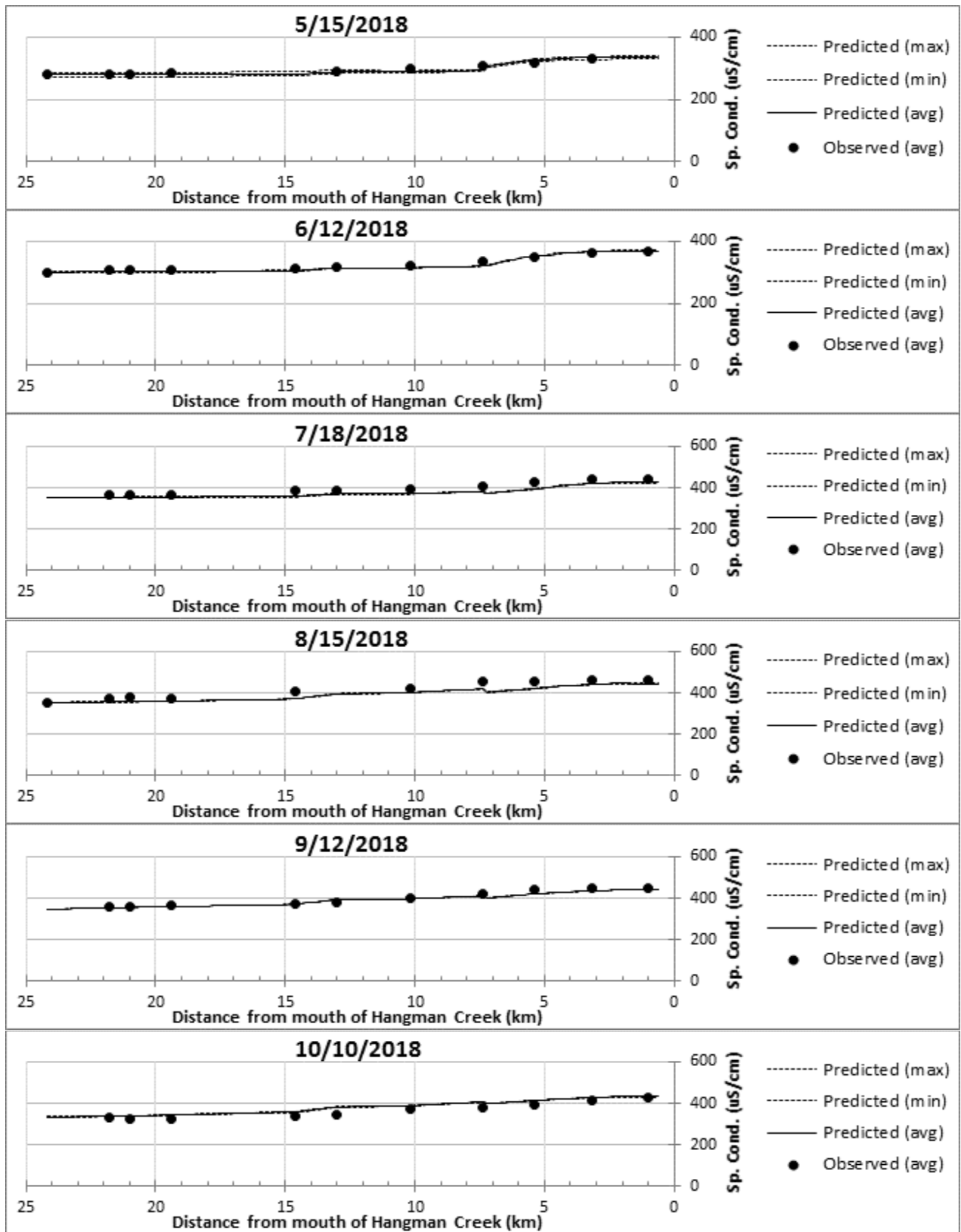


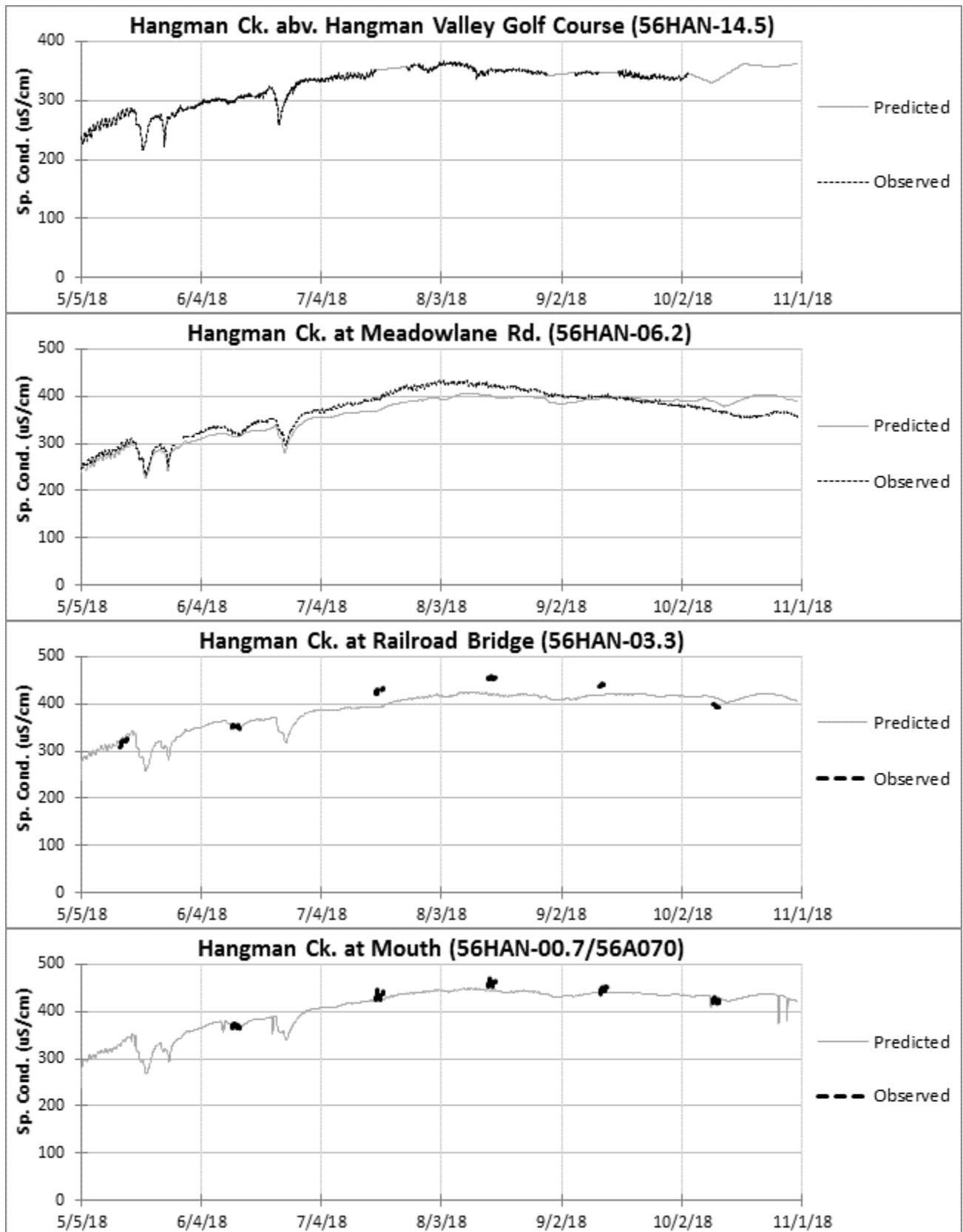


pH

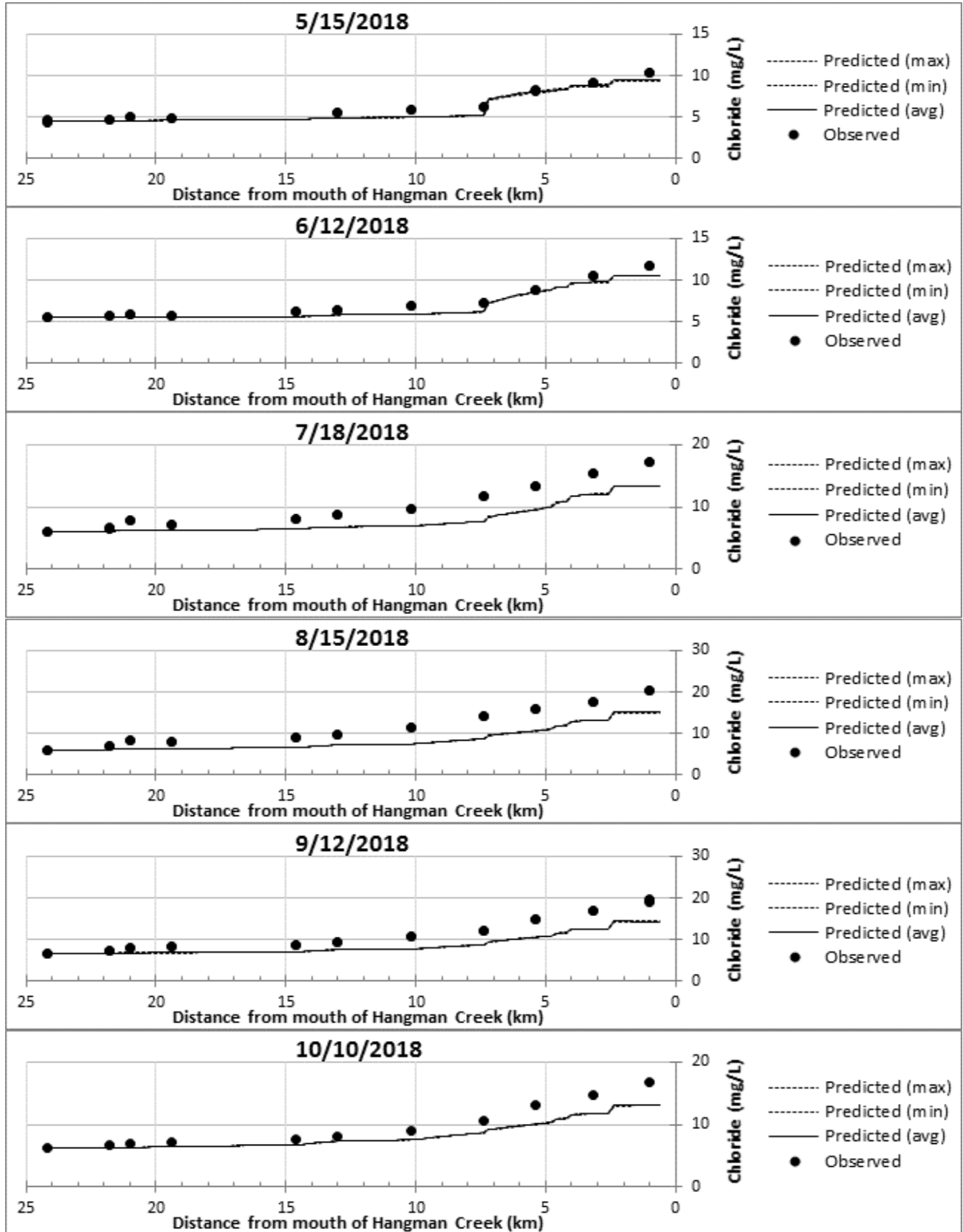


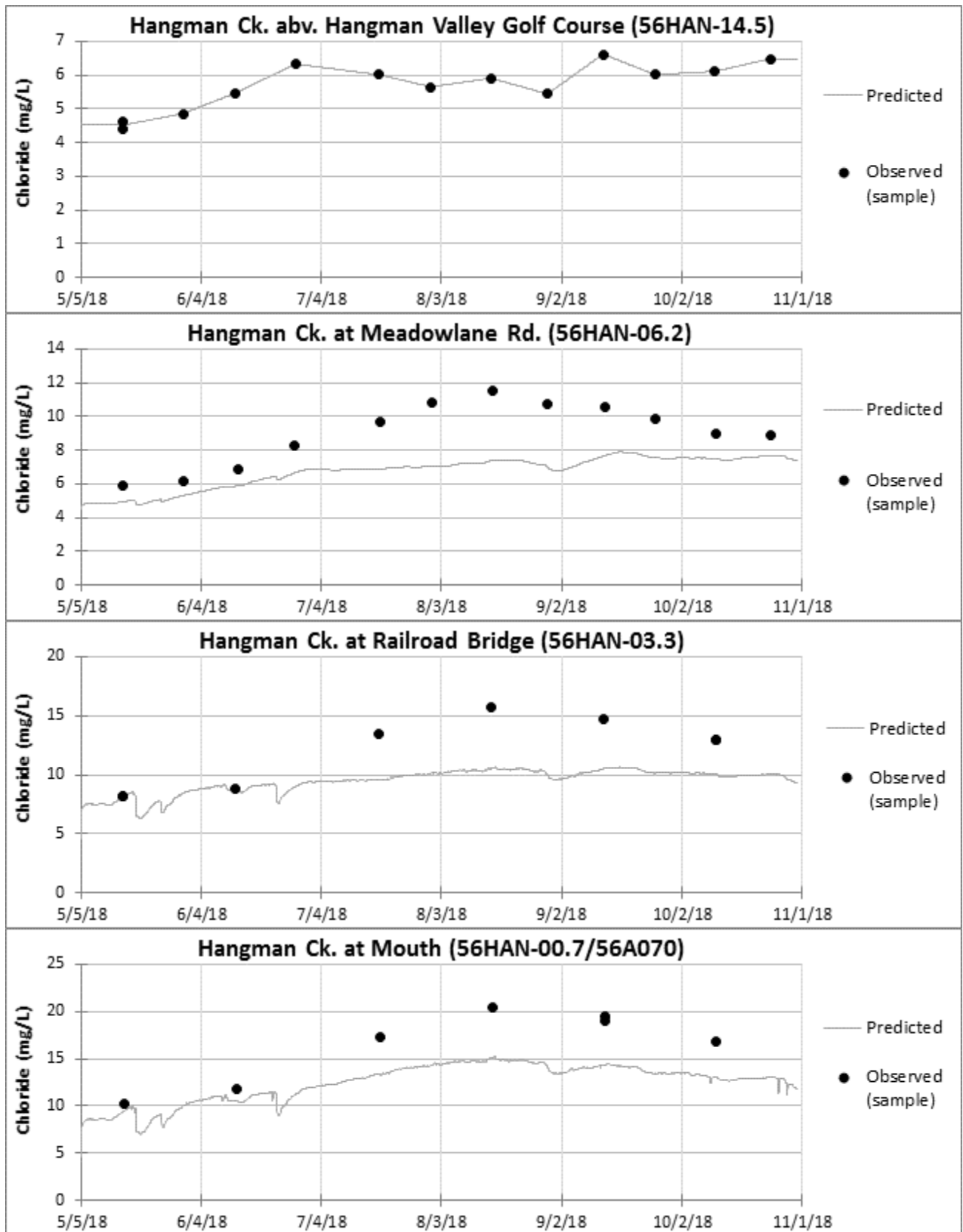
Specific Conductivity



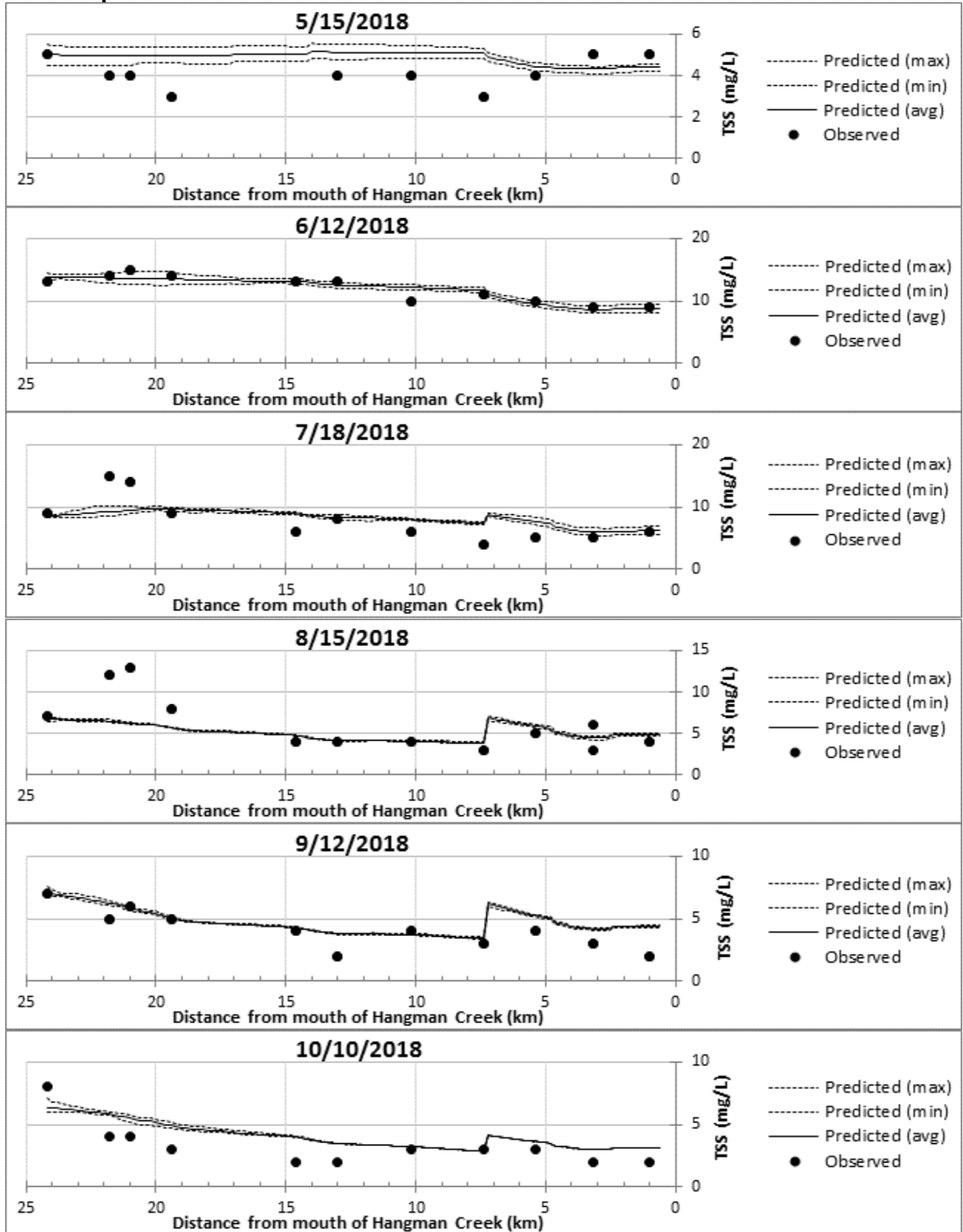


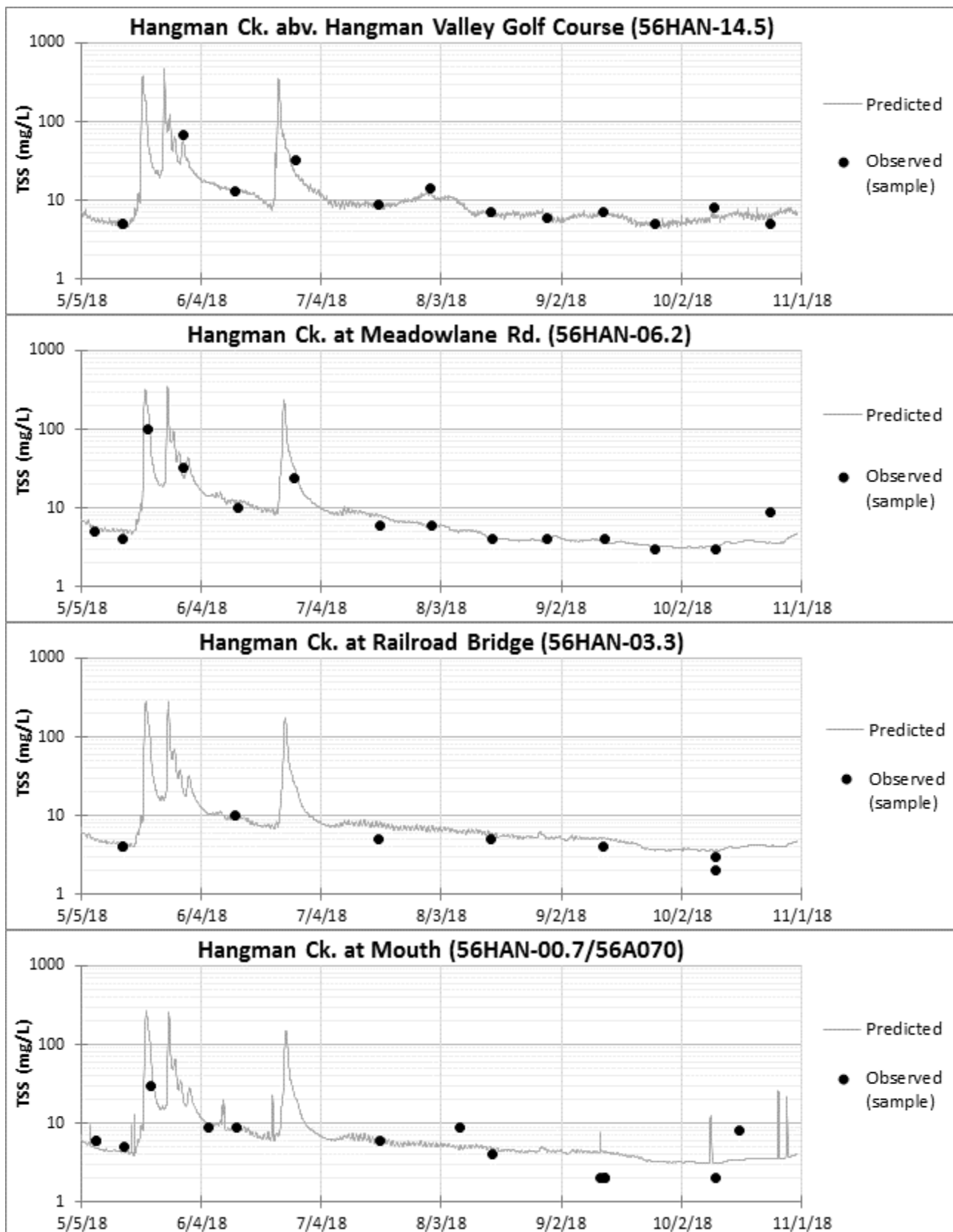
Chloride



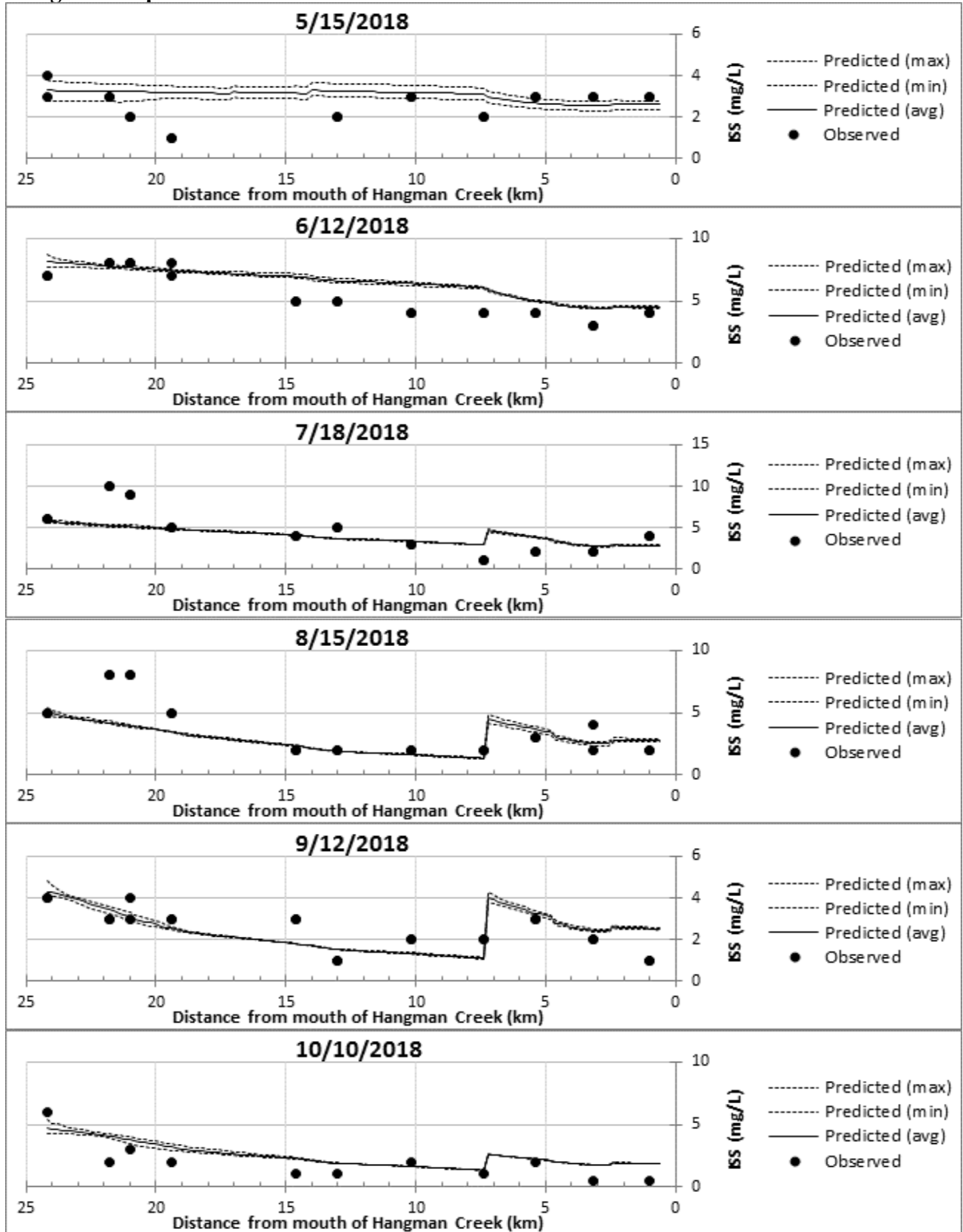


Total Suspended Solids

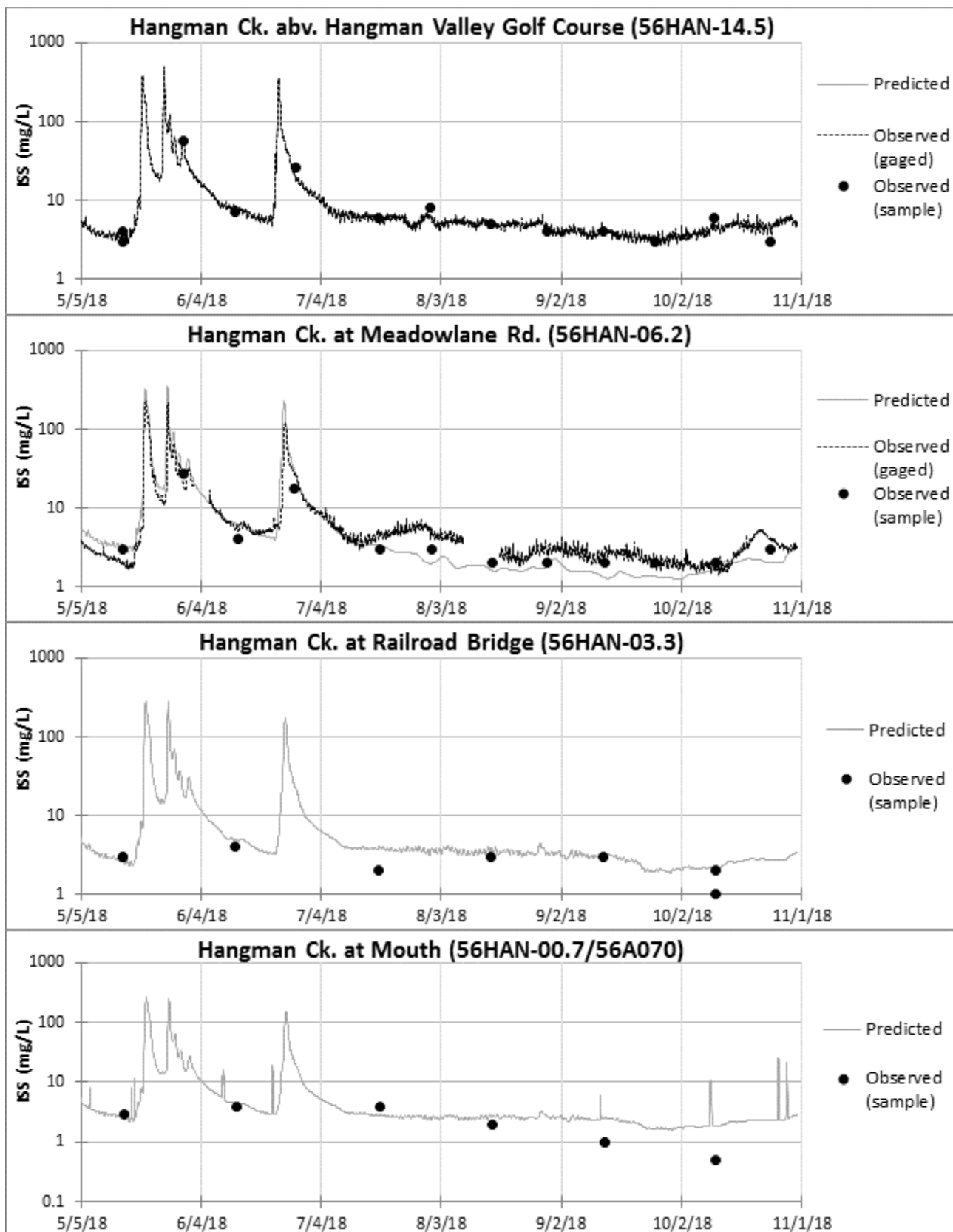




Inorganic Suspended Solids



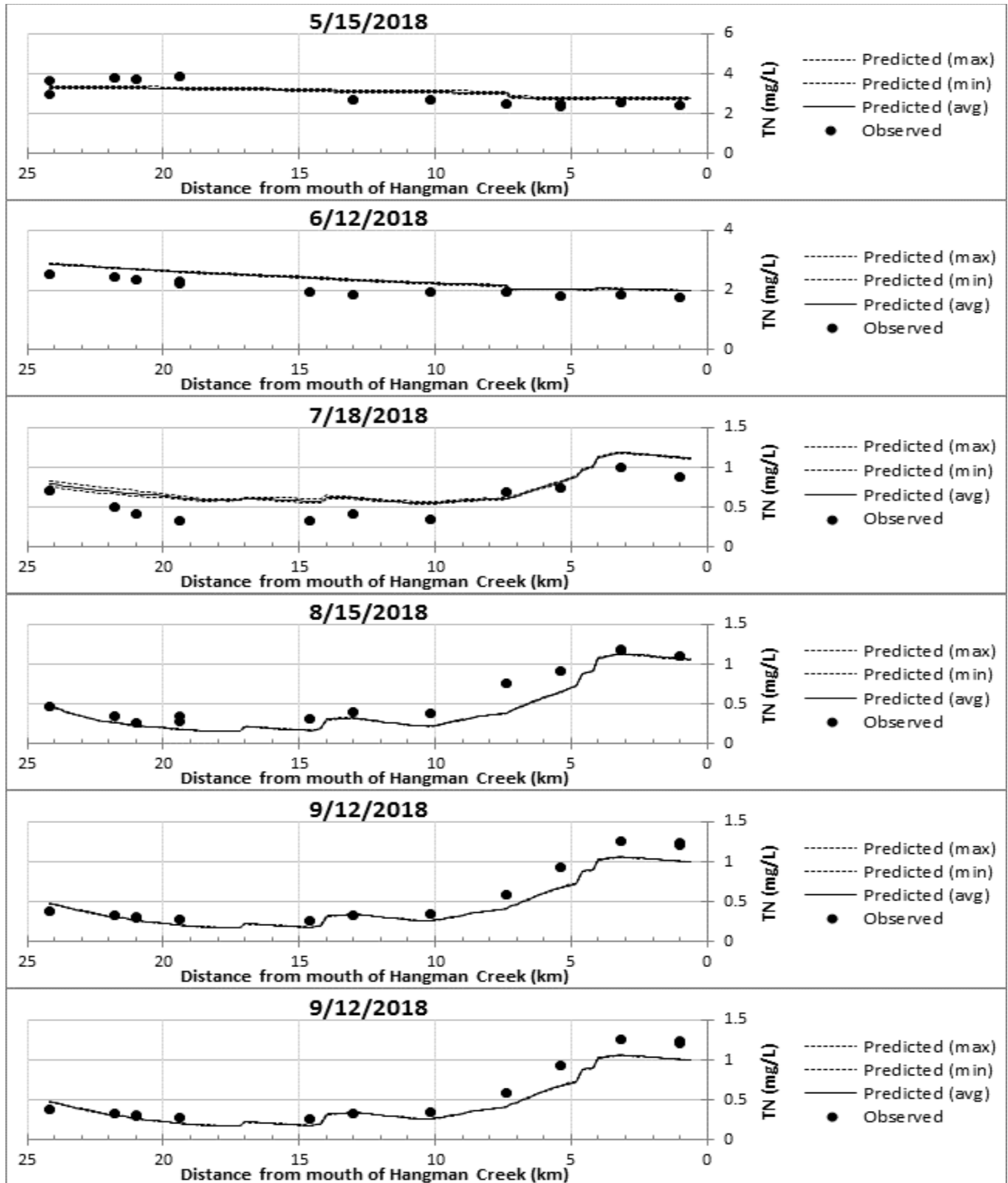
"Gaged" ISS values are estimated from continuous turbidity monitoring data.

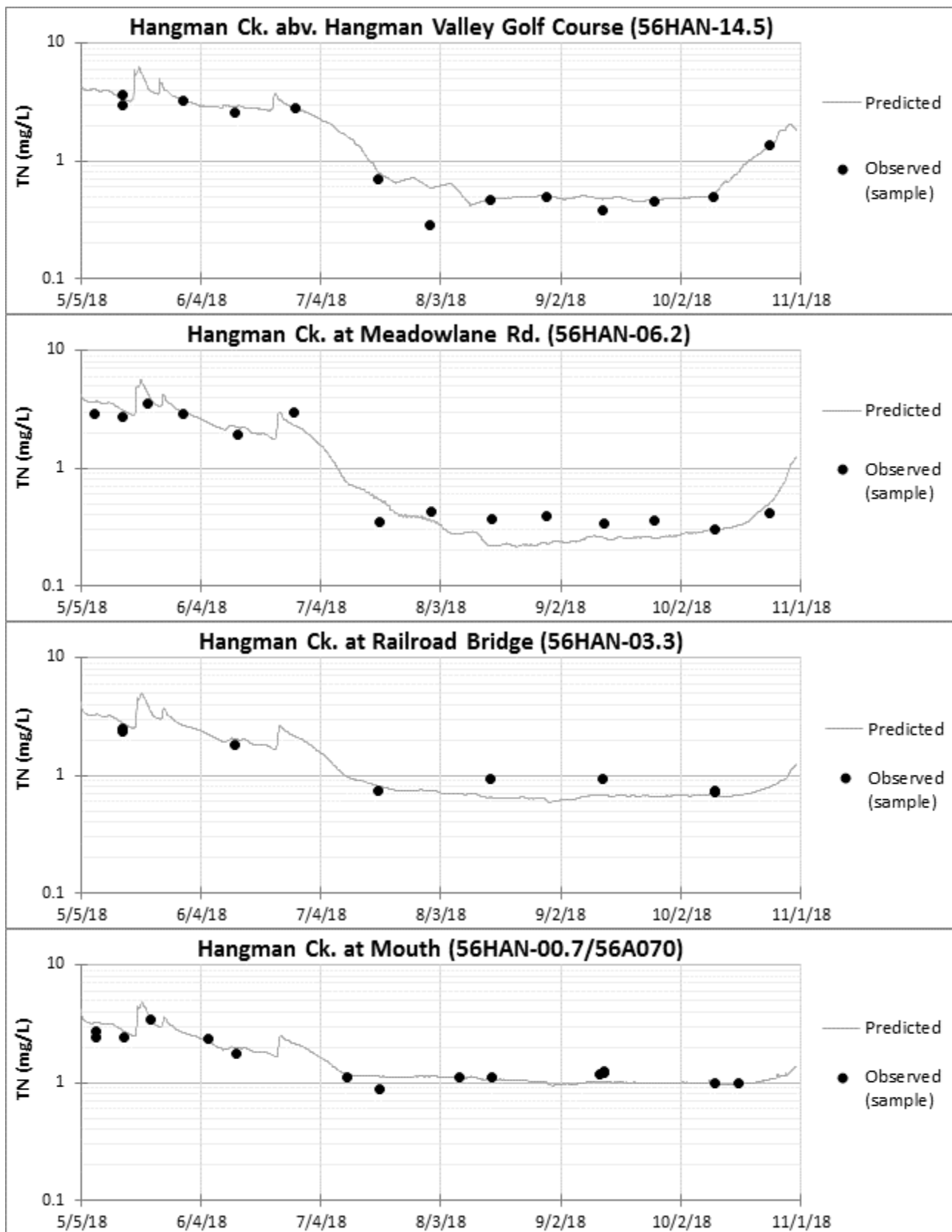


Total Nitrogen

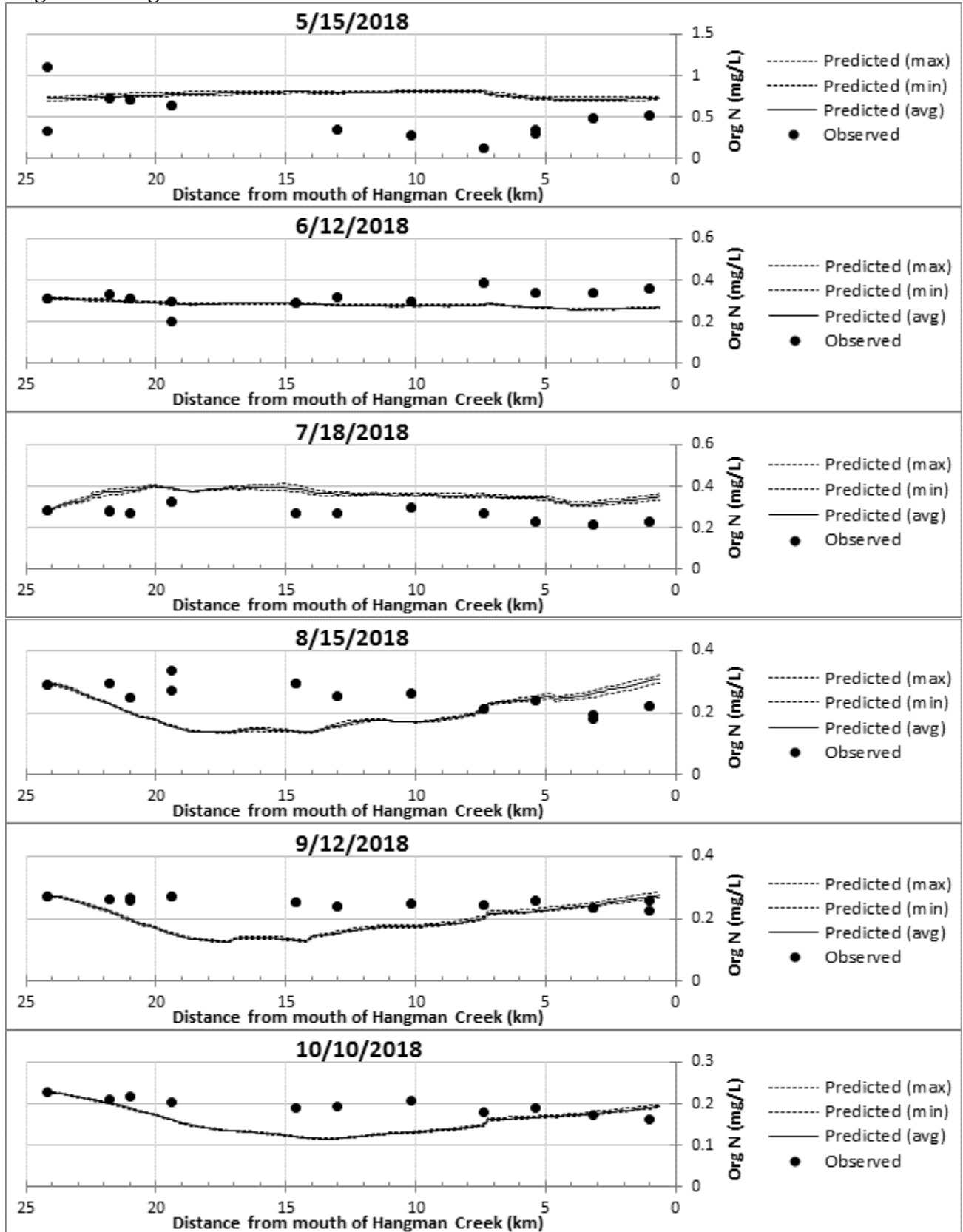
Predicted TN includes organic N, ammonium N, nitrate-nitrite N, and N included in phytoplankton.

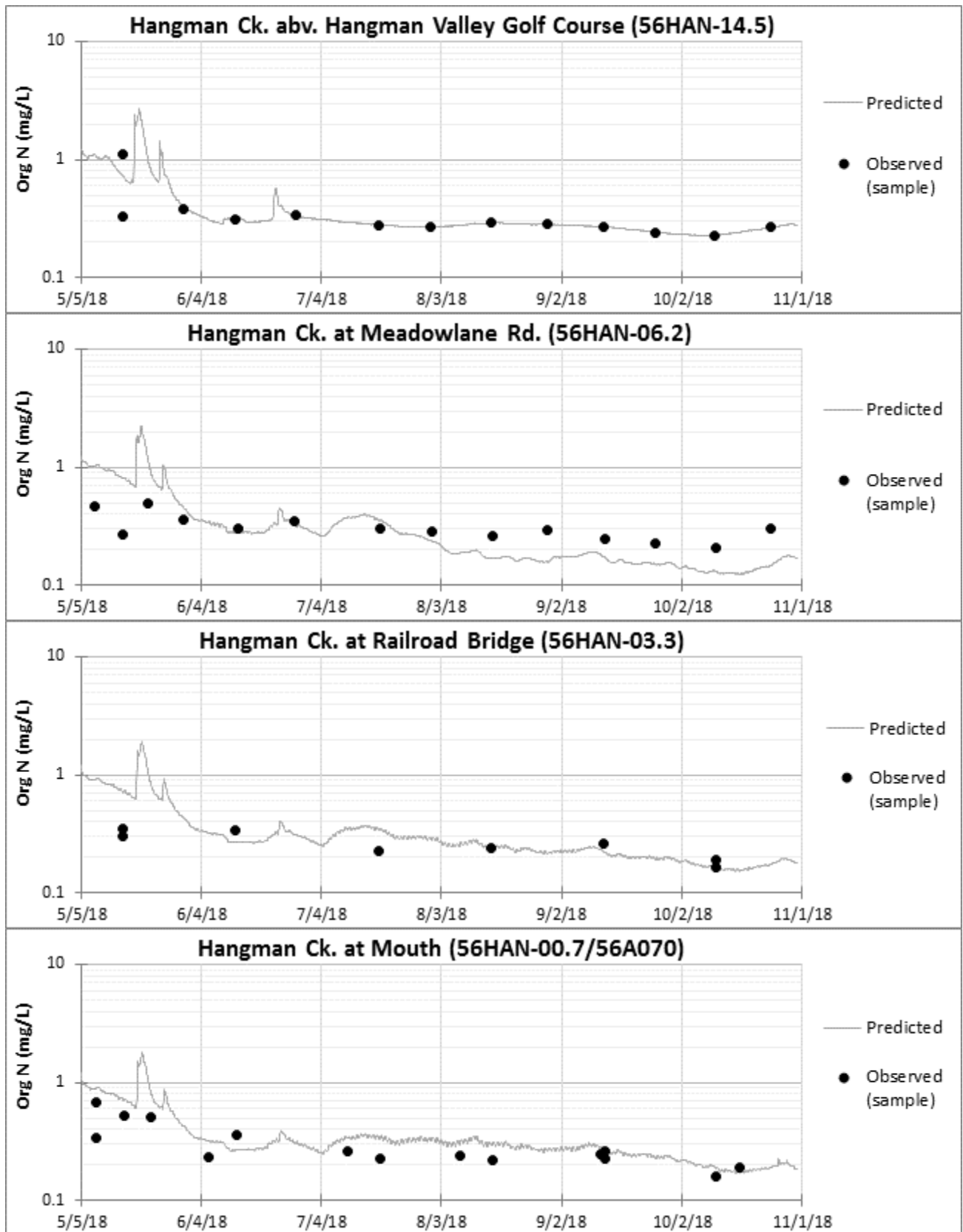
Observed data do not include the phytoplankton component, as the lab procedure for total persulfate nitrogen (TPN) includes a decanting step that removes particulate material. Thus, the model appears to overpredict TN during June and July phytoplankton blooms.



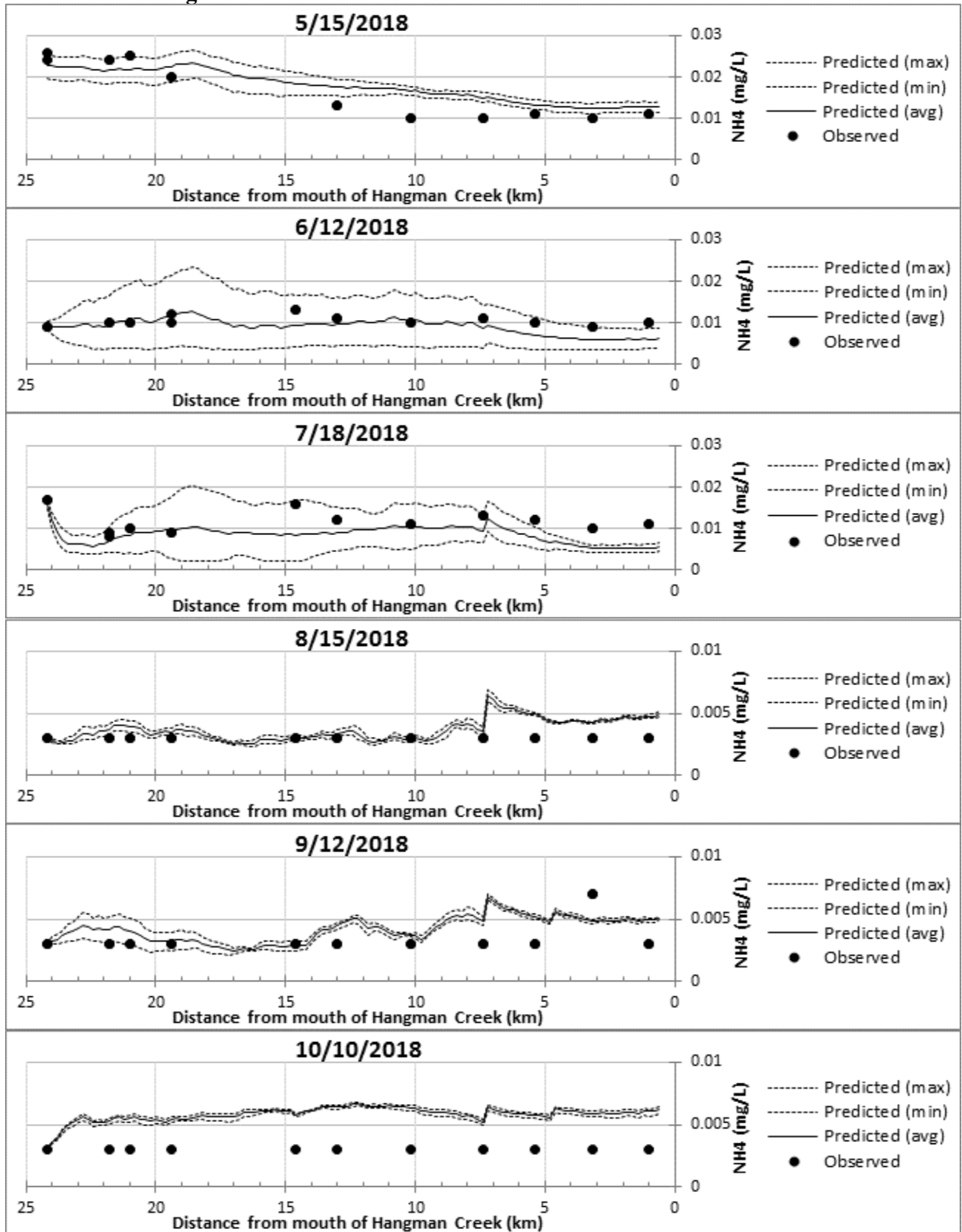


Organic Nitrogen

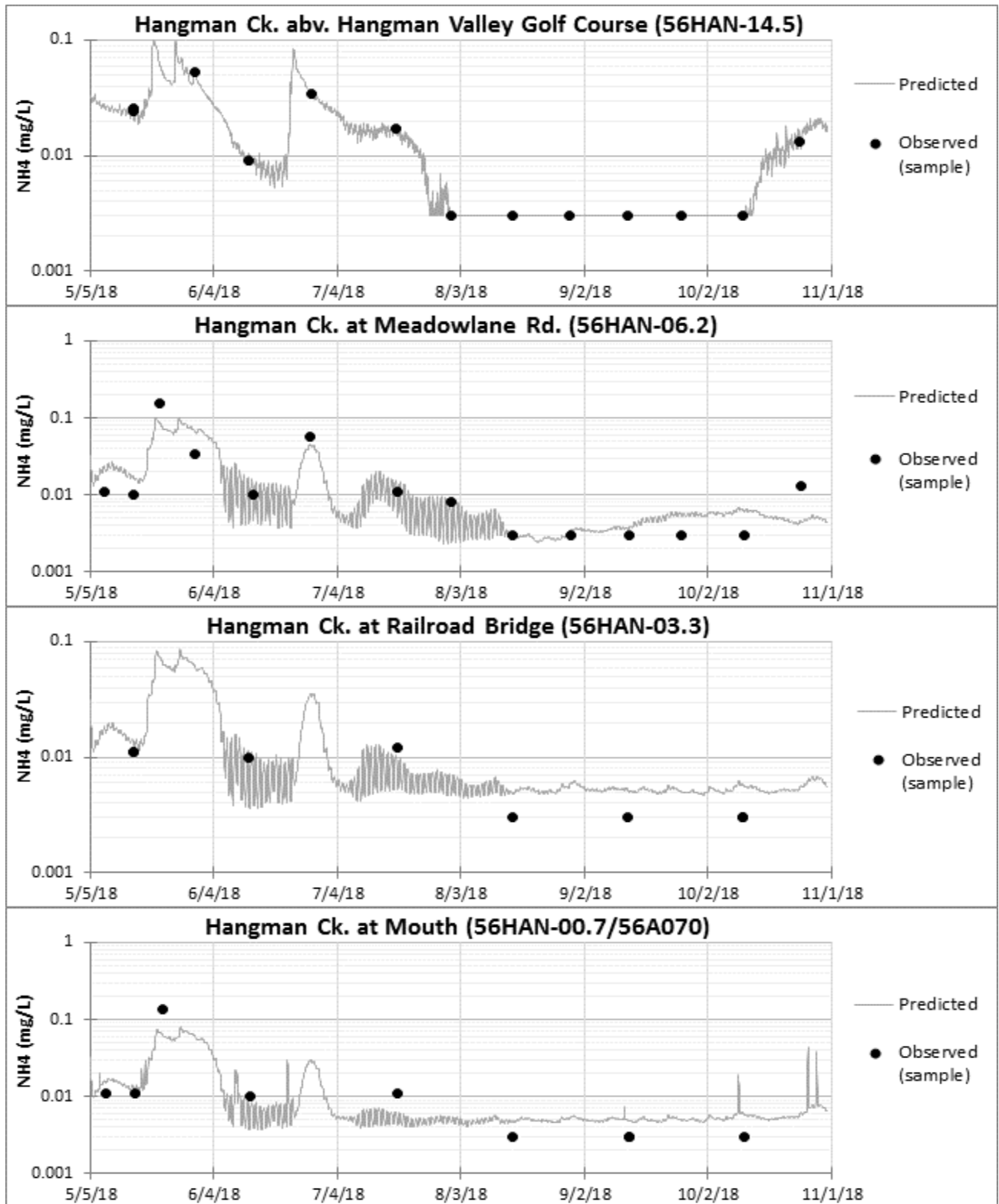




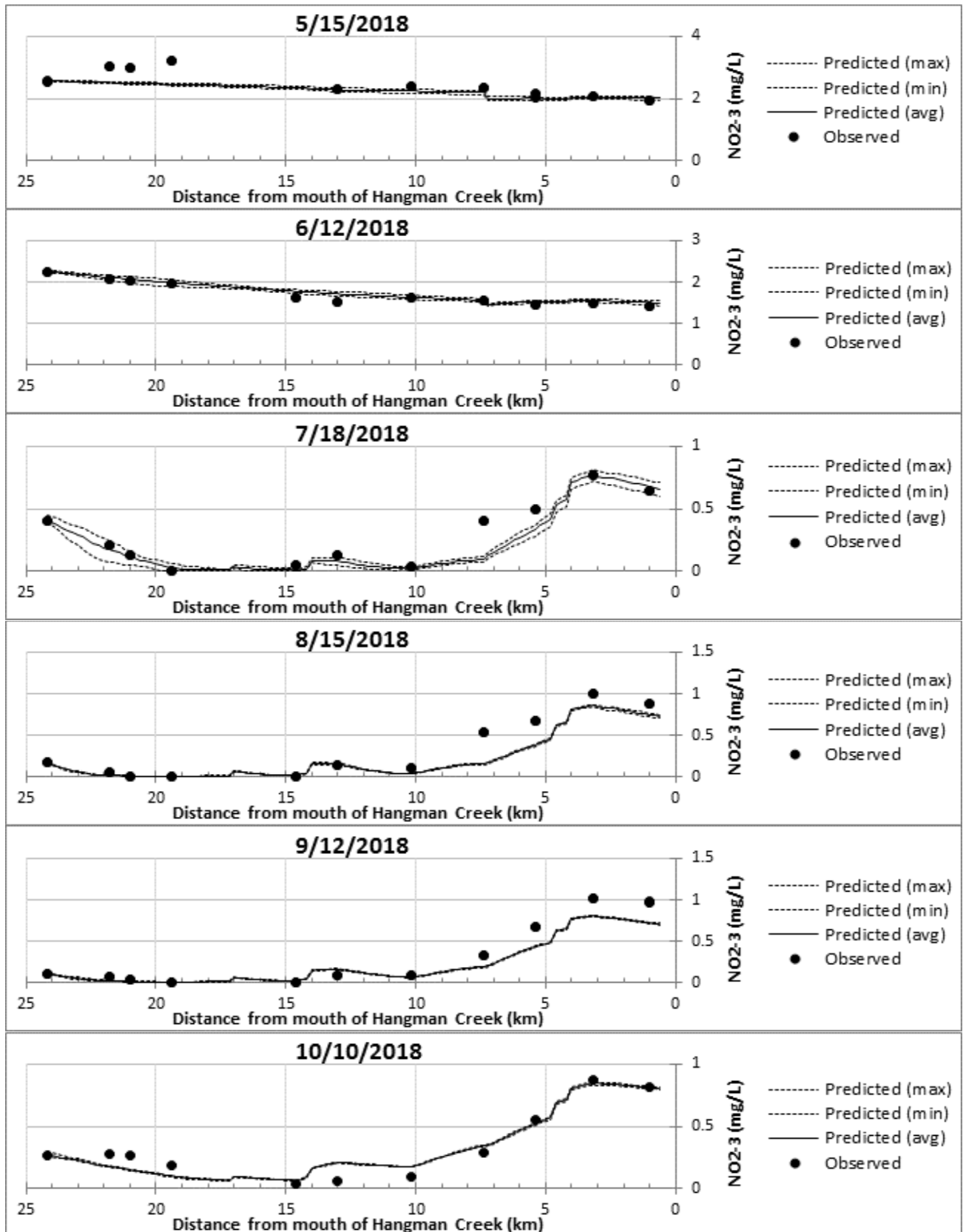
Ammonium Nitrogen



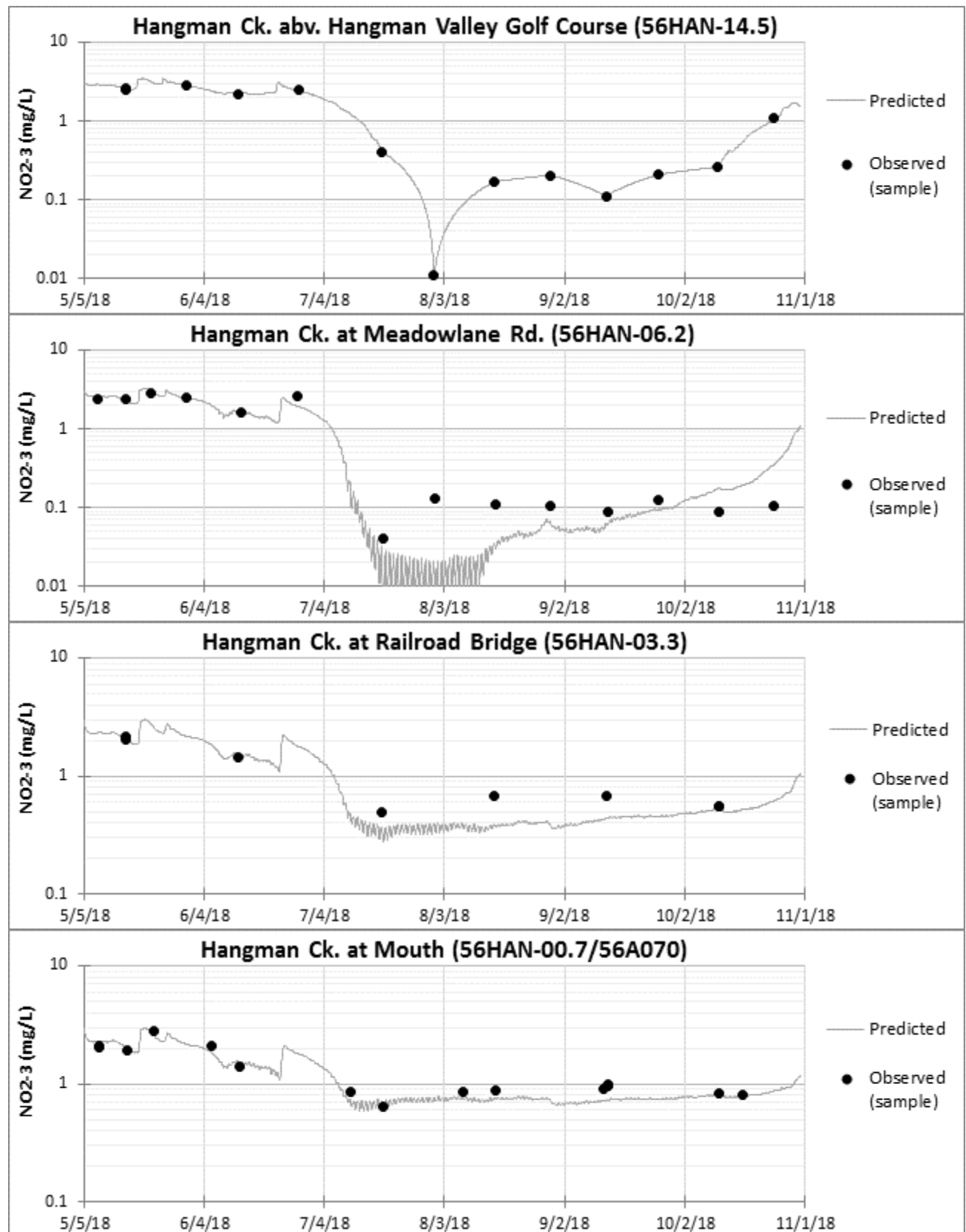
Large diel fluctuations in predicted inorganic nutrients (NH_4 , $\text{NO}_2\text{-3}$, Inorg P) result from simulated uptake by phytoplankton. The QUAL2Kw formulation for phytoplankton, unlike for bottom algae, does not include luxury nutrient uptake. These fluctuations are an expected model artifact and should not be construed as representing reality.



Nitrate-nitrite Nitrogen

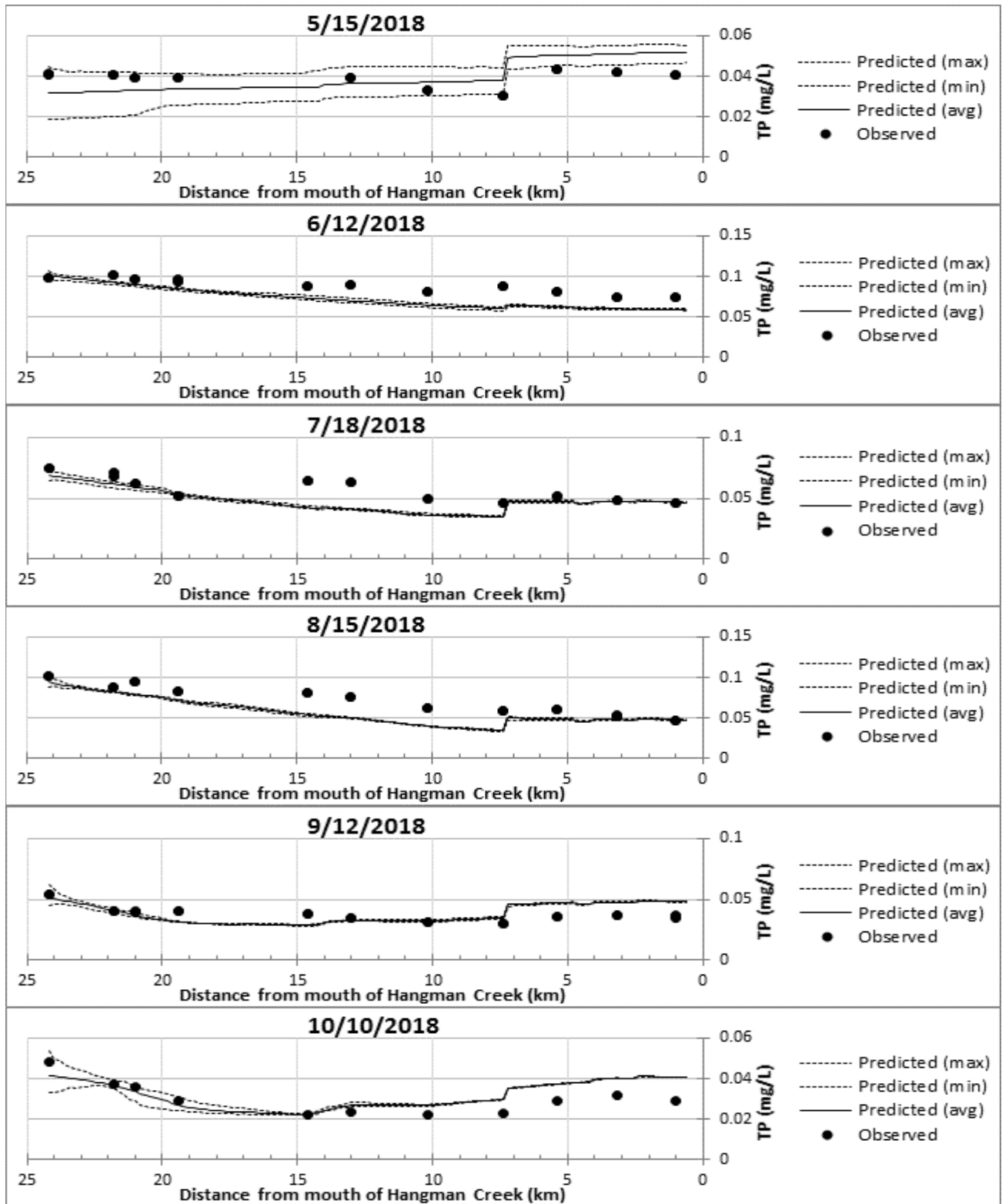


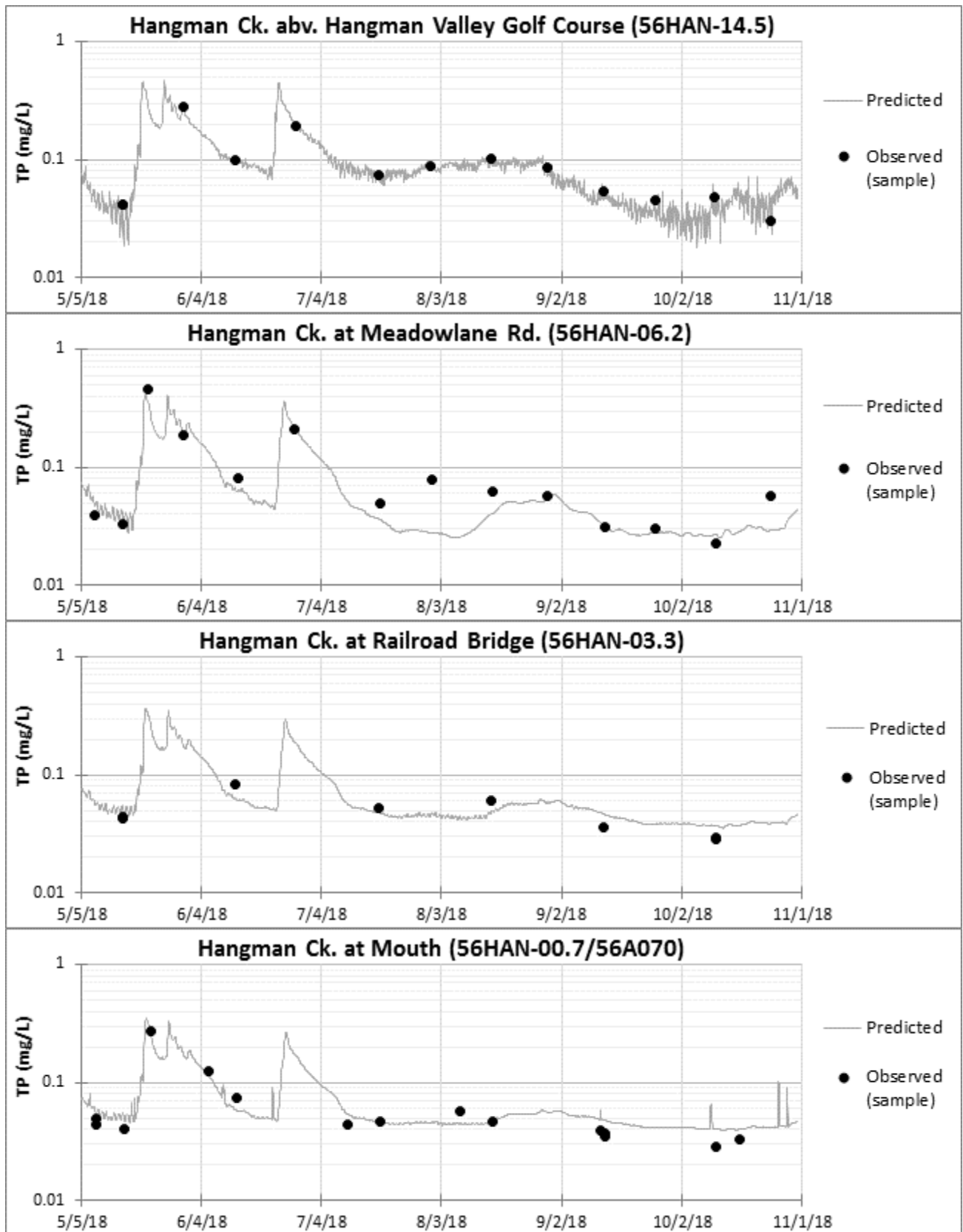
See note accompanying ammonium-N time-series plots concerning predicted diel fluctuations.



Total Phosphorus

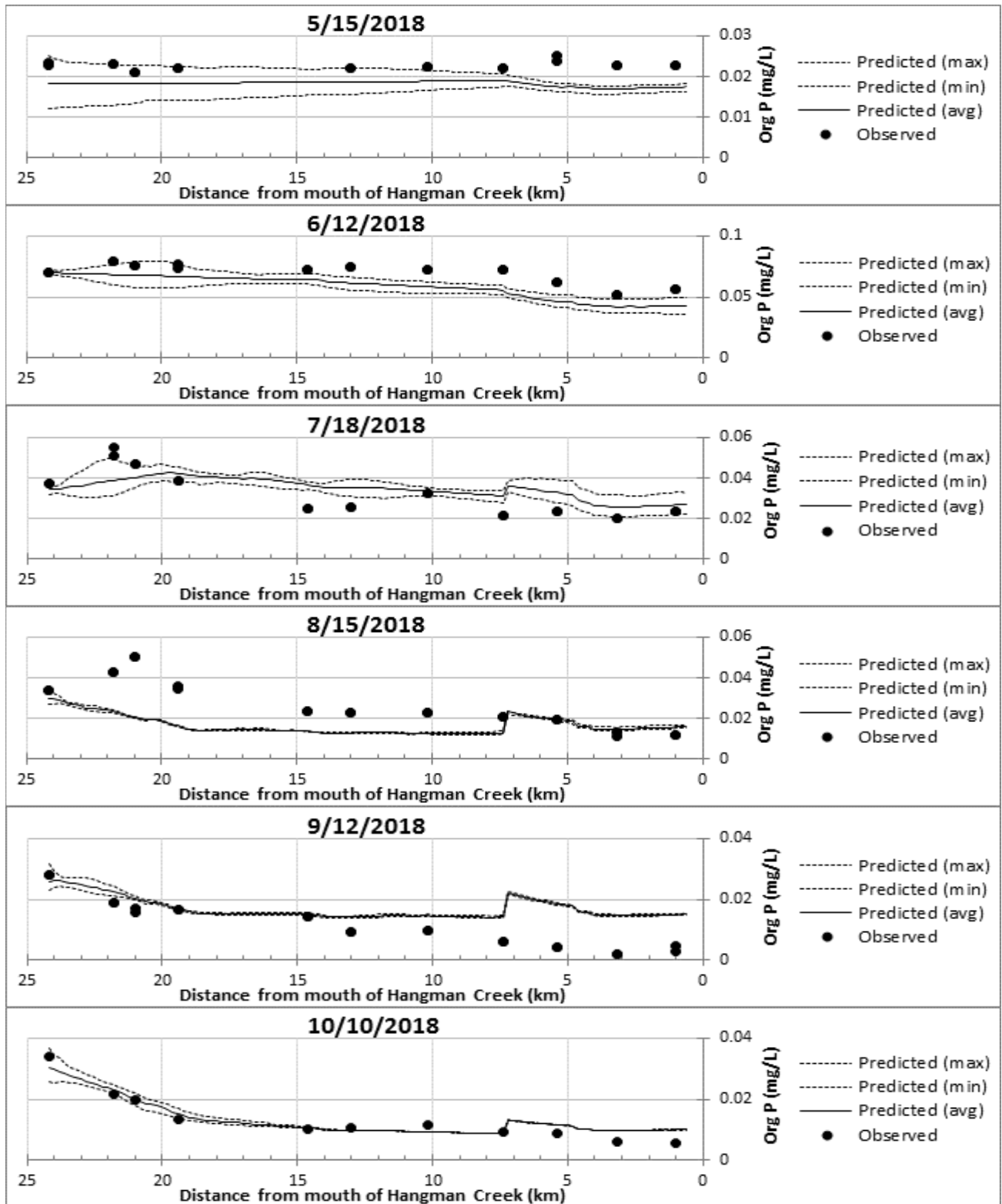
In contrast to the situation for total N, the lab method for total P includes all P in the sample, including particulate material such as phytoplankton. Predicted and observed data should be directly comparable.

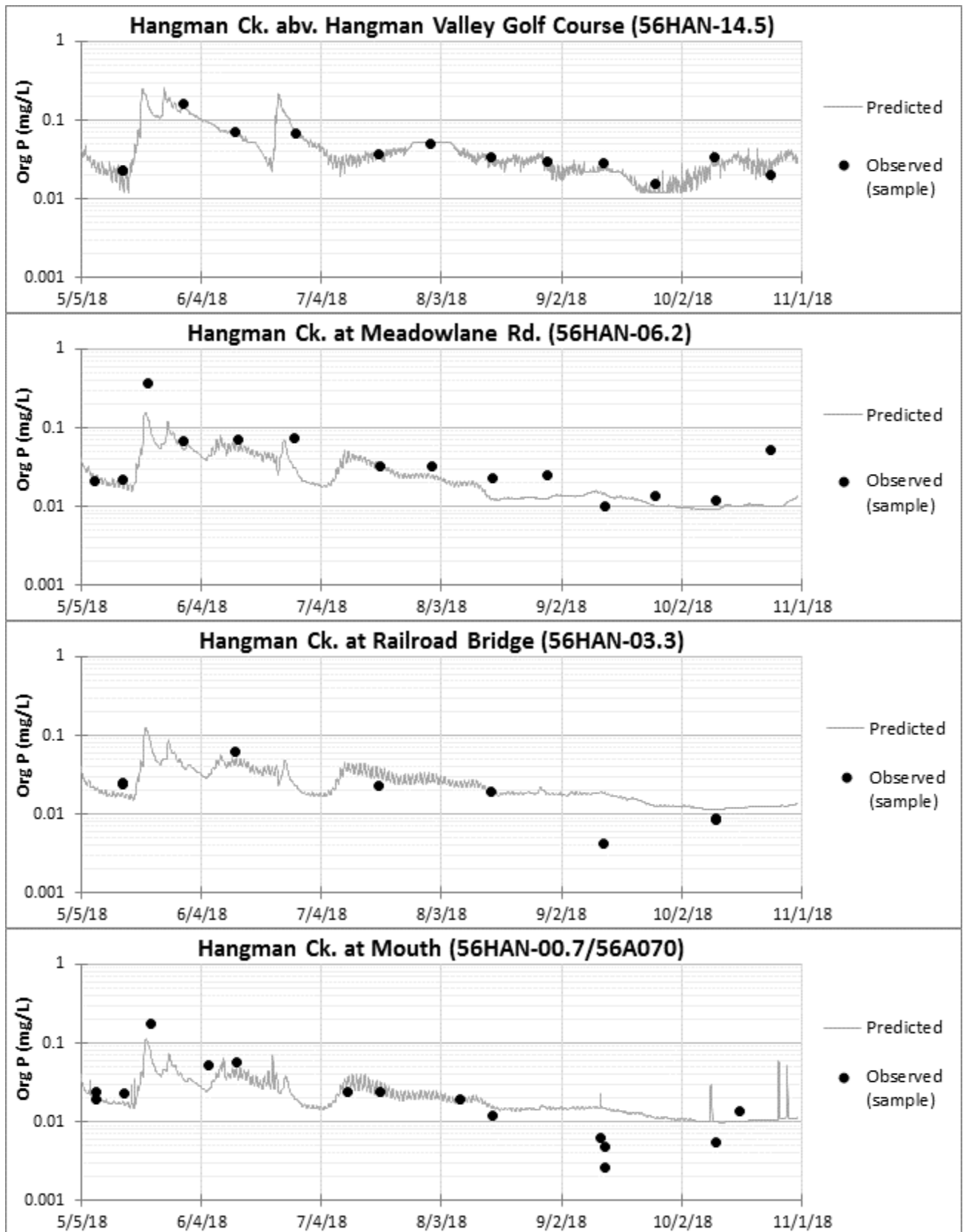




Organic Phosphorus

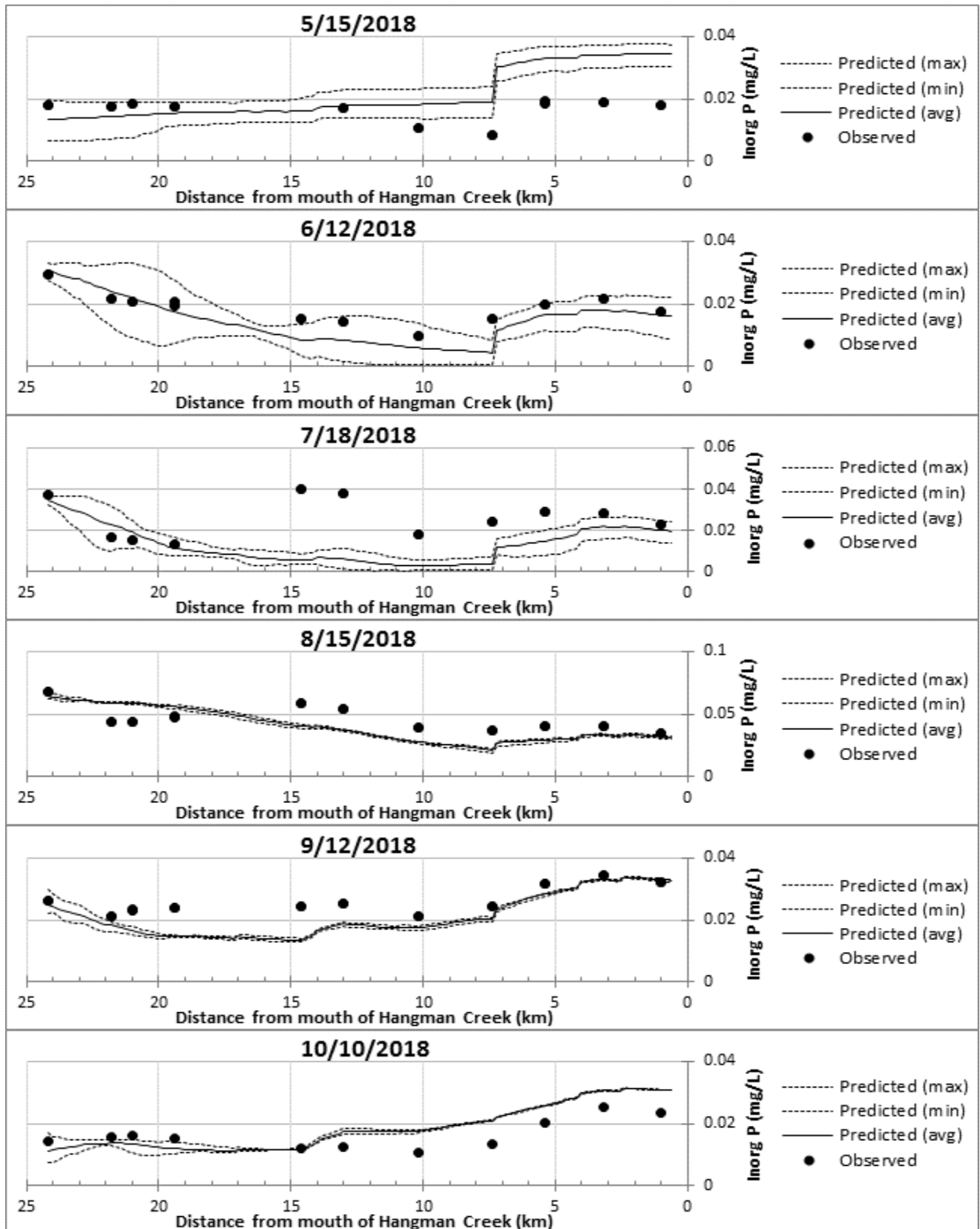
The predicted values shown here include the organic P fraction as defined by QUAL2Kw (which does not include P in phytoplankton) plus the phytoplankton P fraction. This makes the predicted and observed data directly comparable.

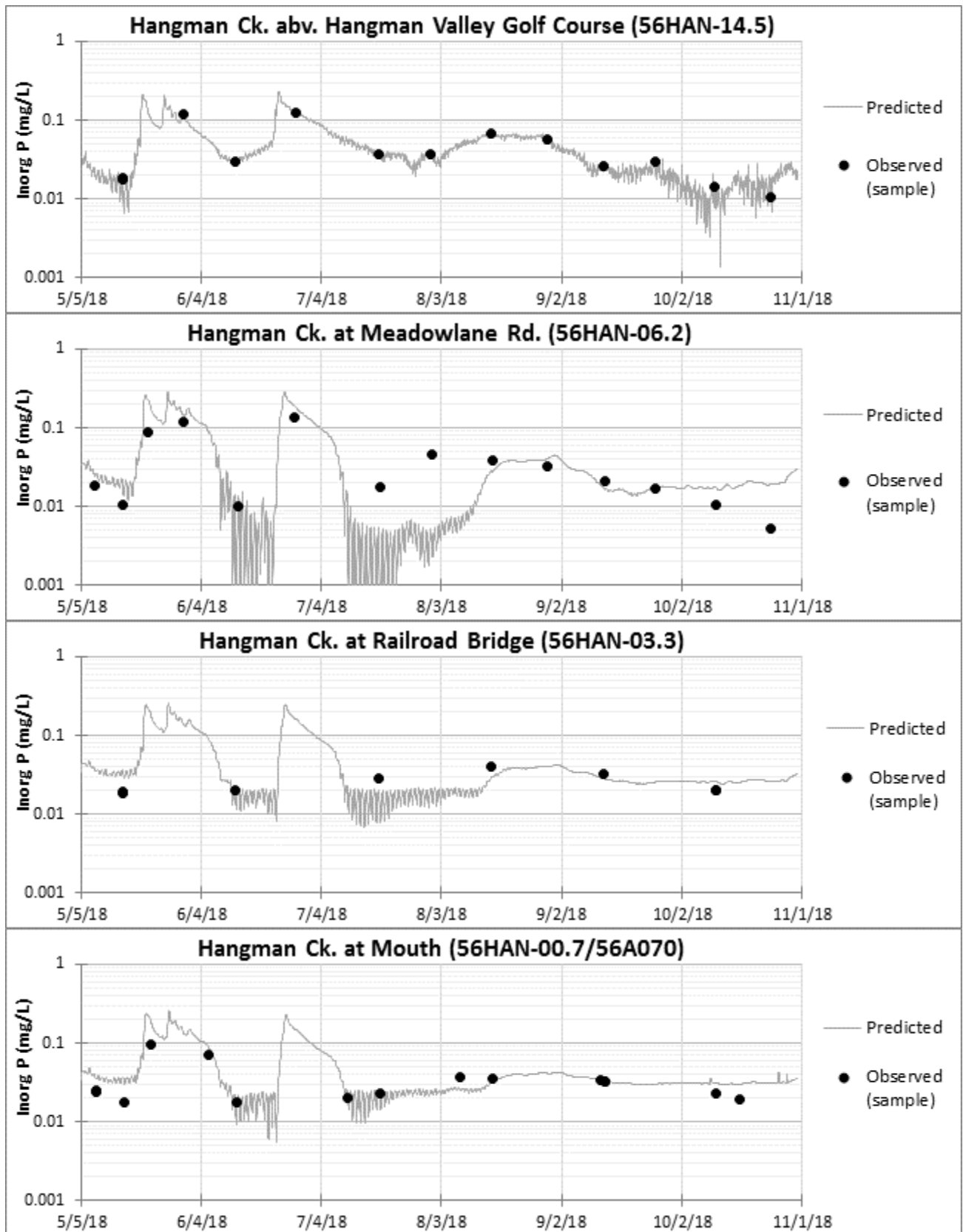




Inorganic Phosphorus

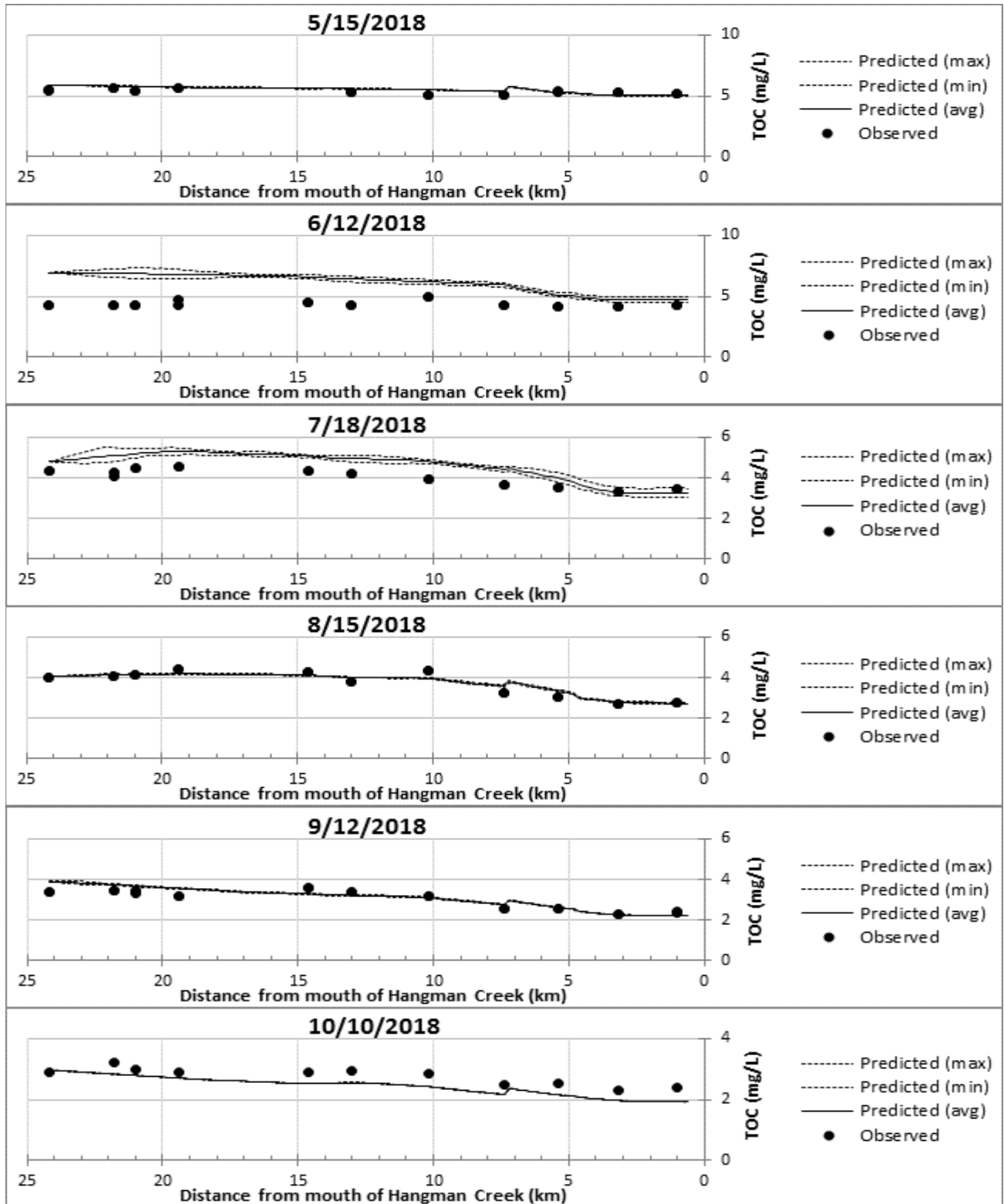
See note accompanying ammonium-N time-series plots concerning predicted diel fluctuations.

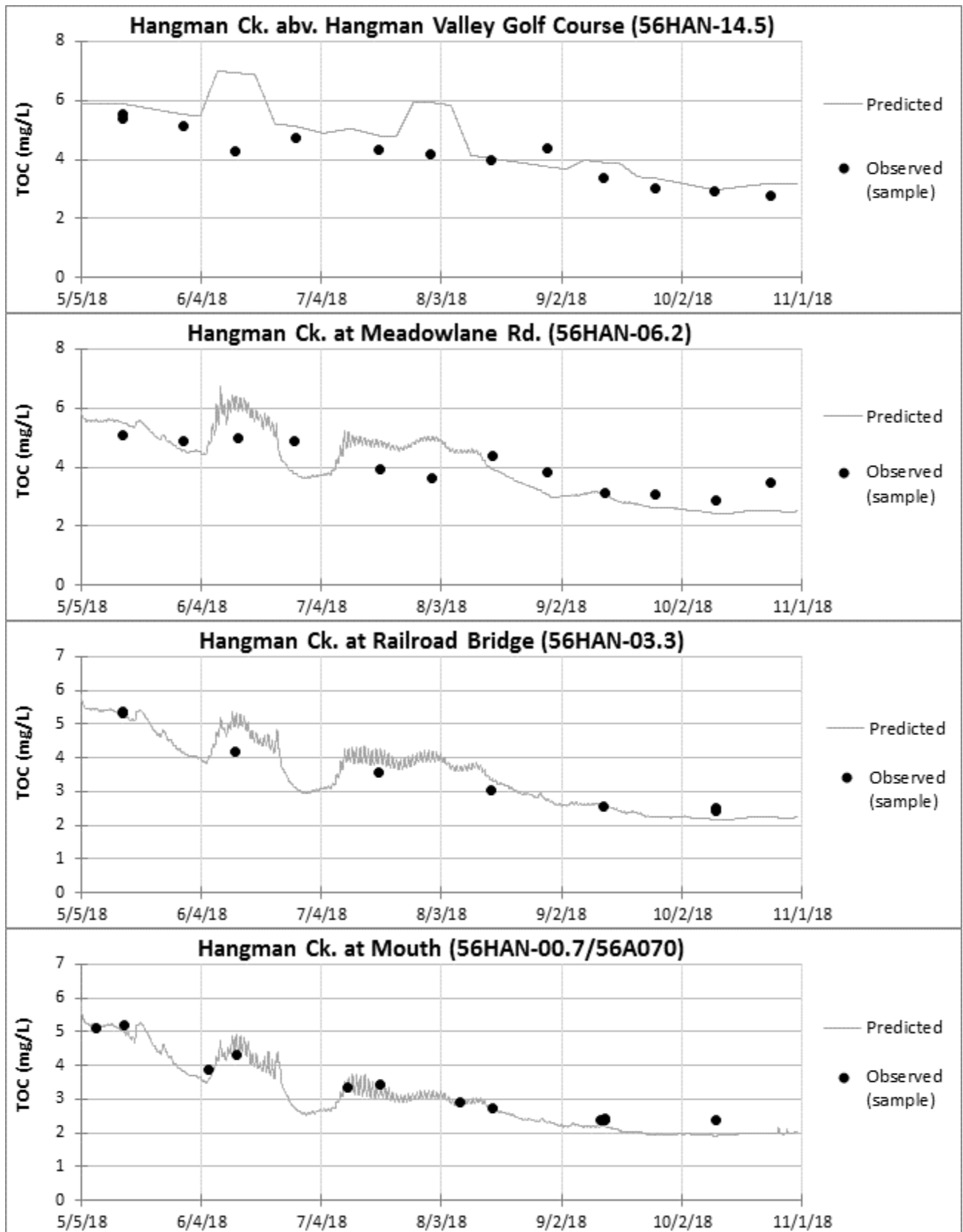




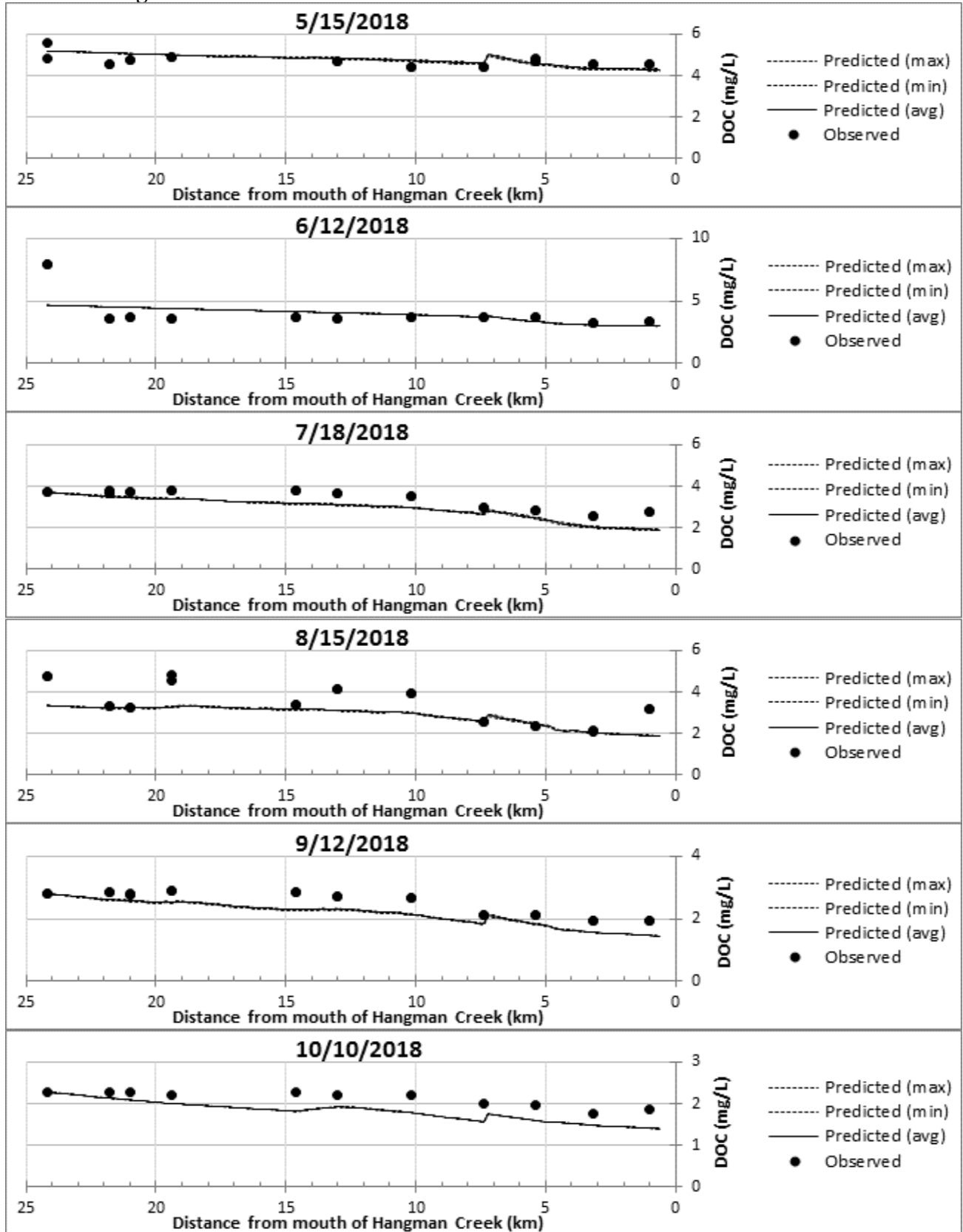
Total Organic Carbon

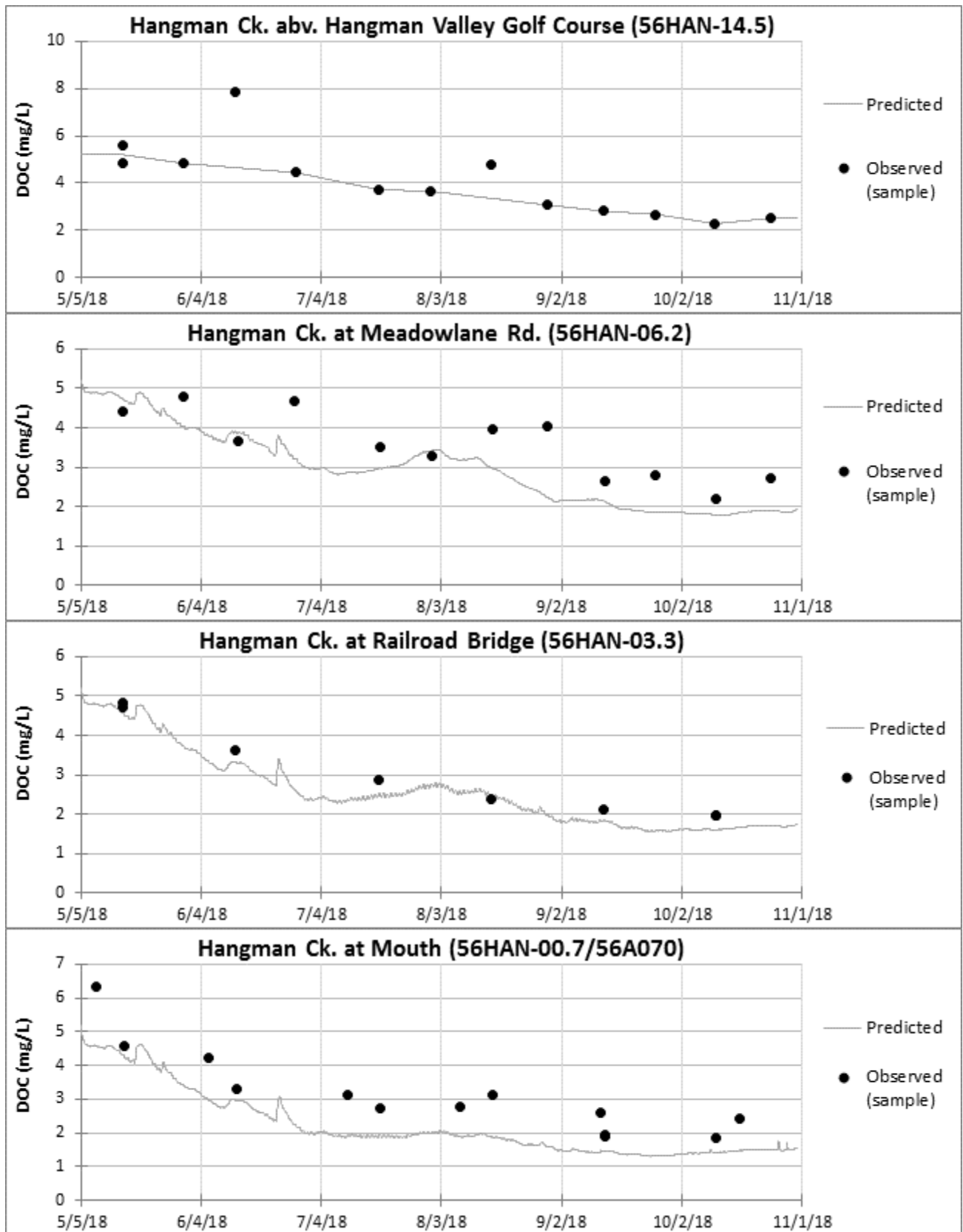
Similar to the case for total N, observed TOC data do not include the phytoplankton component of C, as the lab procedure includes a decanting step that removes particulate material. Thus, the model appears to overpredict TOC during June and July phytoplankton blooms.





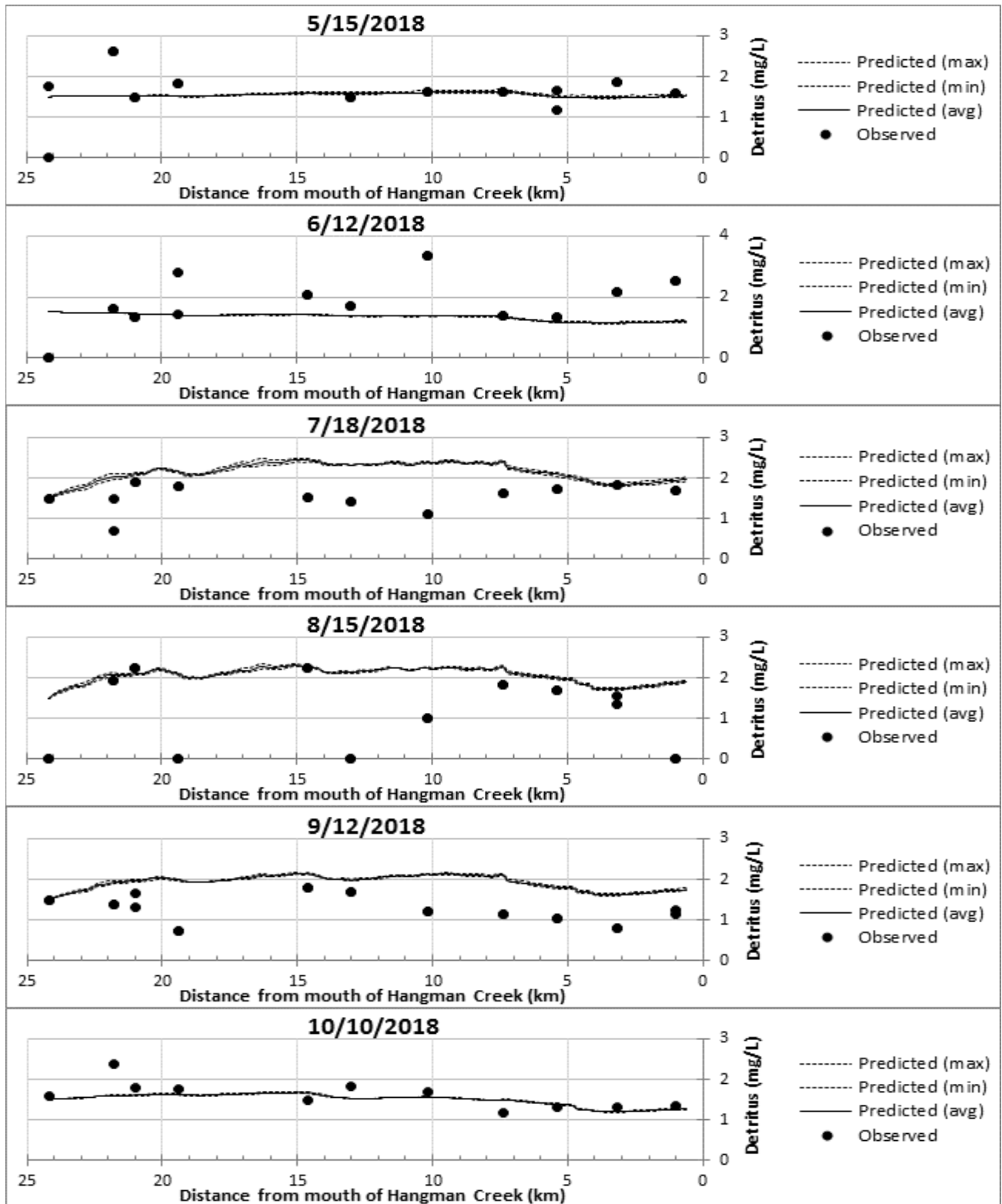
Dissolved Organic Carbon

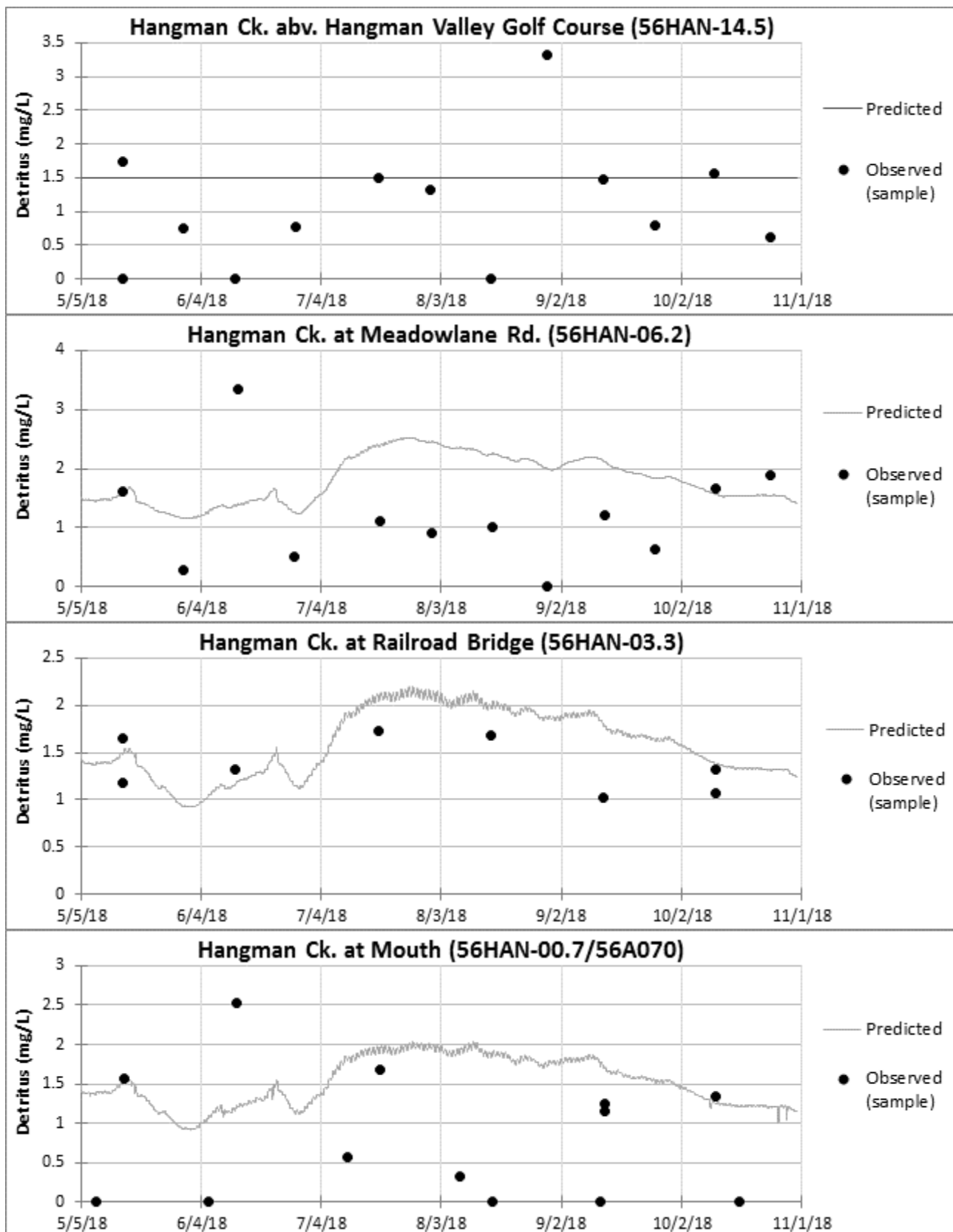




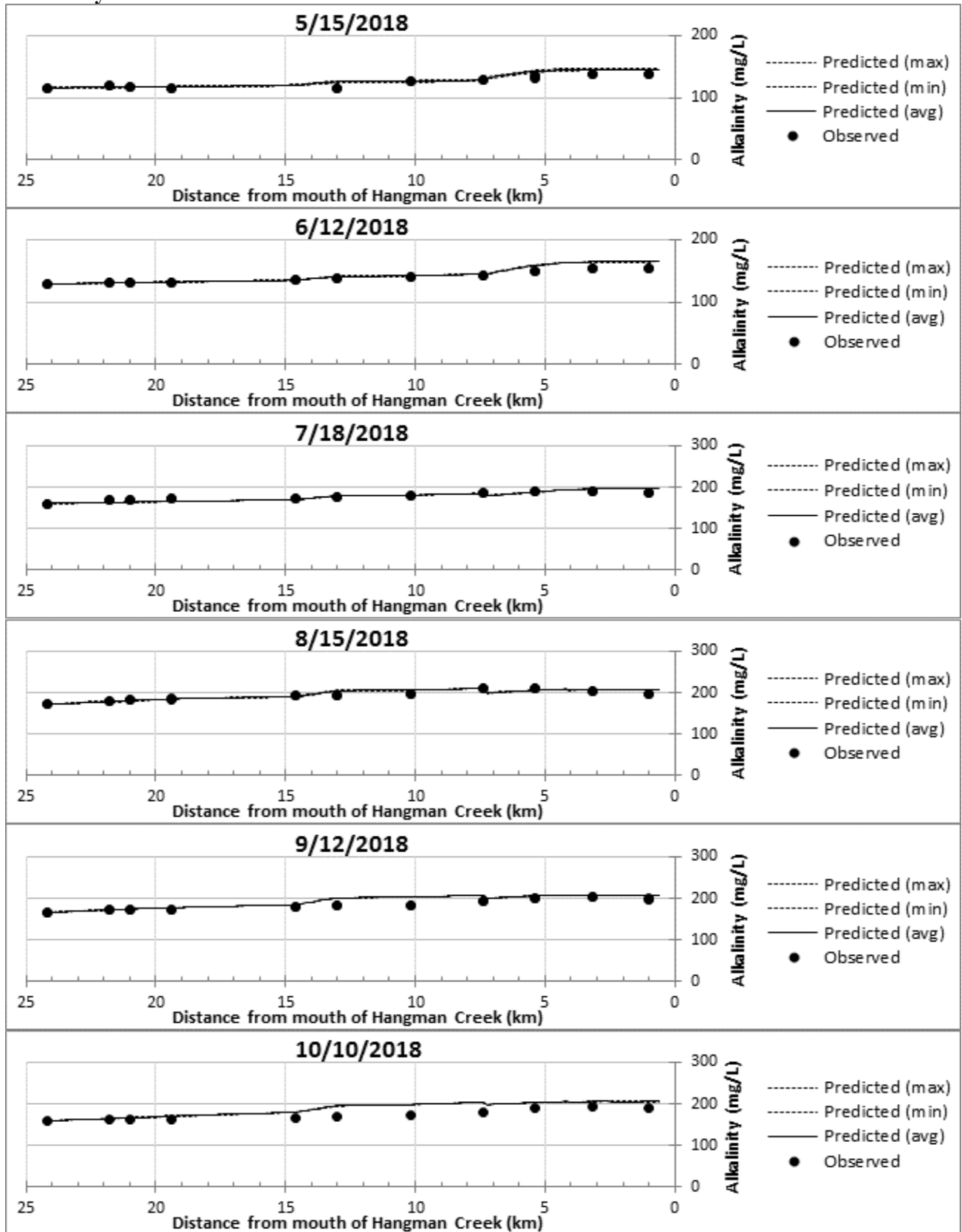
Detritus

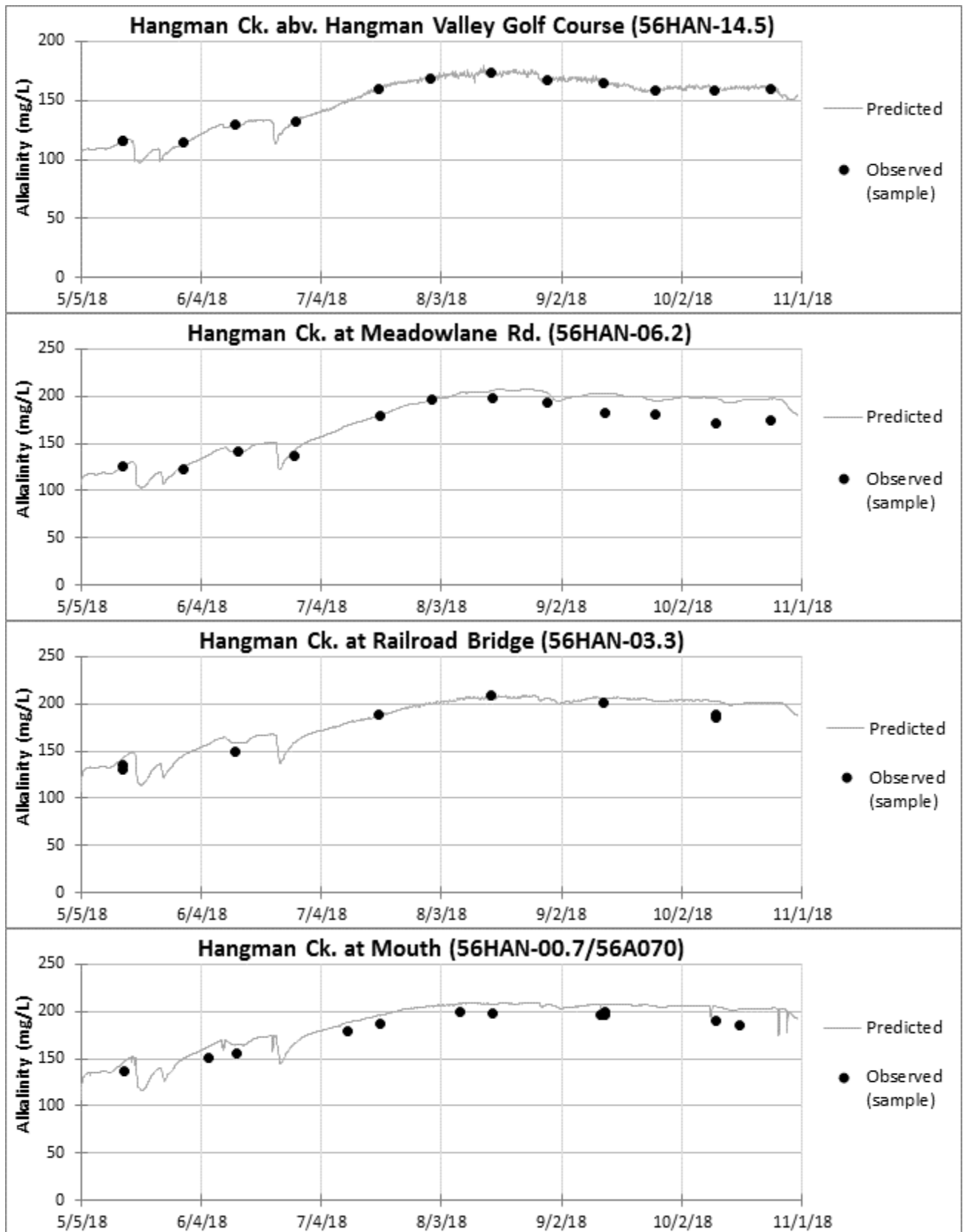
We calculated observed detritus data as $(TOC-DOC)*2.5$, where 2.5 is the stoichiometric ratio of dry weight to carbon. The TOC-DOC subtraction results in data that is highly variable. We used the observed data as a general guide to magnitude only.





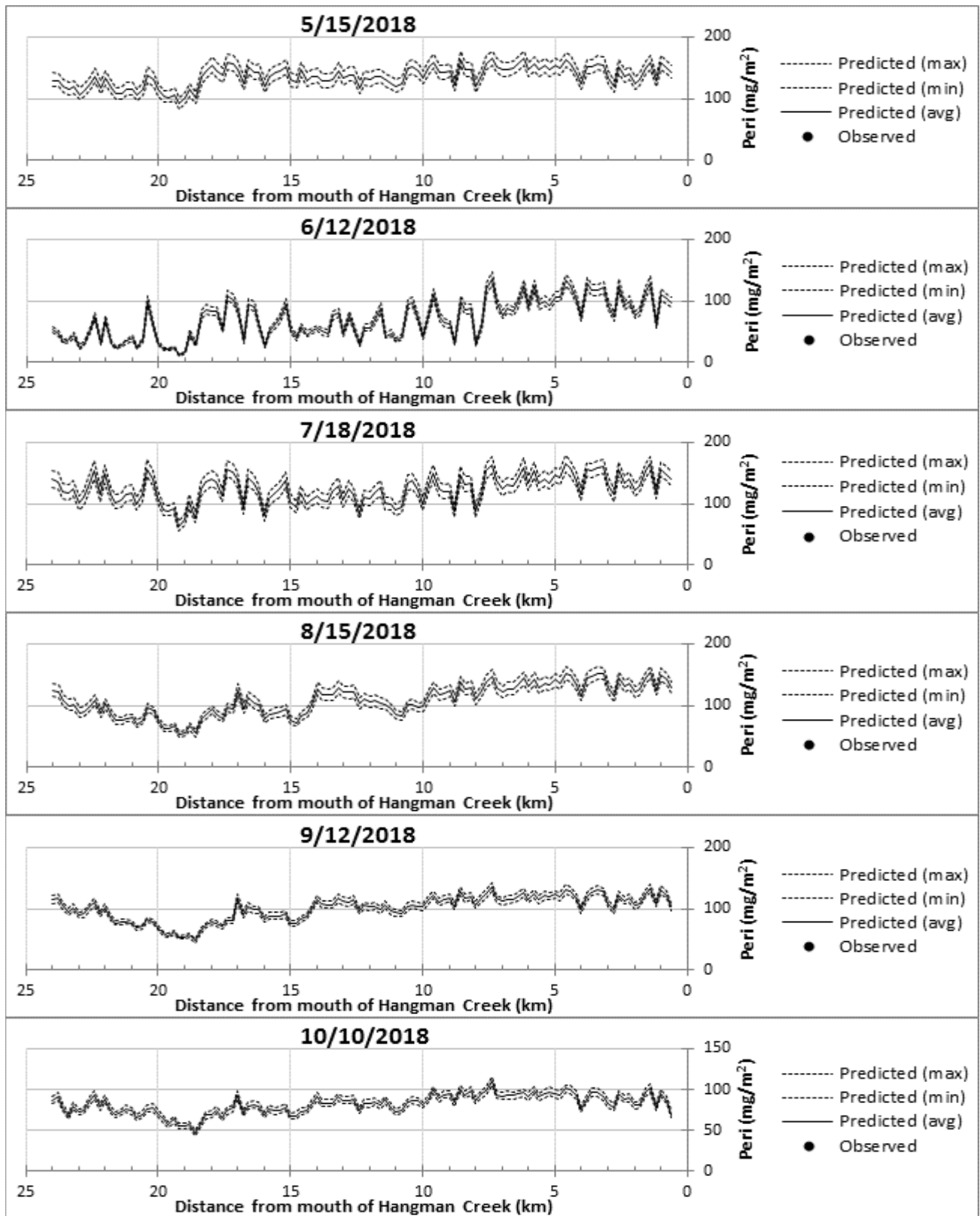
Alkalinity

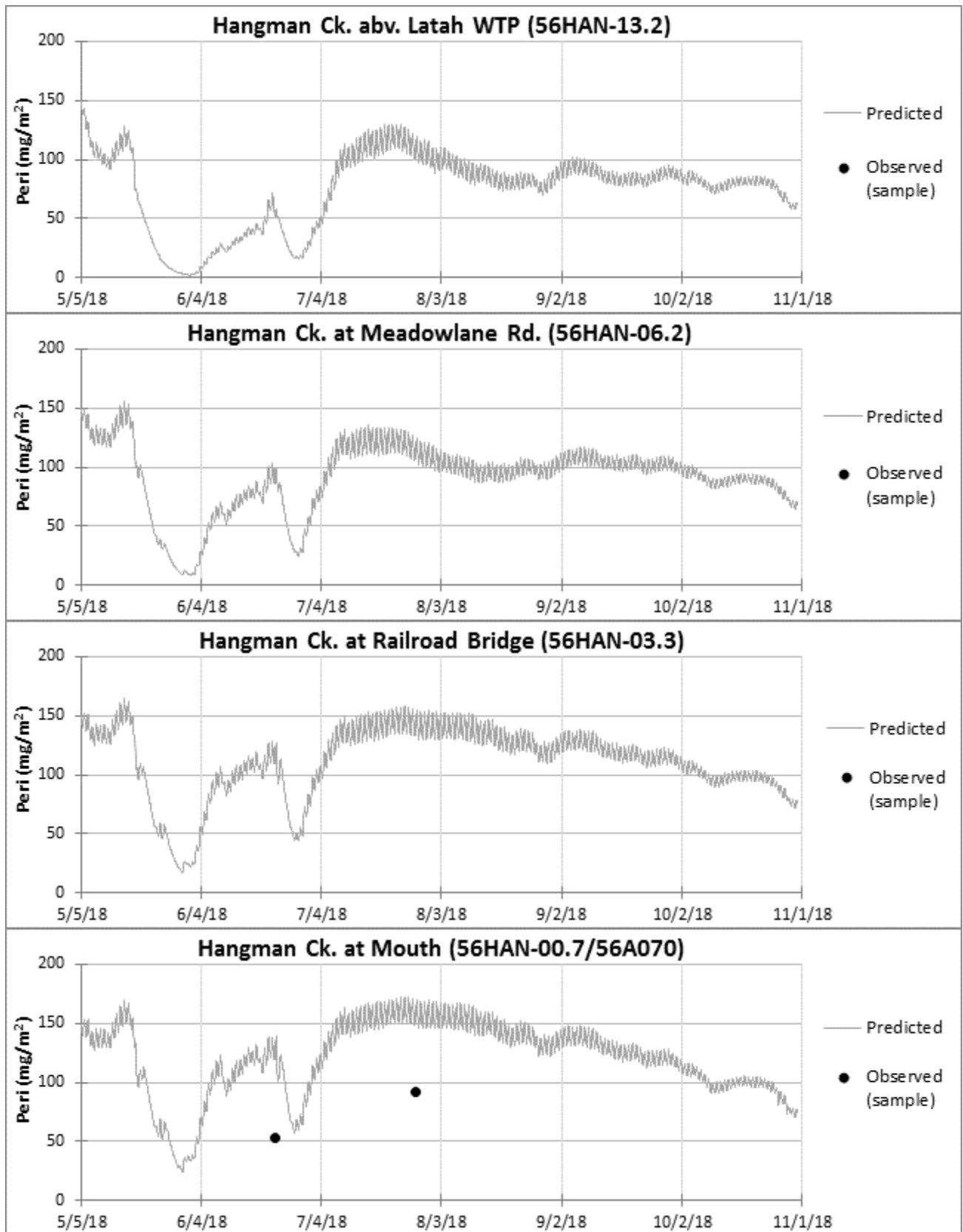




Periphyton (bottom algae) as Chlorophyll a

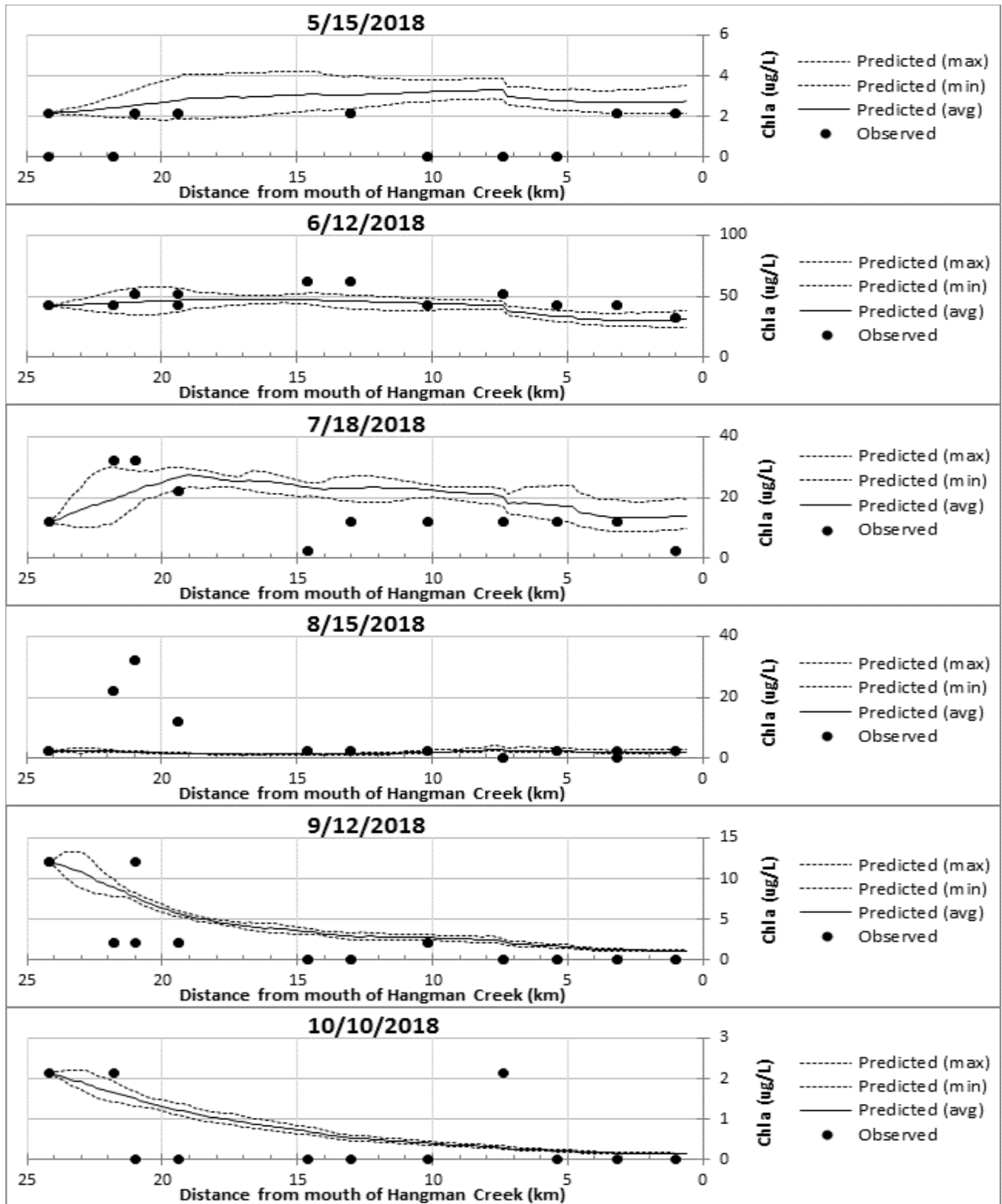
We collected the observed data in June and July, 2009. We show them here on the equivalent dates in 2018.

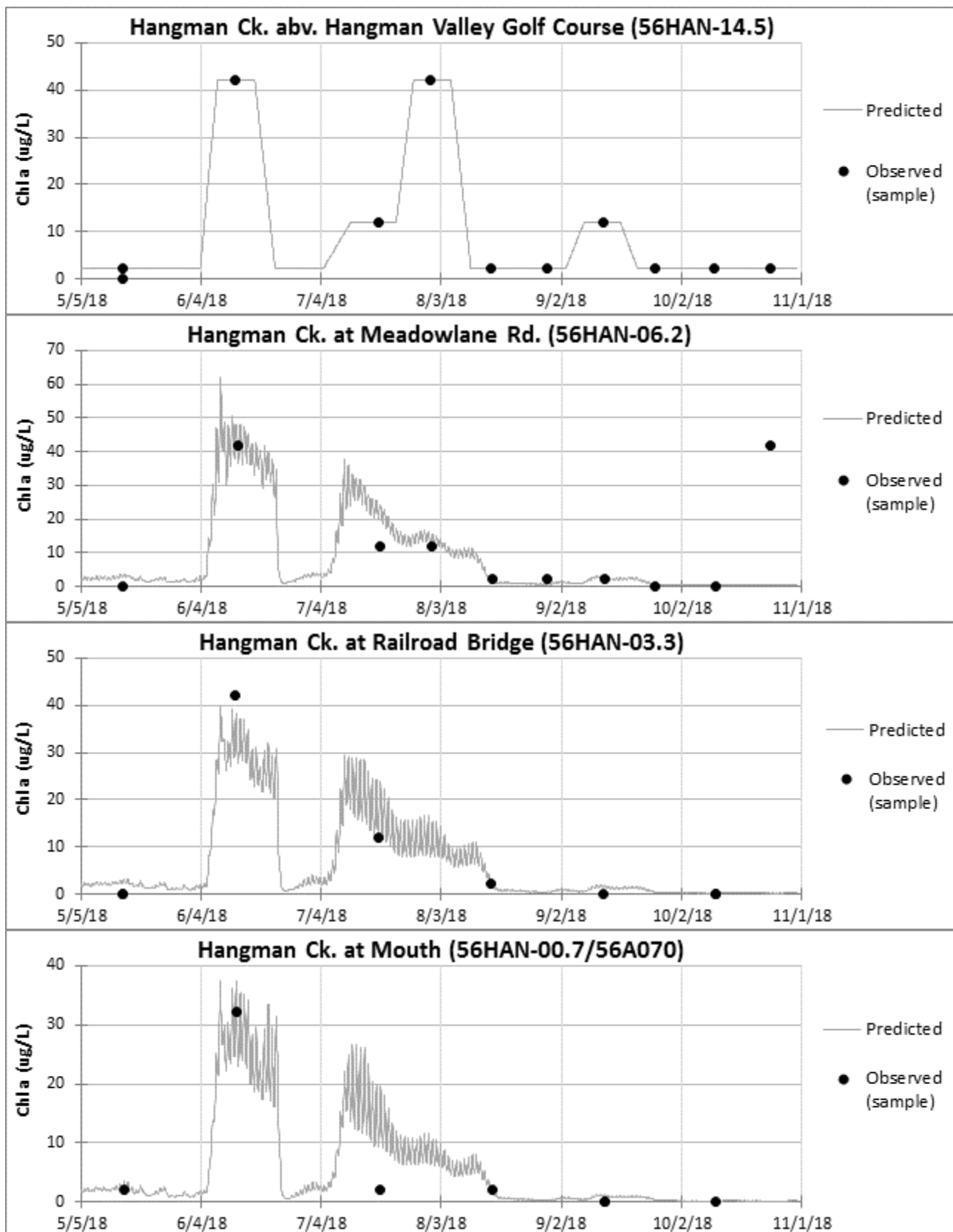




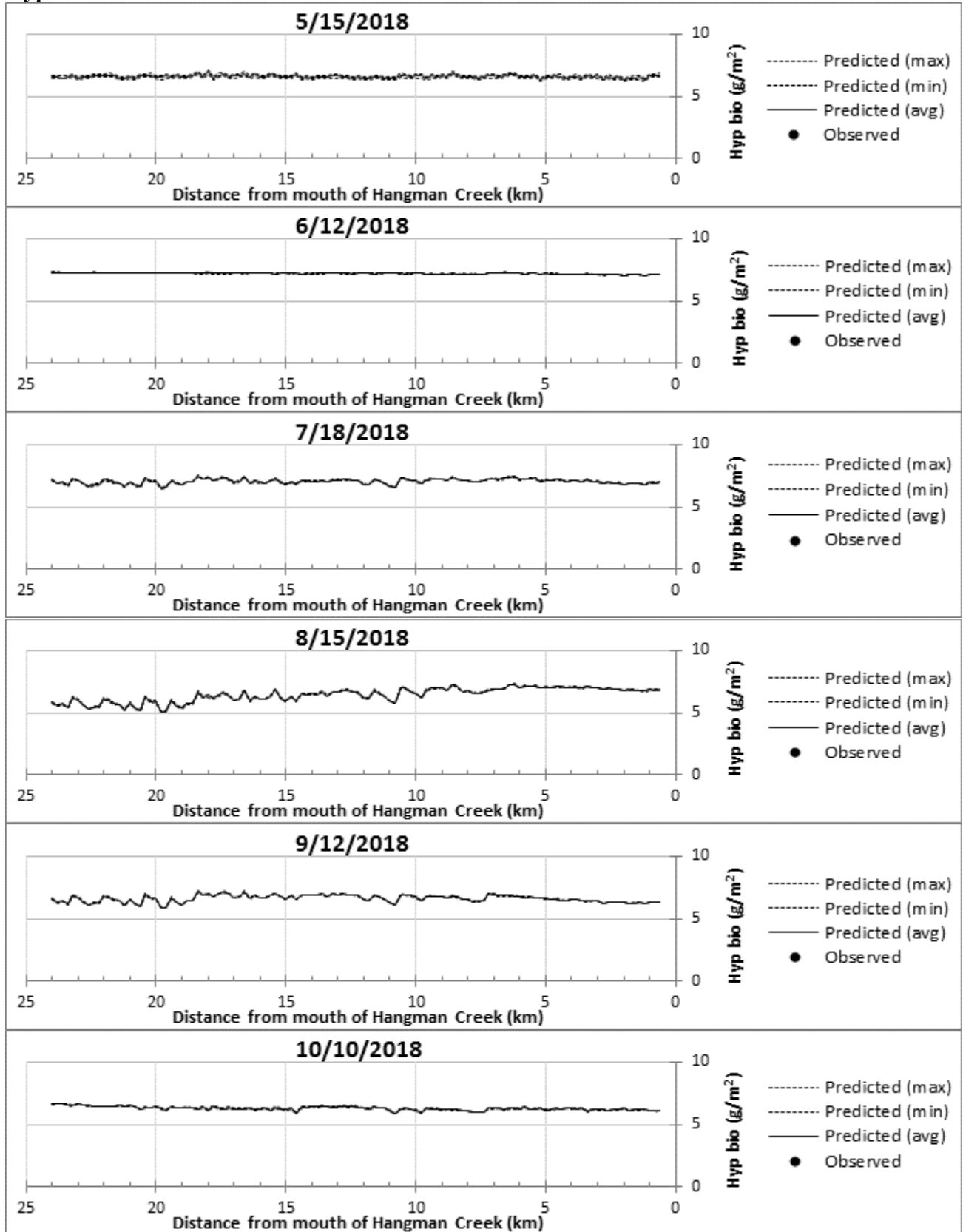
Phytoplankton as Chlorophyll a

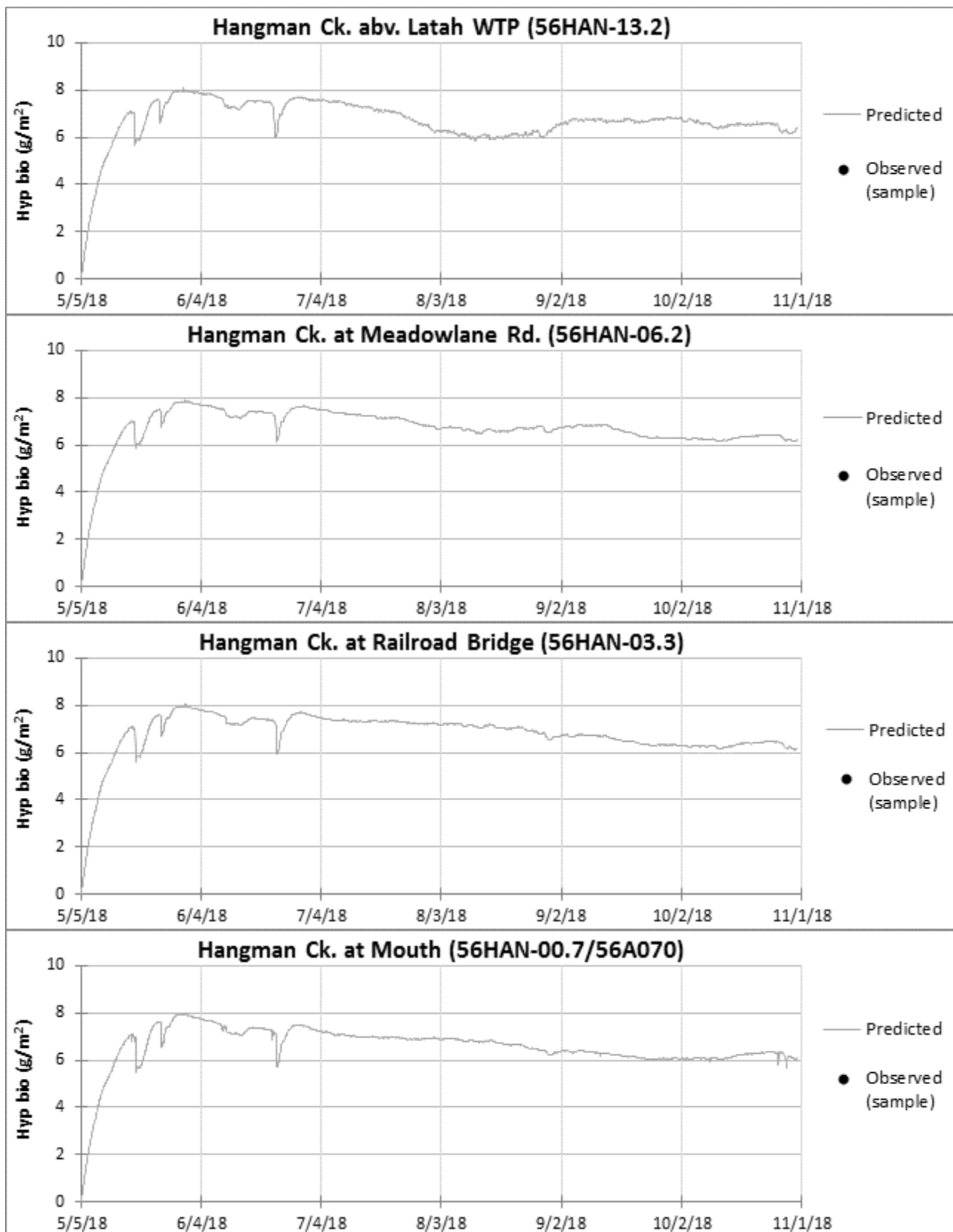
Observed phytoplankton values shown here are estimated from organic suspended solids (OSS) data. See *phytoplankton* section earlier in this appendix for details. These values should be considered approximate.





Hyporheic biofilm





Model Sensitivity to Nutrients

A model's sensitivity to nutrients refers to the relationship between the model's predictions of nutrient concentrations and algal productivity. This determines how the model predictions of DO and pH will respond under scenario conditions where nutrients are reduced relative to current conditions.

The sensitivity of algae to the presence of a limiting nutrient can be conceptualized as a relationship between primary productivity and the concentration of the limiting nutrient, using algorithms such as the Monod equation (Figure E-11). This relationship is not linear. Rather, at low concentrations of the limiting nutrient, a small increase in limiting nutrient concentration will have a large impact on productivity. At higher concentrations, additional increases in concentration will have a smaller impact on productivity.

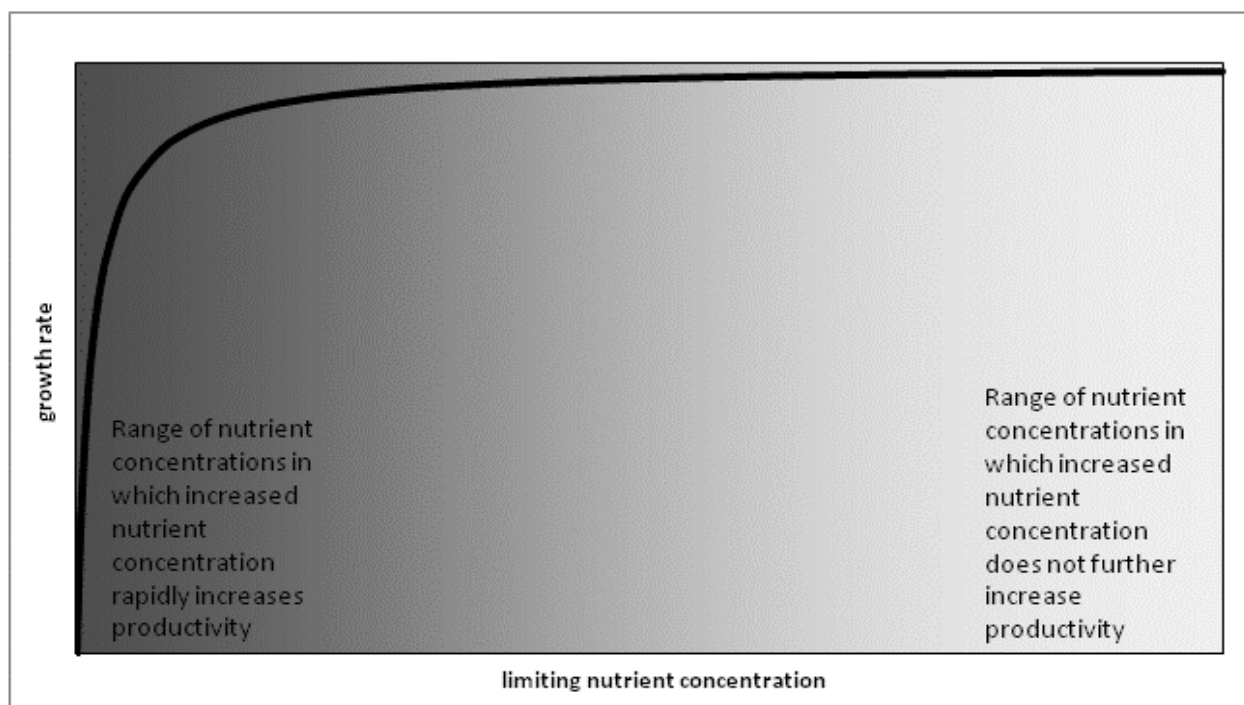


Figure E-11. Conceptual diagram of the relationship between limiting nutrient concentration and algal growth rate, using Monod equation (Monod, 1950; see Borchardt, 1996).

Research literature, along with previous TMDL studies, provides a guide to algal sensitivity to nutrients. All studies on this topic have concluded that the productivity of periphyton communities dominated by diatom algae is saturated by extraordinarily low concentrations of nutrients. This is likely because these organisms have evolved to be extremely efficient at extracting nutrients from very dilute water.

Bothwell (1985) observed approximately half-saturated growth at soluble reactive phosphorus (SRP) concentrations of 1.1 ug/L, and about 90% saturated growth at SRP concentrations of 3-4

ug/L. Rier and Stevenson (2006) found 90% saturated growth at 16 ug/L SRP, which is higher than the Bothwell value, but still extremely low. Data collected by Ecology from the Palouse River, which is a nitrogen-limited system, suggest about 90% saturated growth at dissolved inorganic nitrogen (DIN) concentrations of about 16 ug/L (Snouwaert and Stuart, 2015; Ecology, unpublished data). Rier and Stevenson (2006) found 90% saturated growth at 86 ug/L DIN.

To assess the sensitivity of the calibrated QUAL2Kw model to nitrogen and phosphorus, we compared model predicted bottom algae growth limitation factors for N and P to values that we might expect, given observed DIN and SRP levels. To estimate the expected growth limitation factors, we used the Monod equation, selecting half-saturation constants based on research literature and previous TMDL studies. We initially chose half-saturation constants of 7.2 ug/L for DIN and 1 ug/L for SRP, consistent with Bothwell (1985) and Snouwaert and Stuart (2015). However, these turned out to be a bit too low to explain the observed contrast in DO diel ranges between low-DIN sites and higher-DIN sites. Therefore, we chose slightly higher values of 15 ug/L for DIN and 2.08 ug/L for SRP, maintaining the 7.2:1 Redfield ratio.

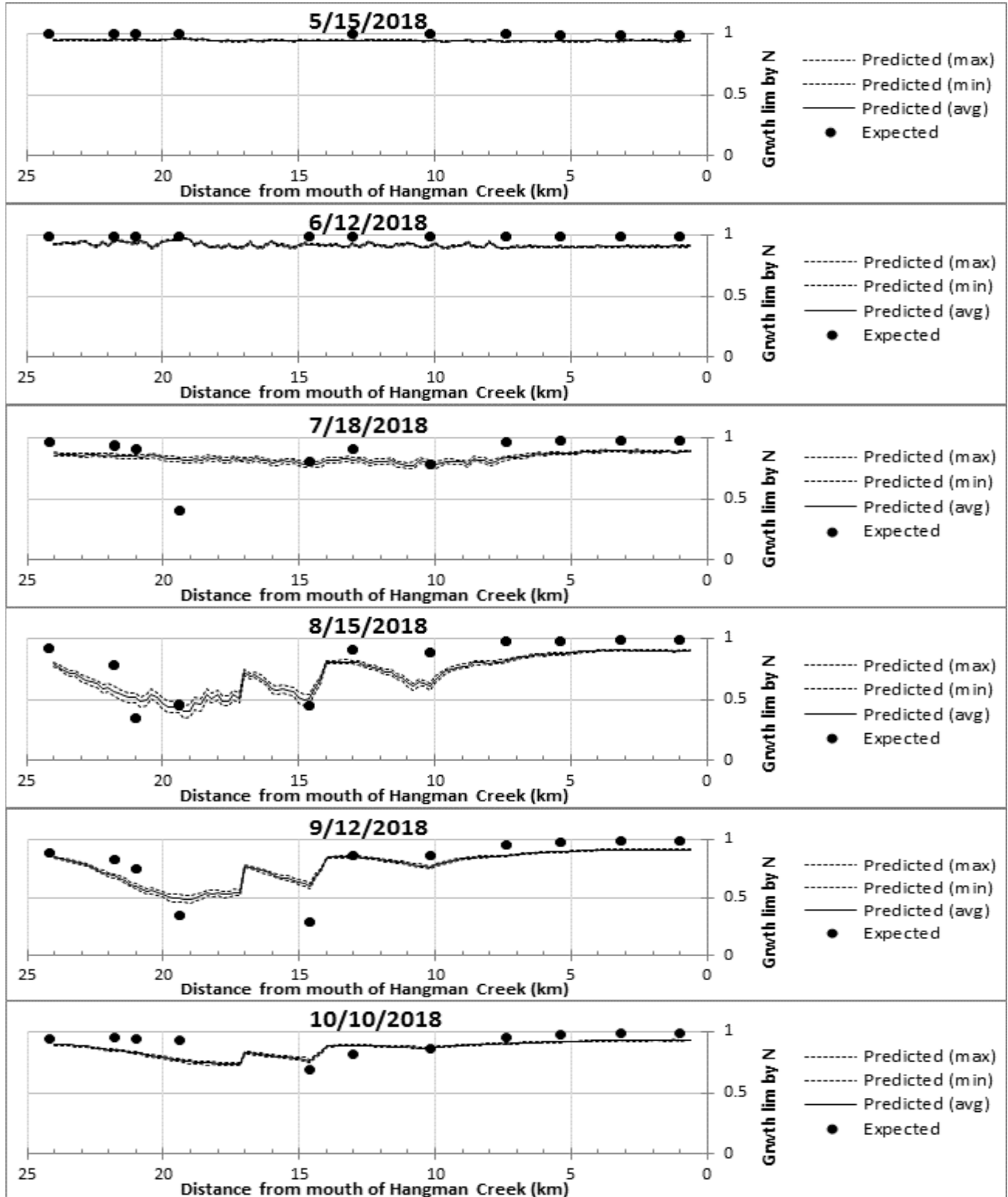
Figure E-12 presents model predicted bottom algae growth limitation factors for N and P alongside the expected factors based on observed DIN and SRP. These values range from 0 to 1, with 0 meaning total limitation and no algae growth, and 1 meaning no growth limitation. Observed late-summer DIN levels from downstream of Latah WWTP to about Hatch Rd. (km 20-14) are low. Both the QUAL2Kw model and our Monod curve analysis predict N-limited algal growth in this reach. Downstream of the Qualchan Golf Course/Marshall Ck. area, groundwater inflows containing nitrate mean there is no nutrient limitation of algae growth. SRP levels are generally not low enough to create P-limitation anywhere in Lower Hangman Creek during the summer months.

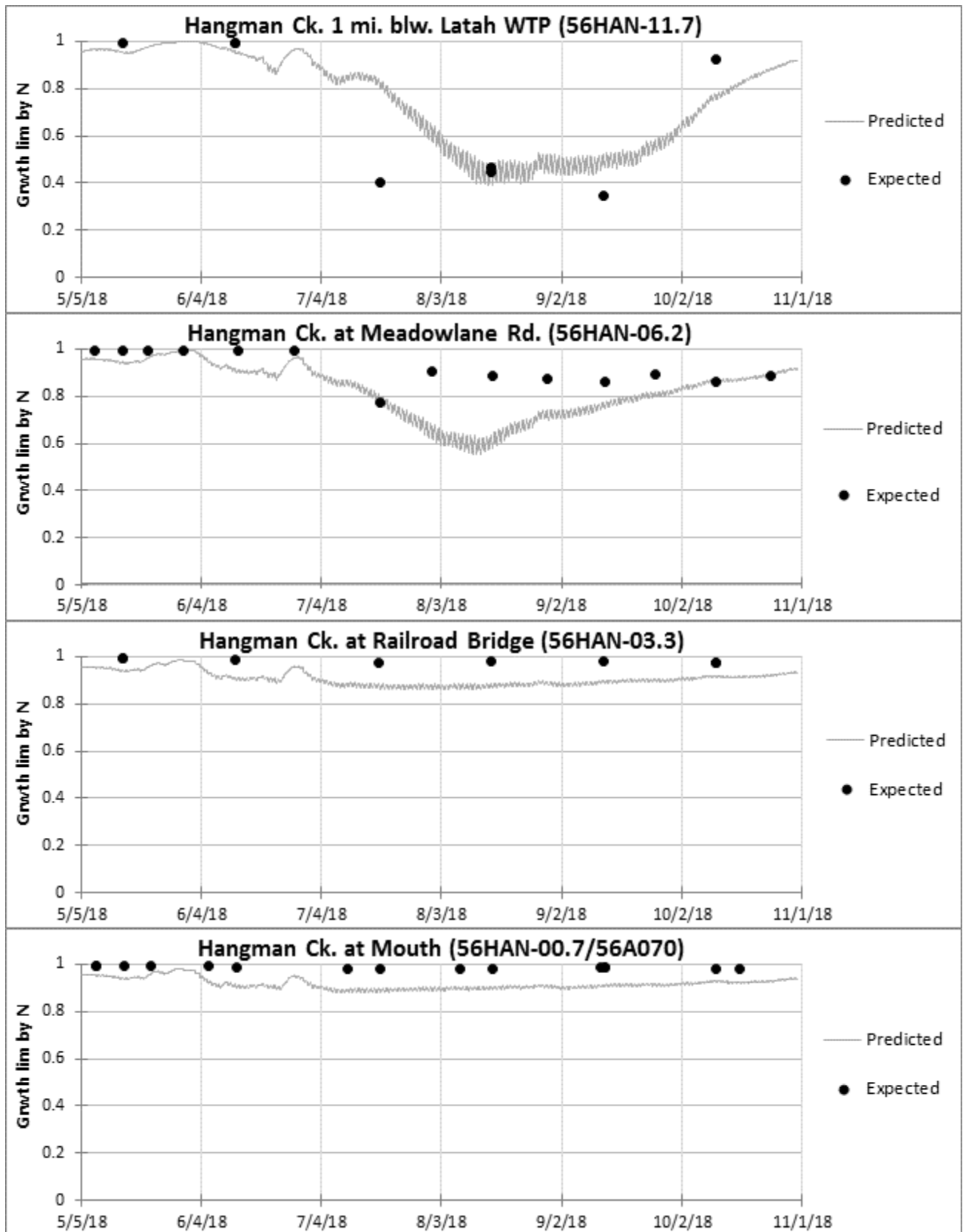
For phytoplankton, QUAL2Kw uses a simple growth model that allows the user to directly select half-saturation constants for nutrient limitation. We used the default values of 15 ug/L for DIN and 2 ug/L for SRP. This is essentially the same sensitivity we assumed for bottom algae (periphyton). This represents an assumption that phytoplankton consisted mainly of diatoms.

Figure E-12. Longitudinal and time-series plots of modeled vs. expected values for bottom algae growth limitation by nitrogen and phosphorus.

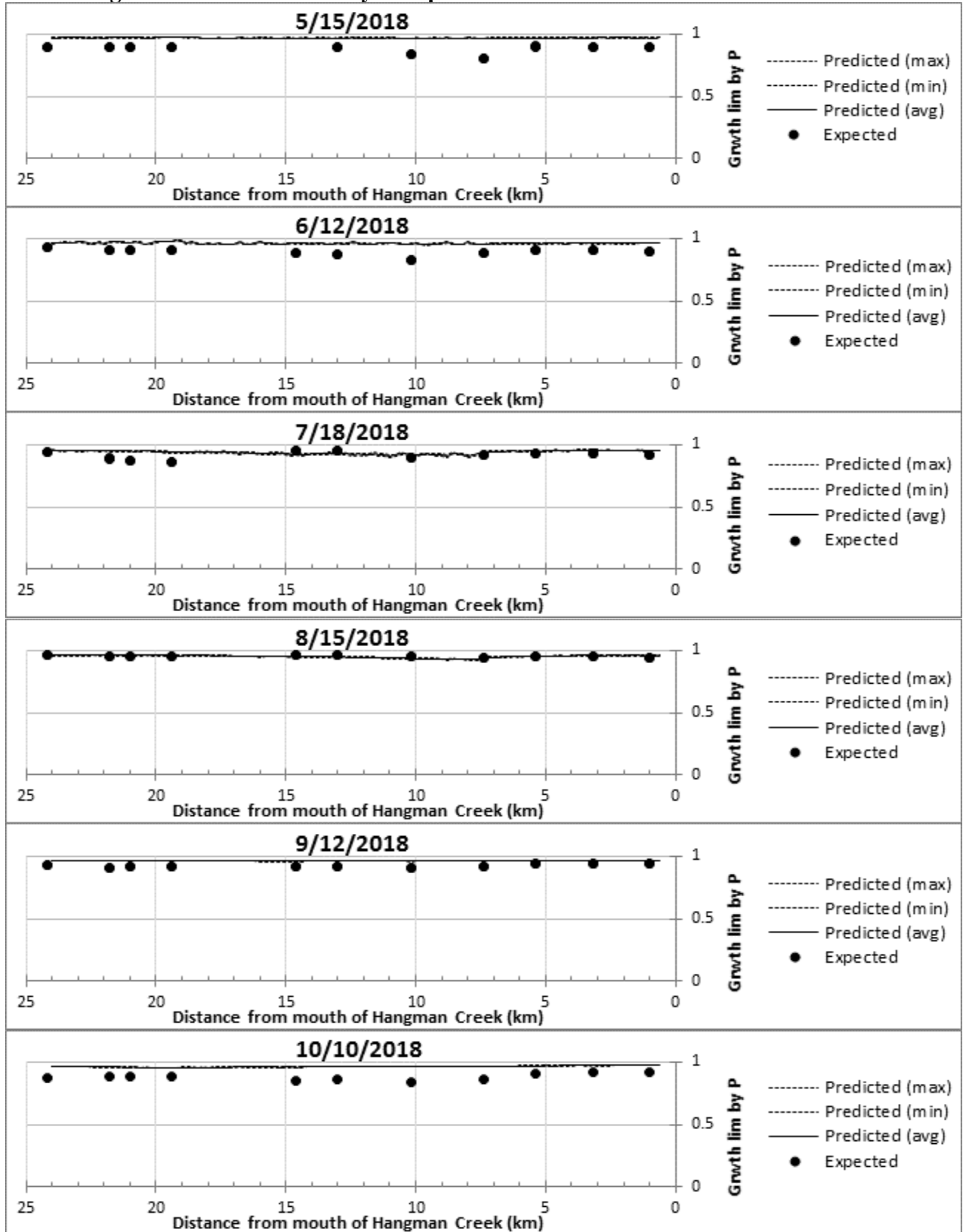
This figure includes all plots in the next 4 pages.

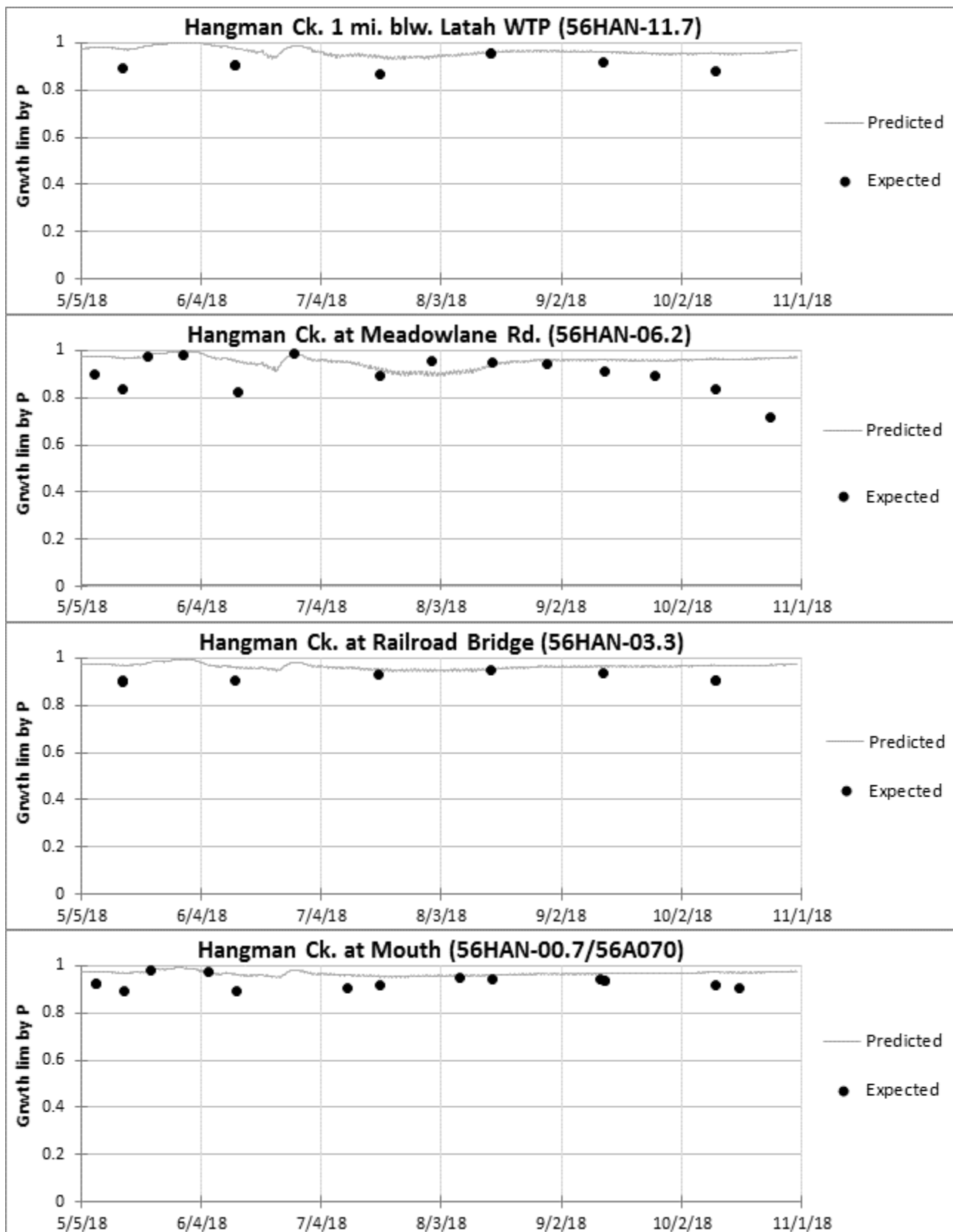
Bottom Algae Growth Limitation by Nitrogen





Bottom Algae Growth Limitation by Phosphorus





Appendix F. Stormwater load estimation

Several stormwater outfalls discharge to Hangman Creek in the Spokane area. Most of these outfalls discharge in the vicinity of the I-90 and Sunset Ave. bridges. These outfalls include stormwater from bridge and street infrastructure in the nearby vicinity, as well as draining parts of downtown Spokane, Browne's Addition, and the lower South Hill. We estimated total stormwater loads and flows from all outfalls together for the time period from 2008-2018. We did not attempt to quantify loads from individual outfalls.

Stormwater flow volume

The USGS Hangman Creek at Spokane gaging station (ID# 12424000) is located just downstream of the cluster of outfalls that constitute the vast majority of stormwater discharge to Hangman Creek. Because background flows in Hangman Creek are low during much of the year, and because stormwater discharges can be significant, albeit short-lived, stormwater flows often show up in gaging station data as clear signals that are distinct from the natural watershed response to the precipitation.

Figure F-1 demonstrates these stormwater flow signals. Stormwater flow typically appears as a fluctuation in the USGS gaging station data that neatly matches the precipitation pattern, like a fingerprint. These fluctuations do not appear in gaged flow data from Hangman Creek at Meadowlane Rd. (RM 6.2) and Hangman Creek at Railroad Bridge (RM 3.3), which are upstream of the stormwater outfalls.

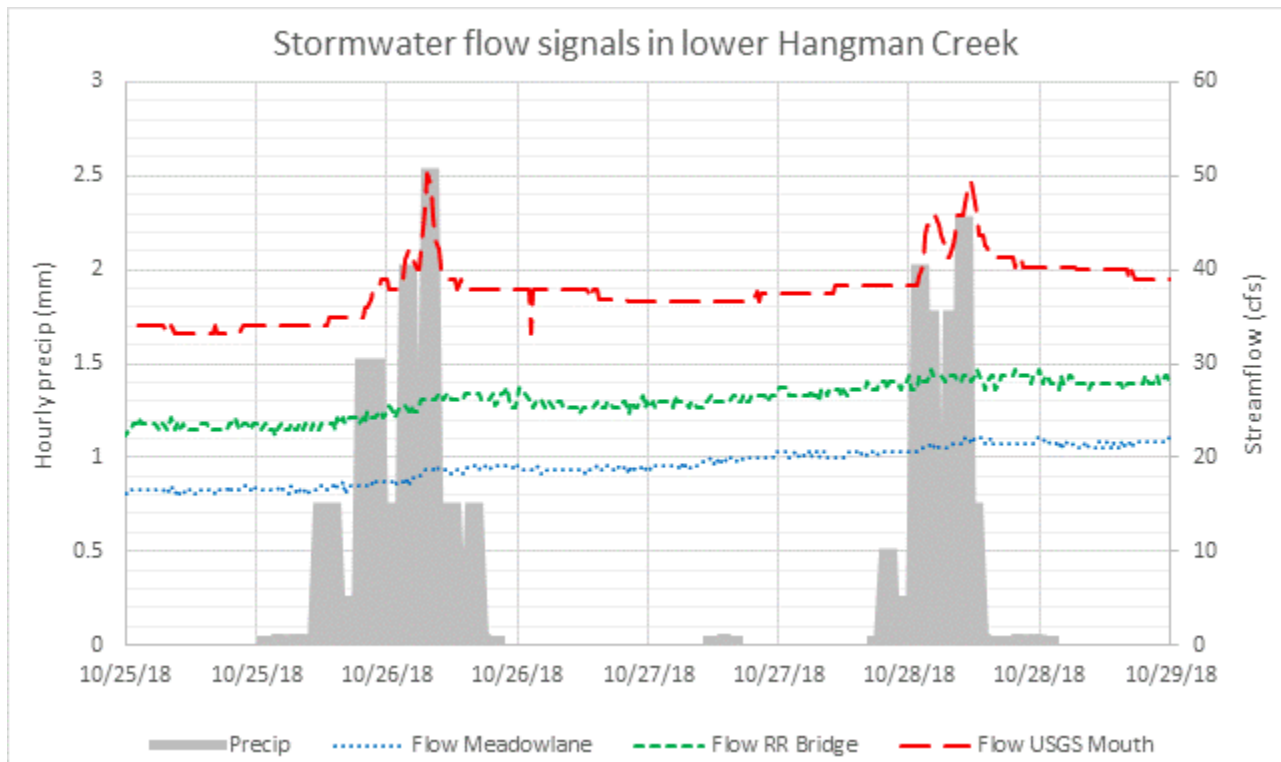


Figure F-1. Hourly precipitation data from Spokane Airport, along with gaging station flow data for Hangman Creek at Meadowlane Rd. (RM 6.2), Railroad Bridge (RM 3.3), and the USGS gage station (RM 0.8).

Stormwater flows are visible as fluctuations in the USGS RM 0.8 flow data (red line) that nearly mirror the patterns of the precipitation event.

Defining rain events

The first step of our analysis was to define and quantify all rain events that occurred during 2008-2018. We used precipitation data from the National Weather Service (NWS) station at Spokane International Airport (KGEG). Precipitation in the Spokane region typically falls during discrete events with dry periods of at least a few hours in between. This makes it relatively straightforward to connect specific rain events with specific stormwater flow events most of the time. We defined rain events as follows, and quantified the total precipitation during each event.

- We defined any rain ≥ 0.254 mm (0.01in) as an event. Trace precipitation (0.025mm, or 0.001 in) did not constitute an event.
- We did not count precipitation in the form of snow or ice.
- For events that contained a mix of rain and snow, we made a judgement call. If the event started as rain and then turned to snow, then we only counted the part of the event that was rain. If it started as snow and then turned to rain, and if the quantity of rain was likely enough to wash off the snow that had fallen earlier, then we included everything.

Defining stormwater flow events

For each defined rain event, we then examined the USGS continuous streamflow record to see if there was a fluctuation in flow that would indicate stormwater discharge. For each rain event, we defined the stormwater flow in one of three categories:

- **Zero stormwater flow** – During the summer and fall when background streamflows in Hangman Creek are low, it is possible to see even small stormwater discharges in the flow record. If a rain event during low background flows produced no fluctuations, then we could infer that there was no significant stormwater discharge. It is common for small rain events during otherwise warm, dry summertime conditions not to produce stormwater flow.
- **Unknown stormwater flow** – During higher background flow conditions, stormwater discharges are harder to see in the flow record. High background streamflows may obscure fluctuations due to stormwater discharge, especially if the stormwater discharge is small. If we could not see a stormwater signal, but could not confidently eliminate the possibility that a small signal was hidden by the high background flows, then we defined stormwater flow as unknown. We never assumed zero stormwater flow during background flows >200cfs.
- **Positive stormwater flow** – If we could see a fluctuation in the flow record indicative of stormwater discharge, then we estimated stormwater flow. To do this, we drew a “baseline” under the flow spike to estimate streamflow without the stormwater discharge effect. We defined the baseline using linear interpolation from the last 15-minute interval before flow began to rise, to the first interval when flows returned to the post-stormwater flatline. The post-stormwater flatline was often higher than flows before the event. This is because streamflows naturally tend to rise during rainfall anyway, as seen in two upstream flow records in Figure F-1. We then defined stormwater flow as the difference between the gaged flow and our defined baseline (Figure F-2). We totaled the stormwater flow for each event in acre-feet. One can visualize the total stormwater flow as the shaded area in Figure F-3 between the defined baseline flow and the gaged flow.

For the 11-year period, 2008-2018, we defined 200 zero stormwater flow events, 431 unknown stormwater flow events, and 341 positive stormwater flow events.

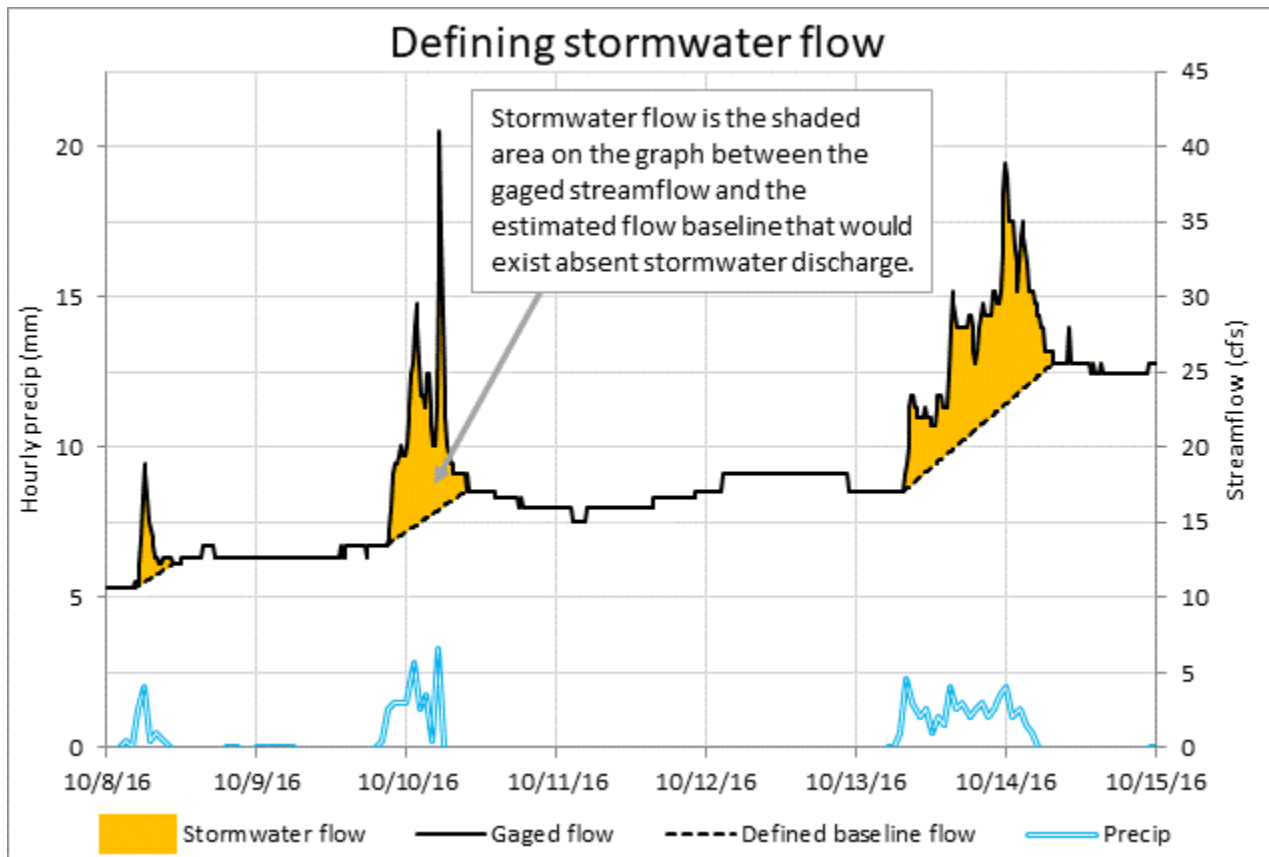


Figure F-2. Method for estimating stormwater discharges to Lower Hangman Creek.

Estimating discharge for unknown stormwater flow events

To estimate stormwater flow for unknown flow events, we used flow estimates from positive stormwater flow events to build a regression model. We explored a number of covariates while building this model, including:

- Total event precipitation
- Precipitation intensity (max hourly precipitation during the rain event)
- Antecedent precipitation over the previous 1, 2, 4, 8, 15, and 30 days
- Antecedent snow depth
- Change in snow depth over course of event
- Average Penman evaporation (Valiantzas, 2006) over the previous 1, 2, 4, 8, 15, and 30 days

However, the total event precipitation and 30-day antecedent precipitation were the only covariates that related strongly to stormwater discharge. We formulated the regression model as follows, using the PIKAIA genetic algorithm (Charbonneau and Knapp, 1995) to optimize the five model parameter constants:

$$S = \max[0, 2.3086((0.3083p - 1.1280) + (0.0303a - 1.0862))]]$$

Where:

S = total event stormwater volume (acre-feet)

p = total rain event precipitation (mm)

a = antecedent precipitation over the previous 30 days (mm)

Unsurprisingly, there was some scatter in the model fit (Figure F-3). Stormwater events are inherently variable. However, the model correlated strongly with the observed data ($R^2 = 0.6352$). We calibrated the model to minimize bias over the full range of predictions. The model does a good job predicting overall flow volumes (Table F-1).

We used the regression model to predict stormwater volumes for “unknown stormwater flow” events, as described above.

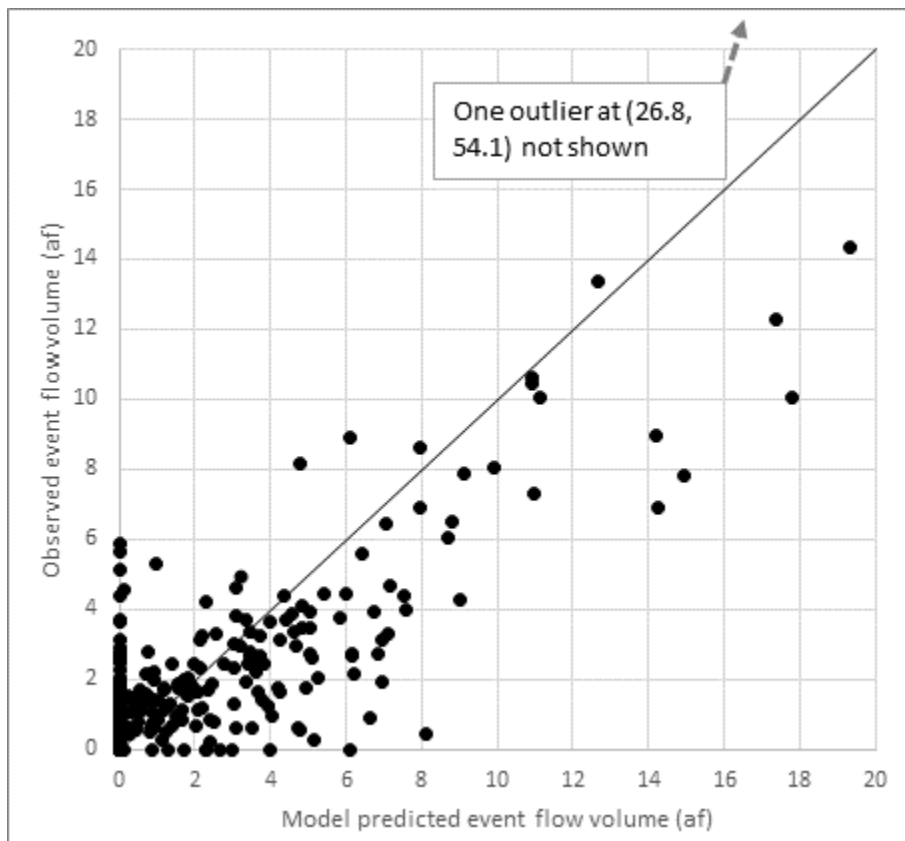


Figure F-3. Predicted vs. observed stormwater event flow volumes (acre-feet).

The black line is the ideal 1-to-1 line.

Table F-1. Stormwater event flow model bias.

Event flow range	Total modeled stormwater flow volume for all events (af) ^a	Total observed stormwater flow volume for all events (af) ^a	Bias (af)	% Bias	# of events
Zero flow events	24.4	0.00	+24.4 ^b	-- ^c	199
0.01 – 1 af events	61.7	61.7	+0.01	+0.0%	170
>1 af events	577	586	-9.1	-1.6%	167
All events	663	648	+15.2	+2.4%	536

^a Note that this is only for events where we were able to estimate stormwater flow from the gage record (i.e. “positive stormwater flow” events). Care should be taken not to misuse these values as estimates of actual total stormwater flow, since “unknown stormwater flow” events are not yet included.

^b Bias from zero flow events is by definition positive, unless the model correctly predicted zero flow for every one of these events. The only way to achieve a near-zero bias, given the amount of scatter, would be to allow the model to predict negative flows some of the time, which is of course absurd.

^c % bias is the bias divided by the observed value. It cannot be calculated when the observed value is zero.

Stormwater flow results

For the 11-year period, 2008-2018, we estimated stormwater flows for all events:

- **Zero stormwater flow** – Zero
- **Unknown stormwater flow** – Estimated using regression model
- **Positive stormwater flow** – Estimated from USGS Hangman Creek gage flow record, as described above.

Table F-2 summarizes estimated stormwater flow totals by month and year. Table F-3 provides summary statistics by month. Figure F-4 charts mean monthly flows along with minimum and maximum for each month.

Stormwater flows are highly variable by month and year, depending on the chance occurrence of short-lived discrete rain events. Stormwater flows are the lowest during the July-September dry summer period, typically around 1-2 acre-feet/month. Stormwater flows are typically an order of magnitude higher during the rest of the year. High monthly stormwater flows can happen at any time except for summer. Dry spells with zero monthly flow can occur any month of the year.

Table F-2. Estimated stormwater flow volumes by month, 2008-2018, in acre-feet.

Month	2008	2009	2010	2011	2012	2013	2014	2015	2016	2017	2018
January	4.1	9.8	21.1	27.6	5.1	6.2	0.5	17.4	19.8	4.4	35.2
February	0	6.0	5.1	0	7.3	0	8.4	7.2	4.8	45.9	8.2
March	0	22.4	9.2	43.4	70.1	6.4	46.3	21.9	44.0	96.2	3.0
April	6.3	11.6	7.8	23.2	21.5	1.4	5.9	3.0	9.0	33.0	26.5
May	5.5	3.7	14.5	21.0	3.7	3.6	4.9	3.7	7.2	11.3	9.0
June	12.6	16.2	33.9	4.0	30.4	15.1	22.8	0.2	1.9	6.4	10.9
July	0	1.3	2.4	2.9	9.4	0	0.3	1.0	0.5	0	0
August	1.5	2.6	0.2	1.0	0	4.5	5.3	0.2	1.5	0	0
September	1.5	3.5	2.9	0	0	6.8	0.0	1.7	0.5	6.7	0.3
October	0.7	21.5	6.2	1.3	8.0	0	7.7	4.6	116.7	7.2	8.4
November	3.8	8.2	10.8	6.0	26.5	9.4	6.5	1.5	18.2	22.2	17.7
December	3.8	20.6	27.3	6.6	23.4	2.0	15.3	25.3	0.0	11.4	26.2
Total	39.8	127.4	141.3	136.9	205.4	55.4	124.0	87.6	224.1	244.6	145.5

Table F-3. Estimated stormwater flow volume summary statistics by month, 2008-2008, in acre-feet.

Month	Min	10 th %ile	Median	Mean	90 th %ile	Max
January	0.5	1.3	9.8	13.8	33.7	35.2
February	0	0	6.0	8.4	38.4	45.9
March	0	0.6	22.4	33.0	90.9	96.2
April	1.4	1.7	9.0	13.6	31.7	33.0
May	3.6	3.6	5.5	8.0	19.7	21.0
June	0.2	0.5	12.6	14.1	33.2	33.9
July	0	0	0.5	1.6	8.1	9.4
August	0	0	1.0	1.5	5.1	5.3
September	0	0	1.5	2.2	6.8	6.8
October	0	0.1	7.2	16.6	97.7	116.7
November	1.5	1.9	9.4	11.9	25.6	26.5
December	0	0.4	15.3	14.7	27.1	27.3

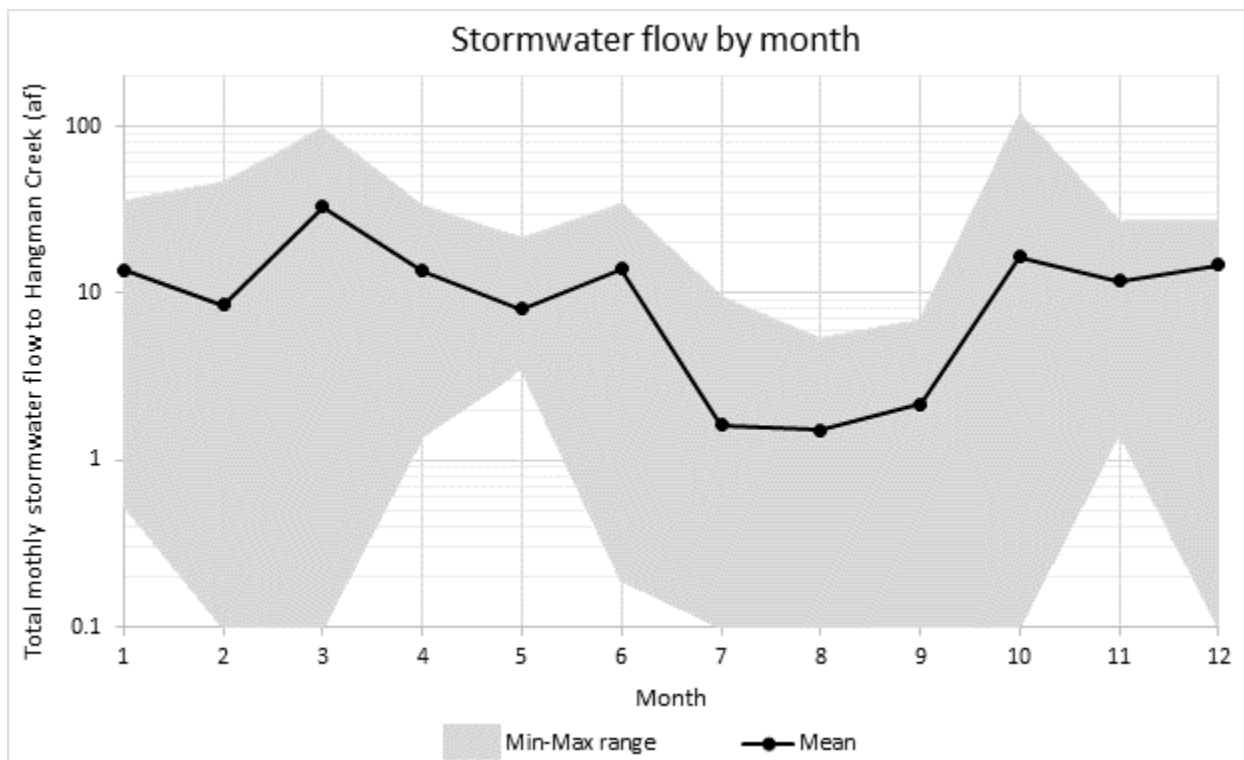


Figure F-4. Mean estimated monthly stormwater flow volumes along with range from minimum to maximum, 2008-2018.

Stormwater sediment and nutrient concentrations

We collected samples and flow measurements from stormwater outfalls on two occasions during spring 2018. During each event, we sampled the four outfalls that were flowing. The March 14, 2018 event was early in an event during rising outflows, while the April 12, 2018 event was late in an event after many hours of rainfall during falling outflows. Unsurprisingly, concentrations were higher during the March 14 than during the April 12 event.

Table F-4 presents stormwater sample concentration results. For each event, we estimated the overall average concentration as the flow weighted average of the four outfalls. We then averaged the two events to provide a general characterization of stormwater entering Hangman Creek.

To check the representativeness of these results, we compared the values to other stormwater data from Spokane for selected parameters (Table F-5). Note that these other comparison results are mostly from different outfalls that discharge to the Spokane River, not to Hangman Creek. Our results were in the same general range as these comparison data, suggesting these are reasonably representative values.

Table F-4. Stormwater sediment and nutrient concentration results.

Location ID	Date	Flow (cfs)	TP (mg/L)	SRP (mg/L)	TPN (mg/L)	NO2-3 (mg/L)	NH4 (mg/L)	DIN (mg/L)	SSC (mg/L)	TSS (mg/L)
56MS4-I90LB	3/14/2018	0.44	0.215	0.122	2.96	2.62	0.099	2.719	56	51
56MS4-I90RB1	3/14/2018	0.4	0.62	0.0548	1.33	0.381	0.522	0.903	323	265
56MS4-I90RB2	3/14/2018	0.23	0.539	0.125	0.828	0.15	0.286	0.436	157	100
56MS4-Sunset	3/14/2018	0.022	3.1	0.182	2.85	0.787	0.983	1.77	1220	1070
Flow-weighted average for 3/14/2018:			0.490	0.0992	1.91	1.24	0.311	1.55	199	160
56MS4-I90LB	4/12/2018	1.4	0.1645	0.0693	2.135	1.725	0.0995	1.8245	45	44.5
56MS4-I90RB1	4/12/2018	1.8	0.38	0.0518	1.15	0.484	0.32	0.804	190	167
56MS4-I90RB2	4/12/2018	1.4	0.319	0.0955	0.485	0.09	0.133	0.223	89	87
56MS4-Sunset	4/12/2018	0.03	0.548	0.0864	0.745	0.355	0.183	0.538	212	205
Flow-weighted average for 4/12/2018:			0.297	0.0705	1.244	0.739	0.196	0.935	116	106
Average of the two events:			0.394	0.0849	1.58	0.991	0.254	1.24	157	133

TP = total phosphorus
 SRP = soluble reactive phosphorus
 TPN = total persulfate nitrogen
 NO2-3 = nitrate-nitrite nitrogen
 NH4 = ammonium nitrogen
 DIN = dissolved inorganic nitrogen (calculated as NO2-3 plus NH4)
 SSC = suspended sediment concentration
 TSS = total suspended solids

Table F-5. Comparison of Ecology 2018 stormwater data with other data sources

Data Source	TP (mg/L)	TSS (mg/L)	NH4 (mg/L)
Ecology 2018 (this study)	0.394	133	0.254
Ecology SRUW ^a (median)	0.341	81	--
Ecology SRUW ^a (mean)	0.5381	244	--
City of Spokane Cochran Basin ^b (mean May-Oct)	0.34	142	0.17
City of Spokane Cochran Basin ^b (mean all data)	0.46	190	0.30

^a Ecology's Spokane River Urban Waters monitoring program. This includes data from conveyances and outfalls, but not CSOs or other types of locations.

^b City of Spokane, 2020

Stormwater loads

We used the stormwater flow volumes and concentrations as described above to calculate stormwater loads for the 2008-2018 period. Table F-6 presents total phosphorus loads, and Table F-7 presents total suspended solids loads. We present these two parameters for their relevance to the *Spokane DO TMDL* (Moore and Ross, 2010) and the *Hangman Multiparameter TMDL* (Joy et al., 2009).

Table F-6. Estimated average monthly stormwater total phosphorus (TP) loads to Lower Hangman Creek, in lbs/day.

Month	2008	2009	2010	2011	2012	2013	2014	2015	2016	2017	2018
January	0.142	0.338	0.730	0.952	0.175	0.214	0.019	0.601	0.685	0.153	1.216
February	0	0.228	0.195	0	0.271	0	0.321	0.274	0.178	1.753	0.312
March	0	0.772	0.319	1.498	2.419	0.220	1.598	0.755	1.519	3.320	0.102
April	0.224	0.414	0.277	0.826	0.767	0.050	0.210	0.108	0.320	1.179	0.947
May	0.189	0.129	0.501	0.726	0.128	0.123	0.169	0.128	0.249	0.390	0.312
June	0.451	0.579	1.211	0.142	1.086	0.537	0.814	0.007	0.069	0.227	0.390
July	0	0.045	0.082	0.099	0.324	0	0.010	0.036	0.016	0	0
August	0.052	0.089	0.006	0.035	0	0.155	0.183	0.006	0.050	0	0
September	0.054	0.125	0.102	0.001	0	0.243	0	0.059	0.019	0.238	0.011
October	0.023	0.741	0.213	0.043	0.276	0	0.267	0.159	4.029	0.248	0.291
November	0.135	0.294	0.384	0.214	0.946	0.336	0.233	0.052	0.649	0.791	0.630
December	0.131	0.710	0.942	0.228	0.806	0.070	0.528	0.874	0	0.393	0.905
Mar-May average	0.137	0.439	0.367	1.018	1.109	0.132	0.664	0.332	0.700	1.635	0.448
Jun average	0.451	0.579	1.211	0.142	1.086	0.537	0.814	0.007	0.069	0.227	0.390
Jul-Oct average	0.035	0.086	0.063	0.046	0.109	0.132	0.065	0.033	0.029	0.078	0.004

Table F-7. Estimated average monthly stormwater total suspended solids (TSS) loads to Lower Hangman Creek, in lbs/day

Month	2008	2009	2010	2011	2012	2013	2014	2015	2016	2017	2018
January	48.1	114.4	246.9	321.9	59.2	72.5	6.4	203.4	231.8	51.8	411.2
February	0	77.2	66.0	0	91.5	0	108.4	92.8	60.1	593.1	105.7
March	0	261.1	108.0	506.5	818.2	74.4	540.5	255.4	513.7	1122.9	34.6
April	75.9	140.1	93.6	279.4	259.5	16.9	70.9	36.4	108.1	398.8	320.3
May	63.9	43.7	169.4	245.4	43.3	41.7	57.3	43.1	84.3	131.9	105.5
June	152.6	195.8	409.6	48.1	367.4	181.8	275.2	2.3	23.3	76.8	132.0
July	0	15.3	27.7	33.6	109.5	0	3.5	12.2	5.4	0	0
August	17.4	30.0	2.1	12.0	0	52.5	61.8	2.0	17.1	0	0
September	18.4	42.4	34.5	0.4	0	82.3	0	19.9	6.3	80.6	3.7
October	7.6	250.6	72.1	14.6	93.5	0	90.5	53.7	1362.9	83.9	98.4
November	45.5	99.5	129.8	72.5	319.9	113.8	78.9	17.5	219.5	267.7	213.2
December	44.1	240.0	318.6	77.1	272.8	23.6	178.5	295.5	0	132.8	306.0
Water Year total load (tons/yr) ^{a b}	-- ^c	15.4	26.7	30.3	29.2	18.4	19.2	15.5	21.8	61.3	24.2

a Water years (WY) extend from October – September, so for example WY 2018 includes October 2017 – September 2018.

b We express water year total TSS loads in tons/year rather than lbs/day as the rest of this table. This is for ease of comparison with load allocations in the *Hangman Multiparameter TMDL* (Joy et al., 2009).

c We did not calculate monthly loads prior to calendar year 2008. Therefore we could not calculate a total for WY 2008, which includes October-December 2007.

Appendix G. Idaho high-flow season load estimation

We estimated high-flow season cross-boundary sediment and nutrient loads originating in Idaho for 2009 and 2018. For 2009 we estimated only total phosphorus loads, while for 2018 we estimated suspended sediment, total phosphorus, and dissolved inorganic nitrogen loads. Because of differences in sampling site locations and study design, we used a different approach for each of the two years. For 2009 we estimated loads for each of the five cross-boundary waterways at sampling locations located at the Washington/Idaho state line. For 2018, we started with subbasin load estimates derived from the watershed mass balance approach, and used the proportion of the watershed area of each trans-boundary subbasin to estimate Idaho loads.

2009

During water year 2009 (October 2008 – September 2009), Ecology collected nutrient and flow data at the Washington/Idaho state line in the five main cross-boundary waterways in the Hangman Creek watershed (Joy, 2008; Ross, 2011). We estimated seasonal TP loads for each of these five locations using multiple-linear regression modeling (Cohn et al., 1989).

Estimation of continuous flow record

Estimating seasonal loads using multiple linear regression modeling, or indeed any other method, requires a continuous flow record. The USGS operates a gaging station on Hangman Creek at the Washington/Idaho state line (ID# 12422990). However, for the other four waterways, the only flow data available are the individual monthly and/or twice-monthly flow measurements we took whenever we collected samples. Therefore, we used continuous flow gaging data collected elsewhere in the watershed by the Spokane Conservation District (SCD), in conjunction with our flow measurements, to estimate continuous flow records for each state line location (Table G-1).

Table G-1. Continuous flow record estimation for state line sample locations for 2009.

Sampling Location	Location ID	Continuous flow basis	RMSE CV ^a
NF Rock Ck. at State Line	56NFR-03.8	$\text{Log}(Q_{\text{nfr}}) = -0.1531 \cdot \text{Log}(Q_{\text{rm}})^2 + 1.7046 \cdot \text{Log}(Q_{\text{rm}}) - 1.6160$	45%
Rose Ck. at State Line	56ROS-01.7	$\text{Log}(Q_{\text{rose}}) = -0.0833 \cdot \text{Log}(Q_{\text{rm}})^2 + 1.2869 \cdot \text{Log}(Q_{\text{rm}}) - 1.2955$	41%
(SF) Rock Ck. at State Line	56ROC-25.9	$\text{Log}(Q_{\text{sfr}}) = -0.1670 \cdot \text{Log}(Q_{\text{rm}})^2 + 1.6645 \cdot \text{Log}(Q_{\text{rm}}) - 1.8859$	46%
Little Hangman Ck. at State Line	56LIT-02.3 ^b	$\text{Log}(Q_{\text{lhc}}) = -0.1681 \cdot \text{Log}(Q_{\text{rm}})^2 + 1.6527 \cdot \text{Log}(Q_{\text{rm}}) - 1.0195$	40%
Hangman Ck. at State Line	56HAN-57.7	USGS gage station data	N/A

^a RMSE CV is the Root Mean Squared Error coefficient of variation, or the RMSE divided by the average observed value:

$$RMSE\ CV = \frac{\sqrt{[\sum(K_{\text{modeled}} - K_{\text{observed}})^2]/n}}{K_{\text{observed}}}$$

^b One might imagine that the USGS Hangman Creek at State Line gage data would form a better basis for estimating Little Hangman Creek. However, we found that the hydrology of Little Hangman Creek bears more resemblance to Rock Creek. Little Hangman and Rock Creeks are both more responsive/flashy than the Hangman Creek mainstem.

Q_{nfr} = flow (cfs) at NF Rock Ck. at State Line

Q_{rose} = flow (cfs) at Rose Ck. at State Line

Q_{sfr} = flow (cfs) at upper (SF) Rock Ck. at State Line

Q_{lhc} = flow (cfs) at Little Hangman Ck. at State Line

Q_{rm} = flow (cfs) at Rock Ck. at Mouth, as gaged by SCD, offset by 1 day to compensate for the fact that this location is quite a distance downstream from the state line locations

Multiple-linear regression modeling

We estimated seasonal loads at each state line sampling location using multiple-linear regression modeling (MLR; Cohn et al., 1989). We built and calibrated models for each sampling location. The models followed the same form as the MLR models that we used for the 2018 watershed mass balance analysis (Appendix C):

$$\log K = \beta_0 + \beta_1 \log(Q/A) + \beta_2 \log(Q/A)^2 + \beta_3 \sin(2\pi f_y) + \beta_4 \cos(2\pi f_y)$$

Where:

K = constituent concentration (mg/L)

Q = flow (cms)

A = contributing watershed area (km²)

f_y = year fraction (e.g. July 1, 2018 = 2018.50)

β_0 = intercept parameter

$\beta_{1,2}$ = parameters relating to flow dependence

$\beta_{3,4}$ = parameters relating to seasonal variation

Table G-2 presents the parameterization and selected goodness-of-fit statistics for the MLR models for TP for the state line sites, for the 2009 high-flow season.

Table G-2. Parameterization and goodness-of-fit for multiple linear regression models for TP, for Washington/Idaho state line sites for 2009.

Location ID	β_0 intercept	β_1 log(Q/A)	β_2 log(Q/A) ²	β_3 sin(2 π f _y)	β_4 cos(2 π f _y)	RMSE CV ^a	% Bias ^b	Slope ^c	R ² ^d
56NFR-03.8	0.463	0.388	0.046	-0.635	0.109	42.3%	-6.9%	1.10	0.57
56ROS-01.7	1.174	1.210	0.169	-0.299	0.071	32.0%	-3.2%	1.08	0.88
56ROC-25.9	1.652	1.541	0.234	-0.467	0.097	38.3%	-4.9%	1.06	0.82
56LIT-02.3	0.512	0.817	0.105	-0.122	0.074	54.4%	-6.4%	1.13	0.70
56HAN-57.7	1.100	1.305	0.210	-0.395	0.145	68.9%	-11.4%	1.16	0.42

^a RMSE CV is the Root Mean Squared Error coefficient of variation, or the RMSE divided by the average observed value:

$$RMSE\ CV = \frac{\sqrt{[\sum(K_{modeled} - K_{observed})^2]/n}}{\bar{K}_{observed}}$$

^b % Bias is the overall bias divided by the average observed value:

$$\% \text{ Bias} = \frac{[\sum(T_{modeled} - T_{observed})]/n}{\bar{K}_{observed}}$$

^c The slope of the best fit line through the back-transformed predicted vs. observed scatter plot, with a specified zero intercept. The ideal value is 1.

^d The R² value of the best fit line through the back-transformed predicted vs. observed scatter plot, with a specified zero intercept.

At each location, we used the MLR model along with the continuous flow record to estimate constituent concentration at 1 day intervals. We then estimated loads for each day. From this, we calculated seasonal average loads (Table G-3). We did not attempt to apply any adjustment or correction to these model predictions (see Appendix C; Figures C-4 and C-5), because we did not have continuous turbidity in 2009 to provide an independent basis for these estimates.

Table G-3. Estimated phosphorus loads from Idaho, high-flow season 2009.

Waterbody	Idaho Drainage Area (mi ²) ^a	TP (lbs/day) 1/1/09 - 4/30/09 ^b	TP (lbs/day) 3/1/09 - 5/31/09 ^b	Flow (cfs) 1/1/09 - 4/30/09 ^b	Flow (cfs) 3/1/09 - 5/31/09 ^b
NF Rock Ck.	29.7	97	65	44	44
Rose Ck.	19.9	48	40	23	23
upper (SF) Rock Ck.	10.2	34	26	14	14
Little Hangman Ck.	61.3	160	150	94	94
Hangman Ck.	126.6	710	280	270	270
Total from Idaho ^c	--	1100	560	440	440
Estimated load or flow at Hangman Ck. mouth	--	1800	1700	820	860
Estimated % from Idaho	--	60%	33%	54%	52%

^a The drainage areas shown for 2009 are the areas draining to the state line sampling locations for each stream. These may in fact include areas in Washington, and may not include all areas in Idaho, depending on the vagaries of local topography.

^b The 1/1/2009 – 4/30/2009 period represents peak flow season, including an ice dam breakage event that occurred in early January. The season from 3/1/2009 – 5/31/2009 represents the March-May load allocation season established in the *Spokane DO TMDL* (Moore and Ross, 2010).

^c The total from Idaho is the sum of each of the waterbody loads. The values are rounded to two significant digits, and so may not add up exactly.

2018

We estimated high-flow season cross-boundary Idaho loads for 2018 by using the subbasin load estimates from the watershed mass balance analysis (Appendix C, Tables C-7 through C-10). The pour point monitoring stations for these subbasins were all located well within Washington, as we chose these stations based on natural hydrological boundaries. We estimated Idaho loads for each cross-boundary subbasin (Table G-4) based on the simple proportion of the subbasin watershed area located in Idaho.

Table G-4. Estimated sediment, phosphorus, and nitrogen loads from Idaho, high-flow season 2018.

Waterbody	Subbasin Name	Total Subbasin Area (mi ²)	Idaho Drainage Area (mi ²) ^a	% of Subbasin in Idaho	SSC (tons/day) 1/18/18 - 4/30/18 ^b	SSC (tons/day) 3/1/18 - 5/31/18 ^b	TP (lbs/day) 1/18/18 - 4/30/18 ^b	TP (lbs/day) 3/1/18 - 5/31/18 ^b	DIN (lbs/day) 1/18/18 - 4/30/18 ^b	DIN (lbs/day) 3/1/18 - 5/31/18 ^b	Flow (cfs) 1/18/18 - 4/30/18 ^b	Flow (cfs) 3/1/18 - 5/31/18 ^b
NF Rock Ck.	Hoxie Valley - NF Rock Ck	55.3	35.1	63.5%	19	17	48	35	1500	830	54	37
Rose Ck.	Rose Ck.	21.5	17.4	81.0%	9.7	8.4	43	36	1100	690	24	18
upper (SF) Rock Ck.	Upper Rock	36.1	10.1	27.9%	12	8.9	35	26	580	350	15	11
Little Hangman Ck.	Little Hangman Ck.	63.9	52.9	82.7%	92	63	200	140	2500	1500	91	66
Hangman Ck.	Upper Hangman	132.5	126.0	95.1%	75	72	310	250	3900	2400	270	200
Total from Idaho ^c	--	241.5 ^d	--	--	210	170	640	490	9500	5700	450	330
Estimated load or flow at Hangman Ck. mouth	--	677.2 ^e	--	--	300	230	1100	860	22000	15000	940	730
Estimated % from Idaho	--	35.7% ^f	--	--	69%	72%	56%	57%	43%	39%	48%	45%

^a The Idaho drainage areas for 2018 are the exact areas within Idaho that contribute to each subbasin. This is slightly different than the values shown in Table G-3.

^b The period from 1/18/2018 – 4/30/2018 represents the season of peak flows, starting when we installed flow monitoring equipment throughout the watershed. The season from 3/1/2018 – 5/31/2018 represents the March-May load allocation season established in the *Spokane DO TMDL* (Moore and Ross, 2010).

^c The total from Idaho is the sum of each of the waterbody loads. The loading values are rounded to two significant digits, and so may not add up exactly.

^d This is the total area of the Hangman watershed that is located in Idaho.

^e This represents the total area of the Hangman watershed. In fact, this is the drainage area to the Hangman Creek at Mouth monitoring station (56HAN-00.7 a.k.a. 56A070). This does not include the 15.3 mi² of the Indian Canyon subbasin, which we did not monitor during this study. It also does not include a very small area at the mouth of Hangman Creek, downstream of the monitoring station.

^f The percentage of the total Hangman Creek watershed area (as described in footnote e) that is located in Idaho.